Evolution of the Human CD4$^+$ T cell response to Epstein-Barr virus infection - Analysis of systemic and local immune responses

By

Benjamin James Meckiff

A thesis submitted to

The University of Birmingham

For the degree of

DOCTOR OF PHILOSOPHY (PhD)

Institute of Immunology and Immunotherapy

College of Medical and Dental Sciences

The University of Birmingham

April 2019

Abstract

$CD4^+$ T cells are essential for overall control of human virus infections, yet their multiple roles remain ill-defined at the single cell level, and most studies have focused solely on analysis of those present in the circulation. Using Epstein-Barr virus (EBV)-specific human leukocyte antigen (HLA) class II tetramers, we have studied the circulating functional and clonal evolution of circulating antigen-specific $CD4^+$ T cell responses during infection and analysed the $CD4^+$ T cell response at the site of viral replication. We show that primary EBV infection, elicits an acute expansion of oligoclonal antigen-specific T helper-1 (T_H1)-like $CD4^+$ T cell populations in the blood that are armed with cytotoxic proteins and can respond immediately *ex vivo* to challenge with virus-infected B cells. Over time as the primary response contracts, we find that the resultant memory populations show (i) a marked decrease in cells expressing cytotoxic and activation markers, but (ii) increased TCR diversity as new clonotypes join those originally present, and (iii) increased cytokine polyfunctionality. Importantly, the cytotoxic $CD4^+$ T cells responding to acute primary infection differed in their transcriptional program to the classically described CD4-CTLs that accumulate during chronic viral infections. Moreover, we show that EBV infection seeds populations of tissue resident EBV-specific $CD4^+$ T cells in the tonsil. These EBV-specific T_{RM} which expresses cytotoxic proteins, are preferentially retained in the T cell zone and B cell follicles of the tonsils. These findings imply an important effector role for CD4-CTLs in acute EBV infection and at the site of EBV replication, emphasising the need to harness their potential in herpesvirus vaccine design.

Acknowledgments

I would first and foremost like to thank my supervisor Dr Heather Long for her unwavering support and patience with me over the course of my PhD. I have been extremely lucky to be supervised by someone who has always been available to give feedback and advice.

I'd also like to thank Gordon Ryan for teaching me good laboratory practice when I began my project, past and present members of the Graham Taylor and Claire Shannon-Lowe research groups for their assistance, and Richard and Sam for putting up with my colourful language in the office.

Next members of the Burrito Friday club: Nenad, Ben A, Calum, Jack and Ben P as well as the Thursday football crew for providing a welcome escape from the travails of PhD studentship.

I would also like to thank all donors who kindly donated blood and tonsil samples without which none of the experiments would have been possible.

Finally, special thanks go to my parents, Peter, and Michael for their encouragement and emotional support along the way.

Table of contents

CHAPTER 1 INTRODUCTION 1

I. Immunity 1

1. Innate Immunity 1

2. Adaptive immunity 3

3. B cell development 4

1. Maturation 4

2. Activation 4

4. T cell development 6

1. T cell receptor 6

2. Thymocyte selection 8

3. Antigen processing and presentation 9

4. Activation 15

5. $CD8^+$ T cell activation 17

5. $CD4^+$ T cells 19

1. T_H1 20

2. T_H2 22

3. T_H17 23

4. T_H9 and T_H22 24

5. Follicular helper T cells: T_{FH} 26

6. Regulatory $CD4^+$ T cells: T_{reg} 27

7. $CD4^+$ T cell plasticity 28

6. T cell memory 30

II The Epstein-Barr virus 34

1. History 34

2. Life cycle 34

1. Structure and genome 36

1. Structure 36

2. Lytic replication 36

3. Latent genes 37

2. EBV-associated diseases 40

3. Immune control of EBV 41

1. Innate Immune response to EBV 42

2. Adaptive EBV immunity 43

3. EBV vaccines 50
4. Adoptive T cell therapy 54
III $CD4^+$ T cell immunity to viruses 54
1. Cytotoxic $CD4^+$ T cells in humans: CD4-CTLs 54
1. Protective role in immunity 55
2. Chronic viral infection 56
3. Cancer 57
4. Acute Infection 57
5. Development 58
6. CD4-CTL Markers 59
7. Transcription factors 61
2. Tissue resident memory $CD4^+$ T cells: T_{RM} 62
1. Development 63
2. Phenotype 64
3. T_{RM} transcription factors 65
4. Virus-specific T_{RM} 65
5. T_{RM} in cancer 67
Project aims 68
CHAPTER 2 MATERIALS AND METHODS 69
I. Media, reagents and buffers 69
1. Tissue culture reagents 69
2. Culture media recipes 69
3. Peptides 70
4. Flow cytometry 70
II. Donors and ethics 75
1. Peripheral blood 75
2. Tonsils 75
III. Sample preparation 76
1. Isolation of Mononuclear cells 76
2. Cryopreservation 76
3. Cell Lines 76
4. T cell enrichment 77
IV. Molecular Techniques 77
1. DNA Extraction 77

2. HLA-typing by PCR 78
3. EBV VCA IFA 80
4. qPCR for EBV genome load 81
5. CMV IgG ELISA 82
V. Flow cytometry 82
1. pMHC tetramer staining 82
2. Viability and surface staining 83
3. Intracellular staining 83
VI. Cell stimulation and functional profiles 84
1. Peptide stimulation 84
2. Autologous LCL stimulation 84
VII. TCR repertoire analysis 85
1. TCR Vβ segment analysis 85
2. Quantification and characterization of TCR expression 85
VIII. Data analysis 88
1. Flow cytometry 88
2. Statistical analysis 89
CHAPTER 3 THE FUNCTIONAL ROLF OF EBV-SPECIFIC $CD4^+$T CELLS 90
1. Introduction 90
2. Results 92
a. Ex vivo functional properties of EBV-specific memory $CD4^+$ T cells 92
b. Expansion of polyfunctional EBV-specific $CD4^+$ T cells during primary infection 101
3. Discussion 109
CHAPTER 4 CYTOTOXIC PROFILE OF EBV-SPECIFIC $CD4^+$ T CELLS 112
1. Introduction 112
2. Results 114
a. EBV-specific $CD4^+$ T cells degranulate following exposure to EBV-infected B cells. . 114
b. Expression of cytotoxic proteins in EBV-specific $CD4^+$ T cells 115
c. Expression of cellular markers associated with CD4-CTLs in EBV-specific $CD4^+$ T cells 124
3. Discussion 132
CHAPTER 5 CLONAL EVOLUTION OF EBV-specific $CD4^+$ T CELLS 137
1. Introduction 137
2. Results 139
a. TCR Vβ repertoire of EBV-specific $CD4^+$ T cells over the course of infection 139

b. Evolution of the EBV-specific CD4$^+$ T cells TCR repertoire 149
3. Discussion 153
CHAPTER 6 EBV-SPECIFIC CD4$^+$ T CELLS AT THE SITE OF INFECTION 156
1. Introduction 156
2. Results 158
a. EBV-specific CD4$^+$ T cells are enriched at the site of infection 158
b. EBV-specific CD4$^+$ T cells in the tonsil display a T_{RM} phenotype 162
c. Tonsillar EBV-specific CD4$^+$ T cell subset analysis 168
d. Tonsillar EBV-specific CD4$^+$ T cells possess direct effector function and enhanced cytotoxic capacity. 174
3. Discussion 181
CHAPTER 7 FINAL DISCUSSION 187

List of Figures

Figure 1.1 MHCI and MHC-II structure

Figure 1.2 Antigen processing and presentation pathways

Figure 1.3 $CD4^+$ T_{FH} phenotypic profiles in the tonsil

Figure 1.4 $CD4^+$ T cell subsets

Figure 1.5 T cell memory phenotype

Figure 1.6 EBV life cycle

Figure 1.7 T cell responses to EBV

Figure 1.8 CD4-CTLs in chronic and acute infection

Figure 1.9 Resident memory T cells

Figure 2.1 pMHCII tetramer titration

Figure 2.2 Fluorochrome conjugated antibody titration

Figure 2.3 Gating strategy for flow cytometric analyses

Figure 3.1 EBV-$pMHCII^+$ frequencies in healthy carriers

Figure 3.2 Memory phenotype of EBV-$pMHCII^+$ cells in healthy carriers

Figure 3.3 Transcription factor expression of EBV-$pMHCII^+$ cells in healthy carriers

Figure 3.4. Cytokine production of EBV-$pMHCII^+$ $CD4^+$ T cells following peptide stimulation

Figure 3.5 Cytokine production of $CD4^+$ T cells following recognition of autologous LCL in healthy carriers

Figure 3.6 Expanded EBV-$pMHCII^+$ frequencies in acute IM

Figure 3.7 Memory phenotype of EBV-$pMHCII^+$ cells in acute IM

Figure 3.8 Transcriptional profile of EBV-specific $CD4^+$ T cells in acute IM

Figure 3.9 Cytokine production of $CD4^+$ T cells following recognition of autologous LCL in acute IM

Figure 3.10 EBV-specific $CD4^+$ T cells responding to LCL *ex vivo* are polyfunctional

Figure 4.1 Degranulation of EBV-specific $CD4^+$ T upon exposure to EBV-infected B cells

Figure 4.2 Expression of cytotoxic proteins by EBV-specific $CD8^+$ T cells

Figure 4.3 Expression of cytotoxic proteins in memory EBV-specific $CD4^+$ T cells

Figure 4.4 Expression of cytotoxic proteins in CMV and Influenza-specific $CD4^+$ T cells in healthy donors

Figure 4.5 EBV-specific $CD4^+$ T cells express cytotoxic proteins in acute IM

Figure 4.6 Expression of cytotoxic proteins in influenza-specific $CD4^+$ T cells in patients with acute IM

Figure 4.7 Expression of cytotoxic proteins in EBV-specific $CD4^+$ T cells during convalescence

Figure 4.8 Expression of cytotoxicity-associated proteins in $CD4^+$ T cells of healthy carriers

Figure 4.9 Upregulated expression of cytotoxicity-associated proteins in EBV-specific $CD4^+$ T cells in acute IM

Figure 4.10 Transcriptional profile of cytotoxic EBV-specific $CD4^+$ T cells

Figure 4.11 Expanded populations of EBV-specific $CD4^+$ T cells in acute IM are highly activated

Figure 4.12 Expression of cytotoxic protein0 and cellular activation in EBV-specific $CD4^+$ T cells

Figure 5.1 Combinatorial staining with TCR Vβ-specific antibodies and pMHCII tetramers

Figure 5.2 TCR-Vβ repertoire analysis in the total $CD4^+$ T cell pool

Figure 5.3 TCR Vβ chain representation in EBV-specific memory $CD4^+$ T cells

Figure 5.4 TCR Vβ chain representation in the EBV-specific $CD4^+$ T cells in IM

Figure 5.5 Perf/GzmB expression in Vβ defined EBV-pMHCII $CD4^+$ T cells expansions

Figure 5.6 Anti-TCR Vβ-pMHCII interference

Figure 5.7 T cell receptor analysis of EBV-specific $CD4^+$ T cells over the course of infection

Figure 6.1 Frequencies of EBV-specific $CD4^+$ T cells in PBMCs *versus* the tonsil

Figure 6.2 Frequencies of Influenza and CMV-specific $CD4^+$ T cells in PBMCs *versus* the tonsil

Figure 6.3 Memory phenotype of EBV-specific $CD4^+$ T cells in the tonsil

Figure 6.4 Resident memory phenotype of EBV-pMHCII$^+$ $CD4^+$ T cells in peripheral blood and the tonsil

Figure 6.5 Resident memory phenotype of CMV and Influenza-specific $CD4^+$ T cells in the tonsil

Figure 6.6 Expression of the T_{RM} associated transcription factor Hobit and proliferation of EBV-pMHCII$^+$ $CD4^+$ T cells in the tonsil

Figure 6.7 T_{FH} phenotype of EBV-specific $CD4^+$ T cells in the tonsil

Figure 6.8 T_{FH} phenotype of CMV and Influenza-specific $CD4^+$ T cells in the tonsil

Figure 6.9 Differential expression of cellular markers by EBV-specific $CD4^+$ T_{FH} cell subsets in the tonsil

Figure 6.10 Cytokine profile of EBV-specific $CD4^+$ T cells in the tonsil following exposure to autologous LCL

Figure 6.11 Transcription factor expression in EBV-specific $CD4^+$ T cells in the tonsil

Figure 6.12 EBV-specific $CD4^+$ T cells in the tonsil degranulate upon exposure to EBV-infected B cells

Figure 6.13 Expression of cytotoxic proteins in EBV-specific $CD4^+$ T cells in the tonsil

List of Tables

Table 2.1 pMHCI and pMHCII Tetramers

Table 2.2 Surface Antibodies

Table 2.3 Intracellular Antibodies

Table 2.4 HLA antigens typed by PCR

Table 2.5 Primers for HLA typing

Table 2.6 EBV genome load primers and probes

Table 2.7 TCR amplification primers

ABBREVIATIONS

ANKL	Aggressive natural killer leukemia
APC	Antigen presenting cell
BCR	B cell receptor
BL	Burkitt's lymphoma
CCRxx	C-C chemokine receptor type xx
CDxx	Cluster of differentiation xx
CDR	Complementarity determining regions
CLIP	Class II-associated invariant chain peptide
CLP	Common lymphoid progenitor
CMV	Cytomegalovirus
CRTAM	Class-I restricted T cell associated molecule
CTL	Cytotoxic T lymphocyte
CXCLxx	C-X-C motif chemokine xx
CXCRxx	C-X-C chemokine receptor type xx
DC	Dendritic cell
DENV	Dengue virus
DP	Double positive
E	Early
EBER	Epstein-Barr virus encoded small RNA
EBNA	EBV nuclear antigen
EBV	Epstein-Barr virus
ENKTL	Extranodal NK/T cell lymphoma
Eomes	Eomesodermin
ER	Endoplasmic reticulum
FBS	Foetal bovine serum
FoxP3	Forkhead box P3
GATA3	G-A-T-A binding protein 3

GC	Germinal centre
GM-CSF	Granulocyte-macrophage colony-stimulating factor
gp	Glycoprotein
GzmB	Granzyme B
GzmK	Granzyme K
HC	Healthy carrier
HIV	Human immunodeficiency virus
HLA	Human leukocyte antigen
Hobit	Homolog of Blimp-1
HSV	Herpes simplex virus
HuS	Human serum
IAV	Influenza A virus
IFNγ	Interferon gamma
ICOS	Inducible T cell co-stimulator
IE	Immediate early
Ii	Invariant chain
IL-xx	Interleukin xx
IM	Infectious mononucleosis
IRF3	Interferon regulatory factor 3
IS	Immunological synapse
L	Late
Lat	Latency
LCL	Lymphoblastoid cell line
LMP	Latent membrane protein
LN	Lymph node
MHC	Major histocompatibility complex
pMHC	Peptide-MHC
MIP-1α	Macrophage inflammatory protein 1 alpha

miRNA	MicroRNA
MVA	Modified vaccinia Ankara
NK	Natural killer
NKG2D	Natural killer group 2D
NPC	Nasopharyngeal carcinoma
PAMP	Pathogen-associated molecular pattern
PBS	Phosphate Buffered Saline
PCR	Polymerase chain reaction
PD-1	Programmed cell death protein 1
Perf	Perforin
PRR	Pattern recognition receptor
PTLD	Post-transplant lymphoproliferative disorder
RT	Room temperature
S1PR1	Sphingosine-1-phosphate receptor 1
SLO	Secondary lymphoid organ
STAT	Signal transducer and activator of transcription
T-bet	T-box containing protein expressed in T cells
T_{CM}	Central memory T cell
T_{EM}	Effector memory T cell
T_{EMRA}	Effector memory T cell re-expressing CD45RA
T_N	Naïve T cell TCR T cell receptor
T_{NR}^+	Naive receptor positive T cell
T_{SCM}	Stem cell memory T cell
T_{CNP}	Cytokine producing naïve T cell
T_{RM}	Resident memory T cell
TEC	Thymic epithelial cell
TF	Transcription factor
T_{FH}	Follicular helper T cell

TGF-β	Transforming growth factor beta
TIL	Tumour infiltrating lymphocyte
TLR	Toll-like receptor
TNFα	Tumour necrosis factor alpha
TREC	T cell receptor exicison circles
tT_{reg}	Thymically derived regulatory T cell
iT_{reg}	Induced regulatory T cell
VLP	Virus-like particle
VCA	Viral capsid antigen

CHAPTER 1

INTRODUCTION

Viruses are intracellular pathogens that exploit the host cell's metabolic machinery for synthesis and assembly of new viral components. In some cases, infection does not result in death of the host cell and viral DNA is maintained, producing proteins that could alter cellular functions. The innate and adaptive arms of the human immune system have evolved numerous mechanisms to identify virus infected cells in order to maintain homeostasis.

Here we will describe our investigation into the $CD4^+$ T cell response to a persistent virus over the course of infection in the periphery and site of replication.

I. Immunity

1. Innate Immunity

The innate immune system is an ancient form of host defence comprised of molecular modules that can be found in both plants and animals.

Cells of the innate immune system recognise structural and genetic components common to microbial pathogens, called pathogen-associated molecular patterns (PAMPs) through pattern-recognition receptors (PRRs). PRRs can be classified based on specificity for PAMPs and expression profiles in different cell types. Among the most well-defined families of PRRs are: Toll-like receptors (TLRs), C-type lectin receptors

(CLRs), Nucleotide-binding oligomerization (Nod) leucine-rich repeat containing receptors (NLRs) and RIG-I-like receptors (RLRs) (1, 2).

This process can be termed innate as the genes for each PRR are encoded in the germline DNA and therefore host defence using this process does not require gene rearrangement. In order to exert their function these receptors can be localised to the cell surface, as part of the plasma membrane or endosomes, or in intracellular compartments such as the cytosol or lysosomes where pathogens may be encountered. The cellular components of the innate immune system expressing PRRs are macrophages, dendritic cells, mast cells, natural killer cells, basophils, eosinophils, neutrophils and γδ T cells. Following recognition, PRRs can exert a number of different functions such as activation of proinflammatory signal pathways, opsonisation, activation of the complement pathway, phagocytosis and induction of apoptosis (2).

While the main role of the innate immune system is to provide immediate defence from microbial infections, it is also vital for establishment of the adaptive immunity. The response elicited from the innate immune system is dependent on the anatomical compartment in which recognition has taken place. Thus, the distribution of PPRs and their associated immune cells varies throughout the host according to the level of surveillance required. The link between the innate and adaptive arms of the immune response is in a large part mediated by dendritic cells. These professional antigens presenting cells (APCs) migrate to secondary lymphoid organs following recognition of foreign microbes through PRRs where they present antigen to B and T lymphocytes

resulting in activation and establishment of a broader humoral and cellular immune response (3).

2. Adaptive immunity

The adaptive immune system, or acquired immunity is a more recent adaptation of host defence against pathogenic microbes only found in jawed vertebrates. Adaptive immunity is the protection against pathogens mediated by B and T lymphocytes (4). In contrast to innate immunity, the genes encoding the B and T cell receptors are generated by gene rearrangement that occurs during development. This leads to the generation of lymphocytes carrying a hugely diverse repertoire of receptors able to recognise multiple components of pathogens. Both B and T cells develop from common lymphoid progenitors (CLPs) that originate from the foetal liver or bone marrow in adults however B cell maturation occurs in the bone marrow and spleen while T cell maturation takes place in the thymus (5).

Alongside the extensive repertoire that can be generated, the adaptive immune system is also characterised by its ability to establish long-term memory. Following exposure to a pathogen, a subset of long-lived B and T lymphocytes remain in the host which can be quickly activated upon subsequent encounter. This recall response is both quicker and more potent than the primary response and is in part possible due to their high mobility throughout the circulation (6).

Here we will describe components of the adaptive immune system with a focus on the maturation of $CD4^+$ T lymphocytes and their development into diverse functional subsets.

3. B cell development

B cells are responsible for the humoral adaptive immune response mediated by the production of antibodies. Development of B cells occurs in the bone marrow where they arise from CLPs. It is during this stage that B cells acquire antigen specificity, conferred by the B cell receptor (BCR).

1. Maturation

The BCR is composed of a membrane bound immunoglobulin and the signal transduction transmembrane protein CD79. The immunoglobulin contains the highly variable antigen binding region and is composed of two heavy chains and two light chains. The high degree of variability of immunoglobulin arises through recombination and splicing of three genetic regions and is termed V(D)J recombination. Heavy chain recombination involves joining of single D and J regions from their respective *loci* followed by the joining of a single V segment whereas light chain recombination only involves the joining of single V and J region. The resulting VDJ and VJ segments are transcribed and translated to produce heavy chain and light chain proteins which assemble to form the membrane bound IgM immunoglobulin (7). B cells that are not removed as a result of interaction between BCR and self-antigen migrate to the spleen to complete maturation. Thereafter mature B cells migrate to secondary lymphoid organs (SLO) (8).

2. Activation

The antigen-dependent phase of B cell activation occurs in SLO following encounter with cognate antigen, with or without the presence of T cells. In both instances, clustering of

BCRs in a process called cross linking is required to initiate the appropriate signalling pathways. Activation by T-independent antigens requires additional signals from dendritic cells and cytokines in the surrounding environment whereas activation by a T-dependent antigen relies on the formation of an immunological synapse (IS) with co-stimulatory molecules inducing further development. Thereafter, activated B cells differentiate into short-lived antibody secreting plasma cells (9) or long-lived memory B cells that will migrate to follicles within the secondary lymphoid organs and establish germinal centres (10). In the germinal centre memory B cells can undergo class switching which alters the functional properties of antibodies by changing the immunoglobulin isotype without modifying its antigen specificity (11). However, in a separate process called somatic hypermutation, point mutations in the variable regions of both the heavy and light chain are accumulated leading to the generation of antibodies with varying degrees of affinity to their antigen (12). Thereafter preferential selection of antibodies with higher affinity for antigen that occurs in germinal centres is known as affinity maturation.

Class-switching and affinity maturation can take up to 2 weeks during the first encounter, however following re-exposure the secondary response is much faster and memory B cells can produce high affinity antibodies within a few days (13). During this process, B cell are constantly in cell cycle and substantial turnover of cell surface immunoglobulin results in the replacement of the original BCR with newly mutated versions. Thereafter, germinal centre B cells migrate to an antigenic rich region within SLO called the light zone. B cells can interact with follicular dendritic cells in the light zone, capturing antigen that can be processed and presented on MHC-II molecules while

also receiving BCR-mediated pro-survival signals. The highest affinity GC B cells that have picked up and presented the most antigen as a pMHCII complex on the cell surface will outcompete neighboring lower affinity cells for T cell mediated survival and differentiation signals (14). It has also been proposed that B cell clones that recognize self-antigen can be selectively eliminated by regulatory T cells at this stage (15).

4. T cell development

Like B cells, T cells develop from CLPs however they mature in the thymus. Circulating progenitor cells enter the thymic parenchyma through the vasculature surrounding the cortical medullar junction (CMJ) and seeding occurs as the result of interaction between P-selectin glycoprotein 1, expressed on the surface of the progenitors, and P-selectin present on thymic epithelial cells (TECs). In the parenchyma, the Notch-1 dependent double negative stage of thymocyte development is initiated by interaction with TECs expressing Notch-1 ligands. During this stage, developing thymocytes migrate towards the subcapsular zone of the cortex and begin to assemble pre T cell receptor (TCR) complex on the cell surface (16).

1. T cell receptor

Here we will focus on αβ T cell receptors (TCR) assembly. Akin to BCRs, αβ TCRs are produced by V(D)J recombination which determines their specificity. α chains arise from sequentially spliced single V and J regions whereas β chains contain an additional D segment located between V and J segments. V(D)J recombination is mediated by the V(D)J recombinase enzymes RAG1 and RAG2. These enzymes bind to recombinase signal sequences that border individual V, D and J segments, cleaving the DNA and giving rise

to hairpin structures on each region. The endonuclease activity of the enzyme Artemis cleaves the hairpin and juxtaposed V, D and J segments are joined together in a process called non-homologous end-joining mediated by DNA repair enzymes (such as XRCC4) and Ligase IV. Within the process of DNA repair, an inherent imprecision can lead to the non-templated addition or deletion of nucleotides at the junctional boundaries between gene segments thus further increasing the potential TCR repertoire diversity. In addition to the junctional diversity, addition of several nucleotides at the junctions between V and J segments (α chain) and VD and J segments (β chain) is catalysed by the enzyme TdT (17). These sequences at junctional areas encode for one of three complementarity determining regions (CDR) which form the recognition site of the TCR. The CDR1 and CDR2 loops are non-variable germline encoded by the V and J genes however CDR3 is formed by from the V-(N)-J (α chain) and V-(N)-D-(N)-J gene junctions and therefore gives the TCR greater variability. Given the combinatorial diversity possible from 47 V segments and 61 J segment present on the human TCRα chain locus, and the 54 V, 2 D and 14 J genes contained on the TCRβ locus, junctional diversity and variability of the CDR3 region, an estimated 10^{15}-10^{20} different TCRs can be generated by V(D)J recombination (18). Following rearrangement, a gene segment encoding for a full-length TCR protein is deemed productive if during this process no stop codons were introduced. Successful formation of the pre-TCR initiates cellular proliferation and signals further development into $CD4^+$ $CD8^+$ double positive (DP) thymocytes and completion of TCR complex assembly (16).

2. Thymocyte selection

DP thymocytes expressing a productive TCR complexed with the multimeric protein CD3 interact with peptide-MHC (pMHC) complexes on the surface of cortical thymic epithelial cells (cTECs), initiating the selection process. Here, high avidity pMHC-TCR interactions trigger apoptotic signalling pathways and the deletion of thymocytes whereas low-avidity pMHC-TCR interactions trigger survival signals (positive selection). The majority of DP thymocytes do not interact with pMHC on the surface of cTEC and absence of TCR signalling results in cell death (19).

Following positive selection, DP thymocytes differentiate into $CD4^+$ or $CD8^+$ single positive (SP) thymocytes. Lineage commitment is determined by interaction of a DP thymocyte with an MHC-class I bound peptide ($CD8^+$) or an MHC-class II bound peptide ($CD4^+$). SP thymocytes then migrate to the medulla and interact with dendritic cells presenting self-antigens. These self-antigens are produced by medullary thymic epithelial cells (mTECs) expressing the protein AIRE which upregulates transcription of numerous organ-specific genes, thereby exposing developing thymocytes to a wide range of self-proteins (20). Self-reactive SP thymocytes that interact with self-antigens are eliminated (negative selection) (21). A limited number of cells that do recognise self-antigen will become thymically derived regulatory T cells (tT_{reg}, discussed later).

As a result, the TCR repertoire generated by thymocyte selection is both self-tolerant and able to recognise wide range of pathogen-derived antigens. The selection process in the medulla lasts approximately 12 days after which mature thymocytes migrate back

to the CMJ, enter the peripheral bloodstream as mature, antigen naïve T cells (T_N) that will traffic to lymph nodes (LNs).

3. Antigen processing and presentation

a. Major histocompatibility complex - MHC

The efficient processing of antigens by intracellular proteolysis and their subsequent presentation on the cell surface of APCs bound to MHC molecules underpins the T-cell mediated arm of the adaptive immune system. Antigen naïve T cells become activated upon interaction of their TCRs with the cognate peptide bound to MHC molecules on the surface of APCs. MHC molecules are proteins that capture antigens processed by the cell and display them on the cell surface for recognition by T cells. The locus encoding for MHC is the most polymorphic region in the human genome (>10000 described) thus enabling the binding of large variety of different peptides. Each MHC allomorph possesses different peptide binding properties dictated by anchor residues encode by the MHC genes. MHC molecules can be subdivided into two classes: MHC-I and MHC-II. Both molecules are comprised of a peptide-binding domain, an immunoglobulin-like domain, a transmembrane segment and a cytoplasmic tail but possess distinctive peptide binding clefts (22) (Figure 1.1).

b. MHC Class I

MHC class I molecules are made up of two chains: a polymorphic α chain encoded by HLA genes non-covalently bound to a constant β2-microglobulin subunit. The α chain can be further subdivided into three domains: the α1 and α2 domains fold to form the peptide binding groove and bind to TCRs while the α3 domain spans the plasma

membrane and interacts with the CD8 co-receptor. Conserved tyrosine residues on either side of the binding groove of MHC-I molecules form a closed pocket thereby restricting the size of bound peptides 8-10 residues (Figure 1.1).

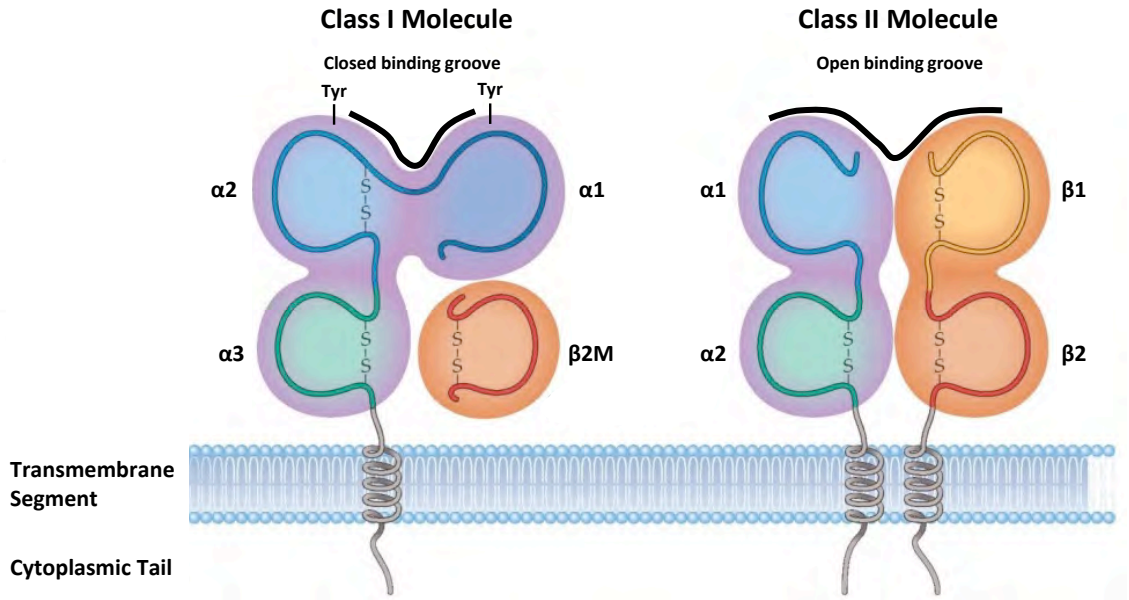

Figure 1.1 Schematic diagram of MHCI and MHC-II structure, as described in sections I.4.3.a to c. Adapted from www.microbeonline.com. Tyr (Tyrosine), β2M (Beta-2-Microglobulin).

b. MHC Class I

MHC class I molecules are made up of two chains: a polymorphic α chain encoded by HLA genes non-covalently bound to a constant β2-microglobulin subunit. The α chain can be further subdivided into three domains: the α1 and α2 domains fold to form the peptide binding groove and bind to TCRs while the α3 domain spans the plasma membrane and interacts with the CD8 co-receptor. Conserved tyrosine residues on either side of the binding groove of MHC-I molecules form a closed pocket thereby restricting the size of bound peptides 8-10 residues (Figure 1.1).

$CD8^+$ T cells will recognise peptides bound to MHC class I of which there are three classes of proteins HLA-A, HLA-B, and HLA-C; with each class exhibiting multiple alleles. Peptides presented on the surface of MHC I^+ cells are predominantly derived from endogenously expressed proteins or the end product of proteolysis of cytosolic proteins by the 26S proteasome (23). Following degradation, peptides are transported to the endoplasmic reticulum (ER) by a protein called transporter associated with antigen processing (TAP). Processed peptides delivered to the ER are generally longer than 10 amino acids and therefore require trimming by aminopeptidases before they are the optimal length for MHC-I binding. These enzymes called ERAPs cleave terminal residues to yield the 8-10 amino acid peptides preferred by MHC-I (24).

Newly translated "empty" MHC class I proteins in the endoplasmic reticulum (ER) are guided towards the TAP transporter by the molecular chaperones calreticulin and ERp57. During this process, these proteins also inhibit any unwanted antigen interaction by blocking the MHC-I binding cleft. In proximity to TAP, MHC-I will interact with a protein called tapasin resulting in the disassociation of the two chaperones, enabling high affinity peptides to bind to the peptide binding groove of MHC-I molecules (25). Thereafter, endosome-mediated transport traffics peptide-loaded MHCI to the cells surface for recognition by a T cell receptor on the surface of a $CD8^+$ T cell.

Some peptides arising from extracellular antigens that have been endocytosed by APCs can be loaded to MHC-I in a process called cross-presentation. Following the internalization of exogenous proteins by endocytic processes such as phagocytosis or pinocytosis, peptides can be degraded and bound to MHC-I through two separate

pathways. Proteins can be exported into the cystosol where they are degraded and loaded onto MHC-I in the ER as described above (the cytosolic pathway) (26-28). Alternatively, exogenous antigens can undergo lyososmal proteolysis by hydrolytic enzymes such as the peptidase Cathepsin S followed by loading onto MHC-I recycled from the cell membrane (vacuolar pathway) (29) (Figure 1.2).

c. MHC class II

MHC-II like MHC-I molecules are also heterodimers however both the α and β peptide chains that form the complex are encoded by HLA genes. Each chain is made up of 2 subunits with the α_1 and β_1 regions coming together to form the peptide binding groove while the α_2 and β_2 regions form an immunoglobulin-like domain. The open binding groove of MHC-II allows for the binding of peptides varying from 13-25 residues in length (30) (Figure 1.1).

Peptides recognised by TCRs on the surface of $CD4^+$ T cells are presented by MHC class II molecules that are encoded at three gene *loci*: HLA-DR, HLA-DQ and HLA-DP. Peptides presented by MHC class II arise from proteolytic degradation of extracellular pathogens and proteins taken up into the endosomal and lysosomal pathways through phagocytsosis or by autophagy. The decreasing pH in maturing endosomes and phagosomes containing internalized proteins creates the optimum condition for proteases to degrade antigens thereby providing a source of peptides suitable for loading onto MHC-II molecules (31). As with MHC-I molecules, MHC-II molecules are assembled within the ER however the loading of peptide does not take place in this organelle. Following dimerization of the α and β chains, MHC-II molecules are transited

to endosomes through the trans-Golgi network with the help of a signalling sequence called invariant chain I (Ii chain or CD74). Ii chains synthesized in the ER trimerize and associate with three MHC-II molecules to form a nonameric complex (three α chains, three β chains, three I chains) critical for stabilising newly generated, unstable "empty" MHC-II molecules (32). Ii chain also functions by preventing antigenic binding to the peptide-binding groove of MHC-II thereby inhibiting early peptide acquisition within the ER (33). Disassociation of the Ii chain from MHC-II within endosomes is facilitated by proteolytic enzymes although this process is incomplete, yielding the class II-associated invariant chain peptide (CLIP) that is maintained within the binding groove to prevent peptide binding (34). The release of CLIP from MHC-II is mediated by a heterodimeric protein homologous to MHC-II called HLA-DM, which is formed of similar α and β subunits but lacks the polymorphic accessible ligand binding groove. HLA-DM transits with MHCII to late endosomes where interaction with the MHC-II-CLIP complex elicits a conformational change resulting in the disassociation of the invariant chain peptide (35). This process involves another MHC-II related heterodimer, HLA-DO, which modulates the function of HLA-DM by inhibiting interaction with MHC-II and the removal of CLIP (36, 37). Following removal of CLIP, HLA-DM further modulates the functional maturation of MHC-II by promoting the binding of high affinity peptides. Similar to the role of tapasin in MHC-I peptide loading, HLA-DM interacts with MHC-II to remove any low-affinity peptides present in the antigenic-rich endosomal compartment (38) (Figure 1.2).

Unlike peptides presented on MHC-I which, due to the closed nature of the binding grove, can be described as having a central "bulge" (39, 40), peptides loaded on MHC-II

assume a “flat” structure in the MHC-II groove (41, 42), resulting in a weaker binding affinity to the TCR (43). This central binding motif consists of 9mer core containing residues that form hydrogen bonds with the MHC-II molecule (44, 45) and sequences that extend out of this core region, either at the N- and C-terminus, are referred to as peptide flanking regions (PFRs). Sequencing of eluted peptides has shown that peptides varying from 12-20 amino acids in length can be grouped together based on a common 9mer core but with variable PFRs (46, 47). These families of peptides are referred to as nested sets. There is increasing evidence to suggest that the variability observed in the PFRs can modulate T cell function (48-50) and studies analysing $CD4^+$ T cell clone activation incubated with peptides containing PFR modifications demonstrated significantly increased responses, in particular when inserting basic residues at the peptide C-terminus (51, 52). It has been suggested that exogenous peptide loaded onto MHC-II can be further trimmed before presentation on the cell surface (53, 54) and that this could vary depending on cell type (B cell, dendritic cell) (55, 56) and the cytokine environment (57). Thus, the distribution of various cell types and inflammation status at different anatomical locations (lymph node, inflamed site of infection etc.) could exert control of the PFR and accordingly, the $CD4^+$ T cell response.

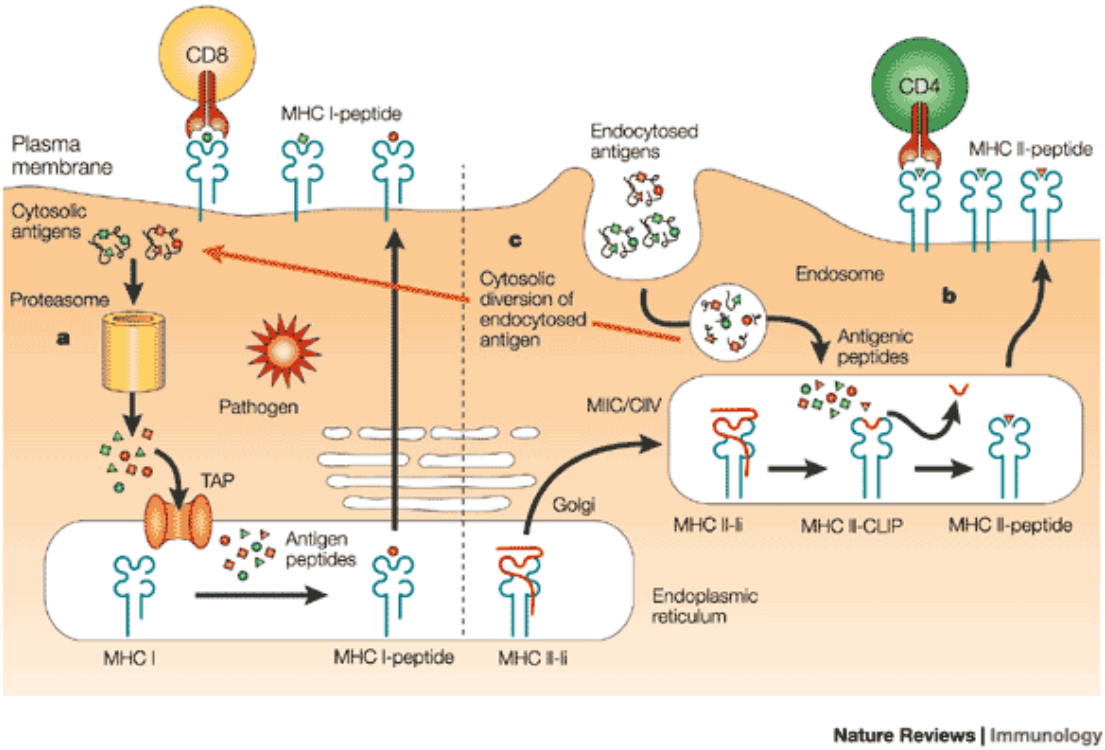

Figure 1.2 Schematic diagram of antigen processing and presentation pathways for MHC-I and MHC-II as described in sections I.4.3.b and c. TAP (transporter associated with antigen processing), MIIC (MHC-II loading compartment), CIIV (MHC-II vesicles), Ii (invariant chain), CLIP (class-II invariant-chain peptide). Taken from (58).

4. Activation

The recognition of cognate peptide complexed with MHC by a TCR leads to the recruitment of the co-receptors CD8 or CD4 that bind to non-polymorphic regions of MHC, induction of a CD3-mediated signalling cascade and formation of an IS. However signalling through the TCR alone is not sufficient for T cell activation and additional signals from co-stimulatory molecules are required. The most commonly described of the co-stimulatory molecules are the two members of the B7 family (B7.1/CD80 and B7.2/CD86) that bind to CD28 on the surface of T cells. Ligation of these molecules and subsequent signalling contributes to the increased production of IL-2 and therefore modulates T cell differentiation and proliferation (59). Other molecules present on the

surface of APCs that can trigger signalling involved in T cell activation include the inducible co-stimulatory (ICOS) ligand that binds to ICOS present on a T cell and plays an important role in the antibody response (60) (T follicular helper cells, discussed later). There are also several members of the TNF superfamily that appear to function through NF-κB signalling, delivering potent co-stimulation to the T cell itself (ligation of CD70 to CD27 on T cells) but also in a bi-directional manner where both cells receive stimulating signals (61). The CD40-CD40L and 4-1BB/4-1BBL interactions not only provide activating signals to the T cell but also to the APC, increasing their surface expression of co-stimulatory molecules and thus further T cell proliferation (62).

Signalling through TCR is initiated by the tyrosine phosphatase CD45 activating the protein tyrosine kinase Lck. Lck is bound to the intracellular domain of the CD4 and CD8 co-receptors and phosphorylates immunoreceptor tyrosine-based activation motifs (ITAMs) present on the cytoplasmic domain of each of the four CD3 subunits (γ, δ, ε and ζ). Phosphorylation of these motifs results in the recruitment and docking of the tyrosine kinase Zap70 to the ζ chains of CD3. Zap70 subsequently phosphorylates the transmembrane protein LAT (linker of activated T cells), which in turn forms a complex with the adaptor protein Gads (Grb2-related adaptor downstream of Shc) and SLP-76. This complex recruits and activates the enzyme PLC-γ1 (Phosphoplipase C, gamma 1) which catalyses the formation of diacylglycerol (DAG) and inositol 1,4,5-trisphosphate (IP_3). DAG activates protein kinase C (PKC), initiating recruitment of proteins that can activate the RAS pathway. IP_3 increases cytosolic levels of Ca^{2+} through the release of calcium stores and influx of extracellular calcium (63).

5. CD8$^+$ T cell activation

CD8$^+$ T cell activation occurs in SLOs following encounter with a dendritic cell presenting cognate peptides bound to MHCI molecules on the cell surface. Signals elicited during the interaction between pMHCI and TCR dictate the fate of the CD8$^+$T cell. Variables that influence the activation and proliferation of a naïve CD8$^+$ T cell can be broadly separated into three signals: the affinity of the TCR for the presented peptide and the duration of contact; presence of co-receptors of the surface of the dendritic cells and the cytokine environment (64). Naïve CD8$^+$ T cells that receive adequate signalling will rapidly expand to produce a clonal population of effector CD8$^+$ T cells (T_{EFF}) capable of chemokine receptor mediated migration to sites of infection. Recognition of antigen at the site of infection and formation of the pMHCI-TCR complex will trigger the release of cytotoxic effector molecules such as Perforin (Perf) and Granzyme B (GzmB) into the IS to lyse the infected cell alongside secretion of pro-inflammatory cytokines such as IFNγ, TNFα and IL-2 to promote immune cell recruitment (65).

The transcriptional activity that defines the development of memory CD8$^+$ T cells has been shown to emerge early during T cell activation in SLO (66), and distinction between the precursor effector CD8$^+$ T cells with either short or long-lived capacity can be made by the differential expression of the IL-7 receptor (CD127) and killer cell lectin-like receptor G1 (KLRG1). Effector cells with a short lifespan are characterized by low expression of CD127 and high expression of KLRG1 (67). This subset termed short-lived effector cells (SLEC) contains low levels of the pro-survival protein Bcl-2 making them susceptible to apoptosis (68). Conversely, memory precursor effector cells (MPEC) express high amounts of CD127 and low amounts of KLRG1 on the cell surface.

Furthermore, Bcl-2 expression is high and therefore this subset possesses a longer lifespan and thus an increased ability to proliferate. The fate of early activated T_N $CD8^+$ T cells is influenced by the signals received from the DC in SLO. A strong pMHCI-TCR interaction (signal 1) alongside high concentration of cytokines such as IFNγ and IL-12 promote differentiation to SLEC T_{EFF} whereas transitory TCR stimulation and presence of anti-inflammatory cytokines such as IL-10 and TGFβ will promote development of MPEC T_{EFF} (69).

Throughout activation of $CD8^+$ T cells, $CD4^+$ T cell help is essential for proliferation and the subsequent generation of a long-lived memory response following infection. Numerous studies have observed that in the absence of $CD4^+$ T cells both the primary and memory $CD8^+$ T cell responses are impaired (70-73).The most well described mechanism of CD4+ T cell help occurs through a process called dendritic cell licensing (74-77). In this model, $CD4^+$ T cells expressing CD40L activate DCs through the CD40-CD40L pathway leading to upregulated cell surface expression of co-stimulatory molecules such as B7, CD70 and 4-1BBL (reviewed in (78)) and secretion of the cytokines IL-12 and IL-15 (79, 80).

In addition to activation and licensing of DC, $CD4^+$ T cells can further enhance $CD8^+$ T cell activation through the production of IL-2 and IFNγ (81, 82). Furthermore, IL-21 secreted by $CD4^+$ T cells was shown to be required to sustain the $CD8^+$ T cell response in the context of chronic viral infection (83).

Thus, $CD4^+$ T cells play a critical direct and indirect role in promoting the cytotoxic $CD8^+$ T cell mediated arm of the immune response to pathogens however this is just one the functions carried out by this highly heterogenous population of T cells.

5. $CD4^+$ T cells

$CD4^+$ T cells are primarily described as carrying out a "helper" role in the immune system that includes but is not limited to, enhancing the development of cytotoxic $CD8^+$ T cells, promoting class switching in B cells and inducing phagocytic activity in innate immune cells. Following activation in SLOs, $CD4^+$ T cells can differentiate into a number of distinct subsets with different functional properties. This process is influenced by cytokines present during activation that regulate the transcriptional profile of the cell. The first observation that $CD4^+$ T cells could possess different functions was made in 1986 when analysis of T cell clones revealed distinct cytokine production and the T_H1/ T_H2 paradigm was proposed (84). Since then, numerous different T helper subsets have been described revealing the diverse and myriad functions that $CD4^+$ T cells carry out in immunity (85) (Fig 1.4).

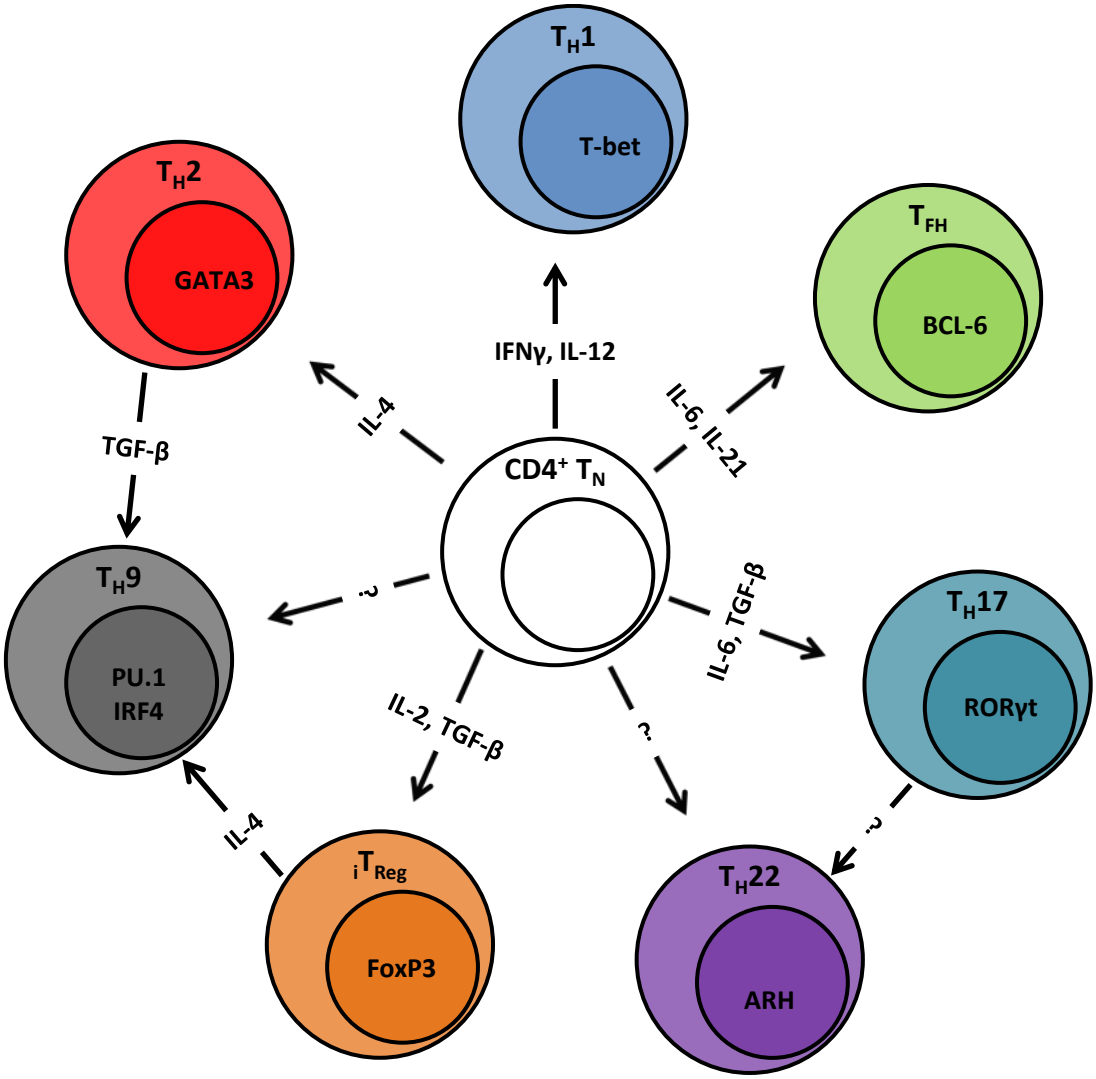

Figure 1.4 Schematic diagram of different helper and regulatory subsets, influence of cytokines in the differentiation and master transcription as described in sections I.5.1 to 6.

1. T_H1

The development of T_H1 $CD4^+$ T cells, is initiated by downstream signalling induced by IL-12 and interferon gamma IFNγ (86). IL-12 is produced by cells of the innate immune system which subsequently induces production of IFNγ by NK cells (87, 88). IL-12 and IFNγ can respectively activate the members of the signal transducer and activation of transcription STAT4 and STAT1. Expression of the master regulator for T_H1 differentiation, T-box transcription factor expressed in T cells (T-bet) is strongly

dependent on the latter (89, 90). T-bet not only promotes differentiation into a T_H1 phenotype, but also inhibits expression of transcription factors (TFs) that drive development of other T helper subsets such as T_H2 and T_H17 (89, 91). T-bet enhances T_H1 differentiation by activating genes encoding for IFNγ and the receptor for IL-12, IL-12R-β2, thereby leading to a positive feedback loop resulting in T-bet amplification. Simultaneously, T-bet suppresses development of T_H2 $CD4^+$ T cells by inhibiting the *IL4* gene and blocking the master regulator for this subset, GATA3 (92, 93). Development of T_H17 $CD4^+$ T cells is also suppressed through T-bet interaction with the RORc promoter encoding for the T_H17 master transcription factor RORγt (91).

T_H1 $CD4^+$ T cells are involved with the elimination of intracellular pathogens. This subset exerts its function by secreting IFNγ which promotes NK cell activity whilst also activating macrophages, increasing their phagocytic capability and enhancing microbial killing (94). IFNγ also modulates components of the adaptive immune system by upregulating expression of MHC class I and class II leading to increased antigen presentation and thus T cell recognition of infected cells (95, 96). Moreover, in conjunction with IL-2, IFNγ promotes development and differentiation of memory cytotoxic $CD8^+$ T cells inducing a robust secondary immune response (97, 98). Importantly, IFNγ also possesses direct anti-viral properties and has been shown to inhibit numerous steps of virus life cycles in infected cells including entry, replication and release (reviewed in (99)). Polarized T_H1 $CD4^+$ T cells also display the chemokine receptors CXCR3 and CCR5 on the surface as a part of their immune function. The corresponding chemokine ligands for these receptors are produced at inflamed sites thus enhancing recruitment of T_H1 cells to infected tissue.

CXCR3 has also been shown to enhance T_H1 cell maturation as well as block T_H2 $CD4^+$ T cell migration (100).

$CD4^+$ T cells with a T_H1-like profile expressing of the signature transcription factor T-bet and production of IFNγ can often be observed during viral infection as a result of type I interferons and IL-12 being produced by innate cells in the priming milieu (101).

2. T_H2

Differentiation of a naïve $CD4^+$ T cells towards the T_H2 subset following antigen recognition is mediated by IL-4, IL-2 and IL-6. IL-4 induced activation of STAT6 leads to upregulated expression of the T_H2 master transcription factor GATA3 which promotes differentiation (102, 103). Much like T-bet during T_H1 differentiation, GATA3 induced production of IL-4 leads to a positive feedback loop. Furthermore, IL-4 induces activation of growth factor independent-1 (Gfi-1) which has been shown to stabilize the GATA3 protein through decreased ubiquitin/proteasome-dependent degradation (104). Concurrently, GATA3 suppresses T_H1 differentiation by downregulating the IL-12 dependent STAT1 pathway (105). IL-2 plays an important role alongside IL-4 in promoting T_H2 differentiation by activating STAT5 which also binds to the *IL4* gene. Co-ordinated binding of STAT5 and GATA3 to two distinct *loci* of the *IL4* gene is required for full T_H2 differentiation (106). Concomitantly, secretion of IL-6 by APCs enhances T_H2 differentiation by upregulating NFAT-mediated IL-4 production while upregulation of suppressor of cytokine signalling-1 (SOCS-1) inhibits the STAT1-IFNγ pathway involved in T_H1 differentiation (107, 108).

The main functions of T_H2 cells are to activate eosinophils and promote defence against extracellular pathogens such as helminths, mediated by the secretion of the effector cytokines IL-4, IL-5 and IL-13. IL-4 promotes class-switching in B cells and the secretion of IgE antibodies whilst also upregulating expression of both the low and high affinity receptors for IgE on the surface of mononuclear phagocytes (109). IL-5 and IL-13 meanwhile promote the cell-mediated immunity against extracellular parasites by activating cells such as eosinophils, the principal cytotoxic effectors in anti-helminth immunity (110, 111). Additionally, T_H2 $CD4^+$ T cells express CCR4 and CCR8 promoting migration to epithelial and mucosal tissues susceptible to infection by extracellular parasites such as the skin and lungs.

3. T_H17

T_H17 development is controlled by the master transcription factor retinoic acid receptor-related orphan receptor gamma-T (RORγt). Activation of RORγt is induced by the presence of transforming growth factor beta 1 (TGF-β) IL-6, IL-21 and IL-23 during T cell activation. TGF-β does not directly promote RORγt activation but inhibits the IL-6/IL-21 induced expression of SOCS3, a negative regulator of STAT3 (112). IL-6, IL-21 and IL-23 signalling activates STAT3, inducing RORγt expression (113). RORγt in turn activates gene promoters for signature cytokines of the T_H17 lineage: IL-17A, IL-17F and IL-22. The self-amplification stage of T_H17 development is exerted by IL-21 which is also produced in abundance (114). Moreover, IL-21 in conjunction with IL-6 can induce expression of IL-23R thereby allowing differentiating T_H17 $CD4^+$ T cells to bind IL-23 and promote stabilization (115).

T_H17 $CD4^+$ T cells are involved in host defence against extracellular pathogens such as fungi and bacteria. IL-17 signals through IL-17Rα expressed on a variety of tissue including lung, skin and intestine (116). Binding of IL-17 to its receptor leads to production of pro-inflammatory cytokines as well as chemokines thereby promoting migration of immune cells to sites of inflammation (117). Expression of IL-22 receptor is restricted to cells with epithelial origin and IL-22 acts by promoting epithelial defence mechanisms to prevent pathogen or inflammatory induced tissue damage (118, 119). T_H17 $CD4^+$ T cells have also been identified during viral infections however their role remains unclear with some reports suggesting production of the effector molecule IL-17 contributes to host protection (120), with others linking it to immune pathology (121, 122).

4. T_H9 and T_H22

More recently, two new T helper subsets have been identified: T_H9 and T_H22. While research into their respective modes of differentiation is still ongoing, some pathways that initiate development have been characterised.

It was initially suggested that the development of IL-9 producing T_H9 subset was the result of TGF-β mediated reprogramming of T_H2 cells (123). However, contemporaneous experiments demonstrated that TGF-β induced T_{reg} cells could in the presence of IL-4, also become IL-9^+FoxP3^- $CD4^+$ T cells (124). More recently, in addition to the STAT6-GATA3 pathway involved in T_H2 differentiation, transcription factors required for the production of IL-9 such as PU.1 and interferon response factor 4 (IRF4) have been shown to be critical in the development of T_H9 subset (125, 126).

Supporting the association of T_H9 and T_H2 $CD4^+$ T cells, the former have been shown to be involved in type 2 immune responses and IL-9 activates an array of immune cells involved in extracellular pathogen immunity. More recently the T_H9 subset has been shown to have potent anti-tumour activity with expression of cytotoxic effectors (127, 128). Accordingly, this subset expresses chemokine receptors associated with recruitment of T_H2 adaptive immunity and mononuclear phagocytes to mucosal tissue (CCR3 and CCR6), but also those associated with recruitment of cytotoxic $CD8^+$ T cells and a type 1 immune responses (CXCR3) (129).

Akin to T_H9 $CD4^+$ T cells, the T_H22 subset was likewise originally classified as part of another subset. Production of IL-22 was detected alongside IL-17 and therefore this subset was initially thought to arise as a result of re-programming of T_H17 cells (130). Additional studies have however shown that $CD4^+$ T cells can produce IL-22 in the absence of IL-17 and more importantly do not express the T_H17 master transcription factor RORγt (131). Instead, aryl hydrocarbon receptor (ARH) has been identified as the key transcription factor with engagement leading to enhanced IL-22 production while also inhibiting IL-17 production (132, 133).

The function of T_H22 is not fully understood however this subset is thought to play an important role in epidermal immunity (134). T_H22 $CD4^+$ T cells express the skin homing chemokine receptors CCR4 and CCR10 and have been shown to be enriched in inflamed skin lesions (131, 134).

5. Follicular helper T cells: T_{FH}

The follicular helper $CD4^+$ T cell subset (T_{FH}) provides the link between humoral and cell mediated immunity by producing factors that promote B cell differentiation. T_{FH} cells are therefore predominantly localized to SLO where they facilitate T and B cell interactions. As such, rather than based on transcription factor expression or cytokine secretion, T_{FH} cells were initially described by their localization to the germinal centres (GC) of lymphoid tissue and expression of CXCR5 (135, 136). Subsequent investigations established the transcription factor Bcl-6 as the key regulator of T_{FH} differentiation (137-139). Bcl-6 antagonises expression of Blimp-1 that is present at high levels during the development of other non-T_{FH} subsets (140). Differentiation of T_N $CD4^+$T cells to the T_{FH} lineage has been shown to be promoted by long-term interaction between T cell and DC in the presence of IL-6 and IL-21 (141, 142). These cytokines signal via STAT3 promoting expression of Bcl-6 and thus repressing Blimp-1. Expression of Bcl-6 results in upregulated surface expression of CXCR5, facilitating migration of T_{FH} into B cell follicles where they interact with B cells to help form germinal centres. Within GC, T_{FH} cells promote affinity maturation through surface expression of the co-stimulatory molecules CD40L and ICOS as well as secretion of the cytokines IL-4 and IL-21.

CD57 had previously been used to identify and study T_{FH} in the germinal centre (143, 144) however, a subsequent study demonstrated that T_{FH} activity was confined to $CXCR5^{hi}$ $ICOS^{hi}$ $CD4^+$ T cells and was independent of CD57 expression (145). Using single cell analysis technology and automated clustering, Wang *et al.* identified several subsets of T_{FH} in the tonsil based on the expression of CXCR5, PD-1, ICOS and CCR7 (146). Expression of CCR7 negatively correlated with increased expression of all the other

markers and the authors suggested that downregulation of the chemokine receptor accounted for $CD4^+$ T cells entering T cell zones from the blood into B cell follicles and germinal centres (Figure 1.3).

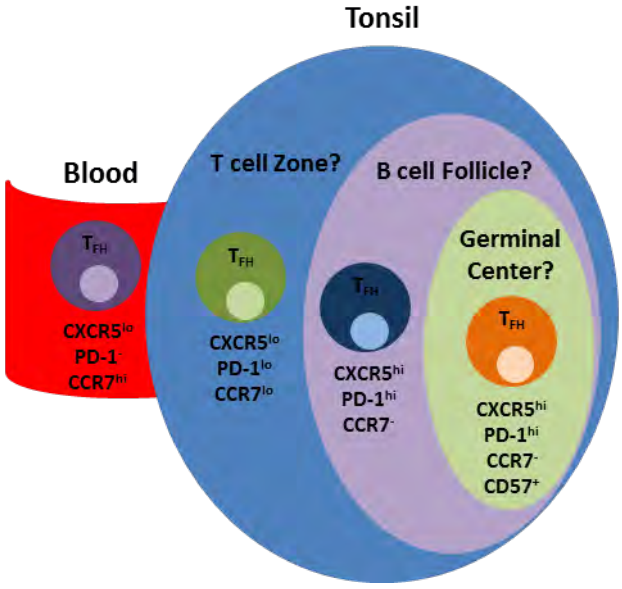

Figure 1.3 Schematic diagram of $CD4^+$ T_{FH} phenotypic profiles and migratory properties. Adapted from (146).

6. Regulatory $CD4^+$ T cells: T_{reg}

In addition to the helper subsets, $CD4^+$ T cells can also differentiate into regulatory T cells (T_{reg}) with immunomodulatory properties. Development of T_{reg} can occur from two distinct pathways. During thymocyte selection, double positive T cells that recognise self-antigen in the presence of CD28 and IL-2 can up-regulate expression of the transcription factor FoxP3. This process is called agonist selection, and $CD25^+$ $FoxP3^+$ naturally occurring regulatory T cells (nT_{Reg}) subsequently exit the thymus and migrate to lymphoid tissue. Unlike nT_{reg}, induced regulatory T cells (iT_{reg}) develop following antigen priming in the lymphoid tissue. Development of iT_{reg} is dependent on the presence of TGF-β and IL-2 during T cell activation to promote expression of the master

transcription factor FoxP3 required for full differentiation (147-149). TGF-β signals through the effectors Smad2 and Smad3 to induce expression of FoxP3, with the latter also decreasing activity of the T_H17 master transcription factor RORγt (150-152).

T_{reg} act as key mediators of immune homeostasis by suppressing excessive inflammation that can arise in the context of autoimmune diseases or an allergic response. The suppressive function of T_{reg} is carried out by a variety of different mechanisms including but not limited to:

- Constitutive expression of the high affinity IL-2 receptor (CD25) and high uptake of exogenous IL-2, thus limiting it's availability to proximate non T_{reg} , inhibiting activation and proliferation and promoting cytokine deprivation-induced apoptosis (153).
- Expression of cytotoxic T-lymphocyte antigen 4 (CTLA-4) that binds to co-stimulatory molecules CD80/86 on the surface of APCs resulting in their downregulation thereby depriving non T_{reg} of co-stimulatory signals (154, 155).
- Secretion of immuno-suppressive cytokines such as IL-10 and TGF-β that inhibit the effector functions of components of the innate and adaptive immune response (156-158).

7. $CD4^+$ T cell plasticity

The differentiation of a naïve $CD4^+$ T cell into a particular functional subset described above was previously thought to be irreversible, and the paradigm of memory $CD4^+$ T cells *in vivo* was one of lineage stability. This was despite the early observation that $CD4^+$

T cell clones could co-express cytokines associated with different subsets *in vitro* (159). However, with the advent of new research techniques studies have shown that $CD4^+$ T cells do possess the ability to modify their functional profile. This concept known as T cell plasticity can be described as the ability of a $CD4^+$ T cell to share characteristics of multiple T_H subsets sometimes losing features acquired during initial activation and converting to a different T_H subset. This capacity to change function under different polarizing conditions further enhances the degree of heterogeneity in $CD4^+$ T cell responses following activation and suggests that plasticity is beneficial for host immunity.

One of the main mediators of T cell plasticity are cytokines. The maintenance of a given T_H cell subset is dependent on individual STAT transcription factors, some of which can perform differing roles in naïve $CD4^+$ T cell differentiation dependant on the cytokines present during activation. Therefore, altered cytokine signals are able to modify the activation of transcription factors involved in $CD4^+$ T helper subset maintenance. Early studies showed that murine T_H1 $CD4^+$ T cells can be re-polarized towards the T_H2 subset *in vivo* following helminth infection, switching from production of IFNγ to IL-4 (160). Similarly, induction of STAT4 by IL-12 can result in T_H17 $CD4^+$ T cells losing expression of RORγt and converting to T_H1 cells (120). Moreover, incubation of T_H2 $CD4^+$ T cells in the presence of the T_H1 polarizing cytokines IFNγ and IL-12 also results in a change to T_H1-like profile (161). Strikingly, studies in mice have shown that T_{FH} cells cultured in IL-12, IL-4 or a combination of IL-6 and TGFβ can be induced to make the cytokines associated with T_H1, T_H2 and T_H17 subsets respectively. Moreover, $CD4^+$ displaying the phenotype of these same subsets can acquire the characteristics of T_{FH} following culture with IL-21

and IL-6 (162). In humans, combined analysis of TCR sequencing and T cell function has demonstrated a high degree of variability in the functional profile of $CD4^+$ T cells generated from the same single cell (163, 164).

There is also clear evidence that thymically derived regulatory $CD4^+$ T cells expressing FoxP3 can adapt to different types of inflammatory responses. In the context of type 1 inflammation, IFNγ-induced expression of the T_H1 master transcription factor T-bet has been observed in T_{reg} cells alongside autologous IFNγ production and surface expression of CXCR3 (165). This subset of T_{reg} cells with distinct T_H1-like properties was critical in controlling the proliferation of T_H1 $CD4^+$ T cells. Likewise, control of T_H2-like inflammatory responses was carried out by T_{reg} cells expressing the transcription factor IRF4, selectively dysregulating the IL-4 mediated immunoglobulin and cellular responses (166).

6. T cell memory

One of the hallmarks of the adaptive immune system is the ability to generate a long-lasting protective response to pathogens through the maintenance of a self-renewing, antigen-experienced, memory T cell population. Accordingly, the frequency of memory T cells increases throughout life with the exposure to multiple pathogens and encounter of a variety of antigens. At birth, memory T cells are absent from the circulation, however their frequency increases rapidly within the first decade, accounting for up to 35% of circulating T cells by the age of 20 (167) and the gradual increase in memory T cell frequency over time coincides with a reduced susceptibility to infectious diseases.

The rapid acquisition of memory T cells early in life is followed by continued exposure to new antigens during adulthood and maintenance of memory T cells. Over time, the age-associated accumulated exposure to antigens, reduction in T cell function and decrease in naïve T cell maintenance is referred to as immunosenescence. Despite the frequency of memory T cells remaining stable, chronic antigen exposure induce clonal exhaustion and T cell replicative senescence. Thus, memory T cells in older individuals possess decreased ability to response to infectious agents and a higher susceptibility to pathogens (168).

Analysis of memory T cells in the laboratory was first made possible following the discovery that CD45RO was ubiquitously expressed on antigen-experienced cells whereas the CD45RA isoform was largely absent (169, 170). Subsequent investigations have revealed memory T cells to be a heterogeneous population with differing functional capacities. The seminal work performed by Sallusto, Lanzavecchia *et al.* classified naïve and memory T cells based on their expression of CD45RO/RA and the chemokine receptor CCR7 (171). Homing and entry of blood-borne naïve T cells to SLO is mediated by expression of CCR7 and CD62L however following activation by DCs, the authors showed that $CD45RA^{-}CD45RO^{+}$ memory T cells displayed different effector functions based on their expression of CCR7. Memory T cells expressing CCR7, termed central memory (T_{CM}), home to SLO where they can assist with the generation of new effector cells by stimulating DCs and helping B cells whereas memory T cells lacking CCR7, termed effector memory (T_{EM}), enter peripheral tissues thereby promoting an inflammatory response and containing invading pathogens.

Furthermore T_{EM} displayed increased production of cytotoxic proteins and effector cytokines following stimulation compared to T_{CM}. Later studies have since demonstrated that T_{CM} are not functionally anergic and could produce inflammatory cytokines akin to T_{EM} (172, 173) as well as showing an increased ability to proliferate (174). Lanzavecchia *et al.* also identified a population of $CCR7^-$ T cells re-expressing CD45RA with a prominent expression of the cytotoxic protein Perforin. This population was subsequently termed effector memory re-expressing CD45RA (T_{EMRA}) and their accumulation in the $CD4^+$ compartment is associated with chronic viral infections (175-177).

Thus, based on the expression of CD45RA and CCR7, T cells can be classified into four memory phenotypes: $CD45RA^+$ $CCR7^+$ naïve (T_N), $CD45RA^-$ $CCR7^+$ central memory (T_{CM}), $CD45RA^-$ $CCR7^-$ effector memory (T_{EM}) and terminally differentiated re-expressing CD45RA (T_{EMRA}) (Figure 1.5).

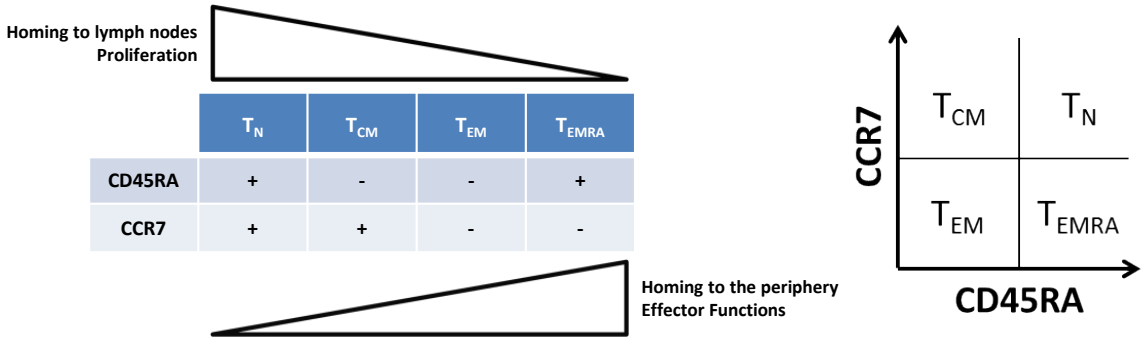

Figure 1.5 Diagram of differential expression of CD45RA and CCR7, migration, proliferation and effector functions in naïve (T_N) , central (T_{CM}), effector (T_{EM}) and terminally differentiated (T_{EMRA}) memory T cells.

More recently, studies have highlighted atypical memory $CD4^+$ T cells displaying a naïve like phenotype. A $CD4^+$ T cell population with cytokine production and chemokine expression associated with T_H1 and T_H2 subsets in the absence of memory cell markers was reported by Song *et al* (178). The number of T cell receptor excision circles (TREC)

was lower compared to the T_N population indicating they had undergone homeostatic division and the authors termed this subset "Naïve Receptor$^+$" CD4$^+$ T cells (T_{NR}^+). Gattinoni *et al.* described a novel population of CD4$^+$ T cells specific for viral and self-tumour antigens displaying a naïve-like CD45RO$^-$ CD45RA$^+$ CCR7$^+$ phenotype while also expressing migratory markers typical of memory cells (179). This population termed "Stem Cell Memory CD4$^+$ T cells (T_{SCM}) has subsequently been shown to have a restricted TCR repertoire (180, 181) with a higher capacity to proliferate upon antigen re-exposure compared to conventional memory subsets and maintained throughout the human lifespan. Importantly, a population of long-lasting *Mycobacterium tuberculosis (M. tb)*-specific CD4$^+$ T cells displaying a T_{SCM} phenotype identified by Mpande *et al.* was shown to be long-lasting and endowed with effector functions in infected individuals (182). A similar population designated "Cytokine-Producing" Naïve CD4$^+$ T cells (T_{CNP}) were found to be increased during active *M. tb* infection compared to latency indicating a role in controlling the disease (183). Identification of T_{SCM} and T_{CNP} CD4$^+$ T cell populations are reminiscent of reports describing CD8$^+$ T cells with similar characteristics following yellow fever vaccination (184) and West Nile virus infection (185).

II The Epstein-Barr virus

1. History

The Epstein-Barr virus (EBV) was discovered in 1964 when virus particles were observed in the cultured cells of patients suffering from the endemic variant of Burkitt's Lymphoma (BL) (186). The unusual geographic distribution of this malignancy, which matched that of holoendemic malaria, had indicated a viral aetiology; however EBV was soon found to be widespread in all human populations. Nevertheless, the association between EBV and BL proved consistent and the first human oncogenic virus discovered.

2. Life cycle

EBV is an orally transmitted γ-herpesvirus that predominantly infects B lymphocytes through the binding of the envelope glycoproteins gp350 and gp42 to the surface receptor CD21 and human leukocyte antigen class II molecules respectively (187, 188). The virus is also able to infect epithelial cells although this process is much less efficient, and the mechanism of entry is still relatively poorly understood although the involvement of several integrins has been suggested (189). Orally transmitted virus establishes a lytic infection of permissive cells (epithelium and possibly local B cells) within the oropharynx, establishing primary replication *foci* and, leading to high levels of virus shedding in the throat. Thereafter the virus initiates growth-transforming infection of B cells many of which will be removed by the developing T cell response to the virus however some are able to escape immune recognition by downregulating expression of viral proteins and therefore antigen presentation of viral epitopes. This

pool of latently infected, antigen-negative memory B cells continually re-circulate between the oropharyngeal lymphoid tissue and blood with periodic reactivation of the lytic cycle in the latter, producing new virions. These virus particles can initiate new *foci* of replication in epithelial cells or local infiltrating B cells resulting in low level shedding into the oropharynx or initiate new growth transforming infection in local B cells thereby replenishing the EBV-infected B cell reservoir (190).

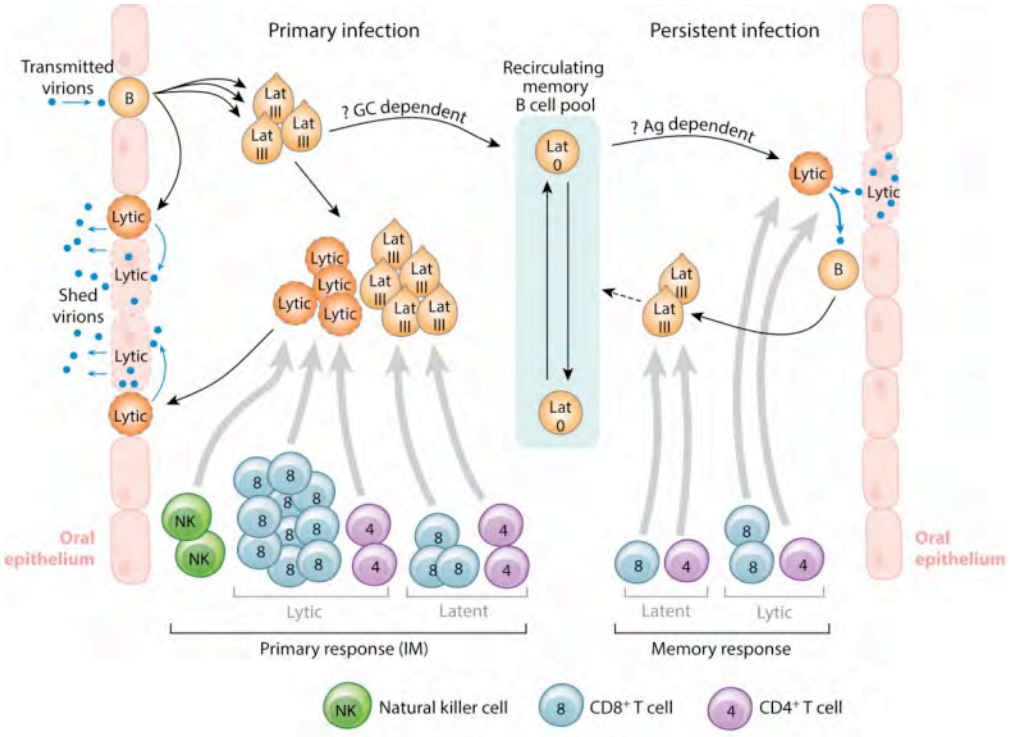

Figure 1.6 Schematic diagram of EBV infection and persistence in immunocompetent individuals as described in section II.2. GC (germinal centre), Ag (antigen), Lat III (latency III), Lat 0 (latency 0), IM (infectious mononucleosis. Taken from (190).

1. Structure and genome

1. Structure

As with other members of the herpesvirus family, EBV is composed of a large, double stranded linear DNA genome. The sequence is approximately 184 kilobase pairs in length and encodes for around 80 proteins. The genetic material is encased in a protein nucleocapsid, which itself is surrounded by viral tegument. The envelope is comprised of both lipids and glycoproteins, essential for infection of target cells (191).

2. Lytic replication

The series of events that lead to the release of EBV virions by an infected cell can be broadly split into three phases of virus gene expression: immediate early (IE), early (E) and late (L).

Following induction of the lytic cycle, two IE genes BZLF1 and BRLF1 are expressed simultaneously functioning as transcription factors and activating the transcription of the E genes (192). These E viral genes encode for proteins involved in viral replication including a DNA polymerase (193). In addition to genes involved in nucleotide metabolism, two bcl-2 homologues are also expressed at this stage. BHRF1 enhances an infected B cell's resistance to apoptosis (194) while BALF1 acts as an antagonist of the cell survival function of BHRF1 (195). L viral genes are transcribed after viral DNA replication and encode the glycoproteins required for binding of the virus to B cells complexes and epithelial cells as well as virus assembly. Genes encoding for structural proteins such as viral capsids and components of the tegument into which viral DNA is packaged are also expressed in the L phase prior to release (191).

As EBV progresses through lytic replication, multiple immune evasion proteins are expressed to avoid recognition by T cells. The E genes BGLF5 and BNLF2a and the L genes BILF1, BDLF3 and BCRF1 encode for proteins that interfere with the MHC-I antigen presentation (196-201) while the EBV proteins BZLF1 (IE), BGLF5 and the glycoprotein gp42 (L) have been shown to target processing and presentation through the MHC class II pathway (199, 202-204). In addition, the product of the E gene BaRF1 has been shown to modulate the immune response to EBV by impairing macrophage differentiation and cytokine release from mononuclear cells (205, 206).

3. Latent genes

In newly infected B cells, the virus initiates a growth-transforming programme known as latency III. At this time the EBV latent proteins involved in B cell transformation are expressed:

- EBV nuclear antigens: EBNA1,EBNA2, EBNA 3A, 3B, 3C and EBNALP
- Latent membrane proteins: LMP1,LMP2A and LMP2B
- Small, non-coding RNAs: *EBER1* and *EBER2*

This is in contrast to circulating EBV-infected B cells which are classified as latency 0, and do not express any EBV antigens (207).

In vitro EBV-transformed B cells display a latency III expression profile with some cells spontaneously entering the lytic cycle which has enabled researchers to investigate the role played by individual proteins in viral replication, maintenance and immunogenicity to the T cell system.

a. EBV-encoded nuclear antigens - EBNA

The EBV encoded nuclear antigens are proteins that localize to the nucleus and can influence both cellular and viral transcription. EBNA1 is a DNA binding protein that is crucial for the maintenance and replication of the viral genome by tagging the viral episome to chromosomes thereby assuring its maintenance following cell division. EBNA1 is expressed in all EBV infected cells and binds to the plasmid origin of replication OriP and to the viral promoters of the EBNAs (including EBNA1) and LMP1, thereby regulating transcription (191). EBNA2 is crucial to the transformation process as it is the main transactivator for the key viral genes *LMP1* and *LMP2A* and interacting with the DNA-binding protein RBP-Jκ which is involved in cell fate determination (208, 209). Furthermore, interaction between EBNA2 and EBNA-LP is required for the efficient outgrowth of EBV-transformed B cells *in vitro* (210, 211). The EBNA3 family of proteins have been shown to modulate the latter, repressing transactivation (212, 213). Additionally, EBNA3A and EBNA3C are required for B cell transformation *in vitro*, however EBNA3B is not essential (214).

b. Latent membrane proteins - LMP

LMPs are membrane proteins capable of activating intracellular signalling pathways. LMP1 is the main transforming protein of EBV and is essential for complete transformation of B cells, acting as a classic oncogene by hijacking multiple cellular pathways to regulate its expression (215, 216). Functionally, the protein resembles CD40, signalling in a ligand independent manner through the NFκB, p38 and JNK pathways to provide growth and differentiation signals to infected B cells (217).

Additionally, LMP1 expression induces activation of genes encoding for anti-apoptotic proteins and immunomodulatory cytokines such as IL-6 and IL-10 (218-220).

The gene encoding for LMP2 can produce 2 distinct proteins: LMP2A and LMP2B. These viral proteins are not required for full transformation of EBV-infected B cells however, LMP2A mimics an activated B cell receptor thereby promoting B cell survival and proliferation in the absence of B-cell receptor signalling (221). In addition, LMP2A induced expression of genes involved in immunity and the inhibition of apoptosis (222). LMP2B does not contain a cytoplasmic region and its function is poorly understood although a modulatory role in regulating LMP2A has been suggested (221).

c. Non-coding RNAs

In addition to genes encoding for proteins, the EBV genome also encodes for two families of non-coding RNA transcripts: Epstein-Barr virus (EBV)-encoded small non-polyadenylated RNAs (EBERs) and microRNAs (miRNAs).

EBER1 and EBER 2 do not play a role in the EBV induced transformation of B cells but are expressed throughout the life cycle in all EBV-infected cells and are critical for maintaining latency in infected cells and have been implicated in immune evasion (223-225).

To date, 44 EBV encoded miRNAs targeting both viral and cellular RNAs have been identified with many studies describing immunomodulatory functions (226). The mechanisms employed by miRNAs to inhibit immune recognition of EBV-infected cells are diverse and include: reduced expression of the NK cell ligand MICB (227) suppression of the T cell attracting chemokine CXCL11 (228), suppression of the proinflammatory

cytokine IL-12, interference with MHCI and MHCII antigen processing and presentation and repressed differentiation of $CD4^+$ T cells to the T_H1 subset (229, 230). Importantly, a recent study using mice with a reconstituted human immune system demonstrated that infection with miRNA-deficient EBV resulted in lower viral titers and a decreased expansion of EBV-specific $CD8^+$ T cells further highlighting the *in vivo* relevance of miRNAs (231).

2. EBV-associated diseases

EBV is carried asymptomatically in the majority of individuals however the global disease burden following EBV infection is considerable, accounting for 200 000 new cases of cancer annually (207) and being linked to several autoimmune diseases such as multiple sclerosis (232-234). In 2010 it was estimated that EBV-associated B cell lymphomas and carcinomas accounted for approximately 1.8% of worldwide cancer deaths (235).

EBV is present in 100% of “endemic” cases of Burkitt’s lymphoma and the virus is known to be associated with a number of B-cell lymphomas including Hodgkin’s lymphoma and post-transplant lymphoproliferative disorder – PTLD. Lymphoproliferative disorders caused by EBV are predominantly observed in patients with acquired or congenital immunodeficiencies where impaired T-cell immunity is no longer capable of limiting the proliferation of EBV-infected B cells (236, 237). Furthermore, EBV infection is associated with epithelial carcinomas (nasopharyngeal carcinoma - NPC, gastric carcinoma) and T and NK cell lymphomas (extranodal NK/T cell lymphoma – ENKTL, aggressive NK leukaemia - ANKL).

While EBV infection is essential to the pathogenesis of some cancers (ENKTL), the influence of the virus in others is less clear. This disparity can be explained by the different cell types infected by EBV, the latency programme activated and the varying contributions of common cellular mutations such as c-myc translocation in BL (238). Expression of latent gene transcripts is not consistent throughout EBV-associated malignancies and individual cancers can be distinguished by latency profiles.

The latency I (Lat I) program characteristic of Burkitt's lymphoma only expresses a single latent protein, EBNA1 (239). A latency II (Lat II) expression profile is commonly observed in Hodgkin's lymphoma, NPC and T and NK cell lymphomas where in addition to EBNA1, all three proteins in the LMP family are expressed (LMP1, LMP2A and LMP2B) (240). A latency III (Lat III) profile is commonly observed in B-cell lymphomas that arise in immunocompromised hosts such as PTLD (241). Here, the full complement of six EBNA and three LMP proteins are expressed as is the case in *in vitro* cultured EBV-infected lymphoblastoid cell lines (LCLs) (242).

3. Immune control of EBV

Following acquisition, EBV is carried for life in the memory B cell pool under control of the immune system. In heathy individuals, the immune response maintains lifelong control resulting in a mutual co-existence. Gaining a broader understanding of the immune cell functional profiles that mediate this continued immune surveillance could help inform both prophylactic and therapeutic treatment for EBV-associated diseases.

Primary EBV infection is asymptomatic in most people but can in some cases be identified through the manifestation of IM. Analysing the evolution of the T cell response to EBV in the early stages of acute infection compared to healthy, long-term carriers represents a useful system with which to study the evolution of immunity to a human oncogenic virus.

1. Innate Immune response to EBV

Initiation of the immune response to EBV infection occurs following the sensing of molecules expressed by the virus such as unmethylated dsDNA and EBERs by Toll-like receptors expressed on the surface of dendritic cells, monocytes and macrophages (243-247). Activation of these innate cells leads to the secretion of cytokines to promote immune cell recruitment (243, 248). In particular, activation of DCs following recognition of EBV PAMPs results in IFNα/β and IL-12 mediated recruitment of NK cells (249).

Expanded populations of NK cells during the early stages of EBV infections have been reported in multiple studies (250-253). However disparate findings between cohorts of IM patients have suggested the innate immune response to EBV mediated by NK cells can either play a role in protection against EBV infection or contribute to disease severity (251, 253). In paediatric IM, the expanded NK cell population expressed markers associated with an early-differentiated phenotype and preferentially degranulated upon exposure to EBV-infected B cells with lytic reactivation (254). Interestingly, frequency of these early differentiated NK cells diminishes with age and the authors proposed that decreased frequencies in adolescents and young adults results in an diminished NK-cell-mediated killing of EBV-infected B cell undergoing lytic replication and therefore an

increased risk of developing IM. In support of this notion, using an immunodeficient NOD-*scid* $_{\gamma c}^{-/-}$ mouse transplanted with $CD34^+$ human hematopoietic progenitor cells that reconstitutes a human immune system, Chijoke *et al.* demonstrated that depletion of NK cells prior to infection with EBV resulted in the development of IM symptoms and promoted EBV-associated tumorigenesis (255). This study also showed that infection with a modified BZLF1 knockout EBV virus, that only establishes a latent program, did not induce an expansion of NK cells, thereby indicating that NK cells exert a limited protective role to latent infections *in vivo*.

2. Adaptive EBV immunity

A robust T cell response is paramount to long-term control of EBV infection and reactivation as highlighted by development of EBV-related lymphoproliferative diseases in individuals with impaired T cell development or function (256, 257).

Studies using pMHCI and pMHCII tetramers have shown EBV elicits a robust T cell response against an array of antigens during primary infection which, while reduced in frequency, is partially maintained into long term-carriage (258, 259).

a. EBV-specific T cell response during primary infection

High numbers of atypical lymphocytes are observed in the peripheral blood of IM patients and further analysis showed that this lymphocytosis was characterised by expanded populations of oligoclonal EBV-specific $CD8^+$ T cells (260). The vast majority of the expanded $CD8^+$ T cells in IM are directed against EBV lytic cycle derived epitopes, in particular those derived from immediate early proteins, with smaller frequencies observed for early proteins and a subdominant response to late antigens (258, 261-263).

Expansions of $CD8^+$ T cells directed against the latent proteins EBNA3A, 3B and 3C and LMP2 are also detectable during EBV primary infection however these are lower in magnitude compared to lytic cycle protein-specific $CD8^+$ T cell responses (258, 264). Phenotypical analysis has shown that during IM, EBV-specific $CD8^+$ T cells are highly activated and proliferating with high expression of HLA-DR, CD38 and Ki-67 (264, 265). Additionally, these cells were positive for CD45RO isoform and negative for the lymphoid homing marker CCR7 or CD62L, consistent with an effector phenotype (258, 264).

Studies of T cell responses during asymptomatic primary EBV infection have been more challenging due to the complication in identifying individuals. However, two separate studies were able to identify young children and adults with a serological pattern consistent with primary EBV infection (anti-VCA IgM antibodies) but that did not develop symptoms of IM. These donors had high viral loads in the blood and expanded EBV-specific $CD8^+$ T cells against immunodominant epitopes, akin to IM patients, but no marked increase in the total number of $CD8^+$ T cells (266, 267). Similarly, a recent prospective study of young adults detected high viral loads in individuals undergoing silent infection and expansion of EBV epitope-specific $CD8^+$ T cell populations but without noticeable change to the total $CD8^+$ T cell pool (268).

Early studies investigating the $CD4^+$ T cell response to EBV during IM relied on measuring cytokine secretion following stimulation with EBV infected B cell lysate or EBV-derived T cell epitopes. While not reaching the magnitude of their CD8 counterparts, expanded populations of EBV-specific $CD4^+$ T cells were detected during IM (262, 269, 270) without

an increase in the total number of $CD4^+$ T cells (253). These assays suggested that, as with EBV-specific $CD8^+$ T cells, a slight bias towards lytic antigen specificities existed however they did not assess responses to all latent proteins. Moreover, these results may have been biased by high concentrations of lytic proteins in virus lysate. A greater knowledge of EBV-derived $CD4^+$ T cell epitopes and the advent of MHCII tetramer technology have enabled researchers to study $CD4^+$ T cells directly *ex vivo* thereby gaining a more accurate representation of the immune response to EBV in the circulation. Using this more sensitive technique it was shown that responses to individual $CD4^+$ T cells during IM could account for as much as 1.5% of the total $CD4^+$ T cell pool revealing a previously underappreciated expansion of EBV-specific $CD4^+$ T cells (259). This study also demonstrated that, in contrast to the coincident $CD8^+$ T cell response, the $CD4^+$ T cell responses to latent proteins outnumbered the lytic epitope-specific responses. Similar to EBV-specific $CD8^+$ T cells, the expanded populations of EBV-specific $CD4^+$ T cells in acute primary infection have an activated phenotype expressing CD38 and display an $CD45RO^+$ $CCR7^-$ $CD62L^-$ effector phenotype (259). Although frequencies of individual epitope-specific $CD4^+$ T cells in IM are not expanded to similar magnitudes as EBV-specific $CD8^+$ T cell populations, the latter targets a much broader range of epitopes with a less clear immunodominance hierarchy. Overall the cumulative response of activated $CD4^+$ T cells in primary infection is sufficient to raise the activation status of the total $CD4^+$ T cell population (259).

In addition to a highly activated phenotype, increased levels of Perforin have been observed in the total $CD4^+$ T cell pool of IM patients (271). To date no studies have investigated whether the expression of this cytotoxic protein is present in EBV-specific

$CD4^+$ T cells. Identifying cytotoxic $CD4^+$ T cells specific for the virus that can recognise and lyse MHC-II expressing infected B cells could reveal a hitherto underappreciated role for $CD4^+$ T cell in IM.

b. EBV-specific T cell responses during persistent infection

Concurrent with the resolution of IM and the associated lymphocytosis, frequencies of EBV-specific $CD8^+$ T cells diminish to levels seen in long-term carriers. In healthy EBV carriers, individual lytic and latent antigen specific populations are maintained at frequencies of up to 2.0% and 0.5% of the total $CD8^+$ pool respectively. The $CD8^+$ T cell memory response to EBV broadly displays a similar immunodominance towards lytic proteins as observed in IM with the IE > E > L hierarchy maintained (258, 262-264). Responses to latent epitopes tend to be focused on the EBNA3 family of proteins however dominant responses against other latent antigens have been observed in individuals with less common HLA types (272). EBV-specific $CD8^+$ T cells in persistently infected individuals are resting, not actively proliferating ($Ki67^-$) with a greater tendency to express the lymphoid homing marker CCR7 (258, 264). Long-term studies have further shown that cytokine production, cytotoxicity and TCR repertoire is stably maintained over many years (273, 274).

In contrast EBV-specific $CD4^+$ T cells are present at much lower frequencies in the circulation of long-term carriers (269, 275-277). HLAII tetramer analysis demonstrated that individual epitope-specific populations account for less than 0.1% of the total $CD4^+$ T cell pool (259). Nonetheless the extensive range of epitopes recognised by EBV-specific $CD4^+$ T cells observed in IM patients is maintained in persistent infection, and latent

specificities continue to outnumber their lytic counterparts in magnitude (259, 276-278). In further contrast to EBV-specific $CD8^+$ T cells, $CD4^+$ T cells targeting lytic proteins in healthy seropositive carriers are not skewed towards the immediate early antigens but are equally distributed across IE, E and L antigens (277, 279). During latent infection circulating EBV-specific $CD4^+$ T cells do not express the activation marker CD38 and are split between resting central or effector memory phenotypes with low frequencies expressing a naïve-like phenotype (259).

Concurrent with the decrease in EBV-specific $CD4^+$ T cells in persistent carriage compared to acute primary infection, several longitudinal studies have observed an analogous drop in responding $CD4^+$ T cells (269, 270, 280). However, these studies investigating the function of EBV-specific $CD4^+$ T cells have to date often been limited to analysis of single cytokine expression following stimulation with overlapping peptide pools or EBV cell lysate. Moreover, as $CD4^+$ T cell responses are not as readily detectable as the EBV-specific $CD8^+$ populations, functional investigations have often relied on the analysis of *in vitro* expanded $CD4^+$ T cell clones or cultures.

Early studies showed that during acute IM, EBV-specific $CD4^+$ T cells within PBMCs could respond to EBV cell lysate and overlapping peptide pools by secreting IFNγ (269, 270). Recently Lam *et al.* further expanded on this work, demonstrating the presence of polyfunctional EBV-specific $CD4^+$ T cells in Chinese children with IM (280). Similarly, in healthy donors, detection of IFNγ secretion has been used in both *ex vivo* studies of EBV-specific $CD4^+$ T cells (270, 275, 279, 280) and also to confirm specificity of *in vitro* cultured $CD4^+$ T cell lines clones (278, 281-283). Production of GM-CSF (279), IL-4 (282)

and IL-10 (284) has also been observed from cultured EBV-specific $CD4^+$ T cell lines following stimulation. Additionally, two separate studies using EBV lysate and overlapping peptide pools have demonstrated that responding EBV-specific $CD4^+$ T cell in healthy carriers are polyfunctional, producing IFNγ, TNFα, IL-2, IL-6 and MIP1α (285, 286).

In contrast to primary infection and other persistent infections such as CMV, there have been no *ex vivo* reports of EBV-specific $CD4^+$ T cells expressing cytotoxic proteins in long-term carriers. Multiple groups have nonetheless demonstrated MHCII restricted killing of EBV infected B cells by *in vitro* cultured $CD4^+$ T cell lines or clones (277, 278, 281, 287, 288). The majority of these studies showed that killing was Perforin-mediated however one group identified the cytotoxic mechanism as being Fas/FasL mediated (289).

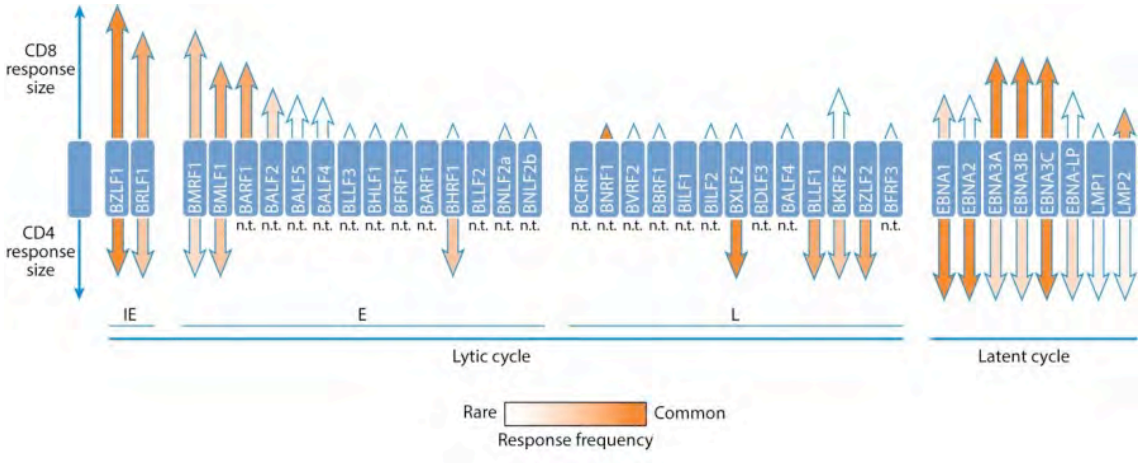

Figure 1.7 Schematic diagram of lytic and latent antigen choice for $CD8^+$ and $CD4^+$ T cell responses as described in sections II.5.2. and b. IE (immediate early), E (early), L (late). Taken from (190).

The critical role played by $CD4^+$ T cells in controlling EBV infection is further highlighted in HIV-infected individuals where $CD4^+$ T cell immunity is severely impaired. Indeed, in HIV-immunocompromised patients, EBV driven B cell lymphoproliferative diseases are

a significant cause of mortality (290, 291). Overall EBV infection has been linked to AIDS-related lymphomas in 40 to 90 % of all cases (292). Accordingly, 80-100% of Hodgkin's lymphoma in HIV-infected persons (293, 294) express EBV proteins while the pathologic subtypes of Burkitt's lymphoma and diffuse large B cell lymphoma commonly occurring in HIV seropositive donors are associated with EBV. Additionally, incidences of primary CNS lymphoma are over 1000 times greater compared to HIV uninfected individuals (295). Thus, the absence of functionally important EBV-specific $CD4^+$ T cells due to HIV infection can result in the uncontrolled proliferation of malignant infected B cells.

c. EBV-specific T cell responses at the site of infection

The tonsil is the main target site for EBV and during primary infection viral replication in the oropharynx is high (296). In some rare cases, IM-induced tonsillar inflammation requires surgery to relieve airway obstruction. Analysis of the mononuclear cells isolated from IM tonsils revealed that $CD8^+$ and $CD4^+$ EBV-specific T cells were present at lower frequencies compared to matched peripheral blood (259, 297). The decreased frequency of EBV-specific T cells in the tonsil is coincident with low expression of the lymphoid homing marker CCR7 during primary infection. Hislop *et al.* also analysed expression of the integrin CD103 to study the ability of EBV-specific $CD8^+$ T cells to bind to tonsillar epithelium that express its ligand, E-cadherin. Infiltrating EBV-specific $CD8^+$ T cell did not express CD103 thus indicating that during primary infection they are not engaging with tissue at the site of virus replication (297).

Interestingly, analysis of EBV-specific $CD8^+$ T cells isolated from tonsils removed from long-term virus carriers due to chronic tonsillitis unrelated to EBV, revealed a 2-5 fold

enrichment of lytic epitope reactivities and, remarkably, a 10-20 enrichment of latent epitope reactivities compared to the periphery (297). Moreover, these EBV-specific $CD8^+$ T cells expressed significant levels of CD103 implying active retention in the tonsil to rapidly control the latent infections, and, to a lesser extent, virus replicative lesions of the B cell pool.

Woon *et al.* further examined the compartmentalization of EBV-specific $CD8^+$ T cells in the tonsil and showed that CD103 expressing cells localized to the epithelial barrier in regions where IL-15 was detected. The authors also demonstrated that IL-15 and TGF-β co-operate to downregulate expression of a surface receptor involved in tissue egress, S1PR1 and its transcriptional activator KLF2 (298).

The accumulation of EBV-specific $CD8^+$ T cell in the tonsil of long-term carriers is facilitated by increased expression of the lymphoid homing marker CCR7 in long-term carriers. A similar change in CCR7 expression is seen in the EBV-specific $CD4^+$ T cell population however whether this results in enrichment in the tonsil similar to $CD8^+$ T cells has yet to be investigated but may be important for development of effective vaccines.

3. EBV vaccines

Given the health burden of EBV-related disease, development of prophylactic and therapeutic vaccines to prevent and treat EBV-associated disease has been the goal for many years.

a. Prophylactic vaccination

To date most efforts have predominantly focused on promoting production of neutralizing antibodies against gp350. Interaction of the EBV glycoprotein gp350 with the complement receptor CD21 results in binding of virions to B cells thereby facilitating fusion with the cell membrane and endocytosis. Gp350 is the most abundant glycoprotein on the surface of virions and while it is not absolutely required for infection, *in vitro* studies have shown that it is important for efficient virus entry (299). Several vaccination studies targeting gp350 carried out in non-human primates have yielded encouraging results, with protection from EBV-induced lymphoma being achieved following inoculation with purified native gp350, recombinant gp350 adenovirus expressing gp350 and vaccinia virus expressing gp350 (reviewed in (300)). Interestingly protection against EBV-induced lymphoma did not always correlate with the production of neutralizing antibodies, suggesting that other immune components may be important to target in the future.

In humans, a phase 1 trial inoculating EBV seronegative donors with vaccinia virus expressing gp350 resulted in delayed infection compared to a control group and production of neutralizing antibodies to membrane antigens (301). However, due to the adverse effects of vaccinia virus it is no longer considered for vaccine strategies. A study using recombinant gp350 and an alum/monophosphoryl lipid A adjuvant progressed to a phase 2 double-bind placebo-controlled trial and individuals were tracked for development of IM-like symptoms as well as presence of antibodies. Fewer cases of IM were observed in the vaccinated group (although this was not statistically significant) and gp350 antibodies were induced in virtually all subjects with the vast majority

developing neutralizing antibodies (302). Given the increased risk of developing Hodgkin's lymphomas following IM (303, 304), reducing the incidence of the disease would be of great benefit.

Human trials to assess whether prophylactic EBV vaccines can prevent the development of EBV-associated malignancies are challenging, primarily due to the length of time that can elapse between infection and disease presentation. Patients awaiting transplant who are at risk of developing PTLD could provide some insight. One such study was performed in EBV seronegative children (who are less likely to be EBV positive) awaiting kidney transplant (305). Following inoculation with soluble gp350 over 6 to 8 weeks, only a limited number of patients produced neutralizing antibodies and these declined rapidly. The relative failure of this trial to elicit a long-lasting immune response could potentially be attributed to the immunosuppressive regiment to which transplant patients are subjected to and the low doses of gp350 used.

More recently, development of virus-like particles (VLPs) containing a broad antigenic spectrum but no detectable EBV DNA have been proposed as an alternative to vaccinations with single proteins. VLPs represent an attractive option for prophylactic vaccination as they contain viral proteins that can be presented by B cells thereby eliciting a strong humoral and cellular immune response. *In vivo* murine studies have demonstrated EBV-based VLPs to be highly immunogenic and efficient in generating both neutralizing antibody titers and EBV-specific $CD8^+$ and $CD4^+$ T cell responses (306, 307). Moreover, in a humanized mouse model, immunogenic particles containing EBNA1 afforded significant protection against EBV infection (308).

b. Therapeutic EBV vaccines

The goal of EBV therapeutic vaccines are to boost cellular immunity in patients with EBV-associated malignancies. Due to EBV's association with undifferentiated NPC, to date most trials have been performed on patients with this disease.

One approach is to administer dendritic cells that have been infected with EBV proteins or incubated with peptides. Thus, following inoculations, these dendritic cells will boost T cell immunity to the chosen EBV antigens. An early trial immunizing 16 patients with DCs pulsed with LMP2 yielded encouraging results, eliciting or boosting $CD8^+$ T cell responses that coincided with, in some patients, tumour reduction (309). In a subsequent phase II trial, 16 patients received DCs transduced with a replication-incompetent adenovirus encoding for an inactive form of LMP1 and full length LMP2 (310). No expansion of LMP1/2-specific T cells was detected in the periphery however clinical responses were observed in 3 patients.

In a separate approach, a modified vaccinia Ankara (MVA) vector expressing a fusion protein of LMP2 and the C-terminal region of EBNA1, was used in two dose escalation phase I trials in NPC patients from the Hong Kong and UK (18 and 16 patients respectively) (311, 312). In both cohorts, higher T cell responses against LMP2 and EBNA1 were detected highlighting the immunogenicity of the vaccine in two ethnic groups with different HLA types. Moreover, these trials demonstrated the ability of the MVA vaccine to stimulate both $CD4^+$ and $CD8^+$ T cell responses.

4. Adoptive T cell therapy

Trials investigating *in vitro* expanded EBV-specific cytotoxic T cells as a treatment option for patients with EBV-related cancers have also shown proof of principle. The first of which in EBV-positive relapsed Hodgkin's disease (313) and it has since been used to treat different types of EBV-associated cancers including lymphomas (314), nasopharyngeal carcinoma (315-317) and PTLD (318, 319). Despite the different protocols used to generate EBV-specific CTLs infusions of both autologous and allogeneic cell preparations have yielded encouraging results.

Importantly, in one trial, better patient outcomes were observed with higher percentage of $CD4^+$ T cells in the infused CTL lines (319).

III $CD4^+$ T cell immunity to viruses

1. Cytotoxic $CD4^+$ T cells in humans: CD4-CTLs

$CD4^+$ T cells possessing the ability to directly recognise and lyse target cells, reminiscent of the role carried out by $CD8^+$ T cells, were first described over 30 years ago (320-322). These early reports of cytotoxic function in $CD4^+$ T cells were from cultured lines and clones, and described lytic function restricted through MHC II. However, for many years, the cytotoxic characteristics were thought to be an artefact of long-term *in vitro* culture.

In recent years, it has become accepted that *ex vivo* $CD4^+$ T cells with cytotoxic capacity, recognising antigen on the surface of MHC class II^+ cells, are widespread in particular in the context of chronic viral infections and cancer. Furthermore, their importance as a

component of the immune response to viruses is supported by numerous studies correlating CD4-CTL frequencies with better clinical outcomes (reviewed in (323)). Thus, generating a long-lived and robust CD4-CTL response following vaccination is now an important consideration of vaccine design (324, 325). Moreover, in a mouse melanoma model, tumour-reactive $CD4^+$ T cells transferred into lymphopenic recipients developed cytotoxic activity and were able to eradicate established tumours (326).

1. Protective role in immunity

Presence of CD4-CTLs in numerous contexts *in vivo* suggests a previously unappreciated function in host immunity. Viruses have evolved mechanisms to avoid detection of CD8-CTLs by interfering with MHCI antigen presentation (327). This is the case in both HIV-1, CMV and EBV where virus-specific CD4-CTLs have been detected and the viruses encode for proteins that lead to downregulation of surface MHCI expression (328) and increased proteasomal degradation of MHC-I (329) respectively. Indications that CD4-CTLs may be compensating for diminished CD8-CTL efficacy due to reduced MHCI antigen presentation, can be found in studies showing that both in patients undergoing CMV reactivation following stem cell transplants and in individuals with acute HIV, frequency of virus-specific CD4-CTLs is a positive predictor of disease outcome (330, 331). Moreover, the CD8-CTL response to influenza is known to be impaired in older adults whereas the CD4-CTL response is preserved (332).

The mounting evidence that a cytotoxic $CD4^+$ T cell response plays a protective role against infections suggests that eliciting CD4-CTL development following vaccination could be advantageous. Vaccination with live attenuated yellow fever and inactive

influenza in mice resulted in the generation of a CD4-CTL response and conferred protection (324, 333). Interestingly, immunization of inactivated influenza with a CpG adjuvant that promotes a T_H1-like response induced significantly higher expression of Granzyme B in persistent $CD4^+$ T cells compared to inactivated influenza alone (333). CD4-CTL responses were similarly induced by SIV vaccination in macaques and their presence correlated with an increased ability to control viremia (325).

2. Chronic viral infection

CD4-CTLs have been predominantly observed in chronic viral infections, thus, most knowledge of this subset has come from this setting. In 2002 Appay *et al.* showed that the low numbers of circulating $Perforin^+$ CD4-CTLs ex vivo in healthy donors were markedly expanded in chronically infected HIV-1 individuals (271). The CD4-CTLs detected in this study displayed a phenotype commonly observed with highly differentiated T cells (CD27-, CD28-, CCR7lo, CD45RA+) but did not show signs of activation or proliferation (CD38lo, CD69-, Ki-67-) (Figure 1.8). Similarly, in patients chronically infected with viral hepatitis, populations of terminally differentiated (CD27-CD28-) $Perf^+$ $CD4^+$ T cells were significantly raised compared to healthy controls (334). More recently, studies investigating the CD4-CTL response to chronic CMV and Dengue virus (DENV) also demonstrated that expression of cytotoxic proteins such as Perforin and GzmB (177, 331, 335-338) and acquisition of direct cytotoxic capacity, as shown by degranulation and killing assays (177, 335) was linked to a T_{EMRA} phenotype akin to *in vitro* cultured cell lines. Moreover, single cell transcriptome analysis performed on $CD4^+$ T cells with previous DENV infection revealed that genes linked to cytotoxic function were expressed at higher levels in the T_{EMRA} population compared to T_{CM} and T_{EM} (339).

Another infectious model where CD4-CTLs have been well described is influenza. In humans, following experimental IAV infection, memory influenza-specific $CD4^+$ T cells from healthy donors expressed GzmB and exhibited cytolytic activity 7 days post-challenge (340).

3. Cancer

Many cancers arise at chronically inflamed sites and as a result $CD4^+$ T cells repeatedly exposed to antigen that have acquire cytotoxic function have also been reported in various tumours affecting $MHCII^+$ cells *in vivo* and *ex vivo*. In a mouse melanoma model it was shown that naïve tumour-specific $CD4^+$ T cells naturally differentiated into CD4-CTLs *in vivo* and led to tumour clearance (341). Moreover, in multiple myeloma patients, $CD4^+$ T cells expressing Perf, GzmA and GzmB were identified and frequency of CD4-CTLs negatively correlated with the frequency of malignant plasma cells (342).

4. Acute Infection

Studies investigating the human $CD4^+$ T cell response during acute infection have been more challenging as identifying and obtaining samples from newly infected individuals seroconverting is difficult. However, there are limited reports of CD4-CTLs in primary infection. In patients undergoing primary HIV-1 infection three reports have detected presence of CD4-CTLs and, unlike in chronic infections, these $CD4^+$ T cells were highly active and proliferating ($CD38^{hi}$, Ki-67^+) (Figure 1.8) (271, 343, 344). These limited observations from human studies that CD4-CTLs are supported by observations in mice showing expression of Perf and GzmB in $CD4^+$ T cells 7 days after infection with influenza (345, 346).

5. Development

Given the potential importance of CD4-CTLs many studies into the signalling pathways involved in their development *in vivo* have been carried out. However, due to the challenges in addressing this issue in humans, most current data has arisen from analysis of CD4-CTLs in mice. $CD4^+$ T cells with cytotoxic activity predominantly have a T_H1 phenotype although the characteristic cytokine of T_H1 IFNγ, is not required for CD4-CTL generation in mice (347). Multiple studies have instead shown that IL-2 is critical for their development (346, 348, 349) along with type I interferons that signal through STAT2 and IRF3 (350). IL-2 activates STAT5 which has been shown to enhance expression of Perf in $CD8^+$ T cells (351) while Granzyme B expression is reduced in STAT2 and IRF3 deficient mice (346, 350). IL-2 also induces expression of the transcription factor Eomes (352). In conjunction with Runx3, Eomes has been shown to be sufficient for cytotoxic protein expression in $CD8^+$ T cells (353), however its role in development of CD4-CTLs remains unclear. IL-15, which is structurally homologous to IL-2 and also signals through STAT5, similarly enhances both Perf and GzmB expression in highly differentiated human CD4-CTLs (354).

With regard to antigen stimulation, in contrast to the early *in vitro* models that suggested chronic stimulation was required for CD4-CTL development, low levels of antigen in mice infected with influenza favoured development of cytotoxic function in $CD4^+$ T cells compared to high antigen concentration (347). However, in the murine gut, CD4-CTL receiving antigenic stimulation only exhibited cytotoxicity with additional signalling from IL-15 (355).

Furthermore, recent work by Carlier *et al*. demonstrated that modification in the peptide flanking regions of class II restricted peptides could induce acquisition of cytotoxic functions (356). Insertion of a CxxC motifs into the regions flanking residues bound to the MHCII peptide binding cleft increased the strength of the interaction between APC and $CD4^+$ T cell, resulting in increased Lck/ZAP70 mediated signalling and promoting expression of cytotoxic proteins (357). Interestingly, the acquisition of cytotoxic properties following recognition of CxxC motif containing peptides could occur in both naïve and memory $CD4^+$ T cells. These findings indicate that the peptide sequence could play an important role in CD4-CTL development.

6. CD4-CTL Markers

The molecular mechanisms that govern the differentiation and development of human CD4-CTLs have yet to be determined and investigation into this subset would be facilitated by the identification of characteristic markers.

With regard to identifying cytotoxic capacity without the need for intracellular staining, numerous cellular markers have been proposed. Early work indicated the presence of CD107a (also called lysosomal associated membrane protein 1 – LAMP 1) on the cell surface of CD4-CTLs following stimulation. CD107a is normally in the internal membrane of lysososmes and is a marker of degranulation, the cellular process whereby intracellular vesicles containing cytotoxic effector molecules such as Perf and GzmB fuse with the plasma membrane resulting in their release into the extracellular matrix (358). In the context of T lymphocytes, following pMHC-TCR interaction, transport of vesicles is carried out by active transport towards the IS. This targeted exocytosis results in

cytotoxic proteins being delivered in close proximity to the target cell, allowing them to exert their function. Thus, in cytotoxic lymphocytes, following the translocation and fusion of lysosomes to the plasma membrane and secretion of granules, CD107a, from the internal lysosomal membrane is left on the cell surface (359). Although, detection of CD107a has been useful for the detection of CD4-CTL, it's presence on the surface requires stimulation. Identification of markers that enable identification of CD4-CTLs without manipulation are needed to further our understanding of this cell type *in vivo*.

More recently, a study of CMV-specific CD4-CTLs isolated from seropositive donors by Pachnio *et al.* showed that highly differentiated $CD4^+$ T cells carrying Perf and GzmB all co-expressed CX_3CR1 (336). CX_3CR1 directs endothelial homing of lymphocytes and has been associated with active development of cytotoxic functions and memory differentiation in $CD8^+$ T cells (360, 361). This finding was corroborated by Shabir *et al.* in a cohort of kidney transplant patients, where in addition to CX_3CR1 positivity, CD4-CTLs also expressed surface NKG2D (337), an activating receptor more commonly associated with NK cells. Expression of CX_3CR1 was also reported to be expressed on the surface of Dengue-virus-specific CD4-CTLs displaying a late differentiated phenotype ($CCR7^-CD45RA^+$ $CD57^+$) (177). Finally, a study published by Takeuchi *et al.* reported that expression of the class-I restricted T cell associated molecule (CRTAM) could be used to identify $CD4^+$ T cells that would develop cytotoxic effector functions (362) (Figure 1.8). However, expression of CRTAM is transient following TCR stimulation, making direct *ex vivo* analysis difficult and limiting its utility as a CD4-CTL marker.

7. Transcription factors

Alongside surface phenotyping, many studies have investigated the transcriptional programme that governs the development and differentiation of CD4-CTLs. Perhaps as a consequence of studying CD4-CTLs in the context of viral infections, many studies have linked CD4-CTL development to the T_H1 $CD4^+$ T cell subset, the polarising conditions present during an anti-viral immune response and its associated cytokine profile (271, 335, 363-365). Nonetheless, reports of cytotoxic activity in other $CD4^+$ T cell subsets have been published indicating that CD4-CTLs are not a distinct lineage and rather have developed cytotoxic function following subset differentiation (347, 366). The master regulators of cytotoxic effector functions in $CD8^+$ T cells are described as T-bet and Eomes together inducing the expression of Perf and GzmB B (367, 368). In $CD4^+$ T cells it has been shown that T-bet alone is not sufficient for GzmB expression and presence of Eomes is required (348, 369). Consequently, Eomes has been detected in both DENV and HIV-specific CD4-CTLs (177, 370) (Figure 1.8). Two other transcription factors reported to be involved in development of CD4-CTLs are Blimp-1 (371) and the homolog of Blimp-1, Hobit (372). Using single cell transcriptional profiling, Donnaruma *et al.* demonstrated that the balance between the TCF-1-Bcl6 nexus and Blimp-1 played a crucial role in determining the direction of $CD4^+$ T cell differentiation to helper or cytotoxic functions. Bcl6 is required for T_{FH} differentiation and its expression suppresses Blimp-1 expression. In the absence of Bcl6, Blimp-1 is expressed at high levels, which favours CD4-CTL development (371). In a study analysing the primary response to CMV, Oja *et al.* showed that $Hobit^+$ $CD4^+$ T cells expressed high levels of Perforin, GzmB B, CX_3CR1, T-bet and Eomes (372).

The lack of a well-defined phenotypic maker for CD4-CTL has precluded researchers from isolating CD4-CTLs to perform single-cell transcriptome analysis.

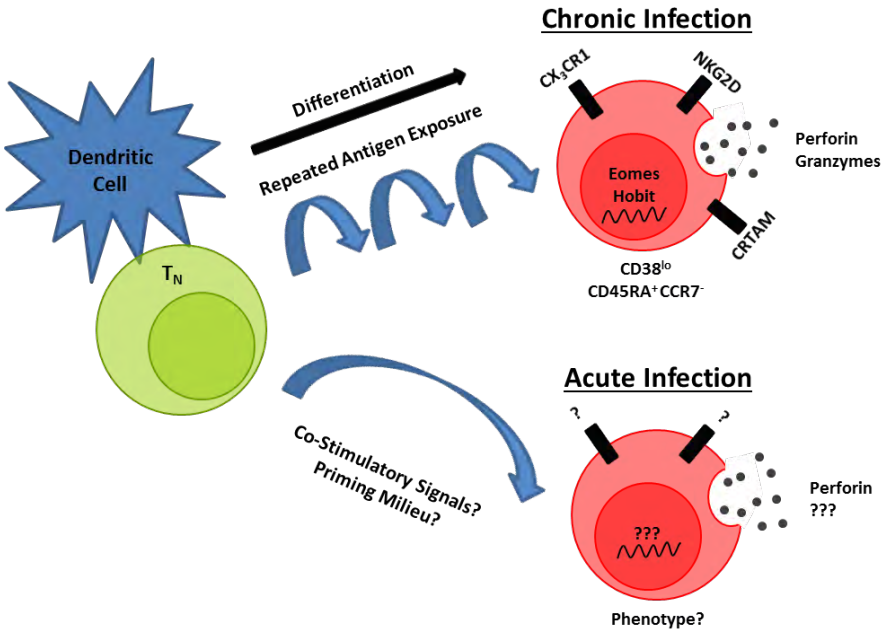

Figure 1.8 Schematic diagram of development, phenotype, cellular markers and effector proteins of CD4-CTLS in chronic and acute infection.

2. Tissue resident memory $CD4^+$ T cells: T_{RM}

Tissue resident memory T cells (T_{RM}) are a subset of cells seeded at specific anatomical sites soon after immune priming (373). The establishment of these non-circulating populations in tissue enables early detection of pathogen entry or reactivation thereby providing an immune response in sites that are susceptible to re-infection (Figure 1.8) (374, 375). Furthermore, this subset is able to respond rapidly and immunity at the site of infection is not solely dependent on the recruitment of circulating memory T cells to a specific location (376).

Until recently, the majority of studies focused on investigating T cell responses to viruses and cancer have focused on peripheral blood, yet T cells in the blood only account for 2-2.5% of an individual's T cell complement (377). Estimates of the number of memory T cells located within tissues such as the skin, lung, gut and lymphoid tissue suggest that the profile of circulating T cells may only represent a small fraction of the immune system's memory response.

1. Development

The signals that are required for the establishment and maintenance of $CD4^+$ T_{RM} are not yet fully understood however cytokines are known to play a prominent role in $CD8^+$ T_{RM} development. Signalling through the IL-2 and IL-7 receptors have been shown to be critical for the establishment (378, 379) and maintenance (380-382) of T_{RM}. $CD8^+$ T_{RM} rely on IL-15 for both generation and maintenance however its role in the context of $CD4^+$ T_{RM} is less clear (383). The requirement for antigen recognition and signalling through the TCR in order to maintain residency is important for $CD8^+$ T cells (384) but less so for their $CD4^+$ counterparts as transferred cells are able to survive in an antigen independent environment (385).

Upon entry into sites of inflammations, inflammatory cytokines (386), oxygen availability (387) and TCR signalling (388), can contribute to re-expression of CD69 although the individual role of these factors to the generation of T_{RM} remains unclear.

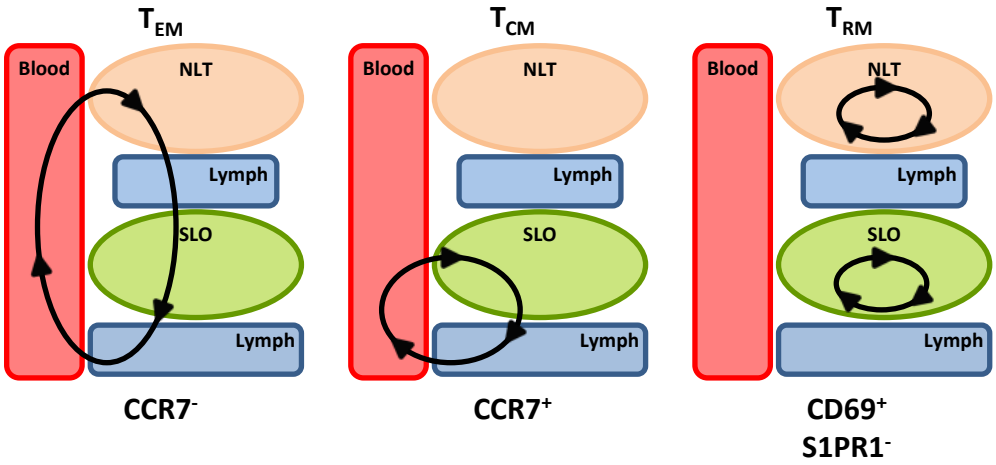

Figure 1.9 Patterns of migration and phenotype of effector (T_{EM}) , central (T_{CM}) and resident memory (T_{RM}) T cells. Adapted from (389).

2. Phenotype

T_{RM}s can be distinguished from circulating memory cells by the downregulated expression of molecules involved in tissue egress. Thus, expression of the C-type lectin CD69 and absence of S1PR1 are hallmarks of T_{RM}. CD69 expressed at the cell surface interacts with S1PR1, facilitating its internalization and degradation and thereby suppressing sphingosine 1-phosphate mediated tissue egress (390-392). Although CD69 is also transiently upregulated on the surface early in T cell activation, it has been shown that it is constitutively expressed in T_{RM} in the absence of activation markers and its expression alone can be used to identify this subset in tissue (393).

The analysis of $CD69^+$ T cells isolated from multiple human organs performed by Kumar *et al.*, also observed upregulation of cell surface markers associated with migration and adhesion in this population namely CD103, CD49a, CXCR6 and CX_3CR1. Expression of the αE integrin CD103 had previously been exclusively associated with $CD8^+$ T_{RM}, although it's presence on the cell surface is not ubiquitous across all tissues. Nonetheless, $CD4^+$

$CD103^+$ T_{RM} have been identified in lung tissue (394) and it has been suggested that environmental cues such as the presence of the anti-inflammatory cytokine TGFβ, which is known to enhance expression of CD103 (395), could be responsible for the differences in surface phenotypes seen.

These observations coupled with the mass cytometry analysis of lymphoid and non-lymphoid T_{RM} populations from eight different human tissues has highlighted the differences in phenotype and functional profile of $CD69^+$ cells (396)

3. T_{RM} transcription factors

The transcription factors Hobit and Blimp-1 have been proposed as central regulators of $CD8^+$ T cell tissue residency in mice (397). However, data from human $CD4^+$ T cell studies isn't as conclusive. Neither Hobit nor Blimp-1 were found to be significantly upregulated in $CD69^+$ $CD4^+$ T_{RM} isolated from the liver, gut or skin (393) and no transcripts were detected in lymph node $CD4^+$ T_{RM} of HIV-infected individuals (398). In lung $CD4^+$ $T_{RM,}$ Hobit was not detected at the protein level however mRNA transcripts were present (394).

4. Virus-specific T_{RM}

Some of the earliest evidence that T_{RM} are retained at specific anatomical sites was demonstrated in models of HSV and LCMV infection in mice. Two laboratories discovered that populations of $CD8^+$ T cells remained in non-lymphoid tissue after infection and did not recirculate through the blood (373, 399). To date, studies investigating virus-specific T_{RM} in have focused mainly on $CD8^+$ T cells (reviewed in (400-402)) despite $CD4^+$ T_{RM} outnumbering $CD8^+$ T cells in some mucosal tissue (403, 404).

However, parabiosis experiments showing that influenza-specific $CD4^+$ T cells did not emigrate from the lung confirmed the existence of virus-specific $CD4^+$ T_{RM} (405).

Nonetheless the functional role of $CD4^+$ T_{RM} in the context of viral infections remains poorly understood and the implication for $CD4^+$ T_{RM} in vaccine design remains limited. Reports in mice have shown that following infection with HSV, a population of polyfunctional virus specific-$CD4^+$ T_{RM} but not their $CD8^+$ counterparts was required for full protection in the skin and genital mucosa (406, 407). Similarly, polyfunctional $CD4^+$ influenza-specific T_{RM} were identified in normal human lung tissue (408) and in the respiratory tracts of mice following secondary infection (409). Data from skin biopsies collected from healthy individuals suggests that, with age, varicella zoster virus-specific $CD4^+$ T cells in the skin decrease in number, increase expression of inhibitory molecules such as PD-1 and can lead to an increased incidence of VZV reactivation (410), thus highlighting their protective role.

Data from virus-specific T_{RM} in lymphoid tissue has also been limited to analyses of the $CD8^+$ compartment. Studies have detected elevated frequencies of HIV-specific $CD8^+$ T_{RMs} in lymph nodes of elite HIV controllers (398) and accumulation and retention of EBV-specific $CD8^+$ T cells in the tonsil and spleen (297, 298) suggesting a hitherto undervalued role of T_{RM} in lymphoid tissue protective immunity.

Studies of T_{RM} in the context of viral infections with known tissue tropism have helped researchers further elucidate the role played by this memory subset in immunity. However there remains a paucity of information regarding $CD4^+$ T_{RM} in lymphoid tissue. A greater understanding of site-specific $CD4^+$ T_{RM} to immunogenic viruses that provide

localised immunity could therefore inform vaccine design to promote development and maintenance of T_{RM} populations.

5. T_{RM} in cancer

In addition to the protective role of T_{RM} in viral infections, studies have highlighted the function of this subset in anti-tumour responses and in cancer-immune equilibrium. Analysis of tumour infiltrating CTLs from treatment-naïve lung cancer patients revealed that enrichment for T_{RM}-associated transcripts correlated was predictive of better clinical outcome (411). Moreover, using a novel epicutaneous mouse melanoma model Park *et al.* demonstrated that T_{RM} were critical in controlling tumour outgrowth and displayed reduced expression of exhaustion markers commonly found on TILs (412).

Project aims

EBV is a clinically relevant virus yet little is known about the $CD4^+$ T cell response important in controlling MHC-II^+ virus infected cells. Furthermore, EBV-infected B cells are maintained in SLO and limited data exists regarding $CD4^+$ T cell immunity at the site of infection. Increased knowledge of the circulating and tissue-specific $CD4^+$ T cell response to EBV could help inform vaccine development.

Using EBV-pMHCII tetramers on peripheral blood and tonsils samples collected at multiple stages of EBV infection we sought to:

1. Analyse the functional properties of circulating EBV-specific $CD4^+$ T cells in acute IM and in long-term carriers.

2. Investigate the presence of EBV-specific CD4-CTLs during natural EBV infection and compare their profile to CD4-CTLs described in the context of chronic infections.

3. Study the evolution of the EBV-specific $CD4^+$ TCR repertoire from acute infection into long term-persistence.

4. Characterize the $CD4^+$ T cell response to EBV at the site of viral replication, the tonsil.

Chapter 2

MATERIALS AND METHODS

I. Media, reagents and buffers

1. Tissue culture reagents

RPMI-1640 (Sigma-Aldrich): RPMI supplemented with L-glutamine and sodium bicarbonate.

Penicillin-streptomycin solution (Pen/Strep, Invitrogen): Solution containing 5000IU/mL penicillin and 5000µg/mL streptomycin

Foetal bovine serum (FBS) (Biosera)**:** Aliquoted and stored at -20°C.

Human Serum (HuS) (Corning)**:** Aliquoted and stored at -20°C.

Phosphates buffer saline (PBS) was prepared by dissolving one Dulbecco A tablet per 100mL of distilled water and autoclaved.

Ethylenediaminetetraacetic acid (EDTA)

MACS buffer: PBS containing 0.5% Bovine Serum Albumin (BSA) and 2.5nm (EDTA).

2. Culture media recipes

Standard medium: RPMI-1640 supplemented with 8% FBS, 100 IU/mL penicillin, 100 µg/mL streptomycin

Freezing media: RPMI-1640 medium supplemented with 20% foetal calf serum, 10% DMSO.

3. Peptides

Synthetic Peptides (Alta Biosciences or Peptide 2.0): Individual EBV CD8 and CD4 epitopes used for stimulation and pMHC tetramer generation were stored in DMSO between 5-10 mg/mL.

4. Flow cytometry

a. pMHCI tetramers

Peptide-MHCI monomers containing EBV CD8 epitopes were manufactured by the University of Birmingham Protein Expression Facility (PEF). Monomers were tetramerised by gradual addition of streptavidin APC on ice over 10 hours.

b. pMHCII tetramers

Peptide MHCII tetramers were either obtained from the Benaroya Research Institute at Virginia Mason or the NIH Tetramer Core Facility.

Optimisation of pMHCII staining using tetramers supplied by the Benaroya Research Institute was performed by a previous member of the laboratory.

pMHCII tetramers generated by the NIH Tetramer Core Facility were initially tested for specificity by staining PBMCs spiked with a known percentage of $CD4^+$ T cell clones specific for the appropriate epitope and restricted through the corresponding HLA type (Fig 2.1; left-hand plots). Thereafter, working concentrations for pMHC staining were determined using matched HLA donors identified with measurable responses. Concentrations with minimal non-specific binding while maintaining the frequency of $pMHCII^+$ $CD4^+$ T cells were chosen for this study (Fig 2.1; right-hand plots).

The full list of pMHC tetramers used throughout this study is shown in Table 2.1.

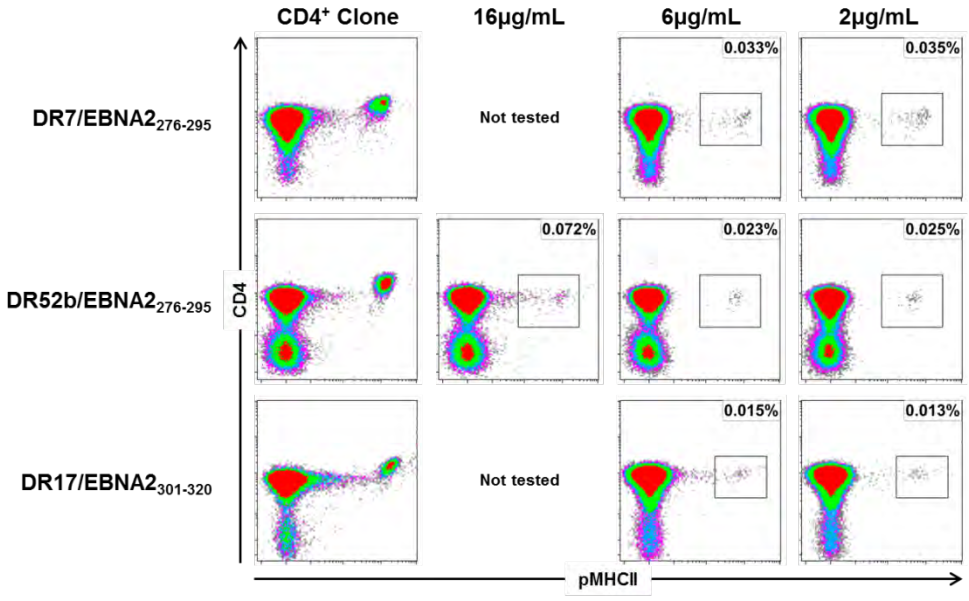

Figure 2.1 pMHCII titration. PBMCs from healthy donors were spiked with CD4⁺ T cell clones specific for an EBV epitope, restricted through a known HLA allele and stained with the relevant EBV-pMHCII to assess specificity (left hand plots). Thereafter PBMCs were stained with different concentrations of EBV-pMHCII to determine optimal working concentrations (middle and right hand plots).

Table 2.1 pMHCI and pMHCII Tetramers

	Pathogen	Virus Phase	Protein	Coordinates	Epitope	MHC restriction
Class I	EBV	Lytic	BMLF1	259-267	**GLC**TLVAML	A2:01
		Latent	EBNA3	379-387	**RPP**IFIRRL	B7
Class II	EBV	Latent	EBNA1 (E1)	474-493	**SNP**KFENIAEGLRVLLARSH	DRB5*01:01 (DR51)
		Latent	EBNA2 (E2)	276-295	**PRS**PTVFYNIPPMPLPPSQL	DRB1*07:01 (DR7)
		Latent	EBNA2 (E2)	279-295	**PRS**PTVFYNIPPMPLPPSQL	DRB3*02:02 (DR52b)
		Latent	EBNA2 (E2)	301-320	**PAQ**PPPGVINDQQLHHLPSG	DRB1*03:01 (DR17)
		Lytic	BMRF1 (BM)	136-150	**VKL**TMEYDDKVSKSH	DRB1*03:01 (DR17)
		Lytic	BaRF1 (Ba)	185-199	**SRD**ELLHTRAASLLY	DRB1*07:01 (DR7)
		Lytic	BZLF1	61-75	**LTA**YHVSTAPTGSWF	DRB3*02:02 (DR52b)
	CMV	N/A	Glycoprotein B	217-228	DYSNTHSTRYVT	DRB1*07:01 (DR7)
	Influenza	N/A	Matrix Protein 1 (M1)	43-59	MEWLKTRPILSPLTKGI	DRB1*07:01 (DR7)

c. Fluorochrome conjugated surface and intracellular antibodies

All conjugated antibodies were pre-titrated for optimal performance.

Populations known to express the appropriate surface or intracellular marker were stained with different concentrations of conjugated antibody. Following analysis, saturating concentrations that resulted in adequate separation between positive and negative populations and reliable measuring of expression levels were chosen. As shown in Fig 2.2, a dilution of 1:80 for CD69 staining on $CD4^+$ T cell from UMs (top plots) and a dilution of 1:8 for Granzyme K staining on $CD8^+$ T cell from PBMCs resulted in identifiable distinct populations suitable for analysis.

The full lists of surface and intracellular antibodies used throughout this study are shown in Table 2.2 and 2.3 respectively.

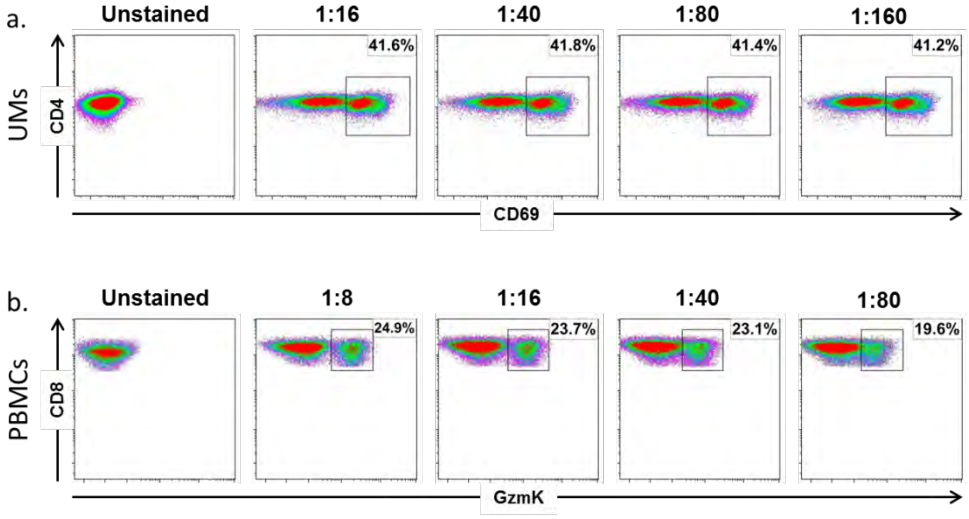

Figure 2.2 Antibody titration. (a) Surface staining of $CD4^+$ T cells from tonsil UMs with decreasing concentrations of BV650 conjugated anti-CD69. **(b)** Intracellular staining of $CD8^+$ T cells from PBMCs with decreasing concentrations of Alexa-Fluor 594 conjugated anti-Granzyme K (GzmK).

Table 2.2 Surface Antibodies

Specificity	Fluorochrome	Clone	Manufacturer	Dilution
CD3	AmCyan	SK7 (Leu-4)	BD	1:40
CD4	APC-Cy7	RPA-T4	Biolegend	1:80
CD4	PE-Texas Red	SFCI12T4D11	Beckman Coulter	1:80
CD4	PerCP	RPA-T4	Biolegend	1:80
CD8	FITC	RPA-T8	BD	1:40
CD8	PerCP-Cy5.5	RPA-T8	eBioscience	1:40
CD14	Pacific Blue	HCD14	Biolegend	1:80
CD14	APC-Cy7	HCD14	Biolegend	1:80
CD19	Pacific Blue	HIB19	Biolegend	1:80
CD19	APC-Cy7	HIB19	Biolegend	1:80
CD38	PerCP-Cy5.5	HIT2	Biolegend	1:80
CD38	BV650	HB-7	Biolegend	1:80
CD45RA	AF700	HI100	Biolegend	1:80
CD45RA	BV510	HI100	Biolegend	1:80
CD45RO	BV605	UCHL1	Biolegend	1:160
CD57	PE-Dazzle 594	J252D4	Biolegend	1:160
CD69	BV605	FN50	Biolegend	1:80
CD103	BV421	Ber-ACT8	Biolegend	1:160
CD103	PE-Dazzle 594	Ber-ACT8	Biolegend	1:160
CD107a	FITC	H4A3	BD Pharmingen	1:50
CD278 (ICOS)	AF700	C398.4A	Biolegend	1:160
CCR7	FITC	150503	R&D Systems	1:8
CCR7	BV785	G043H7	Biolegend	1:80
CRTAM	APC	Cr24.1	Biolegend	1:40
CX3CR1	PE/Dazzle 594	2A9-1	BD	1:160
CX3CR1	BV421	2A9-1	BD	1:16
HLA-DR	AF700	LN3	Biolegend	1:800
NKG2D	BV421	1D11	Biolegend	1:40
PD-1	APC	EH12.2H7	Biolegend	1:160
PD-1	BV510	EH12.2H7	Biolegend	1:80
S1PR1	e660 (APC)	SW4GYPP	Thermo	Undefined

Table 2.3 Intracellular Antibodies

Specificity	Fluorochrome	Clone	Manufacturer	Dilution
GM-CSF	PE-Dazzle 594	BVD2-21C11	Biolegend	1:40
IFNγ	AF700	4S.B3	Biolegend	1:320
IFNγ	FITC	4S.B3	Biolegend	1:40
IL-2	AF700	MQ1-17H12	Biolegend	1:40
IL-2	BV786	MQ1-17H12	Biolegend	1:1600
IL-4	PE-Cy7	MP4-25D2	Biolegend	1:160
IL-4	APC	8D4-8	Biolegend	1:16
IL-10	PE-Cy7	JES3-9D7	Biolegend	1:40
IL-21	APC	3A3-N2	Biolegend	1:80
MIP-1β	BV421	D21-1351	BD Biosciences	1:80
TNFα	PE-Cy7	MAb11	Biolegend	1:160
TNFα	BV650	MAb11	Biolegend	1:160
Granzyme B	AF647	GB11	Biolegend	1:40
Granzyme B	AF700	GB11	BD Biosciences	1:160
Granzyme B	PE Texas Red	GB11	Invitrogen	1:16
Granzyme K	AF594	GM26E7	Biolegend	1:8
Perforin	PE-Cy7	δG9	eBioscience	1:40
Perforin	FITC	B-D48	Diaclone	1:4
Bcl-6	APC-Cy7	K112-91	BD Biosciences	1:40
Bcl-6	PE-CF594	K112-91	BD Biosciences	1:80
Blimp-1	PE	6D3	BD Biosciences	Undefined
Eomes	PE-efluor 610	WD1928	eBioscience	1:16
FoxP3	APC	236/E7	eBioscience	1:40
Gata3	AF488	L50-823	BD Biosciences	1:4
Hobit	AF647	Sanquin-Hobit/1	BD Biosciences	1:40
T-bet	efluor 660	4B10	eBioscience	1:40
T-bet	PE-Cy7	4B10	Biolegend	1:160
Ki-67	BUV395	B56	BD Biosciences	1:40

II. Donors and ethics

1. Peripheral blood

The study cohort included 15 healthy carriers and 14 patients with acute IM, some of which donated subsequent samples. Convalescence was defined temporally as 6 months after the initial diagnosis of IM.

All donors provided written informed consent in accordance with the Declaration of Helsinki. Study approval was granted by the South Birmingham Local Research Ethics Committee (14/WM/1254).

2. Tonsils

Tonsil specimens were obtained from 22 patients undergoing routine tonsillectomy with no history of EBV-related disease. Tonsils were not inflamed at the time of surgery. Matching heparinized blood samples obtained for 15 patients. Samples were collected by the Human Biomaterials Resource Centre (HBRC), University of Birmingham.

All donors provided written informed consent in accordance with the Declaration of Helsinki. Study approval was granted by the North West – Haydock, NRES Committee (14/MW/0079).

III. Sample preparation

1. Isolation of Mononuclear cells

a. Peripheral blood

Heparinised blood was mixed 1:1 with RPMI-1640 and carefully layered onto Ficoll-Paque (GE Healthcare) before centrifuging at 600 x g for 30 mins (no brake). Using a Pasteur pipette, peripheral blood mononuclear cells (PBMCs) were separated by drawing off the upper layer of the interface between plasma and Ficoll. Harvested PBMCs were washed in RPMI-1640 and centrifuged at 800 x g for 10 mins (low brake). A final wash in standard medium was conducted at 400 x g for 5 mins (high brake).

b. Tonsils

Tonsil specimens were disaggregated by teasing apart the tissue and fine mincing with a scalpel. The resulting single cell suspension was diluted in RPMI-1640 and unfractionated mononuclear cells (UMs) were isolated *via* Ficoll-Hypaque centrifugation as described for peripheral blood.

2. Cryopreservation

PBMCs and UMs that were not immediately used in phenotypic or functional assays were cryopreserved by re-suspending a cell pellet in freezing media and immediately transferring to -80°C in a "Mr Frosty" freezing container for a minimum of 2 hours. Thereafter, cells were transferred to liquid nitrogen for long-term storage.

3. Cell Lines

Autologous LCLs were generated by infecting PBMCs with the B95.8 EBV strain. 3-5x10^6 cells were left in 6-8mL of filtered supernatant (0.45µm) from the Marmoset B95.8

producer line overnight in a 5% CO_2 humidified incubator at 37°C. The following day cells were washed in standard medium supplemented with 0.1µg/mL Cyclosporin A and plated in 2mL medium/well in a 24-well plate. The culture was fed weekly by replacing half of the medium with fresh standard medium supplemented with Cyclosporin A. Once *foci* of EBV transformed B cell blasts began to grow, cells were transferred to 25 cm^2 culture bottles and fed biweekly with standard medium.

4. T cell enrichment

$CD8^+$ T cells were depleted by washing PBMCs in RPMI-1640 and incubating with CD8 Dynabeads (Life Technologies) for 30 mins at 4°C on a rotator. Using a magnet, $CD8^+$ T cells were removed and the $CD4^+$ T cell enriched supernatant was harvested for subsequent assays.

Enrichment of $CD4^+$ T cells was carried out by washing PBMCs or UMs in MACS buffer and incubating with Human $CD4^+$ T Cell antibody enrichment cocktail for 5 mins at RT followed by magnetic Dextran RapidSpheres™ for 2 mins (both Stem Cell Technologies). Non-$CD4^+$ T cells were separated using a magnet and $CD4^+$ enriched supernatant was harvested.

Unless indicated otherwise, all experiments were performed using enriched populations of $CD4^+$ T cells, with purities > 95%.

IV. Molecular Techniques

1. DNA Extraction

DNA was required for PCR and qPCR experiments and was extracted from 0.5 – 2.0 $x10^6$ PBMCs or tonsil UMs using the DNeasy Blood and Tissue Kit (Qiagen) as per the

manufacturer's instructions. Briefly, cell pellets were resuspended in 200µL of PBS before addition of 20µL of proteinase K and 200µL of lysis buffer. The solution was thoroughly mixed and incubated at 56°C for 10mins. The lysate was placed in a column containing a DNA binding membrane and centrifuged. Following two washes, elution buffer was added directly to the membrane and left for 1 min. Columns were centrifuged and the concentration of DNA in the eluate was measured using a NanoDrop™ Spectrophotometer (ThermoFisher), and subsequently used immediately or stored at -20°C.

2. HLA-typing by PCR

The HLA types of healthy carriers, IM donors and patients who had undergone routine tonsillectomy was determined using PCR. Genes encoding for 14 class I antigens and 15 class II antigens common in the Caucasian population (Table 2.4), including those for which pMHCI and pMHCII tetramers were available, were amplified using gene specific primers (Table 2.5) (413).

Master Mix (14µL): 6µL TMDH buffer (containing NH_4 reaction buffer, dNTPs, $MgCl_2$ and glycerol); 4µL F and R primer mix (100µM); 1µL control primer mix; 0.06µL BioTaq DNA polymerase; 0.94µL PCR water; 1µL donor DNA (30ng/mL).

Cycling parameters for the PCR reaction were as follows: 96°C 1min. 5 cycles of 96°C 25 sec, 70°C 45 sec, 72°C 45 sec. 21 cycles of 96°C 25 sec, 65°C 50 sec, 72°C 45 sec. 4 cycles of 96°C 25 sec, 55°C 1 min, 72°C 90 sec. 72°C 2min.

Table 2.4 HLA antigens typed by PCR

Antigen	Alleles	Forward primer	Reverse primer	Product size (bp)
A1	A*0101, 0102	286S	431R	629
A2	A*0201-17	296S	302R	489
A3	A*0301, 0302	291S	299R	628
A11, 6601	A*1101, 1102, 6601	290S	167R	552
A1, 11, 36, 80, 3402	A*01, *11, *3601, *8001, *3402	367S	394R	300
B7 (inc. B703), B8101	B*0702-0705, 8101	193S	221R	619
B703	B*0703	312S	221R	600
B8, B51GAC, B*4406	B*0801, 0802, B51GAC, B*4406	195S	212R	543
B8	B*0801, 0802	195S	220R	606
B35[NOT 3505/10/13],53,75,77,5104,1521,4406	B*3501-3504,3506-3509,3511,(3512),5301,1502,1513,5104,1521,4406	193S	223R	369
B35, 18, 78, 1522	B*3501-13, 18, 7801-2, 1522	188S	237R	128
B35, 53, [NOT 3510, 3512-13]	B*3501-3509, 3511, 5301	195S	213R	389/340
			277R	
B44	B*4402-06	202S	393R	546/481
		272S	285R	
B49, 50, 4005, 61, 41, 44 [NOT 4406], 45, 47	B*4002-4006, 4008, 4101, 4102, 4501, 45v, 4901, 5001, 4402-5, 4701	270S	276R	566
DR1	DRB1*0101, 0102, 0104	36S	39R	194
DR15	DRB1*1501-1505	41S	252R	206
DR17	DRB1*03011, 03012, 0302, 0303, 0304, 0305, 1107	68S	255R	211
	DRB1*0301, 0304	46S	38R	216
	DRB1*0302, 0305, 1302, 1305, 1109, 1120, 1402, 1403, 1409, 1413, 1419	44S	37R	188
	DRB1*1301-2/11/16/18-20/22, 1402/03/06/09/12/14/17/19-21, 0301-5	68S	261R	171
DR4	DRB1*0401-22, 1410, 1122	47S	37R	259
			38R	
DR7	DRB1*0701	48S	49R	194
DR51	DRB5*0101, 0102, 0201-03	61S	492R	173
DR52a	DRB3*0101	69S	268R	221
DR52b	DRB3*0201-03	76S	151R	116
DR52b and c	DRB3*0201, 0301	70S	38R	259
DR53	DRB4*0101101, 0102, 0103 (Not DR53 Null)	283S	314R	151
DQ2	DQB1*02	82S	112R	198
DQ7	DQB1*0301, 0304	181S	112R	207

Table 2.5 Primers for HLA typing

	Sense		Antisense	
	Primer Name	Sequence	Primer Name	Sequence
Class I	188S	GCCGCGAGTCCGAGGAC	167R	GAGCCACTCCACGCACCG
	193S	GGAGTATTGGGACCGGAAC	212R	CCTCCAGGTAGGCTCTGTC
	195S	GACCGGAACACACAGATCTT	213R	GAGGAGGCGCCCGTCG
	202S	GGGGAGCCCCGCTTCATT	220R	CCGCGCGCTCCAGCGTG
	270S	GATCGTTCGTGTCCCCACAA	221R	TACCAGCGCGCTCCAGCT
	272S	CGCCACGAGTCCGAGGAA	223R	GCCATACATCCTCTGGATGA
	286S	CGACGCCGCGAGCCAGAA	237R	GCGCAGGTTCCGCAGGC
	290S	ACGGAATGTGAAGGCCCAG	276R	TCCCACTTGCGCTGGGT
	291S	AGCGACGCCGCGAGCCA	277R	GGAGGAAGCGCCCGTCG
	296S	GTGGATAGAGCAGGAGGGT	285R	CGTCGTAGGCGTACTGGCT
	312S	ACACAGATCTACAAGACCAAC	299R	CACTCCACGCACGTGCCA
	367S	TACTACAACCAGAGCGAGGA	302R	CCAAGAGCGCAGGTCCTCT
			393R	GTCGTAGGCGTCCTGGTC
			394R	CCACGTCGCAGCCATACATT
			431R	AGCCCGTCCACGCACCG
Class II	36S	TTGTGGCAGCTTAAGTTTGAAT	37R	CTGCACTGTGAAGCTCTCAC
	41S	TCCTGTGGCAGCCTAAGAG	38R	CTGCACTGTGAAGCTCTCCA
	44S	TACTTCCATAACCAGGAGGAGA	39R	CCGCCTCTGCTCCAGGAG
	46S	GACGGAGCGGGTGCGGTA	49R	CCCGTAGTTGTGTCTGCACAC
	47S	GTTTCTTGGAGCAGGTTAAACA	112R	CGTGCGGAGCTCCAACTG
	48S	CCTGTGGCAGGGTAAGTATA	151R	CGTAGTTGTGTCTGCAGTAATTG
	61S	GTTTCTTGCAGCAGGATAAGTA	252R	CCACCGCGGCCCGCGC
	68S	GTTTCTTGGAGTACTCTACGTC	255R	GTCCACCCGGCCCCGCT
	69S	TTTCTTGGAGCTGCGTAAGTC	261R	CTGTTCCAGTACTCGGCATC
	70S	GTTTCTTGGAGCTGCTTAAGTC	268R	CTGCAGTAATTGTCCACCCG
	76S	GGAGTACCGGGCGGTGAG	314R	CTGGTACTCCCCCAGGTCA
	82S	GTGCGTCTTGTGAGCAGAAG	492R	GCTGTTCCAGTACTCAGCG
	181S	GACGGAGCGCTGCGTTA		
	283S	GATCGTTCGTGTCCCCACAG		

3. EBV VCA IFA

Previous infection with Epstein-Barr virus was determined using an indirect fluorescent antibody method (IFA) designed for the qualitative detection of IgG class antibodies specific for EBV viral capsid antigen (VCA). Briefly, 10µL aliquots of B95.8-LCL and EBV-negative BJAB cell suspensions (10^7 cells/mL) were transferred into the holes of an SM-

011 slide (Hendley-Essex), air dried and fixed in acetone at -20°C. Diluted plasma samples from donors obtained during mononuclear cell, isolation were incubated for 1 hour at 37°C in a humidified chamber and subsequently washed with PBS. 10µL of a FITC-conjugated anti-IgG antibody was added and the slides placed back in a humidified chamber for incubated for 1 hour at 37°C. Following a final wash, slides were covered with coverslips and examined under a UV microscope. Donors where fluorescence was detected against B95.8 but not BJAB were designated EBV positive.

4. qPCR for EBV genome load

EBV genome load in PBMCs and tonsil UMs was assessed by qPCR using primers specific for the EBV DNA polymerase BALF5 (Table 2.6) and compared to DNA standards established using Namwala Burkitt's lymphoma known to contain two copies of integrated EBV genomes per cell. A primer to detect human β-2microglobulin was used as an endogenous control (Table 2.6). Samples containing PCR master mix (Taqman Universal master mix plus EBV and control probes and primers) and sample DNA were placed in a 96-well PCR plate and run in an ABI7500 PCR machine (ThermoFisher Scientific).

Master Mix (25µL): 12.5µL Taqman Universal 2x master mix; 2.5µL BALF5 F primer (2µM); 2.5µL BALF5 R primer (2µM); 2.5µL BALF5 probe (5µM); β2m F primer (3µM); β2m R primer (4µM); β2m probe (5µM); 5µL sample DNA.

Table 2.6 EBV genome load primers and probes

BALF5	
Forward	CTTTGGCGCGGATCCTC
Reverse	AGTCCTTCTTGGCTAGTCTGTTGAC
Probe	(FAM)-CATCAAGAAGCTGCTGGCGGCC-(TAMRA)
β2m	
Forward	GGAATTGATTTGGGAGAGCATC
Reverse	CAGGTCCTGGCTCTACAATTTACTAA
Probe	AGTGTGACTGGGCAGATCATCCACCTTC-(BHQ)

5. CMV IgG ELISA

CMV serostatus was determined using an in-house ELISA. Diluted plasma samples (1:600) were added to plates coated with mock or CMV viral-infected lysate for 1 hour. Following 3 washes an anti-human IgG conjugated to horseradish peroxidase was added to the plate for 1 hour. After washing, the peroxidase substrate TMB was added and the plate kept in the dark for 10 min before the reaction was stopped by adding 1M HCl and plates were read using a spectrophotometer at 450nm. Anti-CMV IgG titres were determined by comparison with a reference standard curve obtained using serial dilutions of a mixture of 3 CMV-positive plasma samples.

V. Flow cytometry

1. pMHC tetramer staining

Total or CD8-depleted PBMCs from healthy carriers, or CD4-enriched PBMCs from patients with IM were washed in Human Serum and stained with optimized concentrations of pMHCI (University of Birmingham) or pMHCII tetramers (Tetramer Core Laboratory of the Benaroya Research Institute) for 1 hour in a 5% CO_2 humidified

incubator at 37°C. Tetramers contained epitopes from EBV, CMV or influenza virus (influenza A/New York/348/03 H1N1) appropriate for the HLA type of each donor (Table 2.1).

CD4-enriched PMBCs and tonsil UMs from patients who had undergone routine tonsillectomy were washed in Human Serum (Corning) and stained with optimized concentrations of pMHCII tetramers (NIH Tetramer Core Facility) containing epitopes from EBV, CMV or influenza virus (influenza A/New York/348/03 H1N1) appropriate for the HLA type of each donor (Table 2.1) for 1 hour in a 5% CO_2 humidified incubator at 37°C.

2. Viability and surface staining

Following staining with pMHCI or pMHCII, cells were washed in PBS and non-viable events were labelled using a LIVE/DEAD Fixable Dead Cell Stain Kit (eBioscience or ThermoFisher Scientific) for 20 mins at RT. Excess viability dye was washed away with PBS and cells were stained with different combinations of pre-determined saturating concentrations of surface antibodies at RT for 30 mins (Table 2.2).

3. Intracellular staining

For detection of effector molecules, cells were fixed by incubation with 4% Paraformaldehyde for 30mins at 4°C and washed with MACS buffer. Next, cells were permeabilised in a 0.5% Saponin solution for 10 mins at 4°C, washed with MACS buffer and stained with various combinations of pre-determined saturating concentrations of conjugated antibodies at RT for 30 mins (Table 2.3).

For detection of transcription factors, cells were fixed and permeabilised by incubating with Fixation buffer for 30 mins at 4°C and washing twice in permeabilisation buffer (both Transcription Factor Staining Buffer Set; ThermoFisher) and stained with combinations of directly conjugated antibodies for 30mins at RT (Table 2.3).

VI. Cell stimulation and functional profiles

1. Peptide stimulation

CD8-depleted PBMCs from $DR7^+$ healthy carriers were stimulated with the $EBNA2_{276-295}$ peptide at a concentration of 0.005 μg/mL, or left unmanipulated, for 4 hr in a 5% CO_2 humidified incubator at 37°C, in the presence of brefeldin A (0.2μg/mL). Cells were gently re-suspended every 15 mins for the first hour. Stimulated cells were washed twice in standard medium and incubated with EBV-pMHCII as described above prior to surface and intracellular cytokine staining for flow cytometric analysis of IFNγ, TNFα, IL-2, IL-4, IL-10, IL-21 and GM-CSF.

2. Autologous LCL stimulation

Bulk PBMCs from healthy carriers or patients with IM or bulk tonsil UMs were stimulated with autologous LCLs at a ratio of 1:1 or left unmanipulated for 16 hr in the presence of brefeldin A (0.2μg/mL), monensin (2.0μM), and α-CD107a in a 5% CO_2 humidified incubator at 37°C. Cells were washed twice in standard medium followed by surface and intracellular cytokine staining for flow cytometric analysis of CD107a, IFNγ, TNFα, IL-2, IL-4, IL-10, IL-21 and GM-CSF, or combinations thereof.

VII. TCR repertoire analysis

1. TCR Vβ segment analysis

$CD4^+$ enriched PBMCs from healthy carriers or IM donors were incubated with a relevant EBV-pMHCII tetramer followed by staining for surface markers and TCR Vβ segments using a TCR Vβ repertoire kit containing antibodies directed against 24 Vβ chains (Beckman Coulter).

2. Quantification and characterization of TCR expression

Cell sorting of EBV-$pMHCII^+$ $CD4^+$ T cells was performed under the supervision of Dr Kristin Ladell in the laboratory of Professor David Price at the Division of Infection and Immunity, Cardiff University School of Medicine.

Unbiased molecular analysis of EBV-specific $CD4^+$ TCR expression was performed by Dr Kristin Ladell and Dr James MacLaren in Cardiff as per Quigley et al (414).

a. Isolation of EBV-specific $CD4^+$ T cells

Serial samples were collected from IM patients during acute infection and at multiple time points post-diagnosis (up to 22months). PBMCs from these samples were stained with EBV-specific tetramers and viable EBV-$pMHCII^+$ $CD4^+$ T cell populations were sorted at > 98% purity directly into RNAlater (Thermo Fisher Scientific) using a custom-modified FACSAria II flow cytometer equipped with DiVa software version 8.0.1 (BD Biosciences). Polyadenylated mRNA was extracted from the sorted EBV-$pMHCII^+$ $CD4^+$ T cells using Oligotex Direct mRNA Mini Kit (Qiagen) according to the manufacturer's instructions.

b. cDNA synthesis

cDNA was synthesised using the SMARTer™ PCR cDNA Synthesis Kit (Clontech). During rapid amplification of cDNA ends (RACE), an oligonucletide of known sequence (SMART oligo) was incorporated into the 5' end of the full length mRNA made possible by the template switching ability of MMLV Reverse Transcriptase, RNase H Minus, Point Mutant. Briefly, reverse transcriptase adds a short deoxycytidine (dC) sequence during terminal transferase activity once it reaches the 5' end of the RNA. The SMART oligo containing a G ribonucleotide sequence hybridizes to the dC sequence and the reverse transcriptase jumps to the 5' of the SMART oligonucleotide and cDNA synthesis is completed.

Unwanted contaminants such as soluble macromolecular components and salts were removed using a NucleoSpin® Extract II Kit (Clontech) as per the manufacturer's protocol. cDNA was loaded onto columns containing a DNA binding silica membrane and contaminations removed with an ethanolic buffer.

c. Amplification of T cell receptor gene products by PCR

Clean Single stranded cDNA encoding TCR genes was amplified using touchdown PCR Advantage®2 PCR Kit (Clontech). Anchor complimentary to the SMART oligo (universal primer mix - UPM) and TCRβ-specific primers specific were used to reduce non-specific binding and enable optimal sequencing of the CDR3 respectively (Table2.7).

Master Mix (50µL): PCR Buffer 10x 5µL; UPM 10x 5µL; MBC2 primer 1µL; dNTP mix 1µL; cDNA 7-13µL; AdvanTaq2 1µL; H_20 to total 50µL.

Cycling parameters for the PCR reaction were as follows: 95°C 30 sec. 5 cycles of 95°C 5 sec, 72°C 2 min. 5 cycles of 95°C 5 sec, 70°C 10 sec, 72°C 2 min. 30 cycles of 95°C 5 sec, 68°C 10 sec, 72°C 2 min.

Table 2.7 TCR amplification primers

UPM	
Long (0.4 µM)	CTAATACGACTCACTATAGGGCAAGCAGTGGTATCAACGCAGAGT
Short (2 µM)	CTAATACGACTCACTATAGGGC
TRBC constant region primer	
MBC2	TGCTTCTGATGGCTCAAACACAGCGACCT

Amplified TCR transcripts were run on a 1% agarose gel and excised. Amplicons were extracted from the gel, dissolved and cleaned up using the NucleoSpin® Extract II kit (Clontech).

d. Ligation and transformation of amplicons into E. coli

TCR gene products were ligated into plasmids for sub-cloning, transformed into competent *E. coli* and spread onto LB agar plates containing X-galactosidase. Following overnight incubations, white colonies (with no functional β-galactosidase) containing inserts were picked and amplified by PCR using primers flanking the insertion site. Cycling parameters for the PCR reaction were as follows: 95°C 5min. 35 cycles of 95°C 30sec, 57°C 30sec, 68°C 3 min. Hold 4°C.

PCR plates were subsequently sent for Sanger sequencing. Gene use was assigned using the IMGT nomenclature (415). All functional TCR sequences were deposited online at VDJdb (416).

VIII. Data analysis

1. Flow cytometry

Data were acquired using an LSR II or a Fortessa flow cytometer (BD Biosciences) and processed using FlowJo (Treestar) or Kaluza Analysis Software (Beckman Coulter).

Gating strategy for all flow cytometry analysis of Live $CD14^{-}CD19^{-}$ $CD3^{+}$ T cells is shown in Fig 2.3.

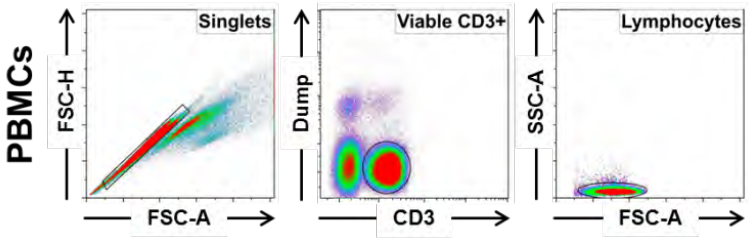

Figure 2.3. Gating strategy for flow cytometric analyses. Single cells were gated in a forward scatter-height (FSC-H) versus forward scatter-area (FSC-A) plot, and a single dump channel was used to exclude dead cells, CD14+ events, and CD19+ events. Viable CD3+ cells were then gated in a side scatter-area (SSC-A) versus FSC-A plot.

Combination gate data from analysis of LCL-responsive EBV-specific $CD4^{+}$ T cells was performed using Funky Cells and SPICE software (Simplified Presentation of Incredibly Complex Results, National Institute of Allergy and Infectious diseases) (417). Background values from unstimulated controls were deducted from all stimulated samples using Funky Cells and cytokine production pie charts generated using SPICE.

2. Statistical analysis

Statistical significance of data was assessed using GraphPad Prism Software (San Diego, USA). The non-parametric Mann-Whitney *U* test and Wilcoxon signed rank test were used to analyse unpaired and paired $CD4^+$ T cell data respectively. The Student's *t*-test with Welch's correction was used to compare total $CD4^+$ and $pMHCII^+$ populations. *P* values below 0.05 were deemed to be significant.

CHAPTER 3

THE FUNCTIONAL ROLF OF EBV-SPECIFIC CD4$^+$T CELLS

1. Introduction

Several studies have reported the cytokine profile of EBV-specific CD4$^+$ T cells and their ability to directly recognise EBV-infected B cells. However, in part due to low frequencies in the circulation, these experiments have been almost exclusively performed on *in vitro* expanded CD4$^+$ T cell lines (276-279, 281, 287, 418, 419). In addition, *ex vivo* studies analysing the functional profile of EBV-specific CD4$^+$ T cells have relied on overlapping peptide pools and virus lysate that may not reliably replicate the encounter between CD4$^+$ T cell and infected B cell *in vivo* (269, 270, 275, 280, 286, 420).

Although numerically outnumbered by their CD8$^+$ counterparts, EBV-specific CD4$^+$ T cells are critical in controlling EBV infection as is evident by HIV/AIDS patients with low CD4$^+$ T cell counts frequently developing EBV-associated malignancies (421), and increased clinical responses in PTLD patients receiving adoptively transferred EBV CTLs containing higher proportions of CD4$^+$ T cells (319). However it is not currently known in the context of the latter whether CD4$^+$ T cells are acting as helpers or possess direct effector functions.

A more comprehensive functional profiling of EBV-specific CD4$^+$ T cells *ex vivo* in IM patients and in long-term healthy carriers would help inform which functions are important in limiting the proliferation of EBV-infected B cells during primary infection

and those required to control the periodic reactivation that occurs in latent infections. Moreover, this knowledge is important to inform future rational vaccine design.

Here, using EBV-pMHCII tetramers and autologous EBV-infected B cells, we sought to analyse the transcriptional and functional profile of EBV-specific $CD4^+$ T cells in long term carriers, and to compare their profiles to the CD4+ T cells induced by acute infection.

2. Results

a. Ex vivo functional properties of EBV-specific memory CD4$^+$ T cells

In order to analyse the functional profile of EBV-specific memory CD4$^+$ T cells we first sought to identify healthy EBV carriers with detectable responses to our panel of EBV-pMHCII tetramers. Table 2.1 describes the eight EBV-pMHCII tetramers used throughout this study. Within the panel, five tetramers were loaded with peptides derived from latent proteins, two from EBNA1 and three from EBNA2, and the remaining three contain epitopes from different lytic cycle proteins, BZLF1 (immediate early) plus BMRF1 and BaRF1 (early). The epitopes are presented through four common HLA-II alleles: DR7 (DRB1*07:01; three epitopes), DR17 (DRB1*03:01; two epitopes), DR52b (DRB3*02:02; two epitopes), and DR51 (DRB5*01:01; one epitope). The specificity of the EBV-pMHCII tetramers have been previously confirmed using CD4$^+$ T cell clones specific for each peptide/MHC combination alongside HLA-matched EBV-seronegative donors as a negative control (259). PBMCs from consented EBV-seropositive healthy carriers with known HLA types were isolated from peripheral blood and stained with relevant EBV-pMHCII tetramers alongside cell surface phenotyping markers and analysed by flow cytometry. Representative examples of EBV-pMHCII responses using five of the tetramers are shown in Fig 3.1. Low frequencies of EBV-pMHCII$^+$ CD4$^+$ T cells were detectable across multiple donors ranging from 0.050% (PER 112, DR52b/EBNA2$_{276\text{-}295}$) to 0.003% (PER149; DR7/EBNA1$_{509\text{-}528}$). These values were obtained by analysing at least 1x10^6 cells per sample and while the responses were low, they were reproducible upon multiple repeats of the assay. Across multiple donors we consistently observed high frequency responses to the EBNA2$_{276\text{-}295}$ epitope presented through the DR7 HLA-II allele

(0.049% of the total $CD4^+$ T cell population in donor PER149, 0.044% in donor PER339 and 0.036% in donor PER344; Fig 3.1 top plots). Interestingly this epitope can also be presented through the DR52b HLA-II allele and we detected responses in numerous HLA-$DR52b^+$ donors. However the frequencies were more variable than among the HLA-$DR7^+$ donors (0.050% in donor PER112 and 0.013% in donor PER 141; Fig 3.1 fourth row). In contrast, responses to the PAQ epitope, also derived from the EBNA2 protein but presented through the DR17 HLA-II allele, were not as high (0.019% for donor PER173 and 0.011% for donor PER038; Fig 3.1 third row). The large panel of EBV-pMHCII tetramers also gave us the opportunity to investigate responses to different epitopes presented through the same HLA-II alleles in the same healthy carriers. In the two donors shown in Fig 3.1 (second row) frequencies of $CD4^+$ T cells staining for the DR7/$EBNA1_{509\text{-}520}$ MHCII tetramer were considerably smaller than those observed for the DR7/$EBNA2_{276\text{-}295}$ MHCII tetramer (0.003% in donor PER149 and 0.002% in donor PER344).

Together these data show that EBV-pMHCII tetramers enable reliable and reproducible investigation of virus-specific $CD4^+$ T cells *ex vivo*. In total we identified 13 healthy carriers with clearly detectable responses, some to multiple epitopes that would enable further phenotyping and functional studies to be carried out.

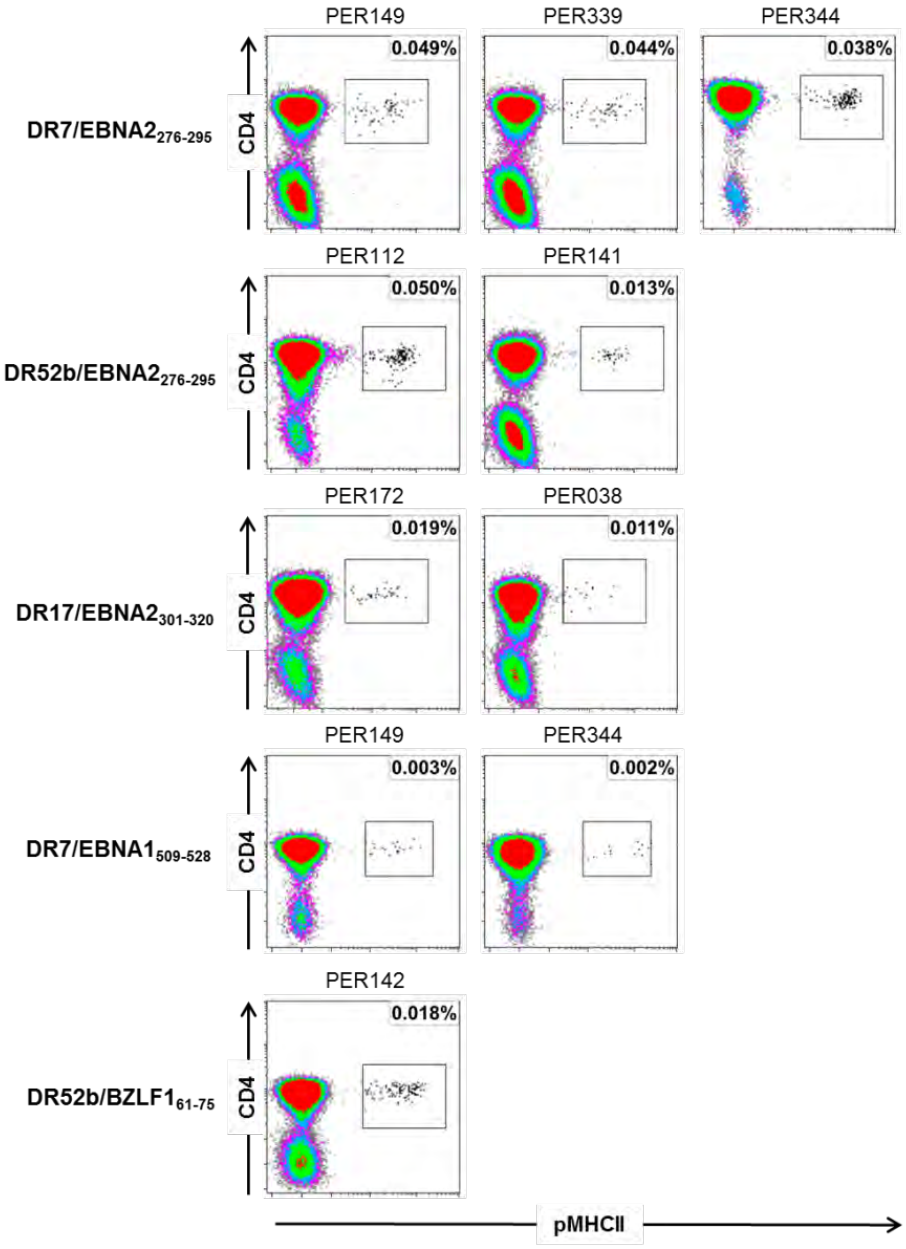

Figure 3.1. EBV-specific CD4$^+$ T cells are detectable in the circulation of long-term healthy carriers. CD4 enriched PBMCs from healthy lab donors were stained with the relevant EBV-pMHCII tetramer according to their HLAII type (Table 2.1). The percentage in each plot indicates EBV-pMHCII$^+$ frequency in the total CD4$^+$ T cell population.

We next investigated the memory phenotype of the EBV-specific CD4$^+$ T cells in our healthy donor cohort. Representative examples of CCR7 and CD45RA staining in the total CD4$^+$ and EBV-pMHCII$^+$ populations of healthy EBV carriers HC211 and HC243 are

shown in Fig 3.2a. In both donors, the EBV-pMHCII$^+$ CD4$^+$ T cells predominantly lay in the CCR7$^+$ CD45RA$^-$ T_{CM} and CCR7$^-$ CD45RA$^-$ T_{EM} compartments. This pattern held true in across the EBV-specific CD4$^+$ T cells in all the donors from our cohort, with a relatively even split between the T_{CM} and T_{EM} compartments (mean 43.4% *versus* 49.8%; NS; Fig 3.2b). The current data corresponds with a previous study using EBV-pMHCII tetramers, in which the majority of EBV-specific CD4$^+$ T cells displayed a T_{CM} or T_{EM} memory phenotype (259). Similarly to the earlier study, we also detected small populations of CD4$^+$ T cells specific for EBV epitopes with a naïve-like CCR7$^+$ CD45RA$^+$ phenotype (mean 5.5%).

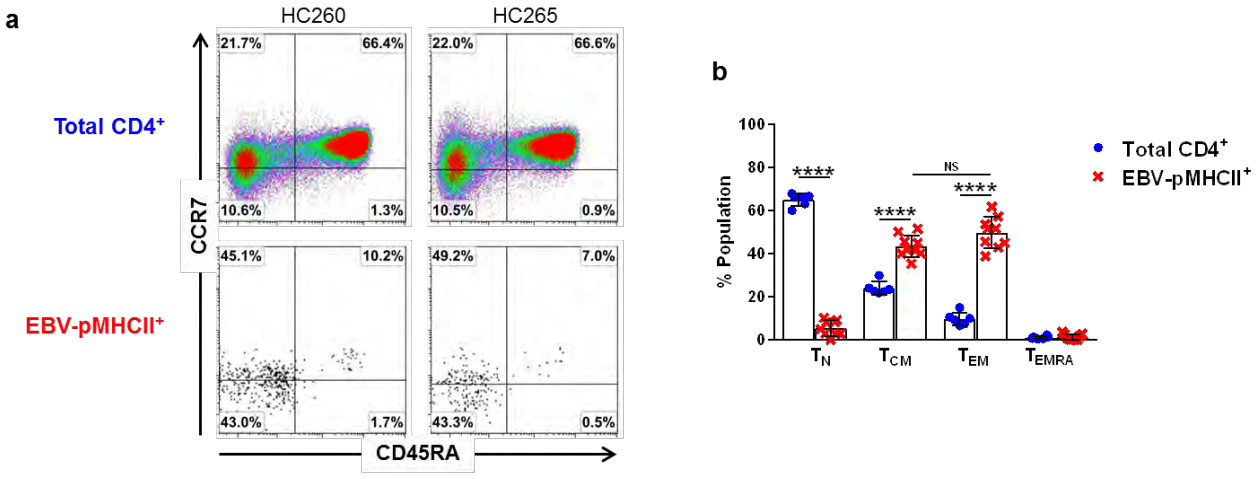

Figure 3.2. Phenotype of EBV-pMHCII$^+$ CD4$^+$ T cells in healthy carriers. (a) Analysis of CCR7 and CD45RA surface expression in the total CD4$^+$ (top) and DR7/EBNA2$_{276\text{-}295}$-specific CD4$^+$ T cells (bottom) of healthy carriers. **(b)** Summary of memory phenotypes within the total CD4$^+$ (blue dots) and EBV-pMHCII$^+$ populations (red crosses). The graph depicts results from 9 independent experiments. Data are shown as mean ± SD. **** $P < 0.0001$; unpaired Student's *t* test with Welch's correction.

The various functional subsets of CD4+ T cells are each associated with expression of a characteristic master transcription factor and secretion of a specific set of cytokines. To date, functional profiling of EBV-specific CD4$^+$ T cells has primarily been based on

analysing cytokine production from cultured T cells stimulated with peptide pools and virus lysate (269, 270, 275, 280, 286, 420). Here, we used our panel of EBV-pMHCII tetramers and multi-colour flow cytometry to analyse transcription factor expression in EBV-specific CD4+ T cells *ex vivo*. Fig 3.3a shows a representative example of total PBMCs (top plots) stained for the transcription factors associated with the T_H1 subset (T-bet), T_H2 (Gata3) and regulatory T cell population (FoxP3). In this donor, 74.15% of the total $CD4^+$ T cell population stained positively for T-bet, 2.77% were positive for Gata3 and 5.81% for FoxP3. Similar analysis in the EBV-pMHCII$^+$ $CD4^+$ population (Fig 3.3a bottom plots) showed that the majority cells were positive for the T_H1 master transcription factor T-bet. However, we did not detect any expression of Gata3 or FoxP3 cells in the EBV-pMHCII$^+$ population. A summary of the transcription factor expression in the total $CD4^+$ T cell and EBV-pMHCII$^+$ populations across all donors tested is shown in Fig 3.3b. In 13 donors assayed, T-bet expression in the EBV-pMHCII$^+$ $CD4^+$ T cells was significantly higher compared to the total $CD4^+$ population (mean 72.4% versus 55.0%; $P < 0.001$). In contrast, we did not detect significant differences in Gata-3 expression between the EBV-pMHCII$^+$ and total $CD4^+$ T cell populations (mean 1.44% *versus* 1.92%; NS). Interestingly, the mean expression of FoxP3 was significantly lower in the EBV-pMHCII$^+$ $CD4^+$ T cells compared to the total $CD4^+$ population (mean 0.83% *versus* 4.12%; $P < 0.0001$). Transcription factor analysis would therefore suggest that the vast majority of EBV-specific $CD4^+$ T cells belong to the T_H1 subset of $CD4^+$ T cells.

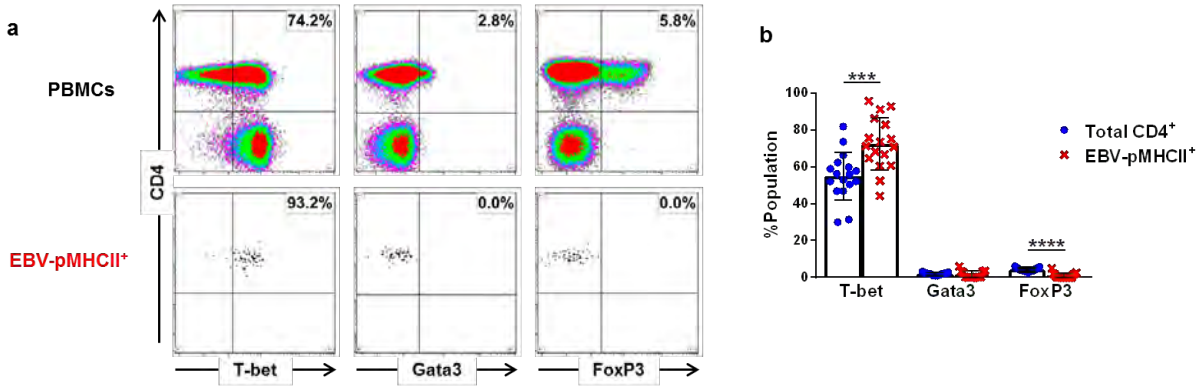

Figure 3.3 Transcription factor expression in EBV-specific memory CD4$^+$ T cells. CD4 enriched PBMCs from healthy EBV carriers were stained with EBV-pMHCII followed by intracellular staining for transcription factors. **(a)** Representative example of T-bet (left), Gata3 (middle) and FoxP3 (right) in the total CD4$^+$ (top) and EBV-pMHCII$^+$ population (bottom). The percentage in each plot indicates frequency in the total CD4$^+$ T cell population **(b)** Summary of transcription factor expression in total CD4$^+$ (blue dots) and EBV-specific pMHCII tetramer$^+$ CD4$^+$ T cell populations (red crosses). The graph depicts results from 17 independent experiments. Data are shown as mean ± SD. *** $P < 0.001$, **** $P < 0.0001$; unpaired Student's *t* test with Welch's correction.

We next investigated the cytokine profile of pMHCII cells when stimulated with their cognate epitope peptide *ex vivo*. These experiments required peptide stimulation followed by staining with the corresponding EBV-pMHCII tetramer, and subsequent intracellular cytokine staining. However, in order to perform this assay, careful optimisation was needed due to TCR competition for peptide and pMHCII tetramer. Downregulation of TCR from the T cell surface occurs following recognition of peptide, thus inhibiting pMHCII tetramer binding. We determined that PBMCs stimulated with peptide at a working concentration of 0.005µg/ml for four hours maintained sufficient TCR on the cell surface to enable EBV-pMHCII tetramer binding and analysis of cytokine production in the antigen-specific population. A representative example of the cytokine

staining observed in DR7/EBNA2$_{276-295}$ pMHCII-specific CD4$^+$ T cells is shown in Fig 3.4a. In this donor an equivalent frequency of EBV-pMHCII$^+$ CD4$^+$ T cells were detected in the cells incubated without peptide (left-hand plot) and with peptide (right-hand plot). Confirming that pMHCII binding alone did not trigger signalling from the TCR resulting in cytokine production from pMHCII$^+$ cells, we did not detect any production of the analysed effector cytokines in the absence of peptide stimulation (Fig. 3.4a left-hand plots). Following short-term *ex vivo* peptide stimulation a significant proportion of DR7/EBNA2$_{276-295}$-specific CD4$^+$ T cells in this donor produced the effector cytokines interferon gamma (IFNγ), tumour necrosis factor alpha (TNFα), and interleukin-2 (IL-2) (Fig. 3.4b right-hand plots). Interestingly, all IFNγ and IL-2 producing T cells also produced TNFα (Fig 3.4b first and third rows) thus indicating that the responding CD4$^+$ T cells are polyfunctional. In contrast, we could not detect production of IL-4 or IL-10, cytokines associated with the Gata3$^+$ T$_H$2 and FoxP3$^+$ T$_{reg}$ subsets respectively (Fig 3.4b bottom panels), or GM-CSF, a cytokine used to identify responding EBV-specific CD4$^+$ T cells *in vitro* (422, 423), or the T follicular helper cell associated cytokine IL-21. Although 21.4% of DR7/EBNA$_{276-295}$-specific CD4$^+$ T cells did not produce any of the cytokines in our flow cytometry panel, overall this data is in accordance with the previous detection of the transcription factor T-bet (Fig 3.3a) and supports a T$_H$1-like CD4$^+$ T cell profile.

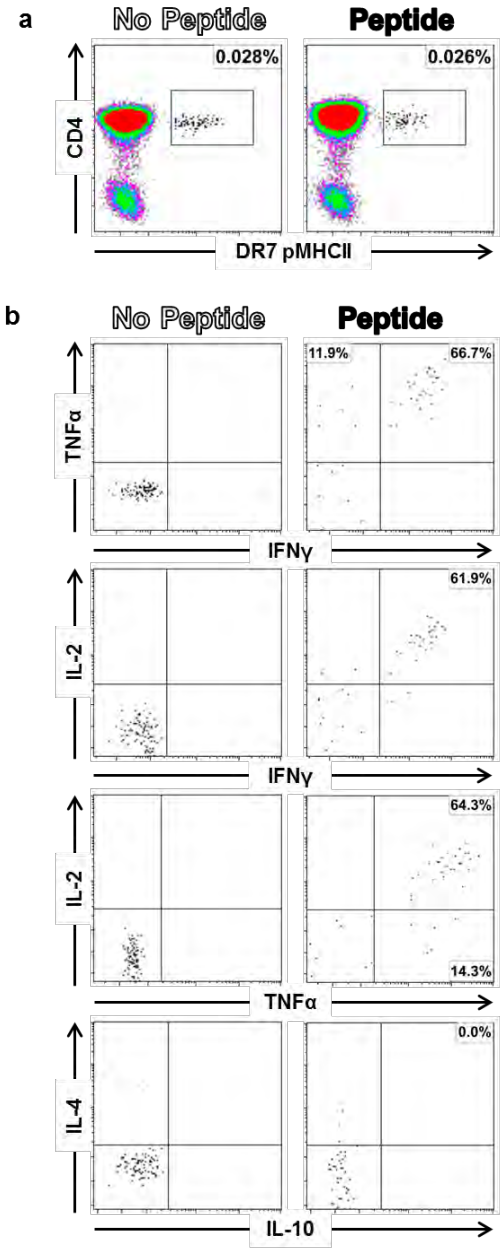

Figure 3.4. Cytokine production of EBV-pMHCII$^+$ CD4$^+$ T cells following peptide stimulation. CD4-enriched PBMCs from a representative DR7$^+$ healthy carrier were either unmanipulated or stimulated with EBNA2$_{276-295}$ peptide in the presence of protein transport inhibitors, stained with DR7/EBNA2$_{276-295}$ tetramer, and analysed by flow cytometry for intracellular expression of IFNγ, TNFα, IL-2, IL-4 and IL-10. **(a)** Representative DR7/EBNA2$_{276-295}$ tetramer staining of unmanipulated (left panel) and peptide-stimulated PBMCs (right panel). The percentage in each plot indicates EBV-pMHCII$^+$ frequency in the total CD4$^+$ T cell population. (**b**) Cytokine production in unmanipulated (left column) and peptide-stimulated DR7/EBNA2$_{276-295}$ tetramer$^+$ CD4$^+$ T cells (right column).

These results provide an interesting insight into the ex vivo functional profile of $CD4^+$ T cells, however we next sought to investigate the response to a more physiologically relevant stimulus by challenging the T cells with EBV-infected cells. To do this we generated autologous lymphoblastoid cell lines (LCLs), which are immortalised EBV-infected B cell lines. Once established, the cell line will naturally process and present viral antigens on the surface through MHCII molecules, enabling recognition by $CD4^+$ T cells (242). LCLs have been used in number of *in vitro* settings to characterise the ability of cultured EBV-specific $CD4^+$ T cells to recognise viral peptides presented on the surface of an $MHCII^+$ EBV-infected B cells. However, performing stimulations directly *ex vivo* allows us to investigate the ability of circulating EBV-specific memory $CD4^+$ T cells in the circulation to immediately respond without prior *in vitro* activation.

A representative example of cytokine production following ex vivo LCL stimulation is shown in Fig 3.5. In the control unstimulated PBMCs we could not detect any spontaneous production of IFNγ, TNFα or IL-2 (left-hand plots). However, following overnight incubation with autologous LCLs we could detect low but reproducible frequencies of $CD4^+$ T cells producing effector cytokines. In this representative donor, 0.1% of $CD4^+$ T cells produced IFNγ in direct response to the EBV-infected B cells, with 0.2% producing TNFα and 0.1% producing IL-2 (right-hand plots). These experiments show that at least some circulating EBV-specific memory $CD4^+$ T cells can directly recognise EBV-infected B cells directly *ex vivo*.

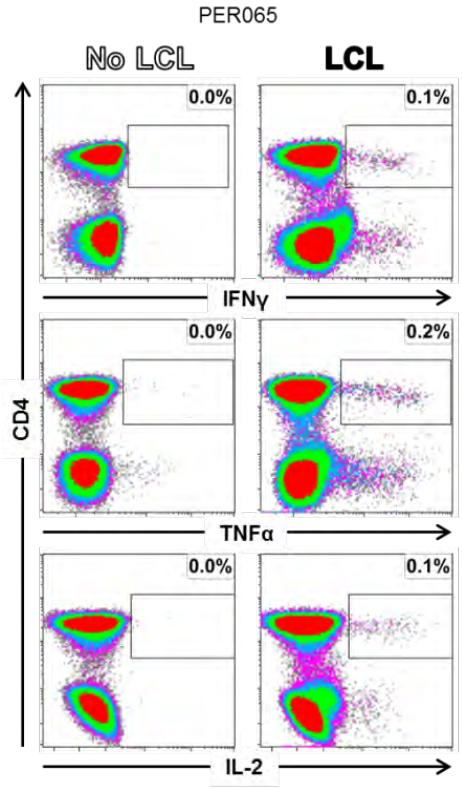

Figure 3.5 EBV-specific memory CD4$^+$ T cells directly recognise autologous LCL *ex vivo*

PBMCs from healthy carriers were either unmanipulated (left panel) or stimulated with autologous LCLs in the presence of protein transport inhibitors (right panel) and analysed by flow cytometry for intracellular expression of IFNγ, TNFα, and IL-2. A minimum of 1 x 10^6 cells were analysed. The percentage in each plot indicates cytokine production in the total CD4$^+$ T cell population.

b. Expansion of polyfunctional EBV-specific CD4$^+$ T cells during primary infection

An advantage of studying the immune response to EBV is the possibility to clinically identify individuals undergoing acute primary infection. This provided an opportunity to compare the functional profile of EBV-specific CD4$^+$ T cells in primary infection, in which our laboratory has previously shown expanded populations of CD4$^+$ T cells against a broad range of viral antigens are present (259). We first screened our bank of IM donors who had donated blood during acute primary EBV infection for amenable HLAII alleles

by PCR and assessed the frequencies of EBV-specific $CD4^+$ T cell populations by EBV-pMHCII staining. In accordance with the earlier research performed in our laboratory, higher frequencies of EBV-specific $CD4^+$ T cells were detected in donors recently diagnosed with acute IM compared to healthy carriers. Representative examples of staining with 4 different EBV-pMHCII tetramers are shown in Fig 3.6. Across all the epitopes tested, frequencies of EBV-$pMHCII^+$ $CD4^+$ T cells were higher in acute IM than in healthy carriers (Fig 3.1). As was seen in our healthy donor cohort, the largest frequencies of EBV-$pMHCII^+$ $CD4^+$ T cells were observed with the $EBNA2_{276-295}$ epitope however this was more striking in the $DR7^+$ donors (0.73% in donor IM211, 1.63% in donor IM243 and 0.37% in donor IM273; top row) compared to $DR52b^+$ donors (0.28 and 0.16% in donors IM201 and IM 271 respectively; second row). Astonishingly, the expanded population of DR7/$EBNA2_{276-295}$-specific $CD4^+$ T cells in donor IM243 accounted for 1.63% of the total $CD4^+$ T cell population. This was more than twice the second largest response seen in any donor (0.73% in IM211) and represented a 33-fold increase compared to the highest frequency observed in our healthy carrier cohort (PER149; Fig 3.1). In contrast, although the DR7/$EBNA2_{276-295}$-specific response was significantly lower in IM211 (0.73%), the frequency of $CD4^+$ T cells specific for the lytic protein derived $BaRF1_{185-199}$ epitope was higher than that seen in IM243; 0.36% compared 0.29% (second row). Throughout our IM cohort, the frequencies of $CD4^+$ T cells specific for latent epitopes were generally higher compared to lytic epitopes.

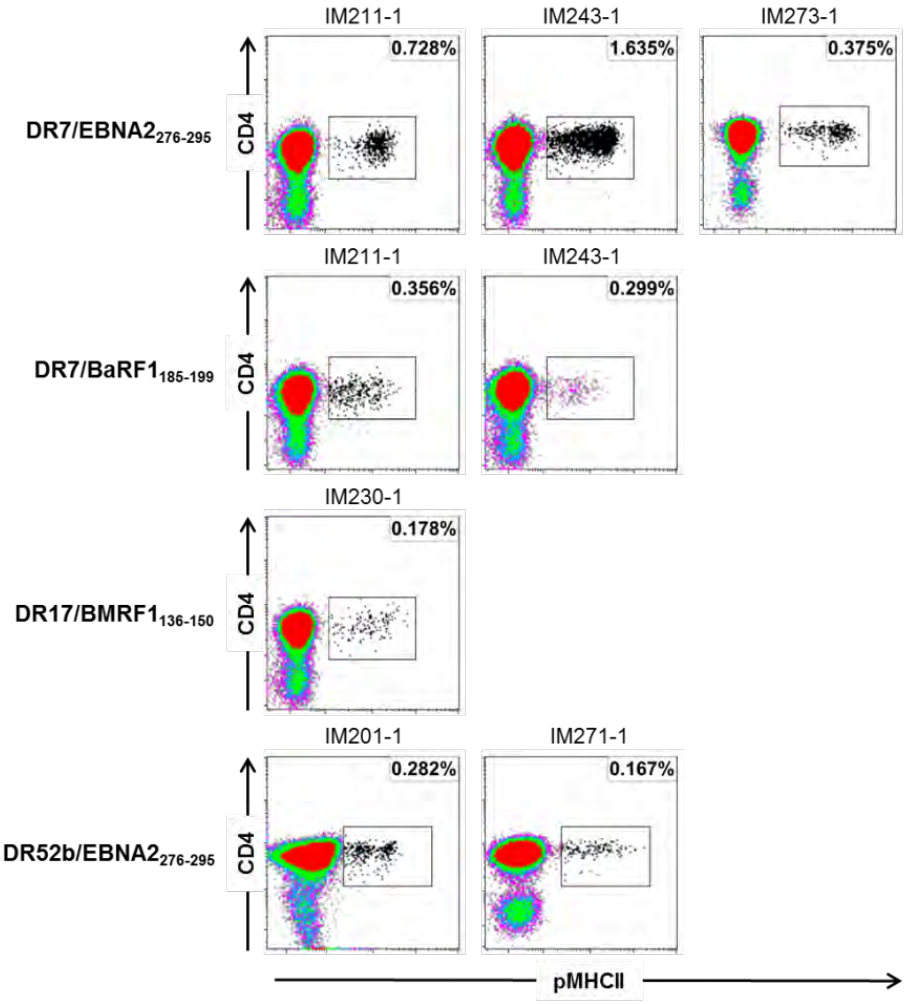

Figure 3.6 Expanded populations of EBV-specific CD4⁺ T cells in acute IM. CD4 enriched PBMCs from patients diagnosed with acute IM were stained with EBV-pMHCII tetramers appropriate for their HLAII type (Table 2.1). The percentage in each plot indicates EBV-pMHCII⁺ frequency in the total CD4⁺ T cell population.

In contrast to healthy carriers where populations of EBV-specific CD4⁺ T cells are split between T_{CM} and T_{EM} phenotypes, previous EBV-pMHCII analysis in IM donors revealed a bias towards to the T_{EM} compartment (259). This was confirmed in the IM cohort in the present study, shown in Fig 3.7a, in which higher frequencies of EBV-pMHCII⁺ CD4⁺ T cells displayed a T_{EM} phenotype compared to T_{CM}. Here, in donors IM211 and IM 243, 62.17% and 83.61% of $EBNA2_{276-295}$-specific CD4⁺ T cells respectively were in the T_{EM}

subset compared to 36.40% and 13.65% in the T_{CM}. This pattern was reflected in all the IM samples tested, with overall frequencies of T_{EM} EBV-pMHCII$^+$ CD4$^+$ T cells significantly higher compared to T_{CM} (mean 66.98% *versus* 28.28%; $P < 0.05$; Fig 3.7b).

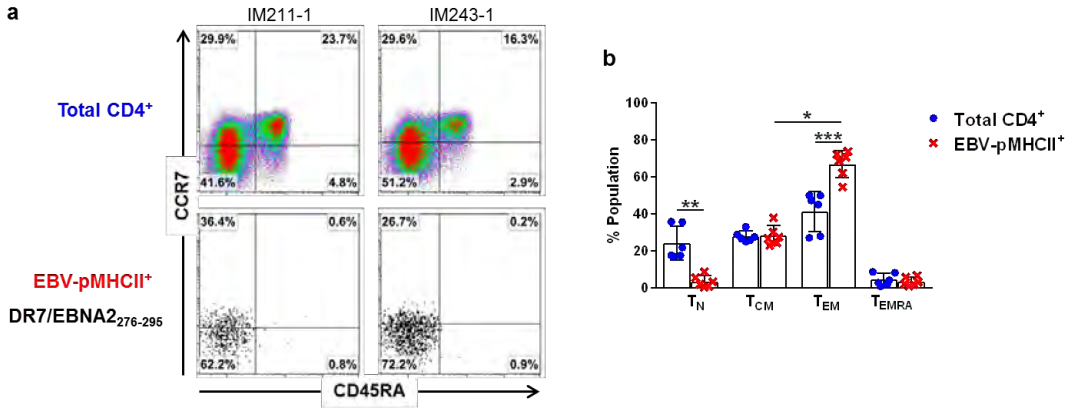

Figure 3.7 Phenotype of EBV-pMHCII$^+$ CD4$^+$ T cells in IM. (a) Analysis of CCR7 and CD45RA surface expression in the total CD4$^+$ (top) and DR7/EBNA2$_{276-295}$-specific CD4$^+$ T cells (bottom) in acute IM. **(b)** Summary of memory phenotype frequencies in the total CD4$^+$ (blue dots) and EBV-pMHCII$^+$ populations (red crosses). The graph depicts results from 6 independent experiments. Data are shown as mean ± SD. * $P < 0.05$, ** $P < 0.01$, *** $P < 0.001$; unpaired Student's *t* test with Welch's correction for comparison between total CD4$^+$ and EBVMHCII$^+$ cells; Mann-Whitney *U*-test for comparison between donor groups.

We next investigated whether CD4$^+$ T cells elicited by primary infection have the same functional profile as those maintained in memory. Initial experiments assessed transcription factor expression. Fig 3.8a shows a representative example of the T-bet and FoxP3 staining in the total PBMCs (top plots) and in CD4$^+$ T cells stained positively for the EBNA2$_{276-295}$ tetramer (bottom plots). In the EBNA2$_{276-295}$-specific CD4$^+$ T cells of IM232 we detected T-bet expression in 96.13% and FoxP3 in 0.00% of the population. A summary of T-bet and FoxP3 expression in the total CD4$^+$ T cell and EBV-pMHCII$^+$ populations from 4 acute IM donors is shown in Fig 3.8b. T-bet expression was near

universal in the EBV-pMHCII$^+$ CD4$^+$ T cell populations, significantly exceeding expression in the CD4$^+$ T cell population (mean 98.5% *versus* mean 79.0%; $P < 0.05$). Furthermore, expression of this T_H1 associated transcription factor in EBV-pMHCII$^+$ CD4$^+$ T cells of IM donors was significantly elevated compared to that previously observed in healthy carriers ($P < 0.01$; Fig 3.3b). Conversely, expression of FoxP3 in the EBV-pMHCII$^+$ CD4$^+$ T cell population in acute IM donors was absent (mean 0.01%).

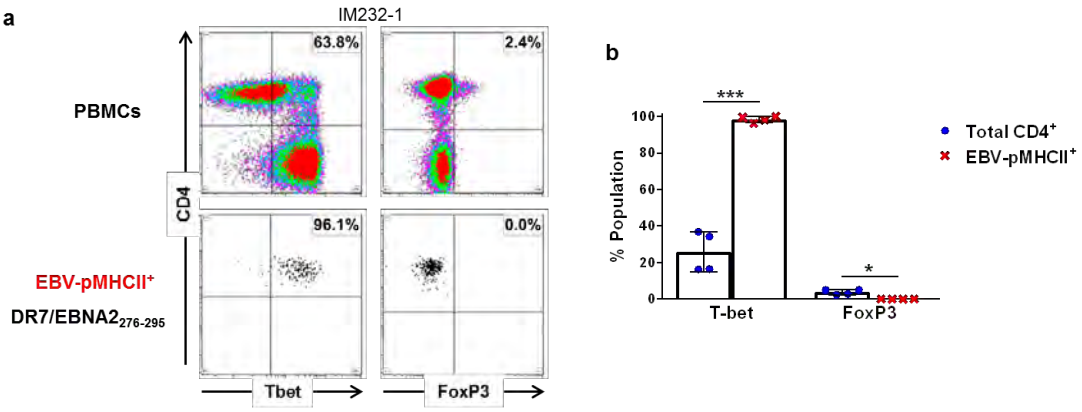

Figure 3.8 Transcriptional profile of EBV-specific CD4$^+$ T cells in acute IM. CD4 enriched PBMCs from IM donors were stained with EBV-pMHCII followed by intracellular staining for transcription factors. **(a)** Representative example of T-bet (left) and FoxP3 (right) in the total CD4$^+$ (top) and DR7/EBNA2$_{276-295}$-specific CD4$^+$ population (bottom). The percentage in each plot indicates TF expression in the total CD4$^+$ T cell population **(b)** Summary of transcription factor expression in unstimulated total CD4$^+$ (blue dots) and EBV-specific pMHCII tetramer$^+$ CD4$^+$ T cell populations (red crosses). The graph depicts results from 4 independent experiments. Data are shown as mean ± SD. * $P < 0.05$, *** $P < 0.001$; unpaired Student's *t* test with Welch's correction.

We next hypothesised that within the expanded T_H1 cells present in IM patients, a higher proportion of EBV-specific CD4$^+$ T cells would be primed to immediately respond to viral antigens *ex vivo*. We therefore attempted to perform sequential peptide stimulation followed by EBV-pMHCII staining as had been possible with PBMCs from healthy carriers (Fig 3.4), but we were unable to successfully optimise the assay as the cells did not

survive the incubation. Furthermore, when we performed overnight stimulations with autologous LCL with the same protocol as was used for healthy carriers (Fig 3.4), relatively few $CD4^+$ T cells remained viable for analysis. This could potentially be explained by activation-induced cell death (AICD) or the absence of the anti-apoptotic protein Bcl-2 T cells from acute IM patients (424, 425). Nonetheless, following LCL stimulation, we could still detect increased frequencies of responding $CD4^+$ T cells producing effector cytokines compared to healthy carriers, a representative of which is shown in Fig 3.9a. In this acute IM donor 1.17% of the total $CD4^+$ T cells produced IFNγ with 0.91% producing TNFα and 0.19% making IL-2. The concatenated data from LCL stimulations performed in 8 independent experiments with 4 IM donors and 4 healthy carriers is shown in Fig 3.10a. Across all 3 effector molecules measured, the frequency of cytokine producing cells was higher in $CD4^+$ T cells from IM patients than healthy carriers, with production of IFNγ and TNFα raised by 12-fold and 6-fold in IM versus healthy carriers respectively. The responding $CD4^+$ T cells in IM also made more IL-2 than in healthy carriers (mean 0.23% *versus* 0.08%) although this only represented a near 3-fold increase. Interestingly, while in healthy carriers a greater frequency of cells made TNFα than IFNγ (mean 0.17% *versus* 0.11%), during acute IM IFNγ was the dominant cytokine made (1.33% *versus* 0.99%). To compare the polyfunctionality of $CD4^+$ T cells responding to autologous LCL, we used software designed for data mining multicolour flow cytometry.

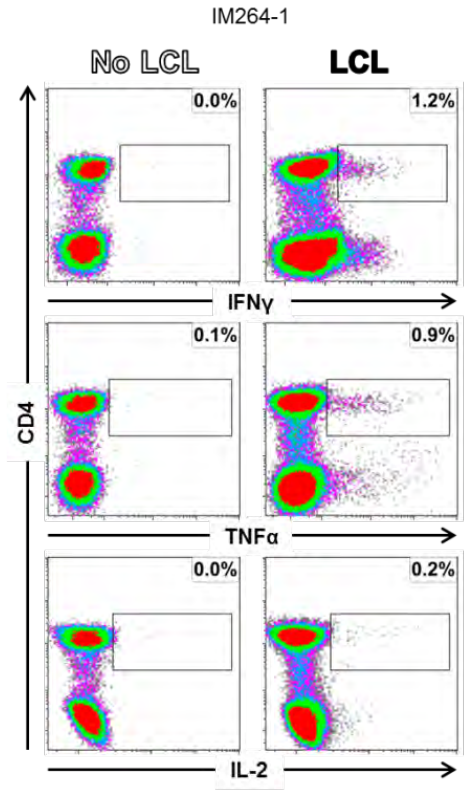

Figure 3.9 Acute IM drives expanded populations of EBV-specific CD4⁺ T cells able to respond to LCL *ex vivo*. PBMCs from IM donors were either unmanipulated or stimulated with autologous LCLs in the presence of protein transport inhibitors, and analysed by flow cytometry for intracellular expression of IFNγ, TNFα, and IL-2. The percentage in each plot indicates cytokine production in the total CD4⁺ T cell population.

Analysis using SPICE software enabled us to visualise and compare the complete cytokine profile of responding CD4⁺ T cells in the two cohorts. The pie charts shown in Fig 3.10b illustrate the number of functions (segments) as well as the individual cytokine or cytokines produced (arcs). As mentioned earlier, substantially higher frequencies of responsive CD4⁺ T cells were detected in patients with IM compared with healthy carriers (Fig 3.8b), however the cytokine profile between the two cohorts was also markedly different. Most noticeable is the increase in polyfunctionality of responding CD4⁺ T cells in healthy carriers compared to IM patients. Indeed, a mean of 23.2% of

cytokine producing CD4$^+$ T cells in healthy carriers simultaneously produced IFNγ, TNFα and IL-2 compared to a mean of 6.5% in IM ($P < 0.05$; Fig 3.8 c light grey sections). A factor contributing to this raised polyfunctionality is the more frequent production of IL-2 during chronic infection (mean 40.0% *versus* 11.4% in IM, $P < 0.05$; Fig. 2d). As noted earlier, IFNγ was the dominant cytokine produced by patients with IM and was present in a mean of 81.9% (blue arcs) of responding CD4$^+$ T cells compared to a mean of 54.0% for TNFα production (orange arcs) ($P < 0.05$). Conversely TNFα was the dominant cytokine produced by responsive CD4$^+$ T cells in healthy carriers (mean 75% for TNFα *versus* mean 64.8% for IFNγ).

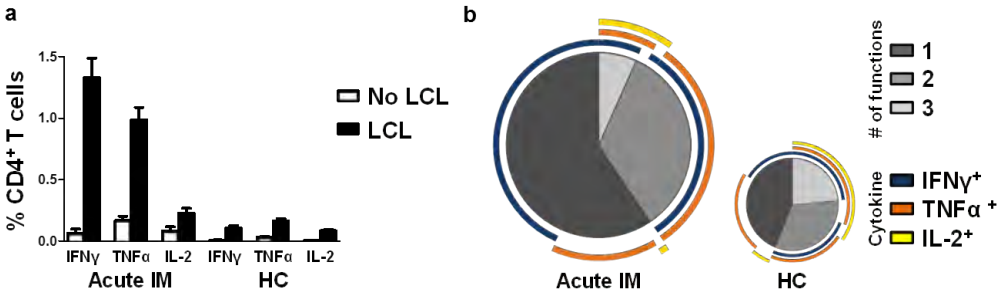

Figure 3.10 EBV-specific CD4$^+$ T cells responding to LCL *ex vivo* are polyfunctional. (a) Summary graphs depicting intracellular expression of IFNγ, TNFα, and IL-2 in unmanipulated PBMCs (unfilled) or stimulated with autologous LCLs (filled) from patients with IM and healthy carriers. Results are from 8 independent experiments with a minimum of 4 donors. HC, healthy carrier. **(b)** SPICE plots illustrating the functional profiles of CD4$^+$ T cells from patients with IM and healthy carriers (HC) responding to autologous LCLs. Image sizes are scaled to reflect the overall numbers of responding cells. Each pie chart segment displays the fraction of responding cells producing the number of cytokines indicated in the key. Arcs show the distribution of each individual function.

3. Discussion

Using EBV-pMHCII we identified a cohort of healthy EBV carriers and a cohort of acute IM patients with detectable responses to one or multiple lytic and latent epitopes that would allow further analysis of the phenotypic and functional evolution of the EBV-specific $CD4^+$ T cells (Fig 3.1 and 3.6).

The cytokine profile typically observed in EBV-specific $CD4^+$ T cells is associated with a T_H1-like phenotype. Here we show using *ex vivo* staining with MHCII tetramers that $CD4^+$ T cells from healthy carriers responding to short term peptide stimulation were polyfunctional, producing IFNγ, TNFα and IL-2, characteristic of the anti-viral T_H1 subset (Fig 3.4). IFNγ in particular plays an important role in viral immune responses by upregulating antigen processing and presentation (95, 96), promoting cytotoxic $CD8^+$ T cell differentiation (426) and enhancing phagocytic ability of macrophages (94). The functional profile of antigen-specific T cells identified using tetramers had previously only been performed in $CD8^+$ T cells showing that detection of IFNγ, TNFα and MIP-1β production in CMV-specific cells following peptide stimulation was possible (358). Furthermore, *ex vivo* transcription factor analysis confirmed the prevalent expression of the T_H1 master regulator T-bet that would drive this functional profile (Fig 3.3). Production of IL-4 and IL-10 by EBV-specific $CD4^+$ T cells that could indicate a T_H2 or T_{reg}-like response has been reported *in vitro* (282, 284). However, we did not detect any *ex vivo* expression of the cytokines or the transcription factors associated with these subsets for the epitopes used. Additionally, production of cytokines was not universal within the stimulated EBV-pMHCII$^+$ $CD4^+$ T cells, which is consistent with a proportion of

cells residing in the T_{CM} pool and do not possess the rapid effector functions of T_{EM} (Fig 3.2) (171, 259, 269).

We were however able to determine the cytokine profile of EBV-specific $CD4^+$ T cells responding directly to EBV-infected B cells in both cohorts using autologous LCLs. The wide array of EBV antigens presented on the surface of infected cells provides a more physiologically relevant stimulus and here we demonstrated *ex vivo* reactivity in both groups in the absence of prior activation or expansion *in vitro* (Fig 3.9 and 3.5). While MHCII restricted direct recognition of LCLs by $CD4^+$ T cells has previously been demonstrated *in vitro* (276-279, 281, 287, 418), our results indicate that direct effector function *in vivo* also occurs. $CD4^+$ T cells responding to stimulation with LCLs produced the same effector cytokines as was previously observed for peptide stimulation but with fewer functions per cell. The natural presentation of epitopes on the surface of EBV-infected B cells providing a weaker antigenic stimulation (427) and the differences in the broadly targeted $CD4^+$ T cell response to EBV could account for these observations (190, 282, 284). Importantly, in primary infection, where expanded populations of EBV-specific $CD4^+$ T cells have been observed (259), significantly greater percentages of circulating $CD4^+$ T cells immediately responding to LCL were detected in comparison to healthy donors (Fig 3.9 and 3.10). The higher proportion of EBV-$pMHCII^+$ $CD4^+$ T cells with a T_{EM} phenotype (Fig 3.7) and higher expression of T-bet observed in these populations in IM may also play a role in the raised responsiveness (420).

Moreover, the cytokine profile in responding $CD4^+$ T cells was different between the two cohorts. In IM, responding $CD4^+$ T cells had fewer functions and IFNγ was the

predominant cytokine detected whereas in healthy donors TNFα dominated, akin to what has been observed in long-term CMV carriers (336). The increase in polyfunctionality during persistent infection is in line with previous *in vitro* studies implicating polyfunctional $CD4^+$ T cells in the long-term control of EBV (280, 286, 420) and CMV (335). Presence of polyfunctional cells in persistent viral infections could reflect the preferential selection of $CD4^+$ T cells with increased function into memory (335) or acquisition of effector functions through repeated antigen exposure (427). Polyfunctional T cells have been associated with better quality long term $CD4^+$ T cell immunity (428).

In summary, we have shown that circulating EBV-specific $CD4^+$ T cells can respond to EBV-infected B cells directly *ex vivo*. Furthermore, they are polyfunctional with a T_H1-like cytokine profile. Importantly, higher frequencies of cytokine producing $CD4^+$ T cells were observed in IM where IFNγ was the dominant cytokine produced in response to EBV-infected B cells however the functional profile of EBV-specific $CD4^+$ T cells changes over the course of infection becoming more polyfunctional dominated by TNFα production.

CHAPTER 4

CYTOTOXIC PROFILE OF EBV-SPECIFIC CD4$^+$ T CELLS

1. Introduction

In recent years, the ability of some CD4$^+$ T cells to exert direct cytotoxicity against antigen-expressing MHCII+ target cells has become appreciated. EBV-infected B cells uniformly express MHC-II, and multiple groups have demonstrated the ability of *in* vitro cultured EBV-specific CD4$^+$ T cell lines and clones to recognise and kill autologous LCL (276-279, 281, 287, 418, 419). Cytotoxic function in CD4$^+$ T cells has long been attributed to the progressive differentiation that occurs *in vitro* as a result of repeated antigen exposure, and the *in vivo* relevance of CD4-CTLs has been poorly studied. Given the constitutive expression of MHC-II on the surface of EBV-infected B cells, such cytotoxic capacity *in vivo* would be highly advantageous. Furthermore, harnessing EBV-specific CD4-CTLs with the capacity to eliminate infected cells could potentially inform the design of treatments to combat EBV-associated malignancies.

Human CD4-CTLs have been identified *ex vivo* in the context of chronic viral infections such as HIV (271, 330), Dengue virus (177, 339) , CMV (336) and hepatitis (334). These early observations have suggested a key role for chronic antigen exposure and advanced stages of differentiation in the acquisition of cytotoxic properties. Thus, identification of cellular markers that would allow further characterization of this subset have predominantly come from studies of chronic infections (177, 336, 337, 339, 360, 370, 372, 429-431). However, occasional studies have also reported CD4-CTLs in the acute

stages of primary HIV (343), CMV (372) and Influenza infection (340) as well as following immune challenge with vaccines (432). Moreover, elevated expression of the cytotoxic protein Perforin has been detected in the total $CD4^+$ T cell pool of IM patients (271). Importantly, in mice, presence of CD4-CTLs following vaccination against yellow fever (324) and influenza (345) has been associated with better clinical outcome. Therefore, inducing CD4-CTLs is now considered an important goal for future vaccine design against many pathogens. However, first a greater understanding of their role in natural viral infection is required.

We have previously shown that EBV-specific $CD4^+$ T cells can directly recognise LCLs *ex vivo* in both acute and persistent infection (Fig 3.5 and 3.9), thus we investigated the presence of $CD4^+$ T cells with cytotoxic capacity in healthy carriers and IM patients.

2. Results

a. EBV-specific $CD4^+$ T cells degranulate following exposure to EBV-infected B cells.

Alongside profiling the cytokine production in EBV-specific $CD4^+$ T cells responding to autologous EBV-infected B cells (Fig 3.5 and 3.9) we also measured mobilisation of CD107a on the surface of T cells.

A representative example of CD107a staining in the PBMCs of a healthy carrier following overnight autologous LCL stimulation is shown in Fig 4.1a (top plots). Concurrent with our observation that low frequencies of EBV-specific memory $CD4^+$ T cells were able to respond to autologous LCL *ex vivo* by producing cytokines (Fig 3.4), we detected small but reproducible increases in CD107a mobilisation between the unstimulated control and stimulated T cells (0.1% versus 0.3% of total $CD4^+$ T cells, respectively). In acute IM, in line with the greater frequency of $CD4^+$ T cells producing cytokines in response to overnight stimulation with EBV-transformed B cells (Fig 3.9), we also observed a much higher proportion of $CD4^+$ T cells mobilising CD107a in this cohort. In the representative IM donor shown in Fig 4.1a (bottom plots), 0.4% of $CD4^+$ T cells degranulated in the unstimulated assay compared to 2.9% of $CD4^+$ T cells following overnight incubation with EBV-infected B cells. The summary data from 4 healthy carriers and 4 acute IM patients is shown in Fig 4.1b. In both cohorts, we detected significant increases in degranulation, as shown by CD107a staining, following autologous LCL stimulation (mean 0.6% versus 2.6% in acute IM; $P < 0.001$ and mean 0.2% versus 0.5% in healthy carriers; $P < 0.001$). However this was significantly more marked in IM patients. Thus,

$CD4^+$ T cells from acute IM patients showed a 5.5-fold increase in CD107a staining compared to healthy carriers following LCL stimulation (mean 2.6% versus 0.5%; $P < 0.0001$).

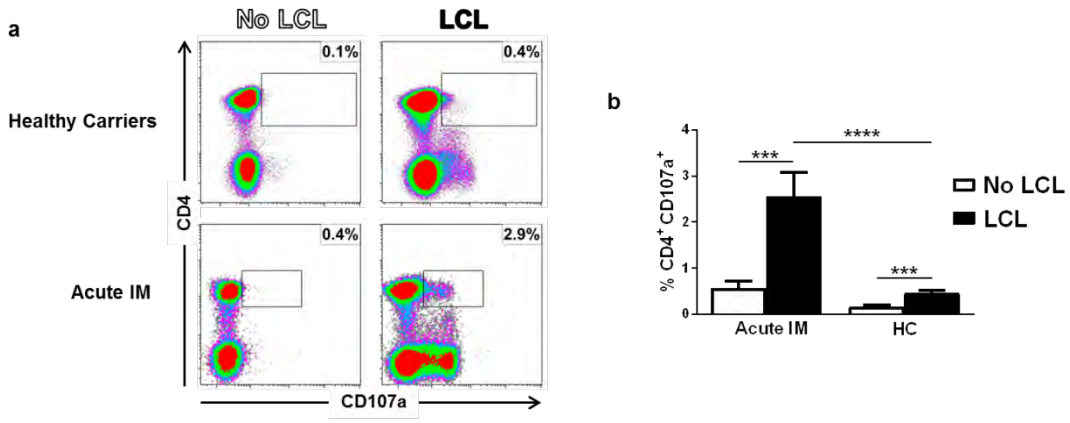

Figure 4.1 EBV-specific $CD4^+$ T cells degranulate upon exposure to EBV-infected B cells. (a) PBMCs from healthy carriers (top row) and IM donors (bottom row) were either unmanipulated (left panel) or stimulated with autologous LCLs overnight (right panel) and analysed by flow cytometry for degranulation as determined by CD107a mobilisation. The percentage in each plot indicates CD107a mobilisation in the total $CD4^+$ T cell population. **(b)** Summary graph representing multiple repeats from a minimum of 4 donors and showing the mean value with SEM. *** $P < 0.001$, **** $P < 0.0001$; Mann-Whitney *U*-test.

b. Expression of cytotoxic proteins in EBV-specific $CD4^+$ T cells

Cytotoxic proteins such as perforin and granzymes can be released into the immunological synapse as a result of degranulation, entering the target cell and initiating apoptotic pathways. Based on our observation that EBV-specific $CD4^+$ T cells can degranulate in both healthy carriers and IM donors, we therefore investigated the possibility that these cells may also contain the cytotoxic effector molecules Perforin (Perf) and Granzyme B (GzmB). To calibrate our measurements of these proteins using flow cytometry, we stained EBV-specific $CD8^+$ T cells which are known to carry both

proteins *in vivo* (433). Fig 4.2 shows the staining of Perf and GzmB in the total CD8$^+$ T cell population of two healthy carriers. As expected, expression of both cytotoxic markers was found in 36.5% of the total CD8$^+$ T cell population in donor PER149 and 30.4% in donor PER213. EBV-pMHCI tetramers loaded with an immunodominant lytic protein and a sub-dominant latent protein derived epitope, presented through the HLA-A2 and HLA-B7 molecule respectively, were subsequently used to detect EBV-specific CD8$^+$ T cells in these healthy carriers (Fig 4.2b top plots). Applying the same gating as for the total CD8$^+$ T cell populations (Fig 4.2a) we detected presence of Perf and GzmB in 69.9% of A2/BMLF1$_{259\text{-}267}$-specific CD8$^+$ T cells in donor PER149 and 43.8% of B7/EBNA3$_{378\text{-}387}$-specific CD8$^+$ T cells of donor PER293.

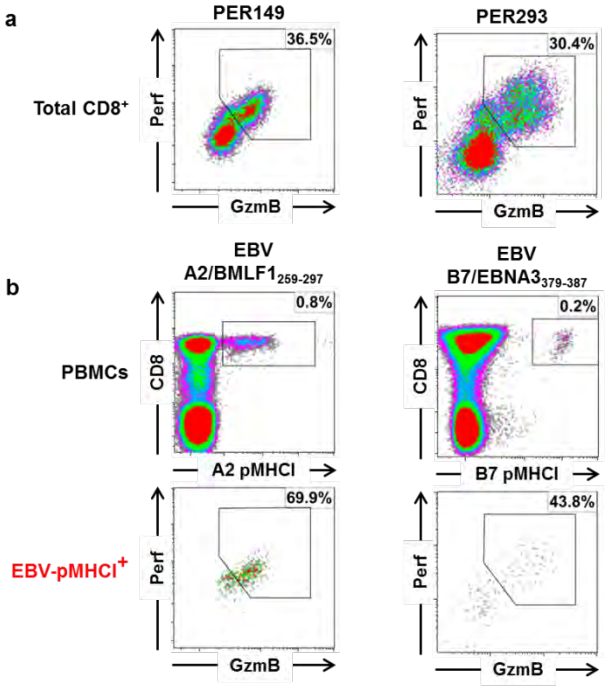

Figure 4.2 EBV-specific CD8$^+$ T cells express cytotoxic proteins. Whole PBMCs from A2$^+$ (left panel) and B7$^+$ (right panel) healthy carriers were stained with A2/BMLF1$_{259\text{-}267}$ and B7/EBNA3$_{378\text{-}387}$ tetramers respectively and analysed by flow cytometry for intracellular expression of Perf/GzmB. **(a)** Perf/GzmB expression in the total CD8$^+$ T cell pool. **(b)** A2/BMLF1$_{259\text{-}267}$ and B7/EBNA3$_{378\text{-}387}$ tetramer staining of CD3$^+$ T cells (top panels), and Perf/GzmB expression in pMHCI tetramer$^+$ CD8$^+$ T cells (bottom panels).

In contrast, when we applied the same analysis to the total $CD4^+$ T cell population in healthy carriers only low frequencies of Perf/GzmB expressing cells were detected, in line with previous reports (434). Fig 4.3a shows that co-expression of these cytotoxic markers accounted for less than 1% of the total $CD4^+$ T cell pool as in PER339 and PER344. However, in some donors, noticeably higher Perf/GzmB was observed, such as donor PER141. Interestingly, this correlated with seropositivity for the herpesvirus CMV (Fig 4.3 a; right plot). In these same donors we then assessed the expression of Perf/GzmB in the EBV-specific memory $CD4^+$ T cell populations using our panel of EBV-pMHCII tetramers. In the DR7/EBNA2$_{279\text{-}295}$-specific $CD4^+$ T cell populations, comprising 0.029% and 0.040% of the respective $CD4^+$ T cell populations of PER339 and PER344 (Fig 4.3 b, top plots), only 6.3% and 2.7% of the corresponding EBV-pMHCII$^+$ $CD4^+$ T cells expressed Perf/GzmB (Fig 4.3 b, bottom plots). Despite the higher frequency of Perf/GzmB expression in the total $CD4^+$ T cell population of donor PER141, the frequency of DR52b/EBNA2$_{279\text{-}295}$-specific $CD4^+$ T cells carrying Perf/GzmB was similar to that observed in the EBV-specific $CD4^+$ T cells in the other healthy carriers.

To compare Perf/GzmB expression in EBV-specific $CD4^+$ T cells with $CD4^+$ T cells specific for other viruses, we used pMHCII tetramers carrying epitopes from another persistent herpesvirus, CMV, and from a virus which is cleared following infection, influenza A. Firstly, we analysed the expression of cytotoxic proteins in CMV-pMHCII$^+$ $CD4^+$ T cells specific for an epitope derived from glycoprotein B, gB$_{217\text{-}228}$ restricted through HLA-DR7.

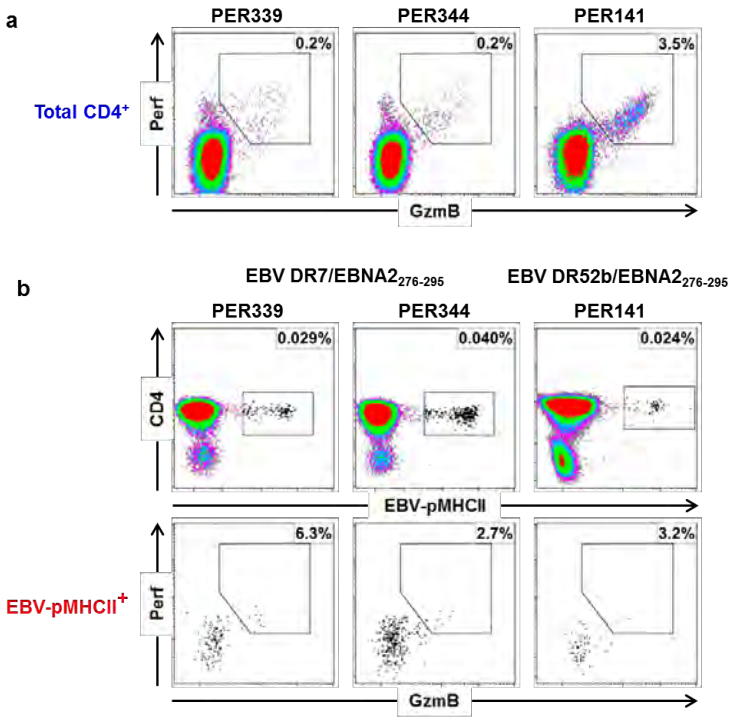

Figure 4.3 Expression of cytotoxic proteins in memory EBV-specific CD4$^+$ T cells. CD4-enriched PBMCs from healthy carriers were stained with the relevant EBV-pMHCII tetramers (Table 2.1) and analysed by flow cytometry for intracellular expression of Perf/GzmB. **(a)** Perf/GzmB in the total CD4$^+$ T cell pool shown for three representative healthy carriers. **(b)** Representative DR7/EBNA2$_{276-295}$ and DR52b/EBNA2$_{276-295}$ tetramer stains (top panels), and Perf/GzmB expression among EBV-pMHCII tetramer$^+$ CD4$^+$ T cells (bottom panels) shown for DR7$^+$ and DR52b$^+$ healthy carriers.

We detected a markedly increase in expression of Perf/GzmB in the CMV-specific CD4$^+$ T cells with 84.2% of DR7/ gB$_{217-228}$ -specific CD4$^+$ T in PER183 and 96.0% in PER213 staining positively for the cytotoxic markers (Fig 4.4a). Secondly we analysed a DR7-restricted CD4$^+$ T cell population specific for an epitope derived from the matrix protein 1 of Influenza virus A. As shown in Fig 4.4b we detected M1$_{43-59}$-specific CD4$^+$ T cells in the circulation of healthy carriers (0.012% of the total CD4$^+$ population in donor PER339 and 0.005% in PER344). In contrast to CMV, and more similarly to EBV-specific CD4$^+$ T

cells, both Perf and GzmB were completely absent from the pMHCII$^+$ CD4$^+$ T cell populations.

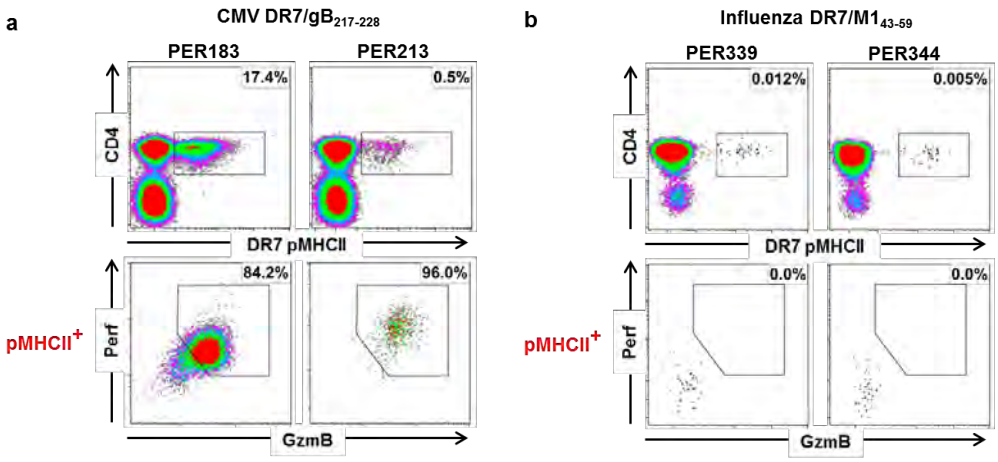

Figure 4.4 Expression of cytotoxic proteins in CMV and Influenza-specific CD4$^+$ T cells in healthy donors. CD4 enriched PBMCs from DR7$^+$ healthy carriers were stained with either gB$_{217-228}$ (CMV) or M1$_{43-59}$ (influenza) pMHCII tetramers (Table 2.1) and analysed for intracellular expression of Perf/GzmB. **(a)** DR7/gB$_{217-228}$ tetramer stains (top panels) and Perf/GzmB expression in pMHCII tetramer$^+$ CD4$^+$ T cells (bottom panels) in two CMV seropositive donors. **(b)** DR7/M1$_{43-59}$ tetramer stains (top panels) and Perf/GzmB expression in pMHCII tetramer$^+$ CD4$^+$ T cells (bottom panels).

We next turned our attention to the EBV-specific CD4$^+$ T cell populations of patients undergoing acute primary infection, where increased frequencies of CD107a mobilisation had been detected in the earlier LCL stimulation assays. Perf/GzmB expression was markedly raised in the total CD4$^+$ T cell populations of individuals undergoing primary EBV infection (Fig 4.5a) compared to that of long-term carriers (Fig 4.3a). As shown in the two representative IM donors, we detected Perf/Gzmb expression in 19.3% of the total CD4$^+$ T cell population in IM211 and 30.1% in IM243. Strikingly, this was further raised in the expanded DR7/EBNA2$_{276-295}$-specific CD4$^+$ T cells in these same donors (Fig 4.5b top plots). In the DR7/EBNA2$_{276-295}$-specific CD4$^+$ T cell

populations of IM211 and IM243 (Fig 4.5b), 79.4% and 72.8% of EBV-pMHCII$^+$ cells stained positively for Perf/GzmB respectively.

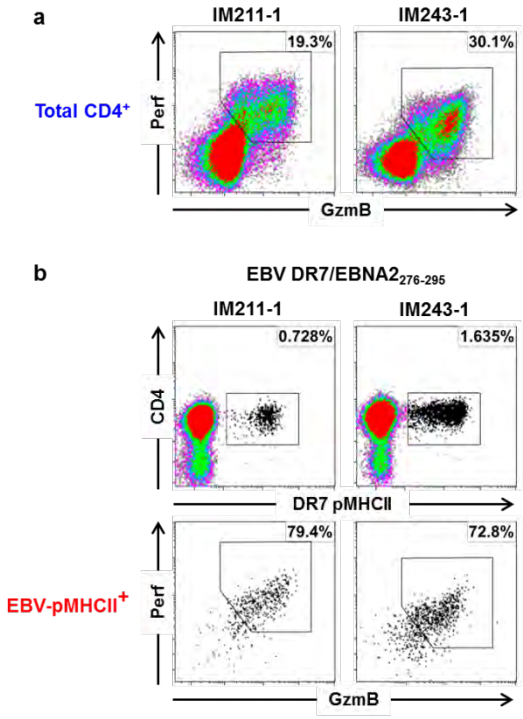

Figure 4.5 EBV-specific CD4$^+$ T cells express cytotoxic proteins in acute IM. CD4-enriched PBMCs from IM donors were stained with the relevant EBV-pMHCII tetramers and analysed for intracellular expression of Perf/GzmB. **(a)** Perf/GzmB in the total CD4$^+$ T cell pool shown for two representative patients with IM. **(b)** Representative DR7/EBNA2$_{276-295}$ tetramer stains (top panels), and Perf/GzmB expression in EBV-pMHCII tetramer$^+$ CD4$^+$ T cells (bottom panels) shown for two DR7$^+$ patients with IM.

During viral challenge it has been reported that nonspecific T cell activation, independent of TCR stimulation, can occur in a process called bystander activation. To verify whether bystander activation was contributing to the high frequency of Perf/GzmB in total CD4$^+$ T cells, we analysed expression of cytotoxic proteins in co-existent influenza matrix protein 1 epitope-specific CD4$^+$ T cells in IM donors. As shown in Fig 4.6, M1$_{43-59}$-specific CD4$^+$ T cells were detectable during primary EBV infection, but

were present at comparable frequencies to healthy carriers; 0.009% of the total $CD4^+$ T cell population in IM241 and 0.011% in IM277 (Fig 4.6 top plots). Importantly, these $M1_{43-59}$-specific $CD4^+$ T cell populations were universally negative for Perf/GzmB (Fig 4.6 bottom plots) indicating that no bystander activation of these cells occurs during acute EBV infection.

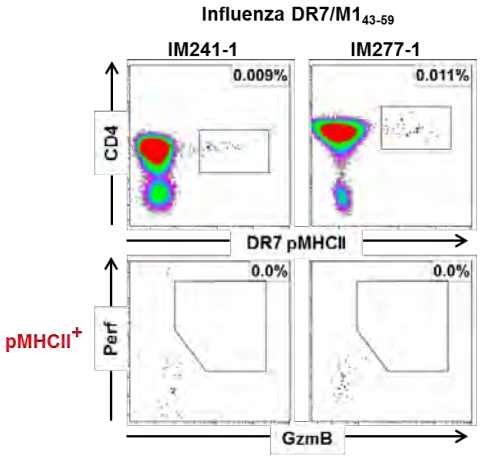

Figure 4.6 Expression of cytotoxic proteins in influenza-specific $CD4^+$ T cells in patients with acute IM. CD4-enriched PBMCs from IM donors were stained with the DR7/$M1_{43-59}$ pMHCII tetramers and analysed for intracellular expression of Perf/GzmB. DR7/$M1_{43-59}$ tetramer stains (top panels), and Perf/GzmB expression in pMHCII $tetramer^+$ $CD4^+$ T cells (bottom panels) shown for two $DR7^+$ patients with IM.

In addition to samples obtained rapidly after initial IM diagnosis, serial samples were collected from some patients in the subsequent months and years, thereby allowing us to track the functional evolution of the $CD4^+$ T cell response to EBV. The samples shown in Fig 4.7 were taken approximately 6 months following IM diagnosis. Interestingly, for both IM230 and IM 243 the frequency of Perf/GzmB expression in the total $CD4^+$ T cells was now similar to that observed in long term healthy carriers (Fig 4.3a). In the case of IM243, the frequency had reduced from 30.1% at acute infection to 2.0% during

convalescence, representing a 15-fold decrease. The frequency of EBV-specific $CD4^+$ T cells, as shown in Fig 4.7b by staining with the DR7 pMHCII $EBNA2_{276-295}$ and $BaRF1_{185-199}$ tetramers had also contracted to frequencies in the range of long term carriage (0.033% in IM230 and 0.011% IM243 respectively). However, Perf/GzmB remained noticeably elevated in the pMHCII $tetramer^+$ cells (Fig 4.7b bottom plots). In the $EBNA2_{276-295}$-specific $CD4^+$ T cell population of IM243-2 20.4% stained positively for Perf/GzmB and in IM230-2 42.2% of the $CD4^+$ T cells specific for the lytic derived epitope $BaRF1_{185-199}$ were positive for the cytotoxic proteins. These data suggest that during convalescence expression of Perf/GzmB is maintained in a proportion of the EBV-specific $CD4^+$ population even though the heavily expanded populations observed during primary infection have waned to levels typical of long term carriage.

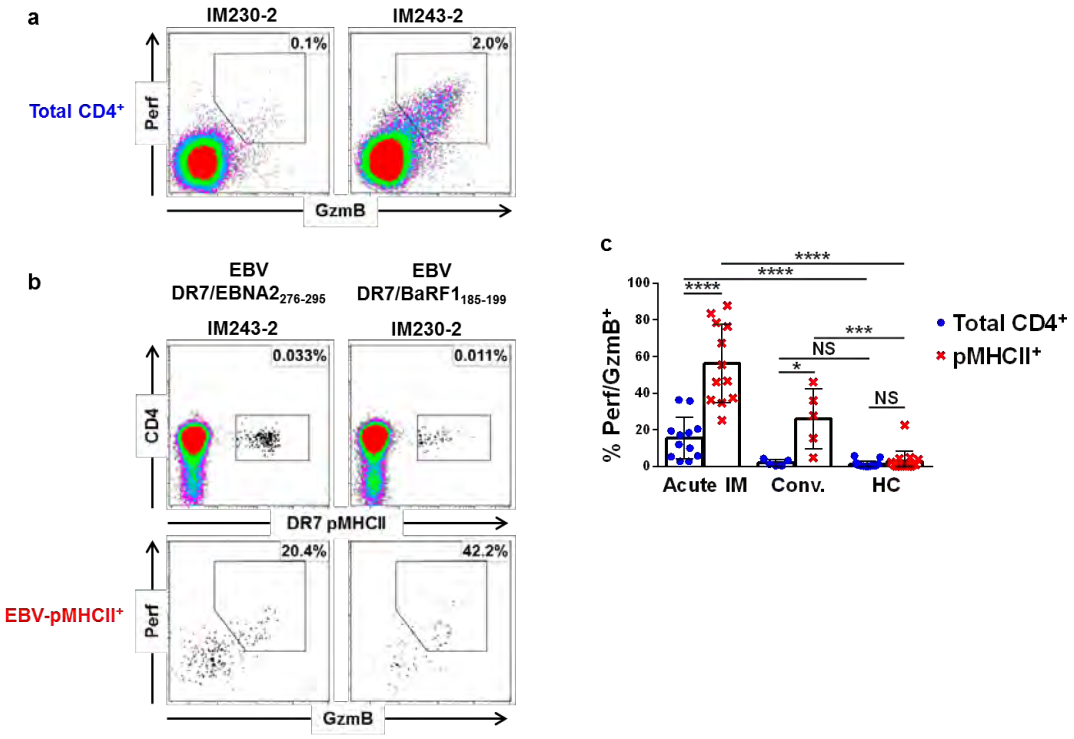

Figure 4.7 Expression of cytotoxic proteins in EBV-specific CD4$^+$ T cells during convalescence. CD4-enriched PBMCs collected six months following IM diagnosis were stained with the relevant EBV-pMHCII tetramers and analysed for intracellular expression of Perf/GzmB. **(a)** Perf/GzmB in the total CD4$^+$ T cell pool shown for two representative donors. **(b)** Representative DR7/EBNA2$_{276-295}$ and DR7/BaRF1$_{185-199}$ tetramer stains (top panels), and Perf/GzmB expression in EBV-pMHCII tetramer$^+$ CD4$^+$ T cells (bottom panels) shown for DR7$^+$ donors. **(c)** Summary of Perf/GzmB expression in the total CD4$^+$ (blue dots) and EBV-specific pMHCII tetramer$^+$ CD4$^+$ T cell populations (red crosses) from patients with IM (acute n = 12 and convalescent n = 5) and healthy carriers (HC n = 15). Data are shown as mean ± SD. * $P < 0.05$, *** $P < 0.001$, **** $P < 0.0001$; unpaired Student's *t* test with Welch's correction for comparison between total CD4$^+$ and pMHCII$^+$ cells; Mann-Whitney *U*-test for comparison between donor groups.

The concatenated data of Perf/GzmB expression in the total CD4$^+$ and EBV-pMHCII$^+$ populations in acute IM, convalescence and healthy carriers is shown in Fig 4.7c. Expression of cytotoxic proteins within both the total CD4$^+$ T cell population and the EBV-pMHCII$^+$ CD4$^+$ T cells of acute IM donors were highly variable, ranging from 2.8% to 36.3% and 25.2% to 87.8% respectively. This is likely due to the differences in time from

onset of symptoms characteristic of IM to clinical diagnosis between donors (typically 10 -21 days). In both acute infection and convalescence, expression of Perf/GzmB was significantly higher in the EBV-pMHCII$^+$ CD4$^+$ T cells compared to the total CD4$^+$ population (mean 56.2% *versus* 15.5%; $P < 0.0001$; mean 26.0% versus 1.9%; $P < 0.05$ respectively). However, in healthy carriers, the frequency of Perf/GzmB$^+$ cells was not significantly different between both populations (mean 2.7% *versus* 1.2%; NS).

c. Expression of cellular markers associated with CD4-CTLs in EBV-specific CD4$^+$ T cells

Multiple surface markers and transcription factors have been described in the context of CD4-CTLS present in persistent infection and we next investigated whether a panel of these cellular markers were expressed by EBV-specific CD4-CTLs during an acute infection. Fig 4.8a shows surface staining for CX_3CR1, NKG2D and CRTAM along with intracellular staining for Hobit and Eomes in the total CD4$^+$ T cells of two representative healthy donors. Low but reproducible frequencies of all 5 cellular markers were detected in all donors, typically accounting for less than 1% of the total CD4$^+$ T cell population. Interestingly in donor PER141, who is CMV seropositive and where a greater percentage of CD4-CTLs were seen (Fig 4.3a), all of the markers except CRTAM were present at noticeably higher frequencies.

As CRTAM was not detected in CD4 $^+$ or CD8$^+$ T cell populations in our assays, we performed short term stimulation assays with OKT3 to verify the antibody staining. Following incubation we detected a marked increase in CRTAM positivity in the CD8$^+$ T

cell compartment of healthy donor PBMCs from 0.2 to 12.7% as shown in (Fig 4.8b). Thus, CRTAM is not expressed in the CD4⁺ T cell populations of healthy individuals.

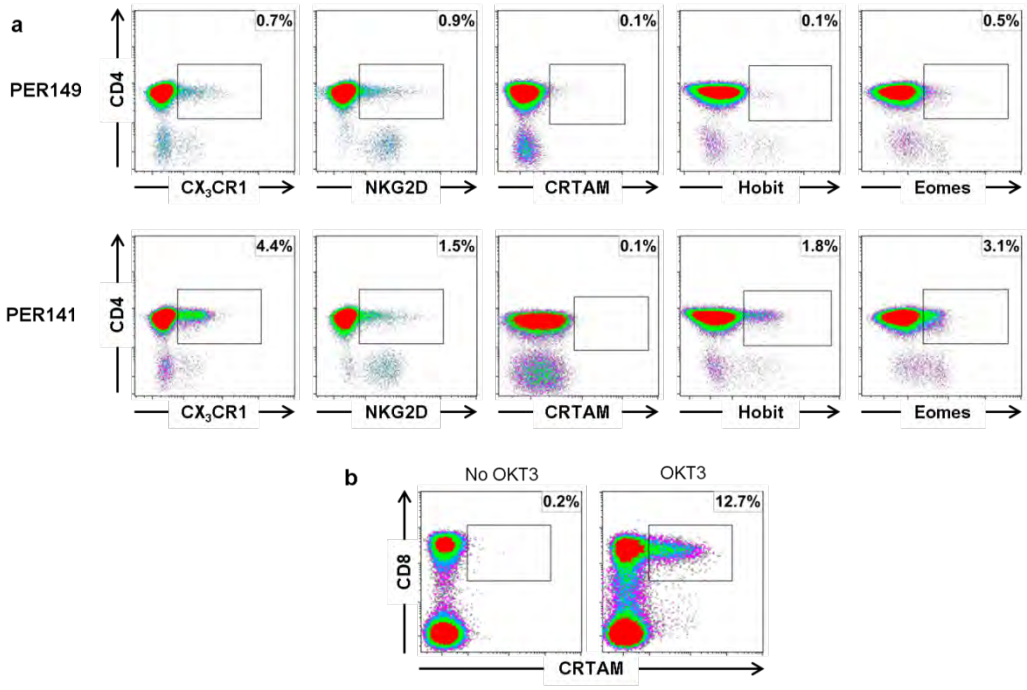

Figure 4.8 Expression of cytotoxicity-associated proteins in CD4⁺ T cells of healthy carriers. (a) Expression of CX_3CR1, NKG2D, CRTAM, Hobit, and Eomes in the total CD4⁺ T cell pool from two representative healthy carriers. The percentage in each plot indicates cytotoxicity marker expression in the total CD4⁺ T cell population. **(b)** PBMCs from a healthy carrier were stimulated with OKT3 and assessed for surface expression of CRTAM.

We next applied this same antibody panel to PBMCs from acute IM donors. Frequencies of all surface markers except CRTAM were noticeably higher in the total CD4⁺ T cells of IM donors, with CX_3CR1 and NKG2D staining positively on 14.4% and 4.6% of the total CD4⁺ T cell pool respectively (Fig 4.9a top plots). Furthermore, expression of Hobit and Eomes was detected in 8.1% and 9.1% of total CD4⁺ T cells (Fig 4.9a; top plots).

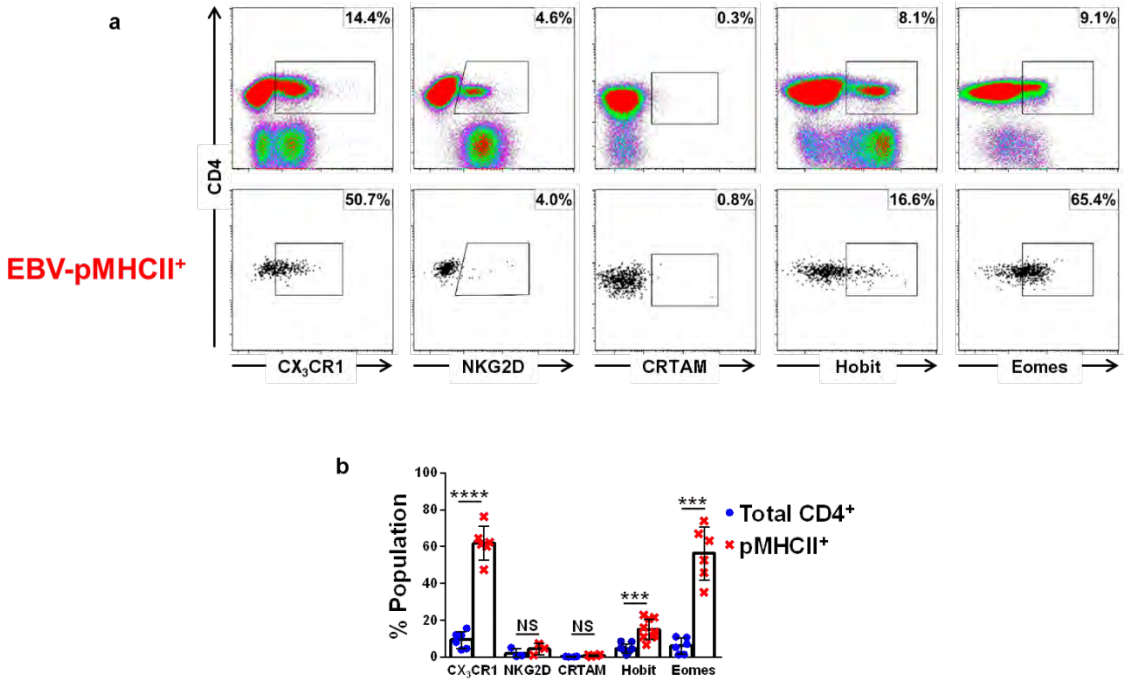

Figure 4.9 Upregulated expression of cytotoxicity-associated proteins in EBV-specific CD4⁺ T cells in acute IM. (a) Expression of CX_3CR1, NKG2D, CRTAM, Hobit, and Eomes in the total $CD4^+$ (top panels) and DR7/$EBNA2_{275-296}$ tetramer$^+$ $CD4^+$ T cell populations (bottom panels) from a representative patient with IM. The percentage in each plot indicates cytotoxicity marker expression in the total $CD4^+$ T cell population. **(b)** Summary of CX_3CR1, NKG2D, CRTAM, Hobit, and Eomes expression in total $CD4^+$ (blue dots) and EBV-specific pMHCII tetramer$^+$ $CD4^+$ T cell populations (red crosses) from patients with IM (n = 6). Data are shown as mean ± SD. *** $p < 0.001$; **** $P < 0.0001$ unpaired Student's *t* test with Welch's correction.

Within the EBV-pMHCII$^+$ $CD4^+$ T cell population, expression of CX_3CR1, Hobit and Eomes was further increased (Fig 4.9a; bottom plots). Here, we detected a 3-fold increase in CX_3CR1 expression in the EBV-pMHCII$^+$ population compared to the total $CD4^+$ T cell population (14.4% to 50.7%); a 2-fold increase in Hobit positivity (8.1% to 16.6%) and a 7-fold increase in Eomes (9.1% to 65.4%). The summary data of the 5 IM donors assayed is shown in Fig 4.9b. While there was no significant difference in the expression of NKG2D and CRTAM between the total $CD4^+$ and the EBV-pMHCII$^+$ T cell populations,

mean expression of CX_3CR1, Hobit and Eomes were all increased on the HLAII tetramer$^+$ cells (9.4% *versus* 62.0% for CX_3CR1, $P < 0.0001$; 4.5% *versus* 15.0% for Hobit, $P < 0.001$ and 6.1% *versus* 56.4% for Eomes; $P < 0.001$). These data indicate that during acute IM, expression of CX_3CR1, Hobit and Eomes are specifically upregulated in the EBV-specific CD4$^+$ T cell population.

We therefore investigated whether expression of these markers correlated with presence of Perf/GzmB in EBV-specific CD4$^+$ T cells. In the representative IM donor shown in Fig 4.10a, both CX_3CR1 and Hobit were present at noticeably higher frequencies in the Perf/GzmB$^+$ population of EBV-pMHCII CD4$^+$ T cells (bottom plots) than in the Perf/GzmB$^-$ (top plots). Frequency of CX_3CR1 was 40.0% compared to 72.1% and Hobit was 2.6% compared to 21.2%. However the percentage of Eomes$^+$ cells was very similar between the two fractions. The concatenated data shown in Fig 4.10b from 5 IM donors shows that there is a significant increase in mean expression of both CX_3CR1 and Hobit in the Perf/GzmB$^+$ EBV-pMHCII$^+$ CD4$^+$ T cells compared to the Perf/GzmB$^-$ fraction (51.7% *versus* 78.5% for CX_3CR1, $P < 0.01$; 6.4% *versus* 29.9% for Hobit, $P < 0.001$). In contrast, we did not observe any significant different in Eomes expression between the two fractions (58.1% *versus* 55.6%, NS). Interestingly however, no single marker was universally expressed in the Perf/GzmB$^+$ EBV-pMHCII$^+$ CD4$^+$ T cell population, and CX_3CR1 and Eomes were also commonly expressed in the Perf/GzmB$^-$ fraction of EBV-specific CD4$^+$ T cells. To determine whether a combination of CX_3CR1, Hobit and Eomes expression may better correlate with presence of Perf/GzmB within the EBV-pMHCII$^+$ CD4$^+$ T cell population, co-expression was analysed using SPICE.

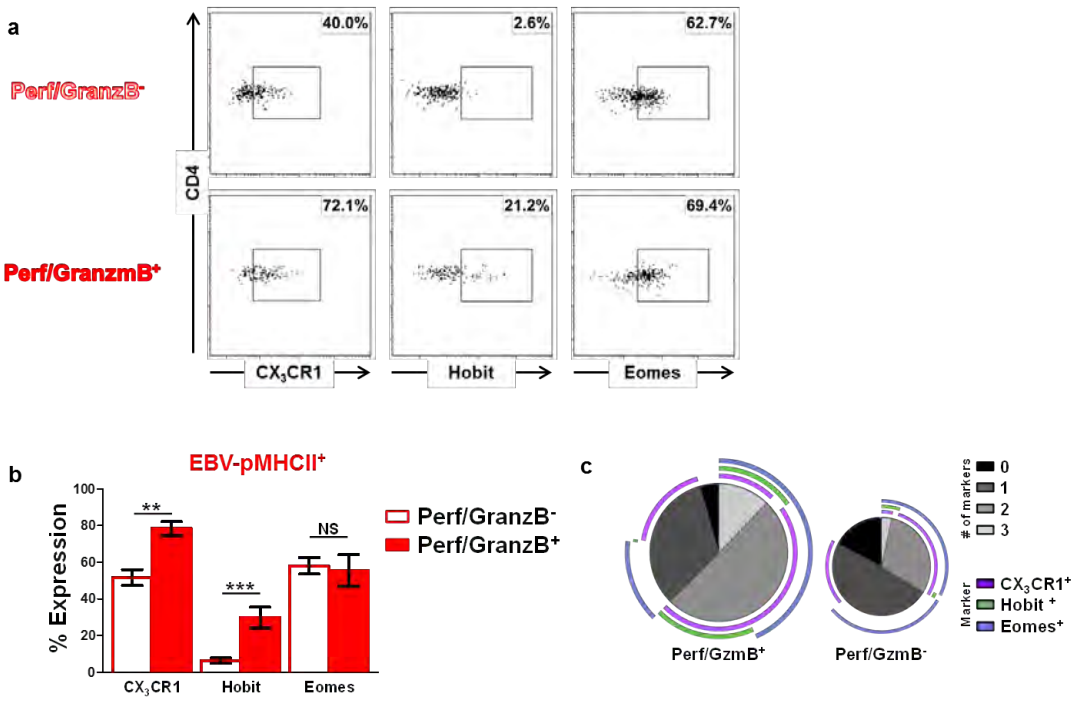

Figure 4.10 Transcriptional profile of cytotoxic EBV-specific CD4⁺ T cells. (a) CX_3CR1, Hobit and Eomes expression in EBV-pMHCII⁺ CD4⁺ T cells from two representative patients with IM. **(b)** Summary of CX_3CR1, Hobit, and Eomes expression in Perf/GzmB⁺ (filled) and Perf/GzmB⁻ pMHCII tetramer⁺ CD4⁺ T cell populations (unfilled). Data are shown as mean ± SD. ** $P < 0.01$, *** $p < 0.001$; Mann-Whitney *U*-test. **(c)** SPICE plots illustrating the expression profiles of CX_3CR1, Hobit, and Eomes among Perf/GzmB⁺ and Perf/GzmB⁻ pMHCII tetramer⁺ CD4⁺ T cells. Image sizes are scaled to depict the distribution of Perf/GzmB⁺ and Perf/GzmB⁻ events among pMHCII tetramer⁺ CD4⁺ T cells. Each pie chart segment displays the fraction of cells expressing the number of markers indicated in the key. Arcs show the distribution of each individual marker. **(b & c)** Results are representative of 6 independent experiments.

As shown in Fig 4.10c, the majority of Perf/GzmB⁺ EBV-pMHCII⁺ CD4⁺ T cells either expressed 2 of the cellular markers associated with CD4-CTLs (50.2%) or all 3 simultaneously (12.3%; left hand plot). The most common profile observed in this fraction was co-expression of CX_3CR1 with either of the transcription factors Hobit or Eomes (19.2% and 28.1% respectively). Interestingly, Perf/GzmB⁺ EBV-pMHCII⁺ CD4⁺ T cells expressing only one of the cellular makers were positive for either CX_3CR1 or Eomes

but not Hobit. Furthermore, in 4.4% of the population we detected no expression of any of the 3 cellular markers (black segment). While the proportion of EBV-pMHCII^{+} CD4^{+} T cells expressing none of these markers was higher in the Perf/GzmB^{-} fraction (17.0%), cells expressing all combinations were present including 3.5% expressing all 3 markers (Fig 4.10c; right-hand plot).

Collectively, this data shows that EBV-specific CD4^{+} T cells elicited by acute infection do express cellular markers that have been associated with CD4-CTL development and function in viral persistence. However, we did not uncover a consistent signature transcriptional profile that defined the Perf/GzmB^{+} virus-specific CD4^{+} T cells.

We therefore wondered whether cellular activation may drive cytotoxic potential in acute infection. Multiple studies have shown that CD4^{+} T cells during primary infections, including acute EBV infection, express high levels of the activation markers such as CD38 (CD38^{hi}) (259, 343, 435). We therefore used CD38 as a surrogate marker to investigate the activation status of the Perf/GzmB^{+} EBV-pMHCII^{+} CD4^{+} T cells in acute IM. As shown in Fig 4.11a, during primary EBV infection the CD4^{+} T cell pool contains a raised population of cells expressing high levels of CD38. Thus, in IM211 27.7% of the total CD4^{+} T cell population were CD38^{hi} whereas in the healthy carrier PER112 only 5.4% were CD38^{hi}. This difference was even more striking in the EBV-specific CD4^{+} T cells, in which 84.7% were CD38^{hi} in IM211 compared to 2.2% in PER112. Concurrent with our previous observations that during acute IM, influenza-specific CD4^{+} T cells were neither expanded nor expressing Perf/GzmB, in representative donor IM243-1 the vast majority of M1$_{43-59}$-specific CD4^{+} T cells were CD38^{lo}, despite significant elevation of CD38^{hi} in the total

$CD4^+$ T cell pool of this individual (Fig 4.11b). The summary data in Fig 4.11c illustrates the significant increase in $CD38^{hi}$ expression in EBV-$pMHCII^+$ T cells populations compared to the total $CD4^+$ pool during acute IM (mean 80.2% *versus* 22.3%; $P < 0.001$). In contrast, $CD38^{hi}$ was expressed only at low frequencies in both populations in healthy carriers.

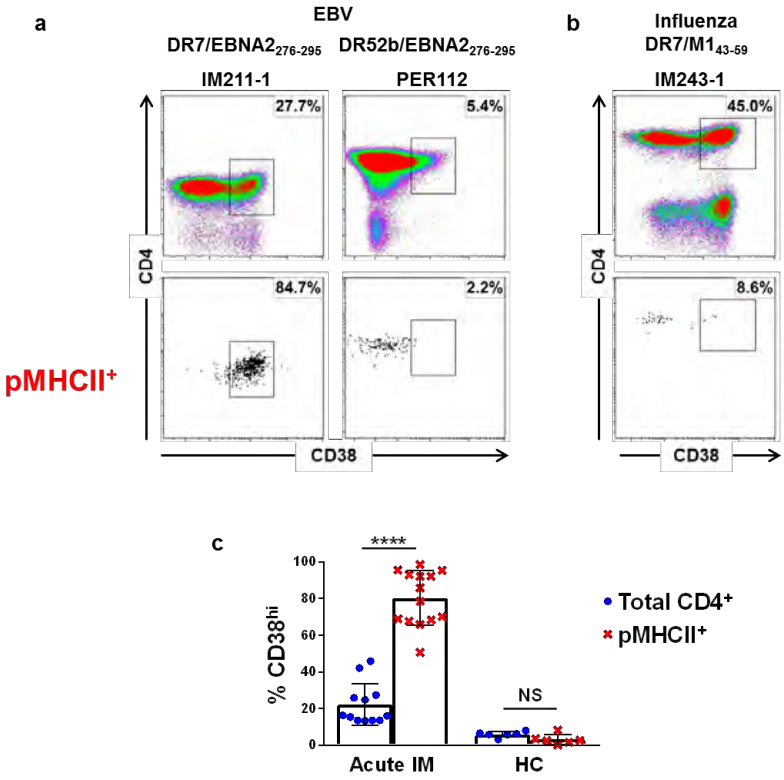

Figure 4.11 Expanded populations of EBV-specific $CD4^+$ T cells in acute IM are highly activated CD4-enriched PBMCs from patients with IM and healthy carriers were stained with the relevant EBV and Influenza pMHCII tetramers (Table 1) and analysed by flow cytometry for surface expression of CD38. **(a)** CD38 expression in the total (top) and EBV-$pMHCII^+$ $CD4^+$ T cell populations (bottom) in a representative IM donor (left panels) and healthy carrier (right panels). **(b)** CD38 expression in the total and infleuenza-specific $CD4^+$ T cells of a representative IM donor. The percentage in each plot indicates CD38i expression in the total $CD4^+$ T cell population **(c)** Summary of $CD38^{hi}$ expression in total $CD4^+$ (blue dots) and EBV-specific pMHCII $tetramer^+$ $CD4^+$ T cell populations (red crosses) from patients with IM (n = 14) and in healthy carriers (n = 6). Data are shown as mean ± SD. **** $P < 0.0001$ unpaired Student's *t* test with Welch's correction.

Within the total $CD4^+$ T cell pool of donor IM243-1, Perf and GzmB expression were both almost exclusively limited to cells expressing high levels of $CD38^{hi}$ (Fig 4.12a, top panel). Accordingly, in the heavily expanded pMHCII $tetramer^+$ population, where $CD38^{hi}$ was almost ubiquitously expressed, the vast majority of cells were positive for Perf and GzmB (Fig 4.12a, bottom panel). In donor IM211-1, where the lower magnitude of the pMHCII tetramer population and lower percentages of Perf/GzmB and $CD38^{hi}$ expression in the total $CD4^+$ T cell pool indicated that this individual had donated blood later after disease onset (Fig 4.12b, top panel), a lower frequency of EBV-specific $CD4^+$ T cells were carrying Perf/GzmB (Fig 4.12b, bottom panel). Crucially, however, expression of cytotoxic proteins was limited to those cells expressing $CD38^{hi}$. The concatenated data from all donors analysed during acute IM and convalescence (Fig 4.12c) shows a strong overall correlation between the percentage frequency of $Perf/GzmB^+$ events and the percentage frequency of $CD38^{hi}$ events, both in the total $CD4^+$ T cell pool (R^2=0.96) and among EBV-specific $CD4^+$ T cells (R^2 = 0.87). Together, these data demonstrate a clear association between cellular activation and cytotoxic potential in EBV-specific CD4-CTLs during primary infection.

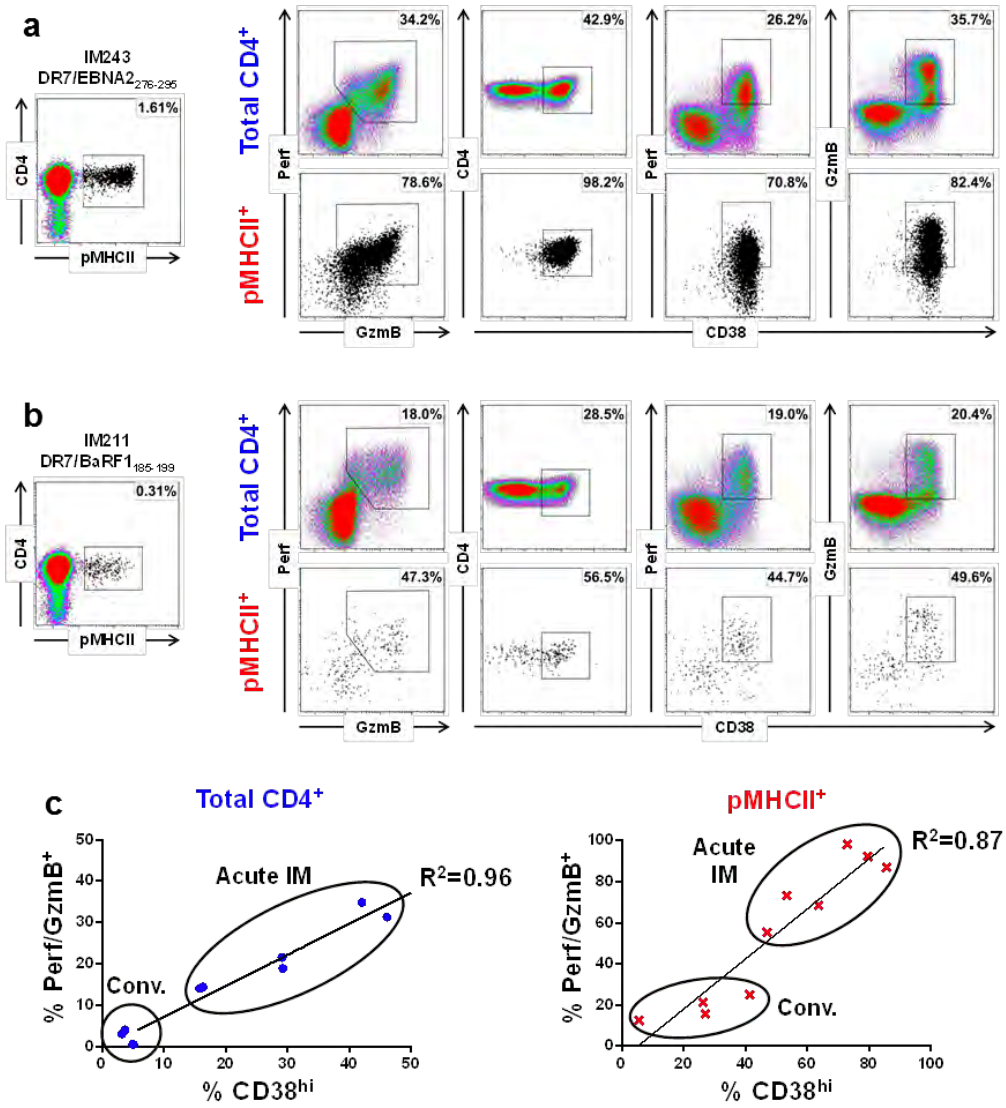

Figure 4.12. Expression of cytotoxic proteins in EBV-specific CD4⁺ T cells correlates with cellular activation. (**a** and **b**) CD4-enriched PBMCs from two representative acute IM donors were stained with the relevant pMHCII tetramers (left plots). Perf, GzmB and CD38 expression were analysed in the total CD4⁺ (top panels) and pMHCII tetramer⁺ CD4⁺ T cell populations (bottom panels). (**c**) Correlation between Perf/GzmB expression and CD38^{hi} events among total CD4⁺ (left plot) and pMHCII tetramer⁺ CD4⁺ T cell populations (right plot) from patients with IM (acute and convalescent). $P < 0.0001$; Pearson correlation.

3. Discussion

Frequencies of CD4-CTLs in the circulation have until recently been underestimated however they are now considered to be an important facet of the immune response to both viruses and cancer (323). Evidence from multiple studies suggests that CD4-CTLs may play important direct role *in vivo* to recognise and eliminate MHC-II$^+$ cells. Specifically, the identification and study of EBV-specific CD4$^+$ T cells capable of lysing infected B cells could have important implications for the design of therapeutics used to treat EBV-driven malignancies.

Here we show that upon exposure to LCL, EBV-specific CD4$^+$ T cells degranulate, indicating the fusion of cytotoxic granules with the cell membrane and the release of effectors molecules such as Perf and GzmB into the immunological synapse. Degranulation was heavily associated with CD4$^+$ T cells from IM patients with only small frequencies detected in healthy carriers. Remarkably, analysis at the antigen-specific level using EBV-pMHCII tetramers revealed that a large proportion of EBV-specific CD4$^+$ T cells in IM were carrying pre-formed Perf/GzmB. Similar observations have been made at the transcript level of CMV-specific CD4$^+$ T cells during primary infection where Oja *et al.* detected upregulation of *PRF1* (Perforin) and *GZMB* (Granzyme B) (372). Interestingly, Perf/GzmB expression was also markedly raised in the total CD4$^+$ T cell pool of IM patients, in line with reports in early primary HIV infection (271, 343). High expression of Perf/GzmB correlated with the largest expansion of EBV-pMHCII$^+$ CD4$^+$ T cell populations. Acute infection and vaccination have been shown to elicit bystander activation in unrelated CD8$^+$ (436) and CD4$^+$ T cells (437, 438) respectively however we detected no such activation in a co-existent memory population of influenza-specific CD4$^+$ T cells during IM. Rather, the cumulative Perf/GzmB expression within the broadly

targeted $CD4^+$ T cell responses to EBV (259) was large enough to skew the overall cytotoxic potential of the total $CD4^+$ pool as has been previously observed (271). Raised expression of Perf/GzmB was maintained in EBV-$pMHCII^+$ $CD4^+$ T cells during convalescence however the epitope-specific populations had contracted to frequencies associated with long term carriage (Fig 3.1 and (259)) and could no longer influence Perf/GzmB positivity within the total $CD4^+$ pool. The elevated expression of Perf/GzmB observed in individual epitope-specific $CD4^+$ T cells during convalescence is possibly driven by continued antigen exposure as lytic replication in the throat endures for several months following primary infection (296, 439).

Unexpectedly, we detected low expression of Perf/GzmB in memory EBV-specific $CD4^+$ T cells in healthy carriers, contrasting with other persistent infections such as HIV, CMV and Dengue virus where cytotoxic molecules are highly prevalent in the virus-specific memory $CD4^+$ populations (177, 336, 370). This may be explained by differences in the differentiation statuses of $CD4^+$ T cells against the different viruses. Late stage differentiation, which is increased in memory HIV (271) and particularly prevalent in CMV-specific $CD4^+$ T cells (336, 372), is associated with acquisition of Perf/GzmB (335, 339). However, memory EBV-specific $CD4^+$ T cells in persistently infected individuals lie in the earlier differentiated T_{CM} and T_{EM} pools (Fig 3.2, (259, 440)), possibly accounting for the lower expression of cytotoxic proteins during viral persistence. Overall our data shows that primary EBV infection induces EBV-specific $CD4^+$ T cells with cytotoxic potential, and that this functionality disappears over time to very low levels in healthy long-term carriers of the virus.

The importance of characterizing cellular markers that would enable the identification and study of CD4-CTLs across viral and cancer settings has led to numerous surface and intracellular proteins being implicated. CX_3CR1, NKG2D, CRTAM, Hobit and Eomes have all recently been described in the development and function of CD4-CTLs, particularly those acquired during chronic infections. We therefore investigated whether these markers were similarly expressed on CD4-CTLs induced by primary infection. Raised expression of CX_3CR1, Hobit and Eomes was detected on the surface of EBV-specific $CD4^+$ T cells during IM, however none of these markers appeared to define Perf/$GzmB^+$ EBV-pMHCII$^+$. CX_3CR1 was the most frequently expressed marker on Perf/$GzmB^+$ EBV-specific $CD4^+$ T cells but was also detectable on a high proportion of the non-cytotoxic EBV-pMHCII$^+$ $CD4^+$ population. Interestingly, Hobit was expressed in all Perf/$GzmB^+$ EBV-specific $CD4^+$ T cells, as previously observed in CMV (372), although Perf/GzmB was also found in the majority of cells that were Hobit$^-$. Consequently, we did not identify any individual marker or combinations thereof that defined all Perf/$GzmB^+$ EBV-specific $CD4^+$ T cells in acute IM.

A caveat of analysing circulating $CD4^+$ T cells from individuals with an ongoing infection is that some cells may not carry Perf/GzmB if they have recently responded to EBV-infected B cells, and released their cytotoxic proteins *in vivo*. Consequently, some cells expressing markers of cytotoxicity may have recently released Perf/GzmB, which may be reflected in the increased degranulation detected on unstimulated $CD4^+$ T cells from acute IM donors (Fig 4.1), and lead to an underestimation of their correlation. Nonetheless, we detected approximately 5% of Perf/$GzmB^+$ EBV-pMHCII$^+$ $CD4^+$ T cells that lacked all three markers, suggesting that neither Hobit, Eomes nor CX_3CR1 are

absolutely required for Perf/GzmB expression in the EBV-specific $CD4^+$ population. Thus, during acute infection, the transcriptional profile that drives cytotoxic function in $CD4^+$ T cells differs from what has been observed in chronic infections, and is as yet undefined.

We did however find a strong correlation between Perf/GzmB expression and cellular activation, defined using the surrogate marker CD38. High levels of activation detected on pMHCII $tetramer^+$ $CD4^+$ T cells *ex vivo* during primary EBV infection is consistent with increased CD38 expression in $CD4^+$ T cells in primary HIV and following vaccinia virus vaccination (343, 435). Although raised Perforin expression was detected in the bulk $CD4^+$ T cell population of primary HIV patients, the authors did not analyse co-expression with CD38. The presence of highly activated effector EBV-specific cytotoxic $CD4^+$ T cells is in contrast to the late differentiated phenotype of described CD4-CTLs in healthy adults, which have been largely characterised in the resting memory steady state (271, 336).

In summary, we have shown that EBV-specific CD4-CTLs elicited during acute primary infection differ markedly from classically reported CD4-CTLs in chronic infections. The characteristics of cytotoxic $CD4^+$ T cells described in viral persistence do not define acutely generated EBV-specific CD4-CTLS (177, 336, 339, 370). The transcriptional programming that regulates CD4-CTL generation in acute infections has yet to be determined with an as yet undescribed pathway possibly driving Perf/GzmB expression in $CD4^+$ T cells (339, 441, 442).

CHAPTER 5

CLONAL EVOLUTION OF EBV-specific CD4$^+$ T CELLS

1. Introduction

To date, studies investigating the clonal composition of the human CD4$^+$ T cell response induced by viral infection have been limited and relatively little is known about the evolution of the TCR repertoire over the course of infection.

Early analysis of the total CD4$^+$ T cell pool in IM patients using heteroduplex PCR detected no biased Vβ expansion (443). However, using flow cytometry, a separate report detected small expansions of individual TCR Vβ chains in acute IM (444). Meanwhile, EBV-specific polyclonal CD4$^+$ T cell lines generated from long term carriers displayed a slight bias towards certain TCR Vβ chains (285).

Studies of CD4$^+$ T cell clonal composition in other chronic viruses have also come to different conclusions. One study analysing CMV-specific CD4$^+$ T cells revealed a TCR Vβ-defined hierarchy dominated by 1-3 clonotypes that could account for up to 50% of CMV-responsive cells (445). In a separate study, CD4$^+$ T cells responding to CMV peptides displayed a less focused response, without dominant clonotypes (335). Additionally, TCR sequencing of CD4$^+$ T cell clones specific for an immunodominant epitope isolated from a patient who developed symptomatic primary CMV infection and healthy carriers exclusively used the *TRBV6-5* gene segment (446).

These early studies were mostly performed using low definition technologies and, in some cases, *in vitro* cultured populations that may not accurately represent the TCR

repertoire *in vivo* (447). Here, using sensitive pMHCII tetramer-based methods we investigated the clonotypic evolution of EBV-specific $CD4^+$ T cells throughout the course of infection through Vβ repertoire analysis and by TCR sequencing of EBV in longitudinal samples.

2. Results

a. TCR Vβ repertoire of EBV-specific CD4$^+$ T cells over the course of infection

In chapters 3 and 4 we observed a change in function of EBV-specific CD4$^+$ T cells from primary infection into long-term carriage and it has been shown that TCR Vβ usage can influence the function of both CD4$^+$ and CD8$^+$ T cells (448, 449). We therefore sought to analyse the clonality of EBV epitope-specific CD4$^+$ T cell populations so as to assess whether clonotypic changes occur over the course of infection and whether we can link these changes to the different functional profiles.

We began by analysing TCR Vβ usage, focussing our efforts on CD4$^+$ T cells specific for the EBNA2$_{276\text{-}295}$ epitope. EBNA2 is the first protein expressed during latent infection of B cells (450) and large responses to the EBNA2$_{276\text{-}295}$ epitope (presented through both HLA-DR7 and HLA DR52b) are commonly detected in acute IM and in healthy donors ((259) and Fig 3.1 and 3.6). Initial experiments used a commercially available TCR Vβ repertoire kit alongside EBNA2$_{276\text{-}295}$ pMHCII tetramers to identify any preferential selection of Vβ chains within epitope-specific CD4$^+$ T cells, as has been observed in the EBV-specific CD8$^+$ T cell compartment (260). A representative example of an EBNA2-$_{279\text{-}295}$-specific CD4$^+$ T cell clone left unmanipulated, stained for the corresponding EBV-pMHCII or stained with an antibody against the Vβ chain used by the clone (previously determined in our laboratory) is shown in Figure 5.1a show. In order to determine whether it was possible for the TCR to bind both the pMHCII and Vβ-specific antibodies, we co-stained EBNA2$_{276\text{-}295}$-specific CD4$^+$ T cell clones with the relevant EBV-pMHCII tetramer and anti-Vβ. Fig 5.1b shows representative examples of EBNA2$_{276\text{-}295}$-specific

CD4$^+$ T cell clones restricted through DR7 (top plots) and DR52b (bottom plots) sequentially stained with EBV-pMHCII followed by the appropriate anti-Vβ antibody (middle) or anti-Vβ followed by EBV-pMHCII (right). Similarly high frequencies of CD4$^+$ T cells positive for both the EBNA2$_{276-295}$-specific tetramer and the anti-Vβ antibodies were observed when stained in either order, thus demonstrating dual staining was possible. For the remainder of our investigation we chose to incubate CD4$^+$ T cells with EBV-pMHCII tetramers prior to staining with anti-Vβ.

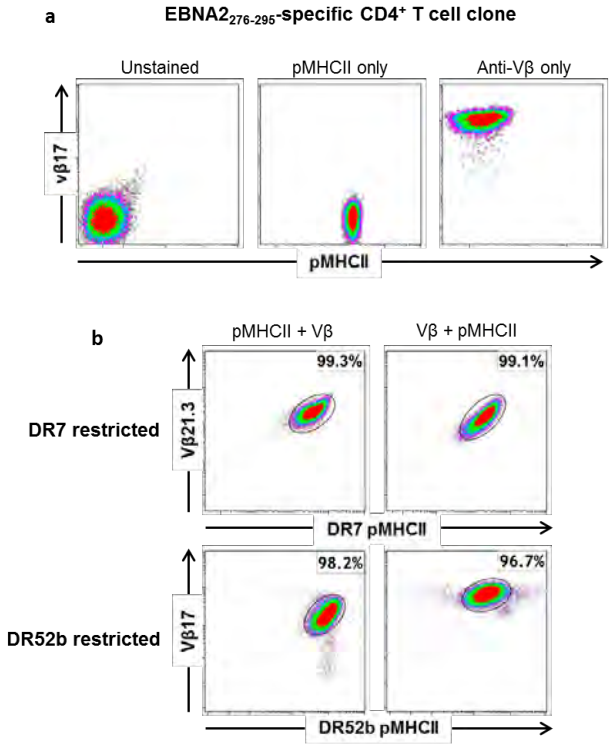

Figure 5.1 Combinatorial staining with TCR Vβ-specific antibodies and pMHCII tetramers. (a) EBNA2$_{276-295}$-specific CD4$^+$ T cell clone was either left unmanipulated (left panel), stained with relevant pMHCII tetramer (middle panel) or with TRBV19-specific antibody (right panel). **(b)** DR7 restricted (top panels) and DR52b restricted (bottom panels) EBNA2$_{276-295}$ CD4$^+$ T cell clone stained sequentially either with the relevant pMHCII tetramer followed by the matched TCR Vβ-specific antibody, or vice versa.

The kit contained antibodies directed against 24 Vβ chains conjugated to either PE, FITC or both fluorochromes, thereby allowing 3 Vβ specificities to be analysed per tube. Examples of staining in the total $CD4^+$ T cell population of a representative healthy donor with all 8 of the Vβ antibody cocktails, covering the 24 Vβs, is shown in Fig 5.2a with the corresponding frequencies for each specificity in Fig 5.2b. With this assay we were able to detect and distinguish $CD4^+$ T cells stained positively for each of the 24 Vβ specificities covered by the kit, including highly expressed chains such as TRBV5-1 and TRBV2 (7.5% and 5.5%; panels C and G respectively) and rarer populations such as TRBV5-6 and TRBV4-3 (0.3% and 0.4%; panels E and H respectively).

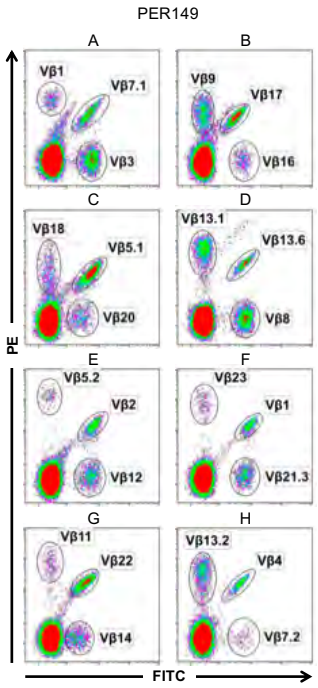

Panel	Vβ specificity	IMGT Nomenclature	% CD4+T cells
A	1	5-5	0.8
	7.1	4-1, 4-2, 4-3	3.2
	3	28	5.3
B	9	3-1	3.3
	17	19	5.5
	16	14	1.0
C	18	18	1.5
	5.1	5-1	7.5
	20	30	1.3
D	13.1	6-5, 6-6, 6-9	4.1
	13.6	6-6	2.0
	8	12-3, 12-4	5.2
E	5.2	5-6	0.3
	2	20-1	2.0
	12	10-3	2.0
F	23	13	0.5
	1	9	1.6
	21.3	11-2	2.0
G	11	25-1	0.6
	22	2	5.5
	14	27	1.9
H	13.2	6-2	2.8
	4	29-1	1.7
	7.2	4-3	0.4

Figure 5.2 Total $CD4^+$ T cell TCR-Vβ repertoire analysis. CD4 enriched PBMCs from healthy lab donors were analysed by flow cytometry for surface expression of defined TCR Vβ segments. Representative example of **(a)** unstained $CD4^+$ T cells and **(b)** $CD4^+$ T cells stained with antibody cocktails covering 24 Vβ chain specificities. Each reagent mixture contained fluorochrome-conjugated antibodies specific for 3 TCR Vβ chains.

The representative frequencies of the 24 Vβ chains in the total and EBNA2$_{276-295}$-specific CD4$^+$ T cell populations of 3 healthy carriers are illustrated in the clonograms shown in Fig 5.3. We detected a high degree of variability in representation of the different in the Vβ chains within the total CD4$^+$ T cell population in all healthy carriers. The highest frequency was 10.2% of CD4$^+$ T cells expressing TRBV20-1 in PER065 (bottom clonogram) and the lowest was 0.3% expressing TRBV5-6 in PER149 (top clonogram). Each individual had a unique signature that was consistent upon repeat assays. However, we did observe some similarities in the clonograms of unrelated donors, specifically a frequency of less than 1% of the total CD4$^+$ population expressing each of TRBV5-5, TRBV14, TRBV13 and TRBV4-3 and high expression of TRBV5-1 in all donors.

We simultaneously applied the same gating strategy to the EBNA2$_{276-295}$-specific CD4$^+$ T cells to establish the Vβ usage of the epitope specific populations. Interestingly, we detected marked differences in the EBV-pMHCII$^+$ pools between healthy carriers. in donor PER149 we detected DR7/EBNA2$_{276-295}$-specific CD4$^+$ T cells expressing 15 of the 24 Vβ chains assayed (Fig 5.3; top clonogram). All the Vβ chains detected were under represented within the EBV-pMHCII$^+$ CD4$^+$ T cells compared to the total CD4$^+$ population except for TRBV10-3, which was carried by 4.6% of the DR7/EBNA2$_{276-295}$-specific population compared to 1.9% in total CD4$^+$ pool (2.4-fold increase). Similarly, in donor PER344 we detected DR7/EBNA2$_{276-295}$-specific CD4$^+$ T cells stained positively for 19 of the 24 Vβ chains in the kit, with all but one being underrepresented compared to the same Vβ chain usage in the total CD4$^+$ T cell population (Fig 5.3, middle clonogram). Indeed, TRBV20-1$^+$ EBV-pMHCII$^+$ CD4$^+$ T cells accounted for 24.1% of the total tetramer$^+$ pool. This chain was the most frequently expressed in the total CD4$^+$ T cell pool (9.2%)

and was further increased 2.5-fold in the EBV-pMHCII$^+$ populations. In the DR52b$^+$ donor PER065 (bottom clonogram), EBNA2$_{276\text{-}295}$-specific CD4$^+$ T cells expressing 12 of the 24 anti-Vβ chains were detected. Both TRBV9 and TRBV6-2 were over-represented compared to the total CD4$^+$ population, although the increases less marked than in the DR7$^+$ donors (1.9% *versus* 3.0% for TRBV9, 1.1% *versus* 1.5% for TRBV6-2). These data indicate that the Vβ chain usage of EBV-specific CD4$^+$ T cell receptors in healthy carriers is diverse, and varies between donors, with occasional preferential selection of particular chains.

We next went on to analyse the Vβ chain usage within the expanded EBV-specific CD4$^+$ T cell populations of acute IM donors. Fig 5.4 shows examples of the EBNA2$_{276\text{-}295}$-specific CD4$^+$ T cell populations from DR7$^+$ (IM273, top) and DR52b$^+$ (IM201, bottom) donors. In both cases total CD4$^+$ T cell population displayed similarities to healthy carriers, including a range of frequencies across the Vβ chains and low usage of certain Vβ chains including TRBV4-3 which was undetectable in IM201 and TRBV30 which was undetectable in both IM donors. However striking differences were seen in the clonograms of the epitope-specific cells. Surprisingly, 24.5% of the DR7/EBNA2$_{276\text{-}295}$-specific CD4$^+$ T cell population in IM273 stained positively for one Vβ chain, TRBV28, which, represented an 18.8-fold increase over the frequency of this chain in total CD4$^+$ T cell population of 1.3% (Fig 5.4, top clonogram). All other Vβ chains were either similarly expressed or present at lower frequency compared to the total CD4$^+$ T cell population.

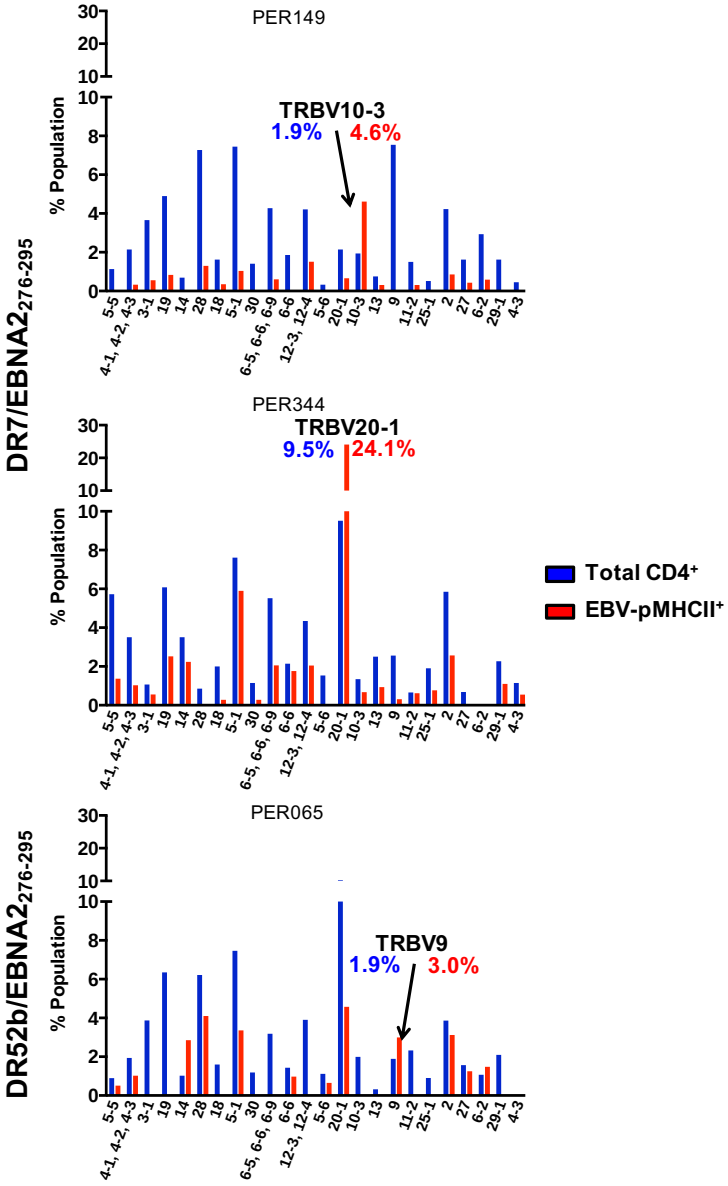

Figure 5.3 TCR Vβ chain representation in EBV-specific memory CD4⁺ T cells. CD4 enriched PBMCs from healthy carriers were exposed to relevant EBV MHCII tetramers followed by a panel of Vβ chain antibodies. Clonograms show the distribution of specific TCR Vβ segments among total CD4⁺ (blue) and EBV-specific pMHCII tetramer⁺ CD4⁺ T cells (red). The dominant TCR Vβ segment is highlighted in each case.

Similarly within the DR52b/EBNA2$_{276-295}$-specific CD4⁺ T cell population of IM201, TRBV11-2 positivity accounted for 16.2% of the EBV-pMHCII⁺ CD4⁺ T cells compared to 2.4% of the total CD4⁺ population, representing a 6.8-fold increase (Fig 5.4, bottom

clonogram). TRBV5-5 was also detected at a higher frequency within the EBNA2$_{276-295}$-specific population compared to the total CD4$^+$ pool but to a lesser extent (2.3% *versus* 1.3% respectively). This data shows that the expanded EBV-specific CD4$^+$ T cell populations in primary EBV infection contain over-representation of individual Vβ chains compared to the total CD4$^+$ T cell pool and could indicate the presence of clonal populations.

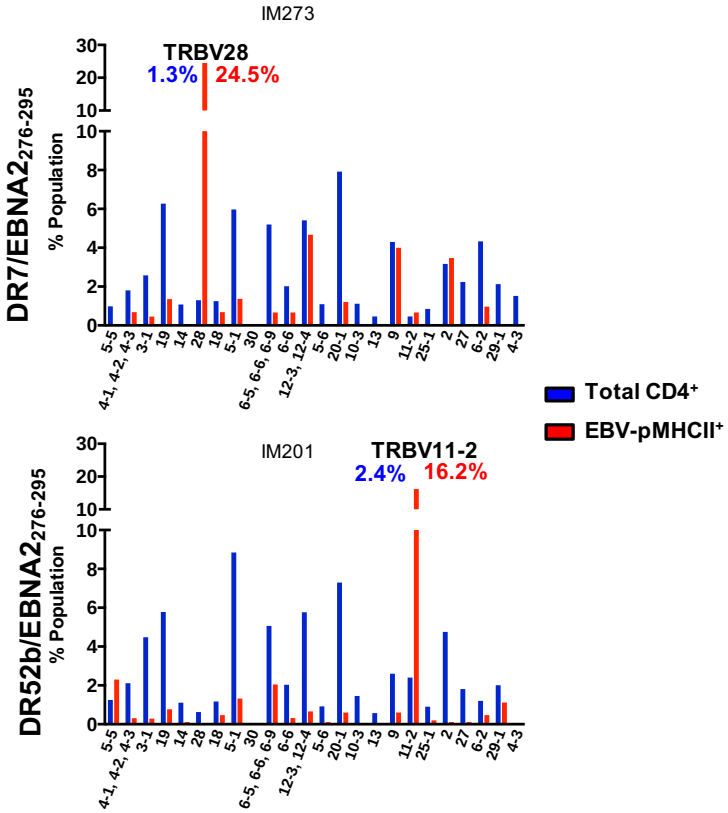

Figure 5.4 TCR Vβ chain representation in the EBV-specific CD4$^+$ T cells in IM. CD4 enriched PBMCs from acute IM donors were exposed to relevant EBV MHCII tetramers followed by a panel of Vβ chain antibodies. Clonograms show the distribution of specific TCR Vβ segments among total CD4$^+$ (blue) and EBV-specific pMHCII tetramer$^+$ CD4$^+$ T cells (red). The dominant TCR Vβ segment is highlighted in each case.

We next aimed to determine if presence of the cytotoxic proteins observe in primary infection was associated with the distinct Vβ-defined expansions. Indeed, given that expression of Perf/GzmB was never universal within the EBV-pMHCII$^+$ CD4$^+$ T cells of IM donors, that markers traditionally associated with CD4-CTLs were not ubiquitously detected within these populations and the absence of over-represented Vβ chains in long term carriers, we hypothesised that overrepresented Vβ chain usage could be linked to cytotoxic potential. As shown in Fig 5.5, in the expanded EBNA2$_{276\text{-}295}$-specific CD4$^+$ T cell population of IM273, 38.0% of the EBV-pMHCII$^+$ CD4$^+$ T cells are positive for Perf/GzmB. In the TRBV28$^+$ pMHCII$^+$ population, Perf/GzmB expression reflected that in the total CD4$^+$ population with 41.2% staining positively (left plots).

Similarly, in the EBNA$_{276\text{-}295}$-specific CD4$^+$ T cell population of IM273, Perf/GzmB expression in the total EBV-pMHCII$^+$ population was comparable to the expanded TRBV11-2$^+$ EBV-pMHCII$^+$ populations (77.7% *versus* 79.7% respectively; right plots). Cytotoxic potential was similar across all vβ subsets indicating that cytotoxic function is not associated with EBV-pMHCII$^+$ CD4$^+$ T cells expressing particular vβ chain usage.

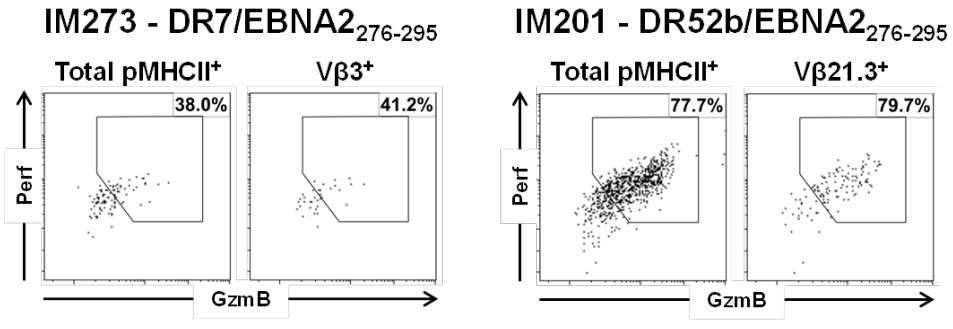

Figure 5.5 Perf/GzmB expression in Vβ defined EBV-pMHCII CD4$^+$ T cells expansions. Perf/GzmB expression among total EBV-pMHCII$^+$ CD4$^+$ (left panels) and dominant Vβ$^+$ pMHCII$^+$ CD4$^+$ T cells (right panels) from the donors shown in Fig 5.4.

The flow cytometry kit we used for establishing Vβ repertoires of healthy carriers and IM donors in Fig 5.3 and 5.4 contained antibodies covering approximately 70% of the normal human TCR Vβ repertoire. Fig 5.6a shows the percentage of the total $CD4^+$ T cell population and EBV-$pMHCII^+$ $CD4^+$ T cells detected by the antibodies present in the kit in the two cohorts. In line with the manufacturer's estimate we detected a mean coverage in the total $CD4^+$ population of 68.1% in healthy carriers and 64.1% in IM donors, with little variation between donors. However, within the EBV-$pMHCII^+$ populations, the frequency covered was variable between donors, and the mean coverage was significantly lower compared to the corresponding total $CD4^+$ T cell populations (68.1% *versus* 30.0% in healthy carriers, $P < 0.05$; 64.1% *versus* 27.7% in acute IM, $P < 0.05$). Therefore, a significant percentage of epitope-specific $CD4^+$ T cells were not staining with any of the 24 TCR Vβ antibodies.

We therefore hypothesised that either pMHCII binding was inhibiting some of the anti-Vβ antibodies not tested in the optimisation assays in Fig 5.1, or that a higher proportion of the EBV-specific $CD4^+$ TCRs used Vβ chains that were not included in the antibody repertoire of this kit.

In order to address the first possibility we performed side-by-side Vβ repertoire analysis in a heathy donor with anti-Vβ staining prior to incubation with EBV-pMHCII (Fig 5.6b top clonogram) or incubation with EBV-pMHCII followed by anti Vβ staining (Fig 5.6b bottom colonogram).

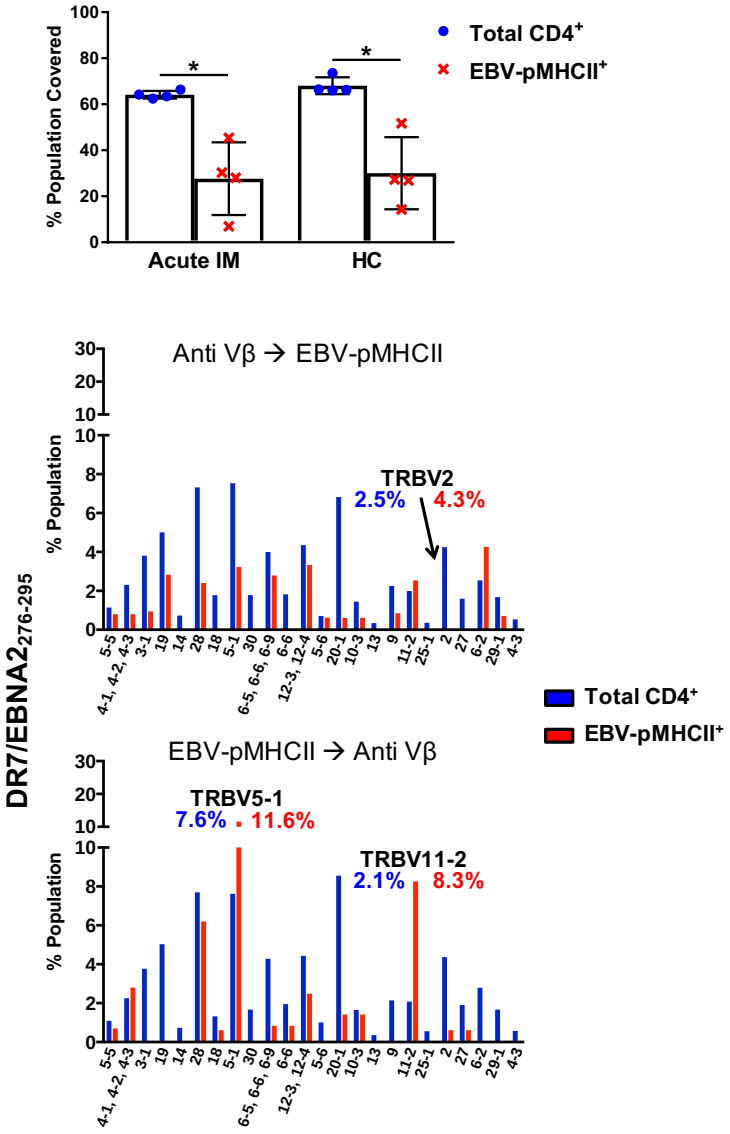

Figure 5.6 Anti-TCR Vβ-pMHCII interference (a) Summary of frequencies covered by the panel of 24 Vβ chain antibodies in the total CD4$^+$ (blue dots) and EBV-pMHCII$^+$ CD4$^+$ T cell populations (red crosses). **(b)** Clonograms showing the distribution of specific TCR Vβ segments among total CD4$^+$ (blue) and DR7/EBNA2$_{276-295}$-specific CD4$^+$ T cells (red) sequentially stained with anti-Vβ chain antibodies followed by pMHCII tetramer (top) or pMHCII tetramer followed by anti-Vβ chain antibodies, in the same donor. Dominant TCR Vβ segments are highlighted (bottom).

As expected, the range of Vβ frequencies detected within the total CD4$^+$ T cell population was very similar regardless of the sequence of staining. However, the

clonograms of the $EBNA2_{276-295}$-specific $CD4^+$ T cell populations were noticeably different between the two methods, with different percentages of EBV-pMHCII$^+$ $CD4^+$ T cells staining with individual Vβ antibodies for a number of chains. In particular detection of TRBV5-1$^+$ and TRBV11-2$^+$ $EBNA_{276-295}$-specific $CD4^+$ T cells was noticeably lower when staining with anti-Vβ antibody cocktails first. Note, the frequencies of these Vβ chains in the total $CD4^+$ populations remained unchanged irrespective of the staining sequence. Furthermore, detection of some Vβ chain subsets the EBV-pMHCII$^+$ $CD4^+$ T cell population was only possible by one method. These data show that despite our ability to co-stain individual $CD4^+$ T cell clones with EBV-pMHCII and anti-Vβ antibodies, variability in the binding domains of some anti-Vβ antibodies between the different specificities likely leads to competition with pMHCII tetramer staining. Nevertheless, our data did indicate that during primary infection, Vβ-defined expansions are present in EBV epitope-specific $CD4^+$ T cells.

b. Evolution of the EBV-specific $CD4^+$ T cells TCR repertoire

To investigate whether these represented expansions of individual T cell clones we performed T cell repertoire sequencing on EBV-pMHCII$^+$ $CD4^+$ T cells. We used an unbiased molecular approach to analyse clonal composition over the course of infection in FACS sorted epitope-specific cells *ex vivo* (414). For these experiments we concentrated on two specificities restricted through HLA-DR7: the latent $EBNA2_{276-295}$ epitope and the lytic $BaRF1_{185-199}$ epitope. Unfixed $CD4^+$ T cells stained positively with $EBNA2_{276-295}$ tetramer or $BaRF1_{185-199}$ tetramer were sorted at > 98% purity into Eppendorf tubes containing an RNA protectant solution and frozen immediately. Thereafter, Dr Kristin Ladell and Dr James McLaren at the Cardiff University School of

Medicine performed unbiased amplification of all expressed *TRB* gene rearrangements using a template-switch anchored RT-PCR with a 3' constant region primer. Amplicons were subcloned, sampled, sequenced, and analysed as described in Chapter 2 (414).

The *TRB* gene re-arrangements expressed in the sorted populations of $EBNA2_{276-295}$-specific $CD4^+$ T at three separate timepoints in donors IM260 and IM265 and $BaRF1_{185-199}$-specific $CD4^+$ T cells in IM260 at two timepoints are shown in Fig 5.7a. Concurrent with our flow cytometric analysis of the Vβ chain usage shown in Fig 5.4, all three populations sorted during acute primary infection showed preferential usage of particular *TRBV* genes use (top panels). The $EBNA2_{276-295}$-specific $CD4^+$ T cell populations of IM260 favoured *TRBV20-1*, which accounted for 39% of sequences, whereas the $BaRF1_{185-199}$-specific population in the same donor, 48% of sequences were matched with *TRBV28*. In contrast, in IM265 the $EBNA2_{276-295}$-specific population favoured *TRBV12-3*, which accounted for 68% of sequences at this acute timepoint. Furthermore, within each of these three dominant *TRBV* sorted populations, a single clone was responsible for the observed *TRBV* gene bias. Clone 1 and clone A identified in IM260 comprised 39% of all sequences in the $EBNA2_{276-295}$-specific $CD4^+$ T cells sequences and 40% of sequences isolated from $BaRF1_{185-199}$-specific $CD4^+$ T cells. Strikingly, in IM265, 69% of all sequences obtained from the $EBNA2_{276-295}$-specific population had the same TRBV usage and CDR3 sequence.

To investigate clonal evolution during the course of infection, we subsequently performed identical analyses on sorted $EBNA2_{276-295}$ specific $CD4^+$ T cells from serial samples collected from the same donors at 2-3 weeks and >18 months after IM

diagnosis. Interestingly, the dominant clonotypes observed during acute primary EBV infection had contracted as early as 2 weeks following diagnosis. Indeed, at this timepoint, clones 1 and 3 from IM260 now accounted for 20% and 8% of all sequences respectively. In the $BaRF1_{185-199}$-specific $CD4^+$ T cells sorted at the same timepoint, the dominant clone A identified in the acute phase remained detectable, however the frequency had dropped to 3.6%. Likewise, the frequency of the $EBNA2_{276-295}$-specific clone I in IM265 at 3 weeks post-IM diagnosis now only accounted for 20% of CDR3 sequences. Alongside the diminished representation of these dominant clonotypes we also observed the appearance of new CDR3 sequences over time, most notably clone 4 in IM260 which accounted for 19.2% of all sequences 22 months following IM diagnosis.

Remarkably, although costs limited analysis to 2 donors, we identified a public *TRBV7-9* specific clonotype in the $EBNA2_{276-285}$-specific sorted $CD4^+$ T cell populations that was present during acute infection in both donors. Moreover, the same clonotype was also detected in all subsequent timepoints for IM260 and IM265. This clone detected during IM therefore persisted into long-term memory and while identical at the amino acid level, the corresponding CDR3 loops were differentially encoded at the nucleotide level, consistent with the principles of convergent recombination (Fig 5.7b) (451).

In summary, these data show that during primary EBV infection, single heavily expanded dominant EBV-specific $CD4^+$ T cell clonotypes can be detected in the circulation. These clonotypes progressively contract as early as 2 weeks post IM diagnosis and can in some cases become undetectable <18 months thereafter. Additionally, clonotypes not

present during the acute phase of infection, can emerge at later timepoints some of which can become dominant.

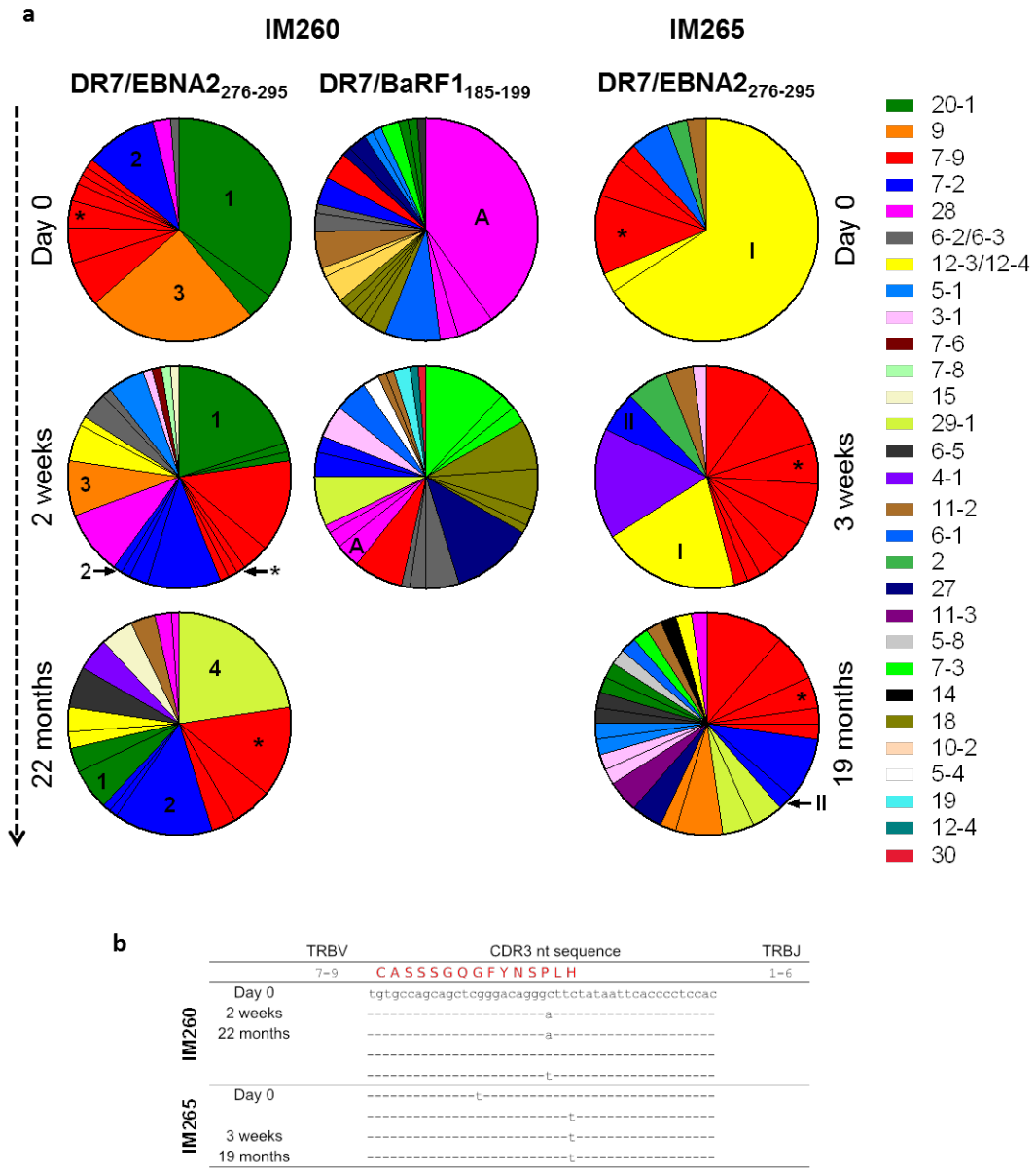

Figure 5.7 T cell receptor analysis of EBV-specific CD4⁺ T cells over the course of infection. Expressed *TRB* gene transcripts in EBV-specific CD4⁺ T cell populations from sequential samples from patients with IM were sequenced using the Sanger method. Each pie chart segment denotes a unique clonotype. Dominant clonotypes indicated as 1–4 in donor IM260, and I and II in donor IM265. A public sequence is indicated with an asterisk (*). (**b**) Nucleotide sequences encoding the public amino acid sequence.

3. Discussion

Preferential expansion of particular Vβ subsets has been detected in the EBV-specific $CD8^+$ T cell population during primary infection (443) and here we show more sensitive MHCII tetramer-based methods that a similar trend occurs in the antigen-specific $CD4^+$ T cells. Perf/GzmB expression was not associated with any particular TCR Vβ usage within the analysed EBV-specific $CD4^+$ T cells, in line with observations from CMV that acquisition of cytotoxicity in antigen-specific $CD4^+$ T cells is not associated with distinct clonotype (335). Furthermore, murine infection models have also shown that members of the same clonotype can exist across different functional states (452).

We have shown using an unbiased molecular approach that similar to the $CD8^+$ T cell population in IM, certain TCR Vβ subsets are over-represented in latent and lytic-epitope specific $CD4^+$ T cell populations and are predominantly composed of a single TCR clone (260).

Individual dominant Vβ chain usage differed not only between epitope-specific populations analysed from the same donor, but also between $CD4^+$ T cells specific for the same $EBNA2_{276-295}$ epitope in unrelated individuals. However, clonotyping of $CD4^+$ T cells specific for the $EBNA2_{276-295}$ latent epitope in two donors did reveal significant common usage of the *TRBV7-9* gene suggesting an important germline-encoded contribution that may confer a structural advantage for recognition of the HLA DRB1*0701:$EBNA2_{276-295}$ complex (453, 454). A similar TRBV bias appeared to be maintained in the CMV-specific $CD4^+$ T cell pool of primary and persistent CMV infected individuals specific for a single CMV-derived epitope (446). Moreover, an identical TCR

sequence was identified within the *TRBV7-9* pool in the acute and subsequent time points in both individuals. This is in line with multiple studies that have identified identical or near-identical class-I restricted TCRs specific for lytic protein derived epitope in the $CD8^+$ T cell repertoire numerous individuals (260, 455-457). Public TCRs can be defined as the same TCR gene rearrangement present across multiple individuals. It has been suggested that public TCRs can arise as a result of a more efficient recombination process that results in preferential selection in thymus (458). In a recent study of HIV-infected individuals who can maintain low viral loads in the absence of retroviral therapy, Galperin *et al.* identified three public class-II restricted TCRs in the $CD4^+$ T cell population of genetically diverse elite controllers, highlighting their importance and suggesting a potential role in the design of TCR based therapies (459).

Clonal expansions of $CD4^+$ T cells have been described in chronic Dengue virus infection (460) and in the context of IgG4-related disease (441). In contrast we show that clonal expansions in the EBV-specific $CD4^+$ T cell repertoire only occur in acute infection when we also observe presence of CD4-CTLs. However, in long-term carriers, we did not observe any clonal focusing which was concurrent with a loss of expression of cytotoxic proteins.

In contrast to what has been observed in the EBV-specific $CD8^+$ T cell pool, clones detected during the acute phase were not maintained at high frequencies in long-term carriers (274). Rather, the dominant clonotypes in acute IM contracted in relative dominance. Nevertheless, each previously dominant clone remained detectable 18 months post infection indicating, that they were not subject to loss through clonal

exhaustion (461) but were instead, along with the public TCR, selected into long-term memory (452). Additional TCR sequences undetectable during the acute phase emerged at later time points as has been seen for CMV-specific $CD8^+$ T cells (462) however, masking of these clones by the dominant clones present in IM cannot be excluded.

Many studies have investigated the structural features of the variable regions of$CD8^+$ TCRs to dominant viral epitopes and found striking similarities in both α and β chain sequences (453, 456, 463). Here we show that public CD4 TCRs may be equally important, and investigating the distinguishing features of long-lived populations of antigen-specific $CD4^+$ T cells could be important in the design of vaccines (464). One explanation for public T cell responses is a process called convergent recombination (465). Instead of biases in the V(D)J recombination, public TCRs could occur as a result of three distinct mechanisms: V(D)J recombination events converging to produce the same nucleotide sequence; different nucleotide sequences converging to encode the same amino acid sequence; different amino acid sequences result in the same amino acid motif (451). Here, the public TCR detected in the EBV-specific $CD4^+$ T cell population may have arisen from the second mechanism with distinct nucleotide sequences at various time points and in each donor giving rise to the same amino acid sequence (Fig 5.7b).

CHAPTER 6

EBV-SPECIFIC CD4$^+$ T CELLS AT THE SITE OF INFECTION

1. Introduction

Long term EBV infection is maintained in the host through latently-infected memory B cells, which constantly recirculate between the blood and oropharyngeal lymphoid tissues such as the tonsil (466). Occasional reactivation of EBV-infected memory B cells into lytic cycle in the tonsil can lead to *foci* of virus replication, thereby producing new virions for transmission in saliva and initiating new growth transformation in the B cell pool (467). These periodic reactivations are contained by the memory T cell response, however very little is known of immunity in the tonsil. Studying the immune response coincident to the ongoing replenishment of EBV-infected B cells within the tonsil would shed important insight into the localised immune response to a pathogen, which may have important implications for vaccine development.

Studies investigating the CD8$^+$ T cell response to EBV in the tonsil have shown that in healthy long-term carriers, epitope-specific populations are enriched compared to the circulation and can express surface molecules associated with tissue residency (297, 298). Specifically, Woon *et al*. demonstrated that EBV-specific-CD8$^+$ T cells, under the influence of cytokines in the tissue, upregulated expression of CD103 thus enabling localization to the epithelial barrier of the tonsil, where EBV reactivation occurs. Interestingly, analysis of matched peripheral blood and tonsil samples from IM patients revealed that not only were EBV-specific CD8$^+$ T cells present at lower frequencies in the

tonsil compared to the circulation at the time of primary infection, but also they did not display a phenotype that would enable retention in the tissue. In a separate study analysing EBV-specific $CD4^+$ T cells in a single matched IM blood and tonsil sample, epitope-specific populations were similarly lower in the lymphoid tissue compared to the circulation, however the phenotype of these cells was not investigated (259).

Most of what is currently known about human $CD4^+$ T_{RM} has come from studies analysing bulk populations of cells isolated from tissue, often from cadavers (393, 396, 404), and few have investigated the compartmentalization of antigen-specific T cells in the context of viral infection (298, 468).

The ability to collect matched blood and tonsil samples from long-term healthy EBV carriers provides us with a unique opportunity to analyse the properties of a human antigen-specific $CD4^+$ T cell population at the site of infection. Isolated mononuclear cells from both compartments allowed us to investigate phenotypical differences between EBV-specific $CD4^+$ T cells at each location and to compare their functional profiles.

2. Results

Collection of matched blood and tonsils

We collected fresh tonsils from 29 patients undergoing routine tonsillectomy paired, with matched blood for 16 donors. At the time of surgery, tonsils were not inflamed. All donors were HLA typed by PCR and screened for exposure to EBV and CMV.

a. EBV-specific $CD4^+$ T cells are enriched at the site of infection

Using the panel of EBV-pMHCII, initial experiments investigated the presence of EBV-specific $CD4^+$ T cells within the unfractionated mononuclear (UM) population isolated from tonsils. The frequencies of EBV-$pMHCII^+$ $CD4^+$ T cells in paired PBMC and tonsillar UM samples for a range of epitopes relevant to each donor's HLA type are shown in Fig 6.1a. In accordance with our analysis in Chapter 3, we detected low but reproducible frequencies of EBV-$pMHCII^+$ $CD4^+$ T cells in the PBMCs of this healthy virus carrier cohort (left-hand plots). These same EBV-$pMHCII^+$ $CD4^+$ T cell specificities were also present in the matched tonsillar UMs (right-hand plots). Interestingly, in donor P014644 the frequency of DR7/$EBNA2_{276-295}$-specific $CD4^+$ T cells within the total CD4+ T cells was of a higher magnitude in the UMs compared to PBMCs; 0.024% versus 0.035% (top plots). Similarly, in donor P015929, the frequency of $CD4^+$ T cells specific for this same latent epitope restricted through DR52b was higher in the tonsillar UMs compared to matched PBMCs; 0.005% *versus* 0.021%, respectively. Additionally, we detected $CD4^+$ T cells specific for two epitopes restricted through the same HLA allele in donor P016375 (bottom plots), latent $EBNA2_{301-320}$ and lytic $BMRF1_{136-150}$. While the magnitude of responses against these two epitopes were smaller than those observed for $EBNA2_{276-}$

$_{295}$ in donors P014644 and P015929, we nonetheless observed an increase in EBV-pMHCII$^+$ cells the tonsillar UMs compared to PBMCs (0.001% in PBMCs *versus* 0.003% in UMs for EBNA2$_{301-320}$; 0.002% in PBMCs *versus* 0.004% in UMs for BMRF1$_{136-150}$). Fig 6.1b summarises the frequencies of EBV-pMHCII$^+$ in the total CD4$^+$ T cell pool in PBMCs and tonsillar UMs. In all the PBMC samples from this cohort, the frequency of EBV-pMHCII$^+$ CD4$^+$ T cells was < 0.05% of the total CD4$^+$ T cell pool, consistent with the healthy lab donor cohort in Chapter 3, and with previous published studies (259). Similarly, in tonsillar UMs, in all but 2 of the samples tested, EBV-pMHCII$^+$ cells accounted for less than 0.05% of the total CD4$^+$ T cell population. Although the mean frequency of EBV-pMHCII$^+$ CD4$^+$ T cells was higher in UMs compared to PBMCs (0.003% *versus* 0.006%; *NS*), this was not statistically significant. EBV-specific CD8$^+$ T cell enrichment in the tonsils is more pronounced in latent epitope reactivities than lytic epitope reactivities (297). We therefore compared the frequencies of EBV-pMHCII$^+$ CD4$^+$ T cells in paired blood and tonsils for latent and lytic epitopes separately, as shown in Fig 6.1c. Interestingly, across the 10 matched samples tested for latent reactive EBV-pMHCII$^+$ CD4$^+$ T cells, frequencies were significantly higher in the tonsil compared to the periphery (left-hand graph). Conversely, there was no significant difference in the frequencies of EBV-pMHCII$^+$ CD4$^+$ T cells specific for lytic reactivities between tonsil UMs and PBMCs. This indicates that, akin to EBV-specific CD8$^+$ T cells, latent protein-specific EBV-specific CD4$^+$ T cells are preferentially recruited and/or retained in the tonsil compared to lytic epitope-specific CD4$^+$ T cells.

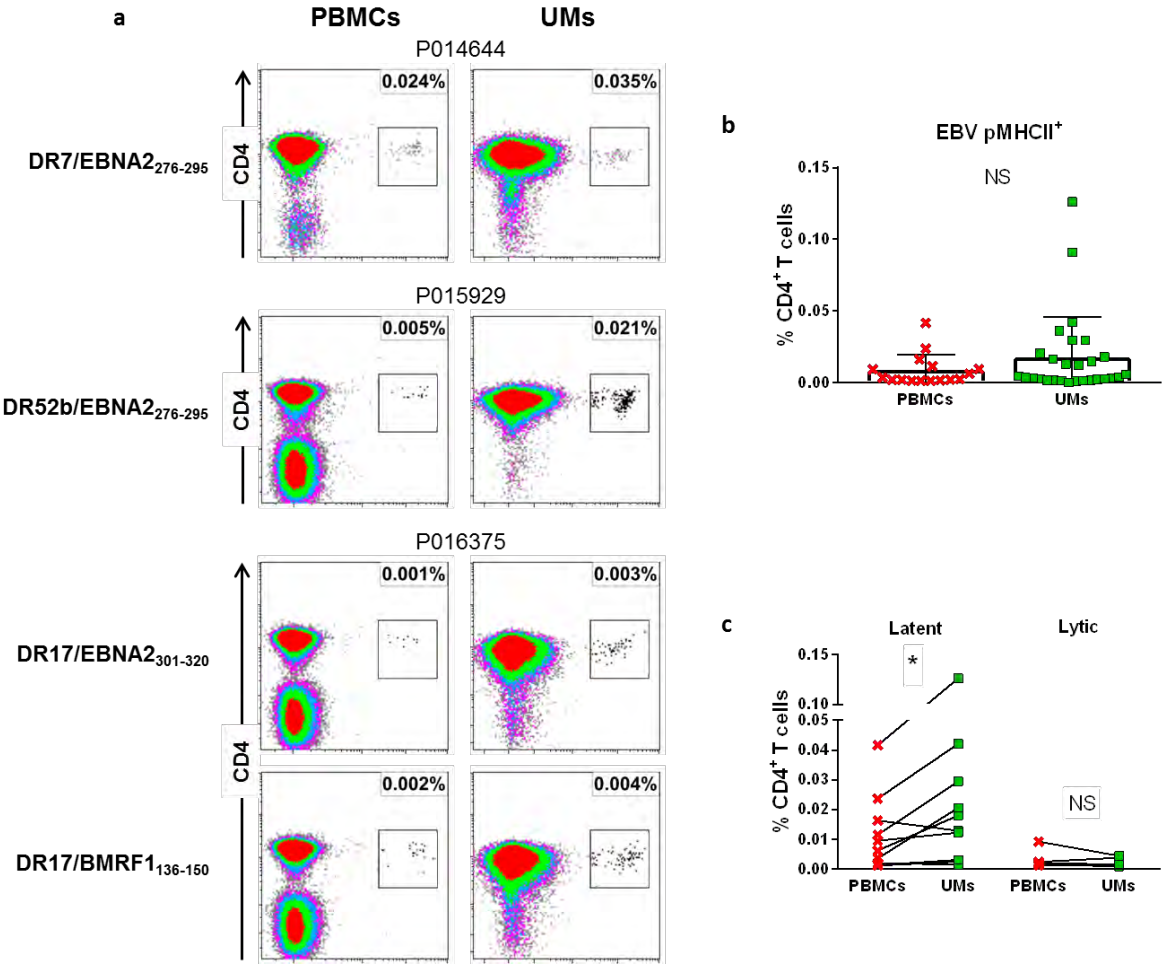

Figure 6.1 Frequencies of EBV-specific CD4⁺ T cells in PBMCs *versus* the tonsil. (a) PBMCs and CD4 enriched UMs from patients undergoing routine tonsillectomy were stained with the relevant EBV-pMHCII tetramers (Table 2.1). The percentage in each plot indicates EBV-pMHCII⁺ frequency in the total CD4⁺ T cell population. **(b)** Summary of EBV-pMHCII⁺ cell frequencies in the total CD4⁺ population of 16 PBMC samples and 28 UM samples and show the mean value with SD. **(c)** Summary graph of latent (left) and lytic (right) epitope specific EBV-pMHCII⁺ cells in the total CD4⁺ population of matched PBMCs and UMs samples from 10 and 6 donors respectively. * *P* <0.05; Wilcoxon signed-rank test.

We next analysed whether the enrichment of virus-specific CD4⁺ T cells was limited to EBV, which infects and replicates at this site, or whether a similar trend could be observed for other virus-specific CD4+ T cells where the tonsils are not the viral reservoir. To address this question, where possible, we compared the magnitudes of

immune responses to CMV and Influenza in the same donors, using pMHCII tetramers loaded with the $M1_{43-59}$ (Influenza) and the $gB_{217-228}$ (CMV) epitopes presented by DR7. Fig 6.2a shows an example of staining in PBMCs (left plots) and UMs (right plots) with the DR7/$EBNA2_{276-295}$ tetramer alongside the DR7/$M1_{43-59}$ tetramer for donor P014644 and the DR7/$gB_{217-228}$ tetramer for donor P015704. As previously observed in Fig 6.1, the frequency of $CD4^+$ T cells specific for the latent derived epitope $EBNA2_{276-295}$ is higher in the tonsil compared to matched blood in both donors (0.024% *versus* 0.002% and 0.035% *versus* 0.007% for P014644 and P015704 respectively). In contrast, the frequency of $M1_{43-59}$-specific $CD4^+$ T cells was lower in the tonsillar compartment of donor P014644 (0.017% in PBMCs *versus* 0.006% in UMs). Even more strikingly, in donor P015704 $gB_{217-228}$-specific $CD4^+$ T cells were 22-fold lower in UMs compared to PBMCs, with only 0.014% of total $CD4^+$ T cells staining positively in the tonsil compared to 0.314% in the periphery. Fig 6.2b shows summary data from the 4 matched pairs tested. In all four donors tested the frequency of $pMHCII^+$ $CD4^+$ T cells was lower in tonsil UMs compared to PBMCs suggesting that unlike EBV-specific $CD4^+$ T cells, CMV and Influenza-specific $CD4^+$ T cells are not preferentially recruited or retained in the tonsil.

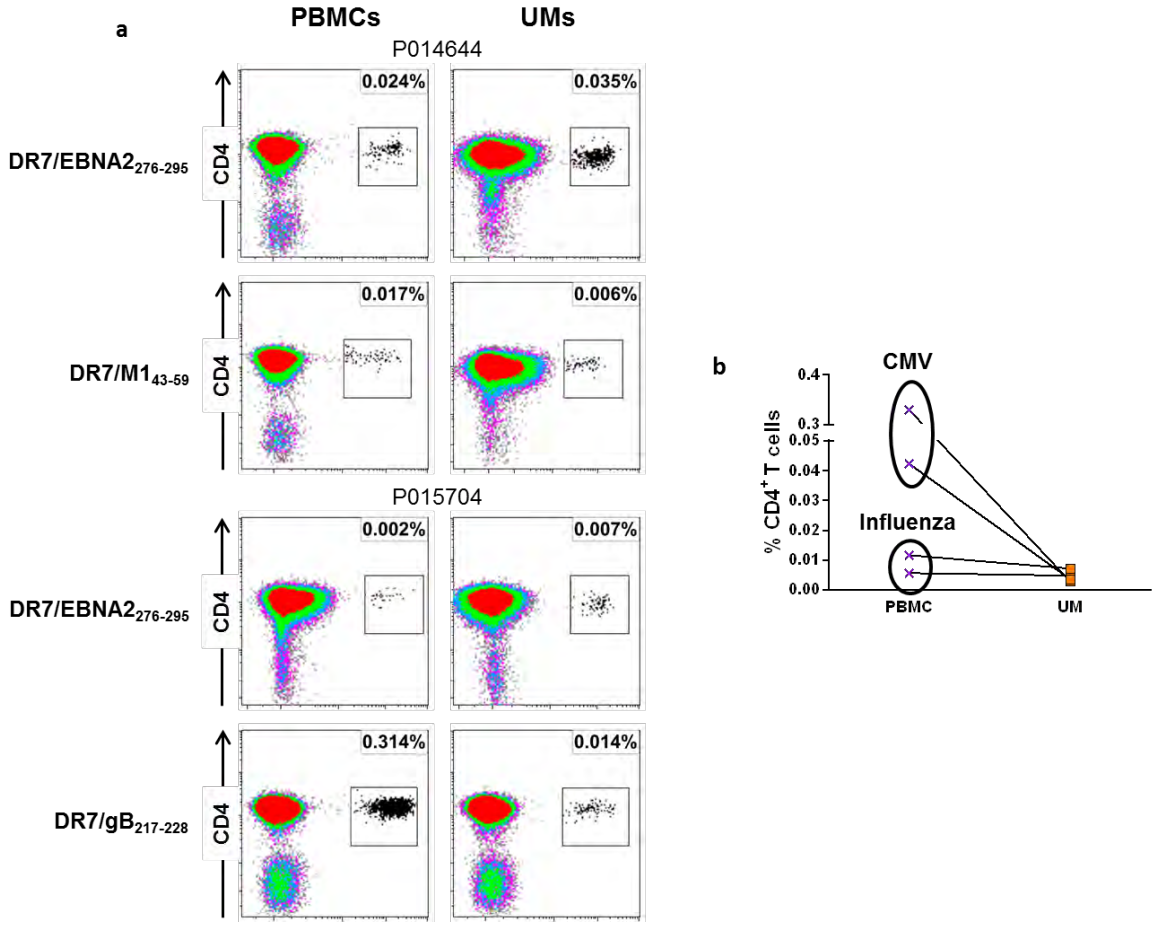

Figure 6.2 Frequencies of Influenza and CMV-specific CD4$^+$ T cells in PBMCs *versus* the tonsil. (a) CD4-enriched PBMCs and UMs from patients undergoing routine tonsillectomy were stained with EBV-pMHCII, DR7/M1$_{43-59}$ or DR7/gB$_{217-228}$ pMHCII tetramer (Table 2.1). The percentage in each plot indicates pMHCII$^+$ frequency in the total CD4$^+$ T cell population. **(b)** Summary graph of control pMHCII$^+$ cell frequencies in the total CD4$^+$ population of matched PBMCs and UMs samples from 4 donors.

b. EBV-specific CD4$^+$ T cells in the tonsil display a T_{RM} phenotype

We next investigated the phenotype of EBV-pMHCII$^+$ CD4$^+$ T cells present within tonsils. We first analysed surface expression of CD45RA and CCR7, markers that enable classification into different memory phenotypes (171). As shown in Fig 6.3a there were marked differences in the distribution of T_N, T_{EM}, T_{CM} and T_{EMRA} between the total and EBV-pMHCII$^+$ CD4$^+$ T cell populations.

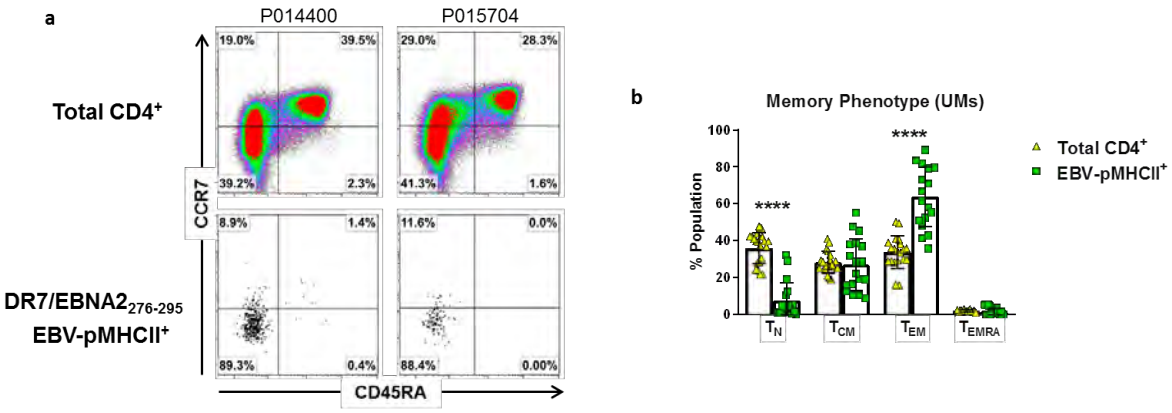

Figure 6.3 Memory phenotype of EBV-specific CD4⁺ T cells in the tonsil. (a) Analysis of CCR7 and CD45RA surface expression in the total CD4⁺ (top) and DR7/EBNA2$_{276-295}$-specific CD4⁺ T cells (bottom) in UMs. **(b)** Summary of memory phenotype frequencies in the total CD4⁺ (yellow triangles) and EBV-MHCII⁺ populations (green squares). The graph depicts results from 18 independent experiments. Data are shown as mean ± SD. **** $P < 0.0001$; unpaired Student's *t* test with Welch's correction.

The vast majority of the EBNA2$_{276-295}$-specific CD4⁺ T cells display an effector memory phenotype (89.3% and 88.4% respectively) with low frequencies in the T_{CM} pool. Naïve-like EBV-pMHCII CD4⁺ T cells were present at low frequencies in P0144400 and undetectable in the antigen-specific population analysed in P015704. The summary data from 18 donors is shown in Fig 6.3b. The majority of EBV-specific CD4⁺ T cells in the tonsil display a T_{EM} phenotype, with a significantly higher proportion of cells lying in this memory compartment than in the total CD4⁺ populations of the same donors (mean 63.9% *versus* mean 33.9%; $P < 0.0001$). Conversely, naïve-like EBV-pMHCII⁺ were virtually undetectable in the tonsil whereas a large percentage of the total CD4⁺ population have a naïve phenotype (mean 2.7% *versus* mean 36.0%; $P < 0.0001$). There was no significant difference in the frequency of cells displaying a T_{CM} memory phenotype between the EBV-pMHCII⁺ and total CD4⁺ populations (mean 27.0% *versus* 28.2%; *NS*), however the frequency of CM cells appeared to be a lot more variable in the

tetramer stained cells. Thus, the enriched populations of EBV-pMHCII$^+$ CD4$^+$ T cells within the tonsil were predominantly CD45RA$^-$ antigen-experienced memory T cells, with few naïve EBV-specific CD4$^+$ T cells present.

To investigate whether tonsillar EBV-specific CD4$^+$ T cells expressed markers associated with tissue residency, we assessed expression of CD69 and CD103, two surface markers commonly associated with T_{RM}. Representative examples of CD69 and CD103 staining in the total and EBV-pMHCII$^+$ CD4$^+$ populations of tonsillar UMs from 2 donors are shown in Fig 6.4a. The total CD4$^+$ T cell pools of both P014400 and P016266 contained cells positive for one or both markers. In particular, CD69$^+$ CD103$^-$ cells accounted for 42.6% and 47.9% of all cells, respectively. In the DR7/EBNA2$_{276-295}$-specific CD4$^+$ populations, elevated frequencies of cells fell within this CD69$^+$ CD103$^-$ phenotype, 65.9% in P014400 and 56.0% in P016266. In donor P014400, a further 10.5% of EBNA2$_{276-295}$-specific CD4$^+$ T cells also expressed CD103, whereas in donor P016266, only 0.6% of EBNA2$_{276-295}$-specific CD4$^+$ T cells expressed this protein. CD69 and CD103 expression in the total CD4 and EBV-pMHCII$^+$ CD4$^+$ T cell populations of tonsillar UMs of 18 donors is summarised in Fig 6.4b. Overall, expression of CD69 was significantly higher in the EBV-pMHCII$^+$ population compared to the corresponding total CD4$^+$ T cell pool (mean 69.2% *versus* mean 49.1%; $P < 0.0001$). Although CD103 expression was not as prominent as CD69, overall it was also significantly increased in the EBV-pMHCII$^+$ CD4$^+$ T cells (mean 6.9% *versus* mean 0.6%; $P < 0.01$). To confirm that CD69 was not expressed on the EBV-specific memory T cells in the blood (393), we analysed the paired PBMC samples from these donors. Although small populations of total CD4$^+$ T cells were positive for either CD69 or CD103, the EBV-pMHCII$^+$ CD4$^+$ T cells were predominantly negative for both (Fig 6.4c).

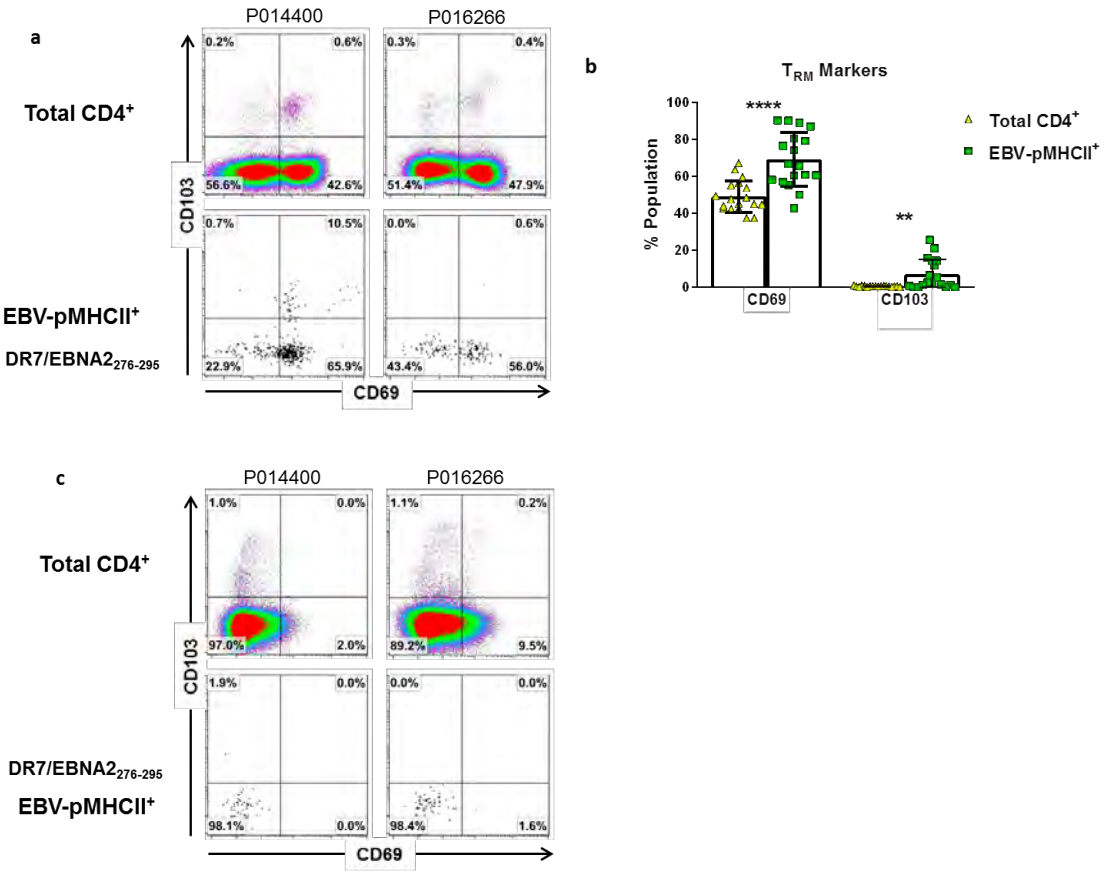

Figure 6.4 Resident memory phenotype of EBV-pMHCII$^+$ CD4$^+$ T cells in peripheral blood and the tonsil. **(a and c)** Analysis of CD69 and CD103 surface expression in the total CD4$^+$ (top) and the DR7/EBNA2$_{276-295}$-specific (bottom) in **(a)** UMs and **(c)** PBMCs. **(b)** Summary of resident memory marker expression frequencies in the total CD4$^+$ (yellow triangles) and EBV-pMHCII$^+$ populations (green squares) of UMs. The graph depicts results from 18 independent experiments. Data are shown as mean ± SD. **** $P < 0.0001$; ** $P < 0.01$; unpaired Student's *t* test with Welch's correction.

Fig 6.5a shows corresponding analysis of the low frequency Influenza and CMV-specific CD4$^+$ T cells in the tonsil. In contrast to the EBV-specific CD4$^+$ T cells, CD69 expression was lower on the M1$_{43-59}$-specfic and gB$_{217-228}$ specific CD4$^+$ T cells compared to the total CD4$^+$ T cell pools of the same donors (46.3% *versus* 15.6% in donor P014644, top plots; 64.3% *versus* 32.1% for P015704, bottom plots) and CD103 expression was entirely absent. Indeed, CD69 positivity was significantly lower in the antigen-specific CD4$^+$

population compared to the corresponding total CD4⁺ T cell pool across all 7 donors tested (mean 36.4% *versus* mean 50.2%; $P < 0.05$; Fig 6.9b). Thus, the tissue residency marker CD69 is specifically upregulated on EBV-specific CD4⁺ T cell populations in the tonsil. Collectively these data suggest that EBV-specific memory CD4⁺ T cells are retained at the site of EBV infection.

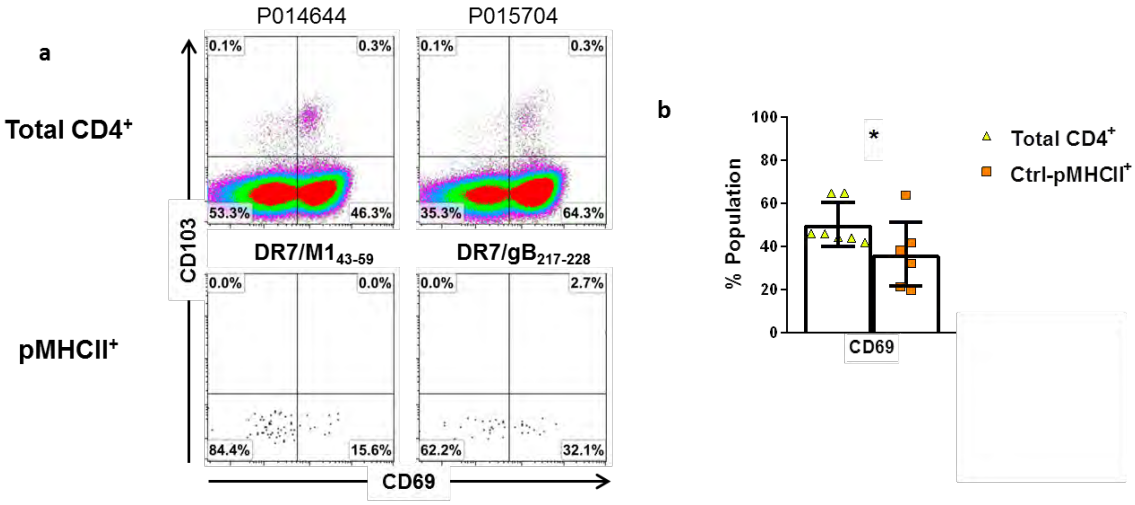

Figure 6.5 Resident memory phenotype of CMV and Influenza-specific CD4⁺ T cells in the tonsil. (a) Analysis of CD69 and CD103 surface expression in the total CD4⁺ (top) and the DR7/M1$_{43\text{-}59}$ or DR7/gB$_{217\text{-}228}$ pMHCII tetramer⁺ CD4⁺ T cells (bottom) in UMs. **(b)** Summary of resident memory marker expression frequencies in the total CD4⁺ (yellow triangles) and pMHCII⁺ populations (orange squares) of UMs. The graph depicts results from 7 independent experiments. Data are shown as mean ± SD. NS; unpaired Student's *t* test with Welch's correction.

In mice, the transcription factors Hobit and Blimp1 have been implicated as central regulators in down-regulating molecules associated with tissue egress thereby maintaining CD8⁺ T cell within the tissue (397), although this has not been verified in CD4⁺ T_{RM} populations. We therefore analysed co-expression of Hobit with CD69. As shown in Fig 6.6a, we were only able to detect a small population of Hobit⁺ CD4⁺ T cells

within tonsillar UMs. In donor S173047, 0.2% of the total $CD4^+$ T cell pool expressed Hobit, yet in the DR52b/$EBNA2_{276-295}$-specific population in the same donor there was no detectable expression. In a further 5 samples, Hobit was expressed in similarly low frequencies of $CD4^+$ T cells, and was not significantly elevated within the EBV-$pMHCII^+$ population. Moreover, expression of Hobit was equally low within the $CD69^+$ and $CD69^-$ antigen-specific $CD4^+$ T cell populations. Despite numerous attempts we were unable to optimise measurement of Blimp-1 by flow cytometry.

In addition to being upregulated in T_{RM} cells, CD69 is also transiently expressed on recently activated T cells (469). Therefore, having only detected low expression of one of the transcription factors that is proposed to govern tissue residency, it was important to verify that CD69 expression on EBV-$pMHCII^+$ $CD4^+$ T cells was not the result of recent activation. We therefore co-stained with CD69 and the proliferation marker Ki-67. As shown in Fig 6.6c, small populations of $CD69^+$ $Ki\text{-}67^+$ cells were present within both the total and EBV-$pMHCII^+$ $CD4^+$ T cell pool (1.9% and 3.2% respectively in donor P014645; 1.3% and 3.2% respectively in donor P016266). However, the vast majority of CD69 expressing cells did not co-express Ki-67. The summary data in the EBV-$pMHCII^+$ $CD4^+$ T cells from 6 donors is shown in Fig 6.6d. These results indicate that the EBV-specific memory $CD4^+$ T cells enriched within the tonsils have a resting T_{RM} phenotype, but do not express the transcription factor associated with tissue residency in murine $CD8^+$ T cells, Hobit.

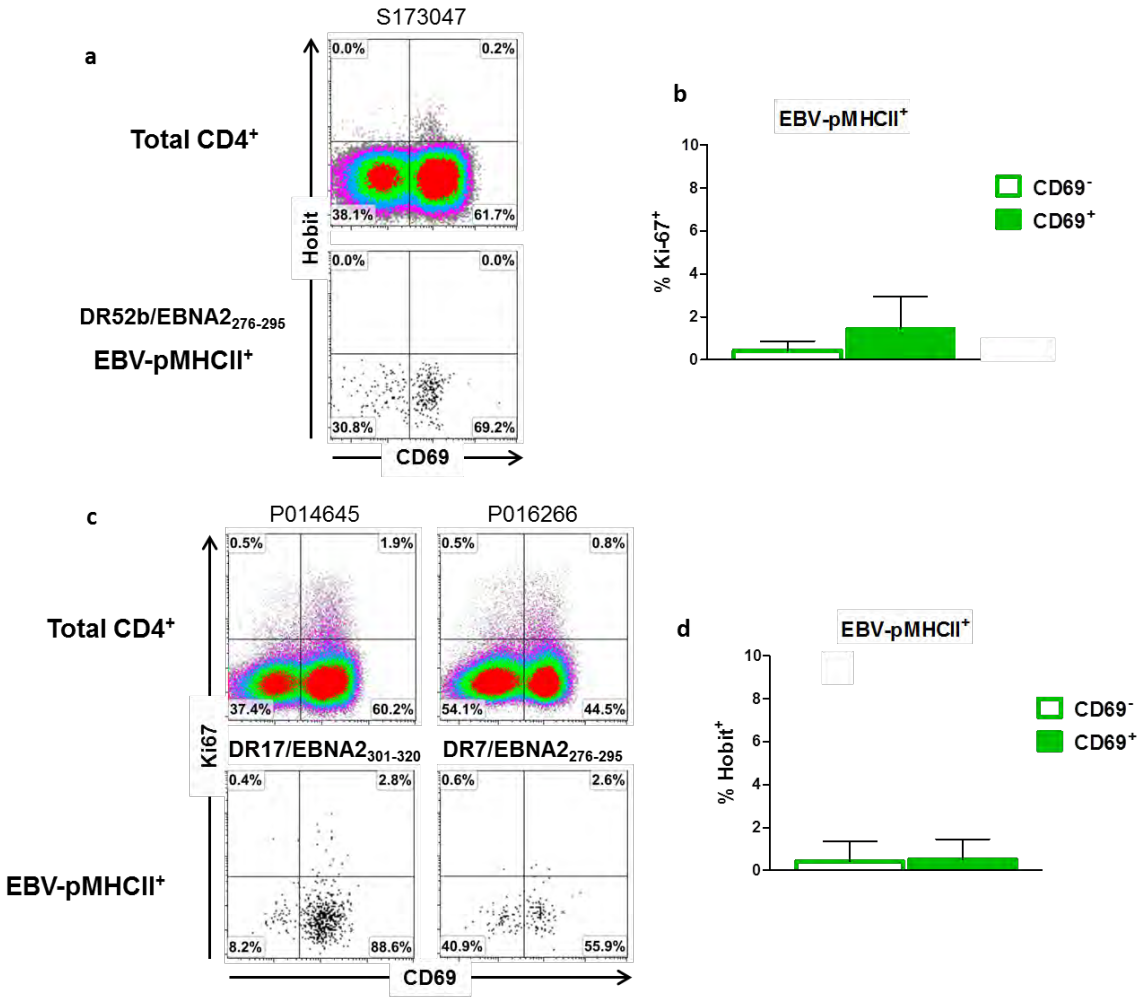

Figure 6.6 Expression of the T_{RM} associated transcription factor Hobit and proliferation of EBV-pMHCII$^+$ CD4$^+$ T cells in the tonsil. (a and c) CD4-enriched UMs were stained with the relevant EBV-pMHCII tetramers (Table 2.1) and analysed by flow cytometry for intracellular expression of **(a)** Hobit and **(c)** Ki-67. Co-expression of Hobit and Ki-67 with CD69 in the total CD4$^+$ population (top) and EBV-pMHCII$^+$ for representative donors. **(b and d)** summary graphs of Hobit and Ki-67 expression in the CD69$^-$ (empty bars) and CD69$^+$ (filled bars) of EBV-pMHCII$^+$ CD4$^+$ T cell populations. The graph depicts results from a minimum of 6 independent experiments. Data are shown as mean ± SD. * $P < 0.05$; Mann-Whitney *U*-test.

c. Tonsillar EBV-specific CD4$^+$ T cell subset analysis

Having identified T_{RM} cells within the EBV-specific CD4$^+$ T cell populations in the tonsil, we next wanted to investigate their functional role. The tonsil is a secondary lymphoid tissue organised into discrete areas where T cells get activated and can also provide help

to B cells. As MHC-II is constitutively expressed on EBV-infected B cells, $CD4^+$ T cells specific for the virus in the tonsil could be acting as direct effectors (as we have observed in the circulation Fig 3.5 and 3.9) or helping promote production of EBV-specific antibodies by B cells (T_{FH}). Recent CyTOF analysis has shown that expression of cell surface molecules on $CD4^+$ T cells reflects their ability to migrate within the tonsil and carried out functions associated with T_{FH} (146). Differential expression of CXCR5, PD-1, ICOS, CCR7 and CD57 enables identification of $CD4^+$ T cells that are present or able to migrate from the blood to the T cell zone, B cell zone and germinal centres (Figure 1.3) (146). Thus, analysis of these markers allows further characterization of the functional subsets of EBV-specific $CD4^+$ T cells present within the tissue.

In initial experiments we investigated whether tonsillar EBV-specific $CD4^+$ populations contained cells with a T_{FH} phenotype. Fig 6.7a illustrates the gating strategy employed to identify cells with phenotypes associated with access to different regions within the structure of the lymph node, as defined by Wong *et al*. (Fig 1.3) (146). Accordingly, $CD4^+$ T cells lacking both CXCR5 and PD-1 were designated as "non-follicular"; $CD4^+$ T cells displaying a $CXCR5^{lo}$ $PD\text{-}1^{lo}$ phenotype were characterised as capable of homing to the T cell zone; and high expression of both CXCR5 and PD-1 suggested the capacity to migrate into B cell follicles. Representative examples of CXCR5 and PD-1 co staining in the total and EBV-$pMHCII^+$ $CD4^+$ T cell populations in tonsillar UMs are shown in Fig 6.7b. Within the total $CD4^+$ T cell pool, the proportion of $CXCR5^-$ $PD\text{-}1^-$, $CXCR5^{lo}$ $PD\text{-}1^{lo}$, $CXCR5^{hi}$ $PD\text{-}1^{hi}$ varied between donors. Donors P014400 and P014425 had similar frequencies of $CD4^+$ T cells with a $CXCR5^{lo}$ $PD\text{-}1^{lo}$ phenotype (30.1% and 32.3% respectively) and a $CXCR5^{hi}$ $PD\text{-}1^{hi}$ phenotype (9.4% and 9.5% respectively). Yet donor P014645 had higher

frequencies of $CD4^+$ T cells with both T cell zone and B cell follicle phenotypes (47.6% and 18.0% respectively). Interestingly, subsequent analysis of EBV-$pMHCII^+$ $CD4^+$ T cell populations, using three different EBNA2 tetramers, showed that the majority of tonsillar EBV-specific $CD4^+$ T cells displayed a $CXCR5^{lo}$ $PD\text{-}1^{lo}$ phenotype, indicating the capacity to migrate into the T cell zone. In each case $CXCR5^{lo}$ $PD\text{-}1^{lo}$ cells were over-represented compared to the corresponding total $CD4^+$ T cell population (30.1% *versus* 79.7% for donor P014400; 32.3% *versus* 67.2% for donor P014425; 47.6% *versus* 66.4% for donor P014645) and very few $CXCR5^-$ $PD\text{-}1^-$ cells were present. The percentage of $CXCR5^{hi}$ $PD\text{-}1^{hi}$ varied between donors. In donor P014400, frequencies of $CXCR5^{hi}$ $PD\text{-}1^{hi}$ cells were lower in the EBV-$pMHCII^+$ population compared to the total $CD4^+$ pool (1.6% *versus* 9.4%) yet in donors P014425 and P0014645 they were substantially higher (18.2% *versus* 9.5% and 27.9% *versus* 18.0% respectively). Fig 6.7b shows a summary of the frequencies of total $CD4^+$ and EBV-$pMHCII^+$ $CD4^+$ T cells exhibiting non-follicular, T cell zone and B cell follicle phenotypes. Non-follicular $CXCR5^-$ $PD\text{-}1^-$ cells were significantly lower in the EBV-$pMHCII^+$ population compared to the total $CD4^+$ pool (decreased in all but 3 donors) (mean 46.2% *versus* 17.8%; $P < 0.001$). Whereas $CXCR5^{lo}$ $PD\text{-}1^{lo}$ cells were over-represented in the EBV-$pMHCII^+$ $CD4^+$ T cells compared to the total $CD4^+$ pool (mean 43.9% *versus* 71.3%; $P < 0.001$). Although EBV-$pMHCII^+$ $CD4^+$ T cells with a $CXCR5^{hi}$ $PD\text{-}1^{hi}$ phenotype were present, their frequency was not significantly different between the total $CD4^+$ and EBV-$pMHCII^+$ populations (mean 10.5% *versus* 10.9%; NS), suggesting no preferential enrichment or differentiation of EBV-specific $CD4^+$ T cells to enable migration into B cell follicles.

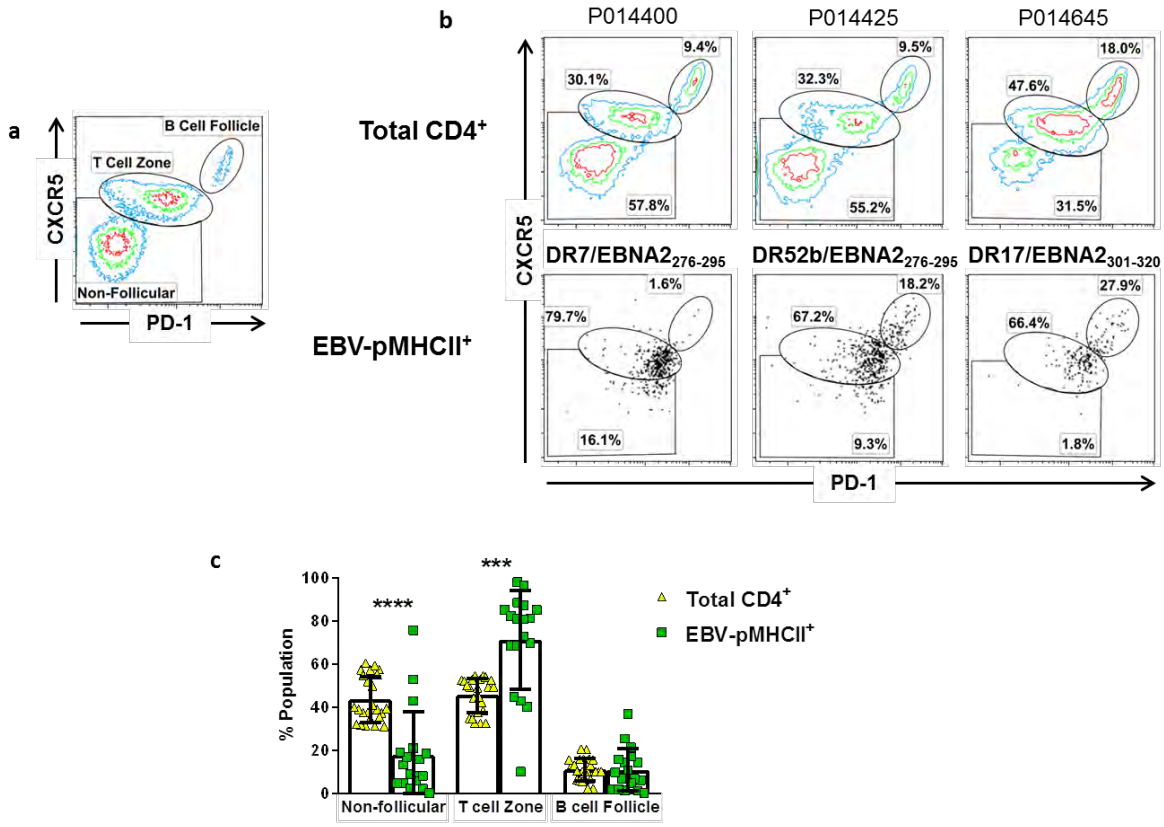

Figure 6.7 T_{FH} phenotype of EBV-specific CD4⁺ T cells in the tonsil. (a-b) CD4-enriched UMs were stained with the relevant EBV-pMHCII tetramers (Table 2.1) and analysed for expression of CXCR5 and PD-1. **(a)** Gating strategy to differentiate subtypes of non-follicular and follicular helper T cells. **(b)** CXCR5 and PD-1 in the total CD4⁺ population (top) and EBV-pMHCII⁺ CD4⁺ T cells of three representative donors (bottom). **(c)** Summary of subtype frequencies in the total CD4⁺ (yellow triangles) and EBV-pMHCII⁺ populations (green squares). The graph depicts results from 18 independent experiments. Data are shown as mean ± SD. **** $P < 0.0001$; *** $P < 0.001$; unpaired Student's *t* test with Welch's correction.

To determine whether the enrichment of cells displaying CXCR5^{lo} PD-1^{lo} and CXCR5^{hi} PD-1^{hi} phenotypes was unique to EBV-specific CD4⁺ T cells, we performed similar analyses on the CMV and Influenza specific CD4⁺ T cells in the DR7⁺ donors. The representative donor in Fig 6.8a and the concatenated data from 7 donors in Fig 6.8b show that, in contrast to EBV, there was no over representation of cells in any defined subset. Rather, the phenotype of the Ctrl-pMHCII⁺ cells mirrored that of the total CD4⁺ pool.

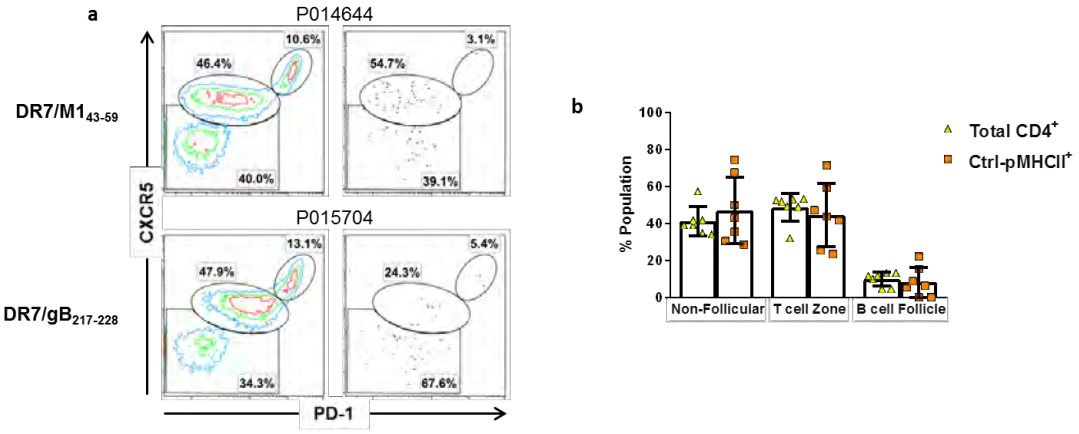

Figure 6.8 T_{FH} phenotype of CMV and Influenza-specific $CD4^+$ T cells in the tonsil. (a) CXCR5 and PD-1 expression in the total $CD4^+$ (top) and the DR7/$M1_{43-59}$ or DR7/$gB_{217-228}$ pMHCII tetramer$^+$ $CD4^+$ T cells (bottom) in UMs. **(b)** Summary of T_{FH} marker expression frequencies in the total $CD4^+$ (yellow triangles) and $pMHCII^+$ populations (orange squares) of UMs. The graph depicts results from 7 independent experiments. Data are shown as mean ± SD. NS; unpaired Student's *t* test with Welch's correction.

To further confirm the T cell zone and B cell follicle phenotypes classifications of the EBV-$pMHCII^+$ cells, as defined by Wong *et al.*, we also analysed expression of ICOS (CD278) and CCR7. In the donors shown in Fig 6.9a, ICOS expression was low in non-follicular $CD4^+$ T cells (grey), intermediately expressed in T cell zone $CD4^+$ T cells (black) and highest on B cell follicle $CD4^+$ T cells (blue). In contrast, CCR7 expression was highest in non-follicular $CD4^+$ T cells and lowest in cells migrating to the B cell follicle. This data fits entirely with the Wong *et al.* classification (146). Interestingly, within the $CXCR5^{hi}$ $PD\text{-}1^{hi}$ B cell follicle population, some cells expressed no CCR7 (right-hand plots). *Bona fide* T_{FH} are present in the germinal centres of lymphoid tissue and provide critical help for B cell maturation. These cells are $CCR7^-$ and express CD57 and Bcl-6 (146). In donors P014425 and P014645 shown in Fig 6.9b, expression of CD57 and Bcl-6 was highest in the $CD4^+$ T cells with a $CXCR5^{hi}$ $PD\text{-}1^{hi}$, B cell follicle, phenotype (blue histogram).

Furthermore, CD57 expression was noticeably raised in the EBV-pMHCII$^+$ CD4$^+$ T cells compared to the total CD4$^+$ pool of these donors (26.5% *versus* 41.6% and 35.5% *versus* 41.5%; Fig 6.9c). Finally, we investigated whether there was any correlation between the enrichment of EBV-specific CD4$^+$ T cells with T cell zone and B cell follicle phenotype and expression of the tissue residency marker CD69. The histograms shown in Fig 6.9.d show there was a clear increase in CD69 expression in total CD4$^+$ T cells with a T cell zone and B cell follicle phenotype (black and blue histograms respectively) compared to those designated as non-follicular cells, which likely circulate back into the blood. Within the EBV-pMHCII$^+$ CD4$^+$ T cells from each donor, CD69 was clearly expressed in the cells with a T cell zone phenotype, and was further increased in those with a B cell follicle phenotype (bottom plots).

Thus, the tonsils of EBV positive healthy carriers contain enriched populations of EBV-specific CD4$^+$ T cells with the capacity to migrate into the T cell zone and B cell follicles; of which a small population express CD57 and Bcl-6, characteristic of *bona fide* T_{FH} cells. These cells have increased expression of the tissue residency marker CD69, indicating their residence in these sites.

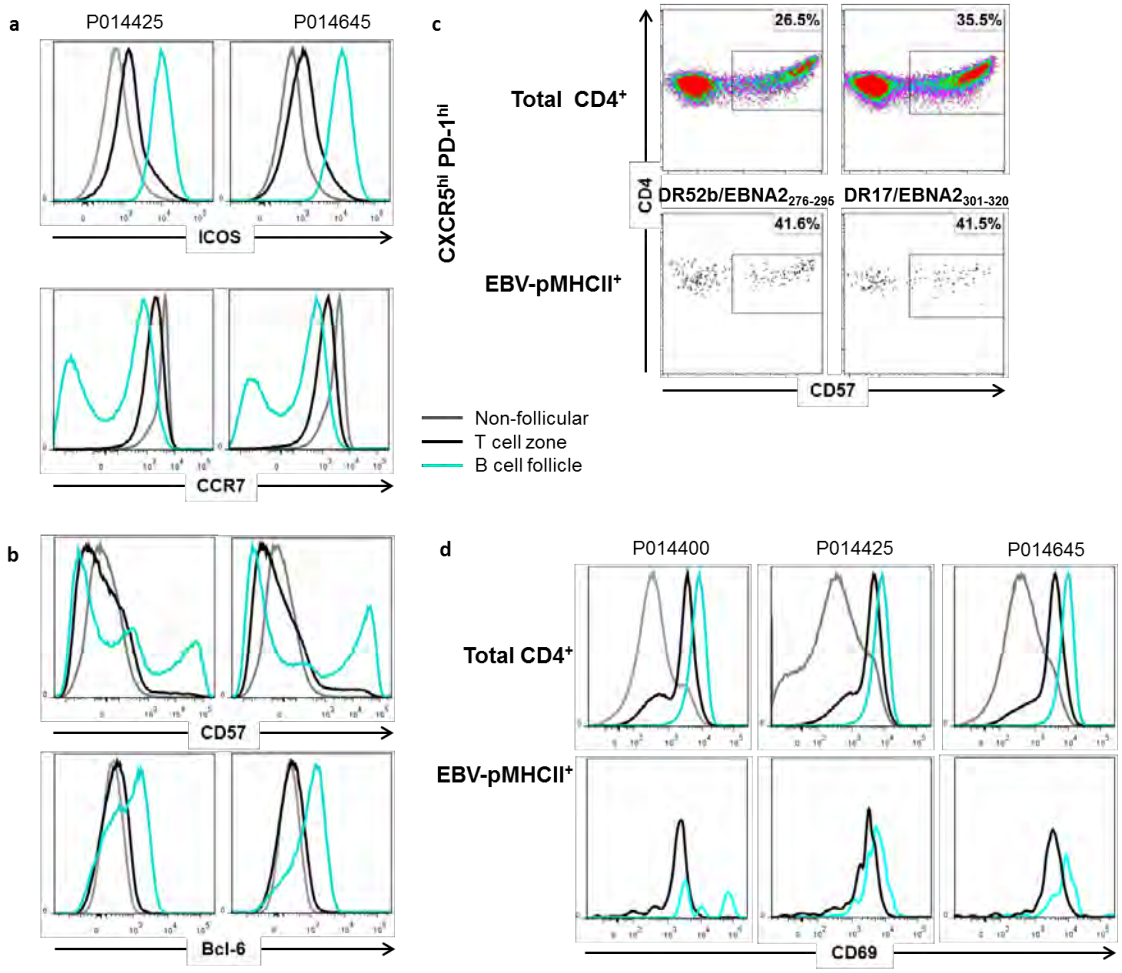

Figure 6.9 Differential expression of cellular markers by EBV-specific CD4⁺ T_{FH} cell subsets in the tonsil. **(a-d)** Relative expression of **(a)** ICOS (CD278), CCR7, **(b)** CD57, Bcl-6 in non-follicular (grey), T cell zone (black) and B cell follicle (cyan) CD4⁺ T cells. **(c)** CD57 expression in the total and EBV-pMHCII⁺ CXCR5^{hi} PD-1^{hi} B cell follicle-designated CD4⁺ T cells of two representative donors. **(d)** Relative expression of CD69 in non-follicular (grey), T cell zone (black) and B cell follicle (cyan) in the total CD4⁺ population and EBV-pMHCII⁺ CD4⁺ T cells of three representative donors.

d. Tonsillar EBV-specific CD4⁺ T cells possess direct effector function and enhanced cytotoxic capacity.

Multiple reports have described the elevated capacity of resident memory T cells to rapidly respond to antigenic challenge in order to control re-infection or viral

reactivation in susceptible tissues (394, 404). Having identified a high proportion of EBV-specific $CD4^+$ T_{RM} cells within the tonsil we sought to investigate their functional capacity, and to compare this to circulating EBV-specific $CD4^+$ T cells in the periphery.

We initially assessed the cytokine profile of the total T cell pool in PBMCs and UMS using non-specific PMA and Ionomycin stimulation. As shown in Fig 6.10a we detected production of IFNγ, TNFα, IL-2, GM-CSF, IL-10, IL-21 and IL-4 in $CD3^+$ T cells from both compartments in response to incubation with PMA/Ionomycin. Of these cytokines only IL-10 and IL-21 were produced in a significantly higher frequency of tonsillar $CD4^+$ T cells compared to PBMCs.

We next assessed the ability of EBV-specific $CD4^+$ T cells in the tonsil to respond to antigenic stimulation using autologous EBV-transformed B cells. Fig 6.11b shows a representative example of IFNγ, TNFα and IL-2 production following overnight stimulations with autologous LCL, performed as described in chapter 3. Following LCL stimulation, we detected noticeably higher frequencies of $CD4^+$ T cells producing IFNγ and TNFα in tonsillar UMs compared to PBMCs (0.9% *versus* 0.1% for IFNγ and 1.0% *versus* 0.1% for TNFα respectively; top and middle plots). Production of IL-2 was comparable between $CD4^+$ T cells from UMs and PBMCs, (0.1% *versus* 0.1%; bottom plots).

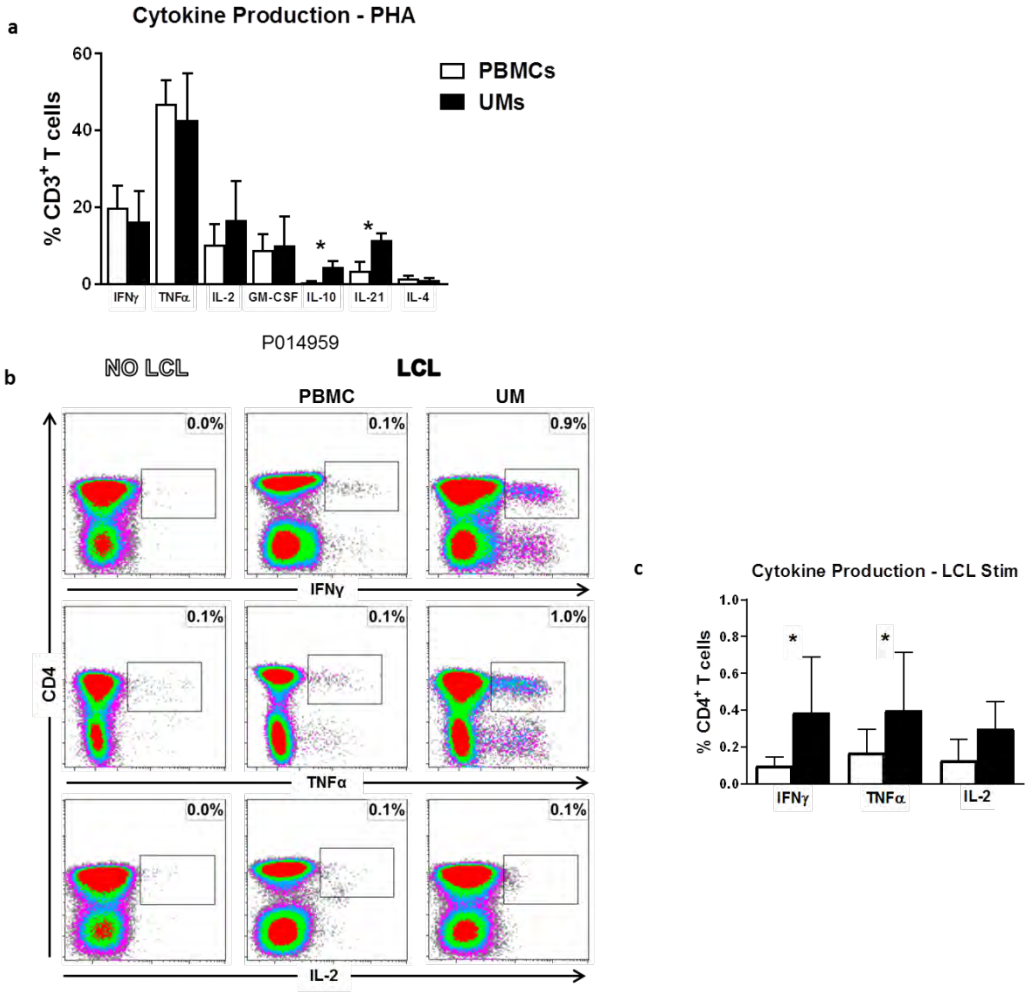

Figure 6.10 Cytokine profile of EBV-specific CD4⁺ T cells in the tonsil. (a) Summary of cytokine production by $CD3^+$ T cells in PBMCs (empty bars) and UMs (filled bars) following overnight stimulation with PMA/Ionomycin. **(b)** PBMCs and UMS were either unmanipulated (left panel) or stimulated with autologous LCLs (middle and right respectively) and analysed by flow cytometry for intracellular expression of IFNγ, TNFα, and IL-2. Percentage in each plot indicates cytokine production in the total $CD4^+$ T cell population. **(c)** Summary graphs depicting intracellular expression of IFNγ, TNFα, and IL-2 in stimulated PBMCs (unfilled) or stimulated UMs (filled). Results are from a minimum of 6 independent donors. Data are shown as mean ± SD. * $P < 0.05$; Mann-Whitney *U*-test.

This held true in matched samples from 6 donors (Fig 6.10c), where we observed significantly higher production of IFNγ and TNFα in tonsillar UMs compared to PBMCs following stimulation (mean 0.4% *versus* mean 0.1%; $P < 0.05$ for IFNγ; mean 0.4% *versus* mean 0.2%; $P < 0.05$ for TNFα), but no significant difference in IL-2 production (mean

0.3% *versus* mean 0.1%; NS). Interestingly, GM-CSF, IL-10, IL-21 and IL-4 production were all undetectable following autologous LCL stimulation.

This cytokine profile suggested a T_H1-like response, as we had previously seen in circulating EBV-pMHCII$^+$ CD4$^+$ T cells. Accordingly, in the representative example of tonsillar staining shown in Fig 6.11a, expression of T-bet was higher in the DR52b/EBNA2$_{276-295}$-specific population than in the total CD4$^+$ T cell pool (59.9% *versus* 82.5% respectively; top plots). Although low frequencies of FoxP3 expression was detected in the total CD4$^+$ T cell population of this donor, no FoxP3$^+$ EBV-pMHCII$^+$ CD4$^+$ T cells were detected. The summary data is shown in Fig 6.11b. Overall, T-bet expression was significantly higher in the EBV-pMHCII$^+$ CD4$^+$ T cells than in total CD4$^+$ T cells (mean 85.3% *versus* 70.0%; $P < 0.01$), whereas FoxP3 was significantly lower (mean 0.5% *versus* 2.4%; $P < 0.001$).

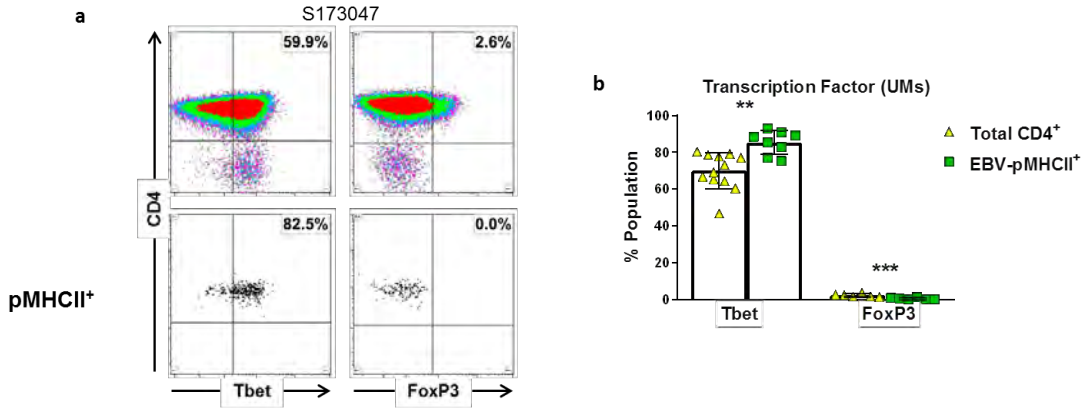

Figure 6.11 Transcription factor expression in EBV-specific CD4$^+$ T cells in the tonsil. CD4 enriched tonsillar UMs were stained with EBV-pMHCII followed by intracellular staining for transcription factors. **(a)** Representative example of T-bet (left) and FoxP3 (right) in the total CD4$^+$ (top) and EBV-pMHCII$^+$ population (bottom). The percentage in the top plots indicates TF expression in the total CD4$^+$ T cell population **(b)** Summary of transcription factor expression in unstimulated total CD4$^+$ (yellow triangles) and EBV-specific pMHCII tetramer$^+$ CD4$^+$ T cell populations (green squares). The graph depicts

results from 12 independent experiments. Data are shown as mean ± SD. ** $P < 0.01$; *** $P < 0.001$ unpaired Student's *t* test with Welch's correction.

Finally, we were interested in whether the EBV-specific $CD4^+$ T cells residing in the tonsil, at the site of EBV infection and reactivation, had increased potential to eliminate EBV-infected cells. We therefore compared the cytotoxic potential of EBV-specific $CD4^+$T cells in the tonsil and periphery by measuring degranulation following overnight incubation with autologous EBV-transformed B cells (Fig 4.1). A representative example of CD107a staining in PBMCs and matched UMs following overnight incubation with LCL is shown in Fig 6.12a. In this donor 0.3% of PBMC $CD4^+$ T cells degranulated in response to LCL stimulation, consistent with our observations in the healthy carrier cohort in Chapter 4. However, the frequency of $CD107a^+$ $CD4^+$ T cells post-LCL stimulation was 4-fold higher in the tonsillar UMs from this donor, accounting for 1.0% of the total $CD4^+$ T cell pool. This assay was repeated on paired PBMC and UM samples from 6 donors, and overall a significantly higher frequency of $CD107a^+$ $CD4^+$ T cells were detected in stimulated tonsillar UMs compared to PBMCs (mean 1.5% *versus* mean 0.3%; $P < 0.01$; Fig 6.12b).

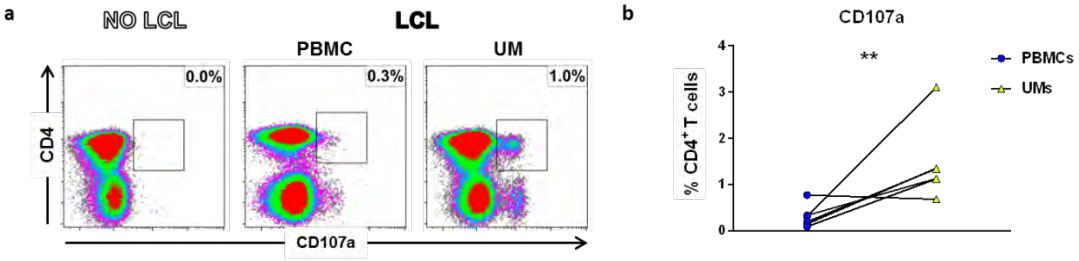

Figure 6.12 EBV-specific $CD4^+$ T cells in the tonsil degranulate upon exposure to EBV-infected B cells. PBMCs and UMs were either unmanipulated (left panel) or stimulated with autologous LCLs (middle and right respectively) and analysed by flow cytometry for degranulation as observed by CD107a mobilisation. The percentage in each plot indicates CD107a mobilisation in the total $CD4^+$ T cell population **(b)** Summary graphs represent repeats from a minimum of 6 donors and show the mean value with SD. ** $P < 0.01$; Mann-Whitney *U*-test.

The increased capacity of EBV-specific $CD4^+$ T cells tonsillar UMs to degranulate following LCL stimulation compared to PBMCs was concurrent with increased constitutive expression of cytotoxic proteins and, moreover, with CD69 positivity. Fig 6.13a shows representative examples of co-expression of CD69 with Perf, GzmB and GzmK in the total (top plots) and $EBNA2_{276-295}$-specific (bottom plots) $CD4^+$ T cell populations in tonsil UMs. Similar to the peripheral EBV-$pMHCII^+$ $CD4^+$ T cells of healthy carriers, the frequency of Perf expression was comparable between the $EBNA2_{276-295}$-specific $CD4^+$ T cell population and total $CD4^+$ pool (0.7% *versus* 0.4%) in this donor, irrespective of CD69 expression. In contrast expression of both GzmB and GzmK was markedly higher in the EBV-$pMHCII^+$ $CD4^+$ T population, with 29.9% and 48.1% of cells staining positively for these cytotoxic proteins compared to only 0.6% and 1.3% in the total $CD4^+$ population respectively. Moreover, GzmB expression was 8-fold higher in the $CD69^+$ $EBNA2_{276-295}$-specific $CD4^+$ T cells compared to the equivalent $CD69^-$ populations, and GzmK expression was 4-fold higher. Fig 6.13b shows a summary of Perf, GzmB, and GzmK expression in $CD69^+$ and $CD69^-$ EBV-pMHCII $CD4^+$ T cells. All 3 cytotoxic proteins were expressed in significantly higher frequencies of $CD69^+$ cells.

Together, these results indicate that EBV-specific $CD4^+$ T cells in the tonsil have increased capacity to degranulate in response to autologous LCL, coincident with their increased expression of cytotoxic proteins. Moreover, Perf, Gzm B and Gzm K expression were all associated with a T_{RM} phenotype, indicating that these cells have greater immediate cytotoxic potential.

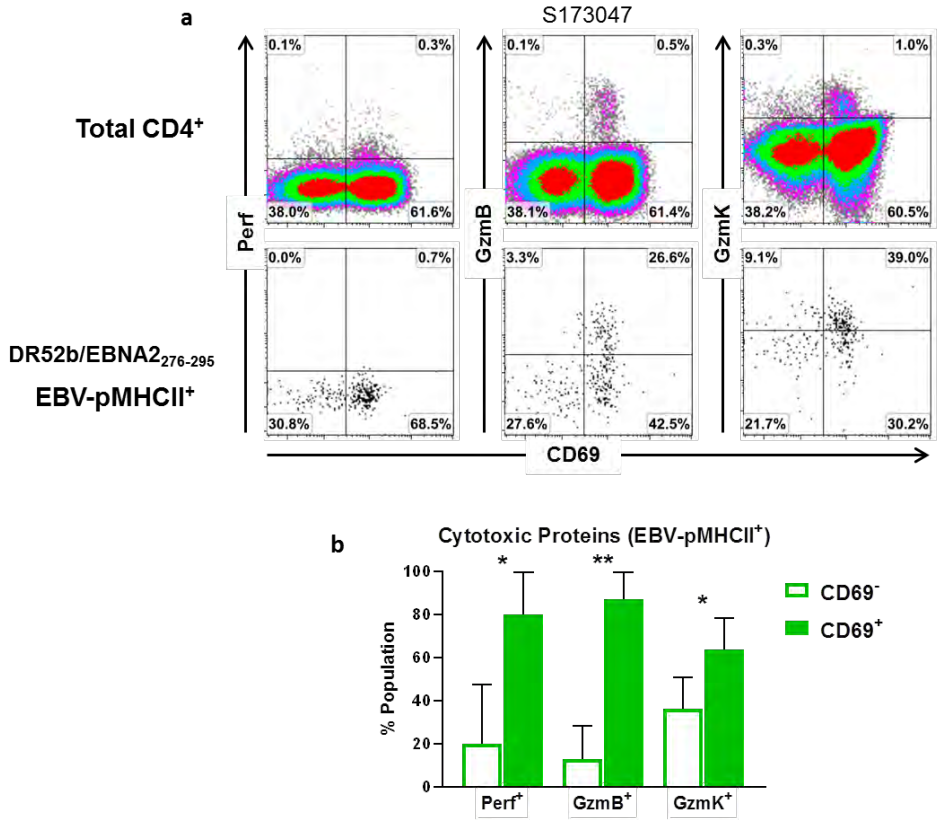

Figure 6.13 Expression of cytotoxic proteins in EBV-specific CD4⁺ T cells in the tonsil. (a) CD4-enriched UMs were stained with EBV-pMHCII tetramer and analysed by flow cytometry for intracellular expression of cytotoxic proteins. Co-expression of Perforin (left), Granzyme B (middle) and Granzyme K (right) with CD69 in the total CD4⁺ population (top) and DR52b/EBNA2$_{276-295}$-specific CD4⁺ T cells of a representative donors. **(b)** summary graph of Perf, GzmB and GzmK expression in the CD69⁻ (empty bars) and CD69⁺ (filled bars) of EBV-pMHCII⁺ CD4⁺ T cell populations. The graph depicts results from 5 independent experiments. Data are shown as mean ± SD. ** $P < 0.01$; * $P < 0.05$; Mann-Whitney *U*-test.

3. Discussion

Most of what is currently known regarding human T cell responses to a virus has come from studies analysing peripheral blood yet this accounts for less than 10% of the total T cell pool. In comparison, relatively little is known about the anti-viral T cell immunity in pathogenic sites or where viral replication occurs.

Here we used matched human blood and tonsil samples to investigate EBV-specific $CD4^+$ T cell immunity at the site of EBV infection and reactivation compared to the peripheral circulation. These experiments showed that EBV-specific $CD4^+$ T cells are detectable and enriched within tonsillar UMs above frequencies observed in matched blood. However, in contrast to EBV-specific $CD8^+$ T cells where both lytic and latent epitope reactivities are enriched in the tonsil, only latent epitope reactive $CD4^+$ T cells were present at significantly higher frequencies compared to the circulation (297). Importantly, $CD4^+$ T cells specific for CMV and Influenza were not enriched in the tonsil, rather the opposite was true, particularly for CMV where dramatically lower frequencies were present in the tonsil than in matched blood, as was similarly observed CMV-specific $CD8^+$ T cells (298). This indicates that EBV-specific $CD4^+$ T cells preferentially accumulate in tonsillar lymphoid tissue.

Importantly, a significant proportion of EBV-specific $CD4^+$ T cells in the tonsil UMs expressed the phenotypic marker associated with tissue residency, CD69, either alone or in combination with CD103, indicating active retention at this site. Heterogeneous populations of $CD69^+$ $CD103^+$ and $CD69^+$ $CD103^-$ EBV-specific $CD8^+$ T cells have been shown to similarly accumulate in the tonsil, suggesting that EBV-specific $CD4^+$ T cells may

also localize to different anatomical regions within the tonsil based on expression of CD103 (298). Although analyses of lung and intestinal epithelial tissues have used CD103 to identify $CD4^+$ T_{RM} populations in humans and mice respectively (394, 470, 471), it is not required for tissue residency (472). CD69 was found to be expressed on the majority of antigen-experienced $CD8^+$ T cells isolated from human SLOs (386, 404, 473) however transient CD69 expression can occur as a result of antigen recognition or cytokines in the surrounding environment (474, 475). Intracellular expression of Ki-67 however was virtually absent in $CD69^+$ EBV-specific $CD4^+$ T cells in the tonsil indicating antigen specific cells expressing the T_{RM} marker were not actively proliferating (393). Some of the early reports analysing T_{RM} in the skin and reproductive mucosa of mice infected with HSV noted that populations of anti-viral $CD4^+$ T cells were highly dynamic, trafficking rapidly through the tissue whereas $CD8^+$ T cell sequestered and maintained at the original site of infection (406). These findings established a precedent that $CD4^+$ T_{RM} are less abundant than their $CD8^+$ counterparts and display a different migratory capacity. Furthermore, $CD8^+$ T_{RM} in SLO were found to be present at low frequencies in mice following systemic LCMV infection (476) while $CD4^+$ T_{RM} remained poorly studied and it was thought that $CD4^+$ surveillance of secondary lymphoid organs was performed by T_{CM} continuously migrating using blood lymphatic vessels. Here, we have identified a population of EBV-specific $CD4^+$ T cells in the tonsil expressing CD69 in the absence of markers for proliferation, indicating a true resident memory phenotype in line with mouse studies that also identified $CD4^+$ T_{RM} populations in SLOs (477, 478).

Additionally, downregulation of cellular markers such as S1PR1, CCR7 andCD62L that would enable egress from tissue have been proposed as another functional signature of T_{RM} (393). While we were unable to assess expression of S1PR1, the vast majority of the EBV-specific $CD4^+$ T cells in the tonsil lacked CCR7 indicating that they would not respond to chemokine concentration gradient and exit the tissue. Interestingly, the mean frequency of $CCR7^-$ EBV-$pMHCII^+$ is higher than the mean frequency of CD69 expressing cells in the same populations thus some EBV-specific $CD4^+$ T cells are not poised to migrate to other lymphoid tissue and may have not initiated the signalling pathways that govern tissue residency. Nonetheless absence of CCR7 was not universal among $CD69^+$ EBV-$pMHCII^+$ $CD4^+$ T cells as has been seen in studies of $CD8^+$ T_{RM} (297, 298, 404). However, in the context of $CD4^+$ resident memory T cells, both $CCR7^+$ and $CCR7^-$ T_{RM} have been detected (404) and recent gene expression analysis of different memory subsets in mice demonstrated a close alignment between SLO T_{RM} with T_{CM} (472).

In mice, Hobit and Blimp-1 have been shown to be critical to the development and maintenance of T_{RM} (397, 479) however; data from human studies is ambiguous (398). Accordingly, we did not detect increased expression of Hobit in the $CD69^+$ EBV-specific $CD4^+$ T cell populations, in line with a study investigating lung $CD4^+$ T_{RM} (394). However, in this case the authors did detect mRNA transcripts of this transcription factor. Protein levels of Blimp-1 could not be investigated in the present study due to the lack of a reliable antibody.

The development and maintenance of T_{RM} in tissues has been shown to largely depend on the cytokine environment, and in particular the presence of IL-15 and TGF-β (480,

481). In combination, these cytokines downregulate the transcription factor Kruppel-like factor 2 (Klf-2) (298) resulting in impaired expression of the receptors CCR7, CD62L and S1PR1 required for tissue emigration (482). We did not assess expression of Klf-2 in our assays, however it would be interesting to see if this inversely correlated with CD69 expression as has been observed in the $CD8^+$ T cell pool of mice infected with LCMV and HSV (391, 392).

Secondary lymphoid organs such as the tonsil contain T_{FH} with specialised functions to promote B cell proliferation, production of high affinity antibodies and also formation of germinal centres (483). Recently, Wong *et al.* applied automated clustering methods to analysis of T_{FH} in the blood and tonsils to characterize different categories of T_{FH} (146). Using this classification, we showed that the vast majority of EBV-specific $CD4^+$ T cells in the tonsils expressed the chemokine receptor CXCR5 and the immune regulator PD-1, indicating localization or an ability to migrate to, the T cell zone, B cell follicles and potentially the germinal centres. This was supported by a progressive downregulation of CCR7 and ICOS in T cell zone and B cell follicle $CD4^+$ T cells populations, as has been observed in multiple studies (146, 484, 485). Furthermore, we identified populations of *bona fide* EBV-specific $CD4^+$ T_{FH} expressing markers associated with presence in germinal centres, including CD57 (486). Interestingly, expression of CD69 progressively increased alongside CXCR5 and PD-1 in EBV-specific $CD4^+$ T cells and was largely absent from $CXCR5^-$ $PD\text{-}1^-$ populations, indicating that T_{FH} localized in B cell follicles had an increased capacity to remain in the tissue. To date this is the first study to demonstrate the expression of T_{FH} markers within $CD4^+$ T_{RM} cells in SLOs. Our data is supported by a report that in LCMV infected mice, Klf-2 downregulation results in increased frequencies of T_{FH}

cells, suggesting that development of the two populations is not mutually exclusive (487).

The final set of experiments addressed the functional profile of $CD4^+$ T cells in the tonsils. The T_{FH}-associated cytokine IL-21 is important for maintaining proliferation of GC B cells (488, 489). Accordingly we detected significant production of IL-21 by total tonsillar $CD4^+$ T cells following non-specific stimulation, which was absent in stimulated PBMCs. IL-4 has been shown to inhibit IL-21 mediated plasma cell differentiation (490), however we did not detect any IL-4 production in tonsil UMs following stimulation. Interestingly, we did detect significant production of the immunosuppressive cytokine IL-10. Production of IL-10 by T cells following stimulation and the absence of detectable IL-4 secretion is in line with a previous study investigating T cell function in the tonsil (146). Furthermore, IL-10 production has however been shown to be induced by IL-21 (491). Although secretion of IL-10 is predominantly associated with regulatory T cells, we detected no expression of the characteristic transcription factor FoxP3.

Moving to antigenic stimulation using autologous EBV-infected B cells, we detected increased frequencies of responding cytokine producing $CD4^+$ T cells in tonsillar UMs compared to peripheral PBMCs. Responding tonsillar EBV-specific $CD4^+$ T cells had a T_H1-like profile, producing IFNγ, TNFα and some IL-2. However, despite the prevalence of cells with a TFH phenotype within the EBV-specific $CD4^+$ T cells, LCL stimulus did not elicit a detectable IL-21 response. GM-CSF, IL-4 and IL-10 were also undetectable, unlike following non-specific stimulation. This could potentially be due to the weaker antigenic stimulus delivered by the virus-infected cells (427). Expression of the T_H1 associated transcription factor T-bet in the majority of the EBV-$pMHCII^+$ $CD4^+$ cells confirmed a T_H1-

like profile, similar to that seen in the EBV-specific $CD4^+$ T cells in the blood. Coupled with the T_{FH} phenotype observed, our data suggest that EBV-specific $CD4^+$ T cells in the tonsil could be classified as T_H1 cell-type T_{FH} cells, a phenotype that has been previously reported in viral infection (139, 492).

A significantly higher frequency of $CD4^+$ T cells degranulating in response to autologous LCL was also seen in the tonsil UMs compared to PBMCs. Furthermore, investigation at the antigen-specific level revealed that the cytotoxic profile of EBV-$pMHCII^+$ $CD4^+$ T cells in the tonsil UMs was markedly different to that previously observed in the PBMCs of long-term carriers (Chapter 4). Expression of cytotoxic proteins in EBV-$pMHCII^+$ $CD4^+$ T cells was significantly increased compared to both the total $CD4^+$ T cell pool in the tonsils, and EBV-specific $CD4^+$ T cells in the PBMCs. Interestingly, recent murine experiments demonstrated that the T_{RM}-associated transcription factors Blimp-1 and Hobit play a critical role in regulating Granzyme B. Blimp-1 and Hobit were required for induction and maintenance of GzmB in $CD8^+$ T_{RM} respectively (493) and in separate experiments, Hobit-Blimp-1 double knock-out mice downregulated GzmB (but not Perf) (470) thus suggesting that the signalling pathways that promote tissue residency may also enhance expression of cytotoxic proteins. Moreover, cytotoxic proteins were preferentially upregulated in the T_{RM} cells within the tonsils, most strikingly seen with Granzyme B, suggesting that the resident $CD4^+$ T cells within the EBV-$pMHCII^+$ populations, that are retained at the site of infection, have increased functionality over those with the capacity to re-circulate into the blood.

CHAPTER 7

FINAL DISCUSSION

Immunity to viruses in humans has traditionally been attributed to the activity of neutralising antibodies produced by B cells along with the ability of $CD8^+$ T cells to lyse infected cells. These two arms of the adaptive immune system during viral infection have been extensively studied (494). Yet, despite the requirement of $CD4^+$ T cell help for both antibody production and $CD8^+$ T cell function, investigating the role of $CD4^+$ T cells in response to infection has been more challenging, exacerbated by the small frequencies of antigen-specific cells, and their heterogeneity and plasticity. In some infectious models, $CD4^+$ T cells have been shown to be the major component of the T cell response (340, 495), and in most others their presence is crucial for viral control. A greater understanding of $CD4^+$ T cell functions that confer the greatest protection from viruses would allow us to better harness the immune system to generate long-lived responses through prophylactic vaccination. Studying the evolution of anti-viral $CD4^+$ T cell responses induced by natural infection is the best way to understand their role.

Here we have shown that the functional properties of EBV-specific $CD4^+$ T cells change from primary infection into persistence where they develop increased polyfunctionality alongside a decreased cytotoxic capacity, as defined by expression of the cytotoxic proteins Perforin and Granzyme B. The high frequency of EBV-specific CD4-CTLs detected in IM patients reveals a hitherto underappreciated direct effector function of $CD4^+$ T cells during an acute human herpesvirus infection. Previous reports have noted

human CD4-CTLs expressing Perf/GzmB during primary HIV, CMV and Influenza infection (340, 343, 372), but have not characterised the antigen specificity or phenotype of these cells. Here we have further characterized the CD4-CTLs generated during acute EBV infection by analysing expression of cellular markers that have been detected on CD4-CTLs present in other chronic infections (177, 336, 337, 339, 360, 370, 372, 429-431). Our results suggest that CD4-CTLs in acute IM can arise from a distinct pathway to those present in chronic infection. Not only did EBV-specific CD4-CTLs express a different phenotypic and transcription profile with regard to these cytotoxic markers (Fig 4.9), in further contrast to CD4-CTLs in chronic infection, we found that levels of activation, as measured by expression of $CD38^{hi}$, correlated with presence of Perf/GzmB (Fig 4.12) (271). EBV-specific $CD4^+$ T cells carrying cytotoxic proteins remained detectable 6 months following IM diagnosis but were virtually absent from long term-healthy carriers (Fig 4.7). Interestingly, using protocols optimised for the generation of T cell lines administered to patients with EBV-associated malignancies, expansion of EBV-specific $CD4^+$ T cells from healthy donors *in vitro* results in upregulation of CD38 (data not shown), suggesting that cytotoxic capacity can be re-acquired upon memory T cell activation. The use of adoptive T cell therapies in EBV-associated malignancies has shown promising results, however the functional profile of $CD4^+$ T cells within donor-specific preparations has yet to be studied. Given our observations of increased $CD38^{hi}$ in these preparations it would be interesting to investigate Perf/GzmB expression and whether higher frequencies of cells carrying these proteins could indicate better clinical responses.

CD4-CTLs in the context of infections such as CMV, Dengue and HIV are heavily linked to the terminally differentiated T_{EMRA} phenotype, associated with chronic antigen exposure (271, 323). Furthermore, single cell RNA sequencing performed on $CD4^+$ T cells from donors with previous DENV infection found that transcripts linked to cytotoxic function, were highly enriched within T_{EMRA} populations compared to T_{EM} and T_{CM} (339). Performing similar analysis on $CD4^+$ T cells from IM patients could help reveal which transcripts are enriched during acute infection and in particular within the $CD38^{hi}$ population that carried cytotoxic proteins. Moreover, such information would allow a direct comparison between CD4-CTLs in acute *versus* chronic infection.

Tonsil tissue collected from healthy long-term carriers allowed us to show that a population of EBV-specific $CD4^+$ T cells is preferentially retained at the site of infection and viral replication, expressing markers associated with tissue residency as has been seen with their $CD8^+$ counterparts (Fig 6.4) (297, 298). We found $CD4^+$ T cell with latent epitope reactivities to be significantly enriched in the tonsil compared to matched peripheral blood and in particular for $CD4^+$ T cells specific for epitopes derived from EBNA2 (Fig 6.1). As EBNA2 is one of the first proteins expressed following B cell infection, this suggests that resident $CD4^+$ T cells may be able to eliminate newly infected B cells. Some donors in our cohort were EBV seronegative and while they were unsuitable for EBV-pMHCII analysis, it would have been interesting to compare whether EBV infection increases the frequency of T_{RM} within the total $CD4^+$ T cell population.

We also showed that the T_{RM} phenotype within EBV-$pMHCII^+$ $CD4^+$ T cells was associated with expression of surface markers allowing migration into the T cell zone, B cell follicle

and germinal centre structures of the SLO. Here, EBNA2-specific $CD4^+$ T cells also appeared to display a higher potential to enter the follicular region of the tonsil compared to other specificities (Fig 6.8). Interestingly, immunostaining performed on tonsil sections from IM patients showed that all EBV^+ B cells in the intrafollicular region and germinal centres were positive for EBNA2 (496). The authors hypothesised that expression of EBNA2 in these cells, in conjunction with CD40 triggering, could promote proliferation and expansion of the EBV-infected B cell pool. Thus, the enrichment of EBNA2-specific $CD4^+$ T cells we observed may be required to contain the propagation of EBV-infected B cells out of the tonsil and into the circulation.

Our functional assays demonstrated that a higher frequency of $CD4^+$ T cells in the tonsil produced effector cytokines and degranulated in response to autologous EBV-infected B cells compared to the periphery (Fig 6.10). However, expression of the T_{RM} marker CD69 was rapidly downregulated in the total $CD4^+$ T cells during the overnight incubation restricting our analysis to the total $CD4^+$ T cell pool. Performing LCL stimulation assays on sorted $CD69^-$ and $CD69^+$ would allow us to determine the recall response of EBV-specific $CD4^+$ T cells with a T_{RM} phenotype in the tonsil. Superior cytokine production observed in lung $CD4^+$ T_{RM} following CD3-CD28 stimulation was partially attributed to rapid translation of mRNA transcripts encoding for effector molecules (394). Quantifying transcripts for effector cytokines in our samples and performing timecourse stimulations assays could reveal whether a similar “trigger-happy” population resides within the tonsil.

In summary we have shown that primary EBV infection elicits the generation of a population of virus-specific CD4-CTLs that display a highly activated phenotype. These cells differ from CD4-CTLs described in chronic infection in their expression of cellular markers and represent a distinct, short-lived subset. In long-term carriers EBV-specific $CD4^+$ T cells become more polyfunctional and carry less cytotoxic proteins, and a population of tissue resident cells is retained in the tonsil. At the site of replication, EBV-specific $CD4^+$ T cells can migrate to the areas where the pool of infected B cells is maintained and these cells possess increased cytotoxic capacity.

These findings highlight the role of $CD4^+$ T cells in viral immunity beyond the traditionally described “helper” subsets and further research into the signals that elicit EBV-specific CD4-CTL development and retention at the site of infection could help inform both prophylactic and therapeutic vaccination.

1. Turvey SE, Broide DH. Innate immunity. J Allergy Clin Immunol. 2010;125(2 Suppl 2):S24-32.
2. Takeuchi O, Akira S. Pattern recognition receptors and inflammation. Cell. 2010;140(6):805-20.
3. Reis e Sousa C. Activation of dendritic cells: translating innate into adaptive immunity. Curr Opin Immunol. 2004;16(1):21-5.
4. Bonilla FA, Oettgen HC. Adaptive immunity. J Allergy Clin Immunol. 2010;125(2 Suppl 2):S33-40.
5. Kondo M. Lymphoid and myeloid lineage commitment in multipotent hematopoietic progenitors. Immunol Rev. 2010;238(1):37-46.
6. Farber DL, Netea MG, Radbruch A, Rajewsky K, Zinkernagel RM. Immunological memory: lessons from the past and a look to the future. Nat Rev Immunol. 2016;16(2):124-8.
7. Schroeder HW, Jr., Cavacini L. Structure and function of immunoglobulins. J Allergy Clin Immunol. 2010;125(2 Suppl 2):S41-52.
8. Pieper K, Grimbacher B, Eibel H. B-cell biology and development. J Allergy Clin Immunol. 2013;131(4):959-71.
9. Nutt SL, Hodgkin PD, Tarlinton DM, Corcoran LM. The generation of antibody-secreting plasma cells. Nat Rev Immunol. 2015;15(3):160-71.
10. Takemori T, Kaji T, Takahashi Y, Shimoda M, Rajewsky K. Generation of memory B cells inside and outside germinal centers. Eur J Immunol. 2014;44(5):1258-64.
11. Stavnezer J, Schrader CE. IgH chain class switch recombination: mechanism and regulation. J Immunol. 2014;193(11):5370-8.
12. Teng G, Papavasiliou FN. Immunoglobulin somatic hypermutation. Annu Rev Genet. 2007;41:107-20.
13. McHeyzer-Williams M, Okitsu S, Wang N, McHeyzer-Williams L. Molecular programming of B cell memory. Nat Rev Immunol. 2011;12(1):24-34.
14. Allen CD, Okada T, Cyster JG. Germinal-center organization and cellular dynamics. Immunity. 2007;27(2):190-202.
15. Zhao DM, Thornton AM, DiPaolo RJ, Shevach EM. Activated CD4+CD25+ T cells selectively kill B lymphocytes. Blood. 2006;107(10):3925-32.
16. Koch U, Radtke F. Mechanisms of T cell development and transformation. Annu Rev Cell Dev Biol. 2011;27:539-62.
17. Bassing CH, Swat W, Alt FW. The mechanism and regulation of chromosomal V(D)J recombination. Cell. 2002;109 Suppl:S45-55.
18. Zarnitsyna VI, Evavold BD, Schoettle LN, Blattman JN, Antia R. Estimating the diversity, completeness, and cross-reactivity of the T cell repertoire. Front Immunol. 2013;4:485.
19. Anderson G, Takahama Y. Thymic epithelial cells: working class heroes for T cell development and repertoire selection. Trends Immunol. 2012;33(6):256-63.
20. Derbinski J, Schulte A, Kyewski B, Klein L. Promiscuous gene expression in medullary thymic epithelial cells mirrors the peripheral self. Nat Immunol. 2001;2(11):1032-9.
21. Klein L, Kyewski B, Allen PM, Hogquist KA. Positive and negative selection of the T cell repertoire: what thymocytes see (and don't see). Nat Rev Immunol. 2014;14(6):377-91.
22. Rock KL, Reits E, Neefjes J. Present Yourself! By MHC Class I and MHC Class II Molecules. Trends Immunol. 2016;37(11):724-37.
23. Michalek MT, Grant EP, Gramm C, Goldberg AL, Rock KL. A role for the ubiquitin-dependent proteolytic pathway in MHC class I-restricted antigen presentation. Nature. 1993;363(6429):552-4.
24. Chang SC, Momburg F, Bhutani N, Goldberg AL. The ER aminopeptidase, ERAP1, trims precursors to lengths of MHC class I peptides by a "molecular ruler" mechanism. Proc Natl Acad Sci U S A. 2005;102(47):17107-12.

25. Cresswell P, Bangia N, Dick T, Diedrich G. The nature of the MHC class I peptide loading complex. Immunol Rev. 1999;172:21-8.
26. Kovacsovics-Bankowski M, Rock KL. A phagosome-to-cytosol pathway for exogenous antigens presented on MHC class I molecules. Science. 1995;267(5195):243-6.
27. Houde M, Bertholet S, Gagnon E, Brunet S, Goyette G, Laplante A, et al. Phagosomes are competent organelles for antigen cross-presentation. Nature. 2003;425(6956):402-6.
28. Guermonprez P, Saveanu L, Kleijmeer M, Davoust J, Van Endert P, Amigorena S. ER-phagosome fusion defines an MHC class I cross-presentation compartment in dendritic cells. Nature. 2003;425(6956):397-402.
29. Shen L, Sigal LJ, Boes M, Rock KL. Important role of cathepsin S in generating peptides for TAP-independent MHC class I crosspresentation in vivo. Immunity. 2004;21(2):155-65.
30. Wieczorek M, Abualrous ET, Sticht J, Alvaro-Benito M, Stolzenberg S, Noe F, et al. Major Histocompatibility Complex (MHC) Class I and MHC Class II Proteins: Conformational Plasticity in Antigen Presentation. Front Immunol. 2017;8:292.
31. Watts C. The exogenous pathway for antigen presentation on major histocompatibility complex class II and CD1 molecules. Nat Immunol. 2004;5(7):685-92.
32. Roche PA, Marks MS, Cresswell P. Formation of a nine-subunit complex by HLA class II glycoproteins and the invariant chain. Nature. 1991;354(6352):392-4.
33. Roche PA, Cresswell P. Invariant chain association with HLA-DR molecules inhibits immunogenic peptide binding. Nature. 1990;345(6276):615-8.
34. Sette A, Ceman S, Kubo RT, Sakaguchi K, Appella E, Hunt DF, et al. Invariant chain peptides in most HLA-DR molecules of an antigen-processing mutant. Science. 1992;258(5089):1801-4.
35. Marks MS, Roche PA, van Donselaar E, Woodruff L, Peters PJ, Bonifacino JS. A lysosomal targeting signal in the cytoplasmic tail of the beta chain directs HLA-DM to MHC class II compartments. J Cell Biol. 1995;131(2):351-69.
36. Liljedahl M, Winqvist O, Surh CD, Wong P, Ngo K, Teyton L, et al. Altered antigen presentation in mice lacking H2-O. Immunity. 1998;8(2):233-43.
37. Yoon T, Macmillan H, Mortimer SE, Jiang W, Rinderknecht CH, Stern LJ, et al. Mapping the HLA-DO/HLA-DM complex by FRET and mutagenesis. Proc Natl Acad Sci U S A. 2012;109(28):11276-81.
38. Kovats S, Whiteley PE, Concannon P, Rudensky AY, Blum JS. Presentation of abundant endogenous class II DR-restricted antigens by DM-negative B cell lines. Eur J Immunol. 1997;27(4):1014-21.
39. Rudolph MG, Luz JG, Wilson IA. Structural and thermodynamic correlates of T cell signaling. Annu Rev Biophys Biomol Struct. 2002;31:121-49.
40. Rudolph MG, Stanfield RL, Wilson IA. How TCRs bind MHCs, peptides, and coreceptors. Annu Rev Immunol. 2006;24:419-66.
41. Hennecke J, Carfi A, Wiley DC. Structure of a covalently stabilized complex of a human alphabeta T-cell receptor, influenza HA peptide and MHC class II molecule, HLA-DR1. EMBO J. 2000;19(21):5611-24.
42. Hennecke J, Wiley DC. Structure of a complex of the human alpha/beta T cell receptor (TCR) HA1.7, influenza hemagglutinin peptide, and major histocompatibility complex class II molecule, HLA-DR4 (DRA*0101 and DRB1*0401): insight into TCR cross-restriction and alloreactivity. J Exp Med. 2002;195(5):571-81.
43. Holland CJ, Cole DK, Godkin A. Re-Directing CD4(+) T Cell Responses with the Flanking Residues of MHC Class II-Bound Peptides: The Core is Not Enough. Front Immunol. 2013;4:172.
44. Brown JH, Jardetzky TS, Gorga JC, Stern LJ, Urban RG, Strominger JL, et al. Three-dimensional structure of the human class II histocompatibility antigen HLA-DR1. Nature. 1993;364(6432):33-9.

45. Stern LJ, Brown JH, Jardetzky TS, Gorga JC, Urban RG, Strominger JL, et al. Crystal structure of the human class II MHC protein HLA-DR1 complexed with an influenza virus peptide. Nature. 1994;368(6468):215-21.
46. Altman JD, Moss PA, Goulder PJ, Barouch DH, McHeyzer-Williams MG, Bell JI, et al. Phenotypic analysis of antigen-specific T lymphocytes. Science. 1996;274(5284):94-6.
47. Carson RT, Vignali KM, Woodland DL, Vignali DA. T cell receptor recognition of MHC class II-bound peptide flanking residues enhances immunogenicity and results in altered TCR V region usage. Immunity. 1997;7(3):387-99.
48. Katz DR. Antigen presentation, antigen-presenting cells and antigen processing. Curr Opin Immunol. 1988;1(2):213-9.
49. Larsen SL, Pedersen LO, Buus S, Stryhn A. T cell responses affected by aminopeptidase N (CD13)-mediated trimming of major histocompatibility complex class II-bound peptides. J Exp Med. 1996;184(1):183-9.
50. Zavala-Ruiz Z, Strug I, Walker BD, Norris PJ, Stern LJ. A hairpin turn in a class II MHC-bound peptide orients residues outside the binding groove for T cell recognition. Proc Natl Acad Sci U S A. 2004;101(36):13279-84.
51. Cole DK, Gallagher K, Lemercier B, Holland CJ, Junaid S, Hindley JP, et al. Modification of the carboxy-terminal flanking region of a universal influenza epitope alters CD4(+) T-cell repertoire selection. Nat Commun. 2012;3:665.
52. Godkin AJ, Smith KJ, Willis A, Tejada-Simon MV, Zhang J, Elliott T, et al. Naturally processed HLA class II peptides reveal highly conserved immunogenic flanking region sequence preferences that reflect antigen processing rather than peptide-MHC interactions. J Immunol. 2001;166(11):6720-7.
53. Lippolis JD, White FM, Marto JA, Luckey CJ, Bullock TN, Shabanowitz J, et al. Analysis of MHC class II antigen processing by quantitation of peptides that constitute nested sets. J Immunol. 2002;169(9):5089-97.
54. Manoury B, Hewitt EW, Morrice N, Dando PM, Barrett AJ, Watts C. An asparaginyl endopeptidase processes a microbial antigen for class II MHC presentation. Nature. 1998;396(6712):695-9.
55. Dudziak D, Kamphorst AO, Heidkamp GF, Buchholz VR, Trumpfheller C, Yamazaki S, et al. Differential antigen processing by dendritic cell subsets in vivo. Science. 2007;315(5808):107-11.
56. Honke N, Shaabani N, Cadeddu G, Sorg UR, Zhang DE, Trilling M, et al. Enforced viral replication activates adaptive immunity and is essential for the control of a cytopathic virus. Nat Immunol. 2011;13(1):51-7.
57. O'Donnell PW, Haque A, Klemsz MJ, Kaplan MH, Blum JS. Cutting edge: induction of the antigen-processing enzyme IFN-gamma-inducible lysosomal thiol reductase in melanoma cells Is STAT1-dependent but CIITA-independent. J Immunol. 2004;173(2):731-5.
58. Heath WR, Carbone FR. Cross-presentation in viral immunity and self-tolerance. Nat Rev Immunol. 2001;1(2):126-34.
59. Shahinian A, Pfeffer K, Lee KP, Kundig TM, Kishihara K, Wakeham A, et al. Differential T cell costimulatory requirements in CD28-deficient mice. Science. 1993;261(5121):609-12.
60. Simpson TR, Quezada SA, Allison JP. Regulation of CD4 T cell activation and effector function by inducible costimulator (ICOS). Curr Opin Immunol. 2010;22(3):326-32.
61. Denoeud J, Moser M. Role of CD27/CD70 pathway of activation in immunity and tolerance. J Leukoc Biol. 2011;89(2):195-203.
62. Croft M, Duan W, Choi H, Eun SY, Madireddi S, Mehta A. TNF superfamily in inflammatory disease: translating basic insights. Trends Immunol. 2012;33(3):144-52.
63. Courtney AH, Lo WL, Weiss A. TCR Signaling: Mechanisms of Initiation and Propagation. Trends Biochem Sci. 2018;43(2):108-23.

64. Mescher MF, Curtsinger JM, Agarwal P, Casey KA, Gerner M, Hammerbeck CD, et al. Signals required for programming effector and memory development by CD8+ T cells. Immunol Rev. 2006;211:81-92.
65. Parish IA, Kaech SM. Diversity in CD8(+) T cell differentiation. Curr Opin Immunol. 2009;21(3):291-7.
66. Mercado R, Vijh S, Allen SE, Kerksiek K, Pilip IM, Pamer EG. Early programming of T cell populations responding to bacterial infection. J Immunol. 2000;165(12):6833-9.
67. Kaech SM, Tan JT, Wherry EJ, Konieczny BT, Surh CD, Ahmed R. Selective expression of the interleukin 7 receptor identifies effector CD8 T cells that give rise to long-lived memory cells. Nat Immunol. 2003;4(12):1191-8.
68. Dunkle A, Dzhagalov I, Gordy C, He YW. Transfer of CD8+ T cell memory using Bcl-2 as a marker. J Immunol. 2013;190(3):940-7.
69. Joshi NS, Cui W, Chandele A, Lee HK, Urso DR, Hagman J, et al. Inflammation directs memory precursor and short-lived effector CD8(+) T cell fates via the graded expression of T-bet transcription factor. Immunity. 2007;27(2):281-95.
70. Shedlock DJ, Shen H. Requirement for CD4 T cell help in generating functional CD8 T cell memory. Science. 2003;300(5617):337-9.
71. Sun JC, Bevan MJ. Defective CD8 T cell memory following acute infection without CD4 T cell help. Science. 2003;300(5617):339-42.
72. Sun JC, Williams MA, Bevan MJ. CD4+ T cells are required for the maintenance, not programming, of memory CD8+ T cells after acute infection. Nat Immunol. 2004;5(9):927-33.
73. Wang JC, Livingstone AM. Cutting edge: CD4+ T cell help can be essential for primary CD8+ T cell responses in vivo. J Immunol. 2003;171(12):6339-43.
74. Bennett SR, Carbone FR, Karamalis F, Flavell RA, Miller JF, Heath WR. Help for cytotoxic-T-cell responses is mediated by CD40 signalling. Nature. 1998;393(6684):478-80.
75. Lu Z, Yuan L, Zhou X, Sotomayor E, Levitsky HI, Pardoll DM. CD40-independent pathways of T cell help for priming of CD8(+) cytotoxic T lymphocytes. J Exp Med. 2000;191(3):541-50.
76. Schoenberger SP, Toes RE, van der Voort EI, Offringa R, Melief CJ. T-cell help for cytotoxic T lymphocytes is mediated by CD40-CD40L interactions. Nature. 1998;393(6684):480-3.
77. Smith CM, Wilson NS, Waithman J, Villadangos JA, Carbone FR, Heath WR, et al. Cognate CD4(+) T cell licensing of dendritic cells in CD8(+) T cell immunity. Nat Immunol. 2004;5(11):1143-8.
78. Borst J, Ahrends T, Babala N, Melief CJM, Kastenmuller W. CD4(+) T cell help in cancer immunology and immunotherapy. Nat Rev Immunol. 2018;18(10):635-47.
79. Bianchi R, Grohmann U, Vacca C, Belladonna ML, Fioretti MC, Puccetti P. Autocrine IL-12 is involved in dendritic cell modulation via CD40 ligation. J Immunol. 1999;163(5):2517-21.
80. Oh S, Perera LP, Terabe M, Ni L, Waldmann TA, Berzofsky JA. IL-15 as a mediator of CD4+ help for CD8+ T cell longevity and avoidance of TRAIL-mediated apoptosis. Proc Natl Acad Sci U S A. 2008;105(13):5201-6.
81. Green AM, Difazio R, Flynn JL. IFN-gamma from CD4 T cells is essential for host survival and enhances CD8 T cell function during Mycobacterium tuberculosis infection. J Immunol. 2013;190(1):270-7.
82. Wilson EB, Livingstone AM. Cutting edge: CD4+ T cell-derived IL-2 is essential for help-dependent primary CD8+ T cell responses. J Immunol. 2008;181(11):7445-8.
83. Elsaesser H, Sauer K, Brooks DG. IL-21 is required to control chronic viral infection. Science. 2009;324(5934):1569-72.

84. Mosmann TR, Cherwinski H, Bond MW, Giedlin MA, Coffman RL. Two types of murine helper T cell clone. I. Definition according to profiles of lymphokine activities and secreted proteins. J Immunol. 1986;136(7):2348-57.
85. Luckheeram RV, Zhou R, Verma AD, Xia B. CD4(+)T cells: differentiation and functions. Clin Dev Immunol. 2012;2012:925135.
86. Trinchieri G, Pflanz S, Kastelein RA. The IL-12 family of heterodimeric cytokines: new players in the regulation of T cell responses. Immunity. 2003;19(5):641-4.
87. Iwasaki A, Medzhitov R. Toll-like receptor control of the adaptive immune responses. Nat Immunol. 2004;5(10):987-95.
88. Trinchieri G, Sher A. Cooperation of Toll-like receptor signals in innate immune defence. Nat Rev Immunol. 2007;7(3):179-90.
89. Afkarian M, Sedy JR, Yang J, Jacobson NG, Cereb N, Yang SY, et al. T-bet is a STAT1-induced regulator of IL-12R expression in naive CD4+ T cells. Nat Immunol. 2002;3(6):549-57.
90. Lighvani AA, Frucht DM, Jankovic D, Yamane H, Aliberti J, Hissong BD, et al. T-bet is rapidly induced by interferon-gamma in lymphoid and myeloid cells. Proc Natl Acad Sci U S A. 2001;98(26):15137-42.
91. Lazarevic V, Chen X, Shim JH, Hwang ES, Jang E, Bolm AN, et al. T-bet represses T(H)17 differentiation by preventing Runx1-mediated activation of the gene encoding RORgammat. Nat Immunol. 2011;12(1):96-104.
92. Djuretic IM, Levanon D, Negreanu V, Groner Y, Rao A, Ansel KM. Transcription factors T-bet and Runx3 cooperate to activate Ifng and silence Il4 in T helper type 1 cells. Nat Immunol. 2007;8(2):145-53.
93. Hwang ES, Szabo SJ, Schwartzberg PL, Glimcher LH. T helper cell fate specified by kinase-mediated interaction of T-bet with GATA-3. Science. 2005;307(5708):430-3.
94. Nathan CF, Murray HW, Wiebe ME, Rubin BY. Identification of interferon-gamma as the lymphokine that activates human macrophage oxidative metabolism and antimicrobial activity. J Exp Med. 1983;158(3):670-89.
95. Shirayoshi Y, Burke PA, Appella E, Ozato K. Interferon-induced transcription of a major histocompatibility class I gene accompanies binding of inducible nuclear factors to the interferon consensus sequence. Proc Natl Acad Sci U S A. 1988;85(16):5884-8.
96. Amaldi I, Reith W, Berte C, Mach B. Induction of HLA class II genes by IFN-gamma is transcriptional and requires a trans-acting protein. J Immunol. 1989;142(3):999-1004.
97. Maraskovsky E, Chen WF, Shortman K. IL-2 and IFN-gamma are two necessary lymphokines in the development of cytolytic T cells. J Immunol. 1989;143(4):1210-4.
98. Williams MA, Tyznik AJ, Bevan MJ. Interleukin-2 signals during priming are required for secondary expansion of CD8+ memory T cells. Nature. 2006;441(7095):890-3.
99. Kang S, Brown HM, Hwang S. Direct Antiviral Mechanisms of Interferon-Gamma. Immune Netw. 2018;18(5):e33.
100. Bromley SK, Mempel TR, Luster AD. Orchestrating the orchestrators: chemokines in control of T cell traffic. Nat Immunol. 2008;9(9):970-80.
101. Pulendran B. Modulating vaccine responses with dendritic cells and Toll-like receptors. Immunol Rev. 2004;199:227-50.
102. Kaplan MH, Schindler U, Smiley ST, Grusby MJ. Stat6 is required for mediating responses to IL-4 and for development of Th2 cells. Immunity. 1996;4(3):313-9.
103. Zhu J, Guo L, Watson CJ, Hu-Li J, Paul WE. Stat6 is necessary and sufficient for IL-4's role in Th2 differentiation and cell expansion. J Immunol. 2001;166(12):7276-81.
104. Zhu J, Jankovic D, Grinberg A, Guo L, Paul WE. Gfi-1 plays an important role in IL-2-mediated Th2 cell expansion. Proc Natl Acad Sci U S A. 2006;103(48):18214-9.

105. Usui T, Nishikomori R, Kitani A, Strober W. GATA-3 suppresses Th1 development by downregulation of Stat4 and not through effects on IL-12Rbeta2 chain or T-bet. Immunity. 2003;18(3):415-28.
106. Zhu J, Cote-Sierra J, Guo L, Paul WE. Stat5 activation plays a critical role in Th2 differentiation. Immunity. 2003;19(5):739-48.
107. Diehl S, Rincon M. The two faces of IL-6 on Th1/Th2 differentiation. Mol Immunol. 2002;39(9):531-6.
108. Diehl S, Anguita J, Hoffmeyer A, Zapton T, Ihle JN, Fikrig E, et al. Inhibition of Th1 differentiation by IL-6 is mediated by SOCS1. Immunity. 2000;13(6):805-15.
109. Steinke JW, Borish L. Th2 cytokines and asthma. Interleukin-4: its role in the pathogenesis of asthma, and targeting it for asthma treatment with interleukin-4 receptor antagonists. Respir Res. 2001;2(2):66-70.
110. Martinez-Moczygemba M, Huston DP. Biology of common beta receptor-signaling cytokines: IL-3, IL-5, and GM-CSF. J Allergy Clin Immunol. 2003;112(4):653-65; quiz 66.
111. Wynn TA. IL-13 effector functions. Annu Rev Immunol. 2003;21:425-56.
112. Qin H, Wang L, Feng T, Elson CO, Niyongere SA, Lee SJ, et al. TGF-beta promotes Th17 cell development through inhibition of SOCS3. J Immunol. 2009;183(1):97-105.
113. Zhou L, Ivanov, II, Spolski R, Min R, Shenderov K, Egawa T, et al. IL-6 programs T(H)-17 cell differentiation by promoting sequential engagement of the IL-21 and IL-23 pathways. Nat Immunol. 2007;8(9):967-74.
114. Nurieva R, Yang XO, Martinez G, Zhang Y, Panopoulos AD, Ma L, et al. Essential autocrine regulation by IL-21 in the generation of inflammatory T cells. Nature. 2007;448(7152):480-3.
115. Stritesky GL, Yeh N, Kaplan MH. IL-23 promotes maintenance but not commitment to the Th17 lineage. J Immunol. 2008;181(9):5948-55.
116. Gaffen SL. Structure and signalling in the IL-17 receptor family. Nat Rev Immunol. 2009;9(8):556-67.
117. Moseley TA, Haudenschild DR, Rose L, Reddi AH. Interleukin-17 family and IL-17 receptors. Cytokine Growth Factor Rev. 2003;14(2):155-74.
118. Sonnenberg GF, Fouser LA, Artis D. Border patrol: regulation of immunity, inflammation and tissue homeostasis at barrier surfaces by IL-22. Nat Immunol. 2011;12(5):383-90.
119. Wolk K, Kunz S, Witte E, Friedrich M, Asadullah K, Sabat R. IL-22 increases the innate immunity of tissues. Immunity. 2004;21(2):241-54.
120. Lee YK, Turner H, Maynard CL, Oliver JR, Chen D, Elson CO, et al. Late developmental plasticity in the T helper 17 lineage. Immunity. 2009;30(1):92-107.
121. Suryawanshi A, Veiga-Parga T, Rajasagi NK, Reddy PB, Sehrawat S, Sharma S, et al. Role of IL-17 and Th17 cells in herpes simplex virus-induced corneal immunopathology. J Immunol. 2011;187(4):1919-30.
122. Hou W, Kang HS, Kim BS. Th17 cells enhance viral persistence and inhibit T cell cytotoxicity in a model of chronic virus infection. J Exp Med. 2009;206(2):313-28.
123. Veldhoen M, Uyttenhove C, van Snick J, Helmby H, Westendorf A, Buer J, et al. Transforming growth factor-beta 'reprograms' the differentiation of T helper 2 cells and promotes an interleukin 9-producing subset. Nat Immunol. 2008;9(12):1341-6.
124. Dardalhon V, Awasthi A, Kwon H, Galileos G, Gao W, Sobel RA, et al. IL-4 inhibits TGF-beta-induced Foxp3+ T cells and, together with TGF-beta, generates IL-9+ IL-10+ Foxp3(-) effector T cells. Nat Immunol. 2008;9(12):1347-55.
125. Staudt V, Bothur E, Klein M, Lingnau K, Reuter S, Grebe N, et al. Interferon-regulatory factor 4 is essential for the developmental program of T helper 9 cells. Immunity. 2010;33(2):192-202.

126. Chang HC, Sehra S, Goswami R, Yao W, Yu Q, Stritesky GL, et al. The transcription factor PU.1 is required for the development of IL-9-producing T cells and allergic inflammation. Nat Immunol. 2010;11(6):527-34.
127. Purwar R, Schlapbach C, Xiao S, Kang HS, Elyaman W, Jiang X, et al. Robust tumor immunity to melanoma mediated by interleukin-9-producing T cells. Nat Med. 2012;18(8):1248-53.
128. Lu Y, Wang Q, Xue G, Bi E, Ma X, Wang A, et al. Th9 Cells Represent a Unique Subset of CD4(+) T Cells Endowed with the Ability to Eradicate Advanced Tumors. Cancer Cell. 2018;33(6):1048-60 e7.
129. Kara EE, Comerford I, Bastow CR, Fenix KA, Litchfield W, Handel TM, et al. Distinct chemokine receptor axes regulate Th9 cell trafficking to allergic and autoimmune inflammatory sites. J Immunol. 2013;191(3):1110-7.
130. Liang SC, Tan XY, Luxenberg DP, Karim R, Dunussi-Joannopoulos K, Collins M, et al. Interleukin (IL)-22 and IL-17 are coexpressed by Th17 cells and cooperatively enhance expression of antimicrobial peptides. J Exp Med. 2006;203(10):2271-9.
131. Duhen T, Geiger R, Jarrossay D, Lanzavecchia A, Sallusto F. Production of interleukin 22 but not interleukin 17 by a subset of human skin-homing memory T cells. Nat Immunol. 2009;10(8):857-63.
132. Trifari S, Kaplan CD, Tran EH, Crellin NK, Spits H. Identification of a human helper T cell population that has abundant production of interleukin 22 and is distinct from T(H)-17, T(H)1 and T(H)2 cells. Nat Immunol. 2009;10(8):864-71.
133. Ramirez JM, Brembilla NC, Sorg O, Chicheportiche R, Matthes T, Dayer JM, et al. Activation of the aryl hydrocarbon receptor reveals distinct requirements for IL-22 and IL-17 production by human T helper cells. Eur J Immunol. 2010;40(9):2450-9.
134. Eyerich S, Eyerich K, Pennino D, Carbone T, Nasorri F, Pallotta S, et al. Th22 cells represent a distinct human T cell subset involved in epidermal immunity and remodeling. J Clin Invest. 2009;119(12):3573-85.
135. Schaerli P, Willimann K, Lang AB, Lipp M, Loetscher P, Moser B. CXC chemokine receptor 5 expression defines follicular homing T cells with B cell helper function. J Exp Med. 2000;192(11):1553-62.
136. Breitfeld D, Ohl L, Kremmer E, Ellwart J, Sallusto F, Lipp M, et al. Follicular B helper T cells express CXC chemokine receptor 5, localize to B cell follicles, and support immunoglobulin production. J Exp Med. 2000;192(11):1545-52.
137. Yu D, Rao S, Tsai LM, Lee SK, He Y, Sutcliffe EL, et al. The transcriptional repressor Bcl-6 directs T follicular helper cell lineage commitment. Immunity. 2009;31(3):457-68.
138. Nurieva RI, Chung Y, Martinez GJ, Yang XO, Tanaka S, Matskevitch TD, et al. Bcl6 mediates the development of T follicular helper cells. Science. 2009;325(5943):1001-5.
139. Johnston RJ, Poholek AC, DiToro D, Yusuf I, Eto D, Barnett B, et al. Bcl6 and Blimp-1 are reciprocal and antagonistic regulators of T follicular helper cell differentiation. Science. 2009;325(5943):1006-10.
140. Martins G, Calame K. Regulation and functions of Blimp-1 in T and B lymphocytes. Annu Rev Immunol. 2008;26:133-69.
141. Kato Y, Zaid A, Davey GM, Mueller SN, Nutt SL, Zotos D, et al. Targeting Antigen to Clec9A Primes Follicular Th Cell Memory Responses Capable of Robust Recall. J Immunol. 2015;195(3):1006-14.
142. Eto D, Lao C, DiToro D, Barnett B, Escobar TC, Kageyama R, et al. IL-21 and IL-6 are critical for different aspects of B cell immunity and redundantly induce optimal follicular helper CD4 T cell (Tfh) differentiation. PLoS One. 2011;6(3):e17739.

143. Chtanova T, Tangye SG, Newton R, Frank N, Hodge MR, Rolph MS, et al. T follicular helper cells express a distinctive transcriptional profile, reflecting their role as non-Th1/Th2 effector cells that provide help for B cells. J Immunol. 2004;173(1):68-78.
144. Kim CH, Lim HW, Kim JR, Rott L, Hillsamer P, Butcher EC. Unique gene expression program of human germinal center T helper cells. Blood. 2004;104(7):1952-60.
145. Rasheed AU, Rahn HP, Sallusto F, Lipp M, Muller G. Follicular B helper T cell activity is confined to CXCR5(hi)ICOS(hi) CD4 T cells and is independent of CD57 expression. Eur J Immunol. 2006;36(7):1892-903.
146. Wong MT, Chen J, Narayanan S, Lin W, Anicete R, Kiaang HT, et al. Mapping the Diversity of Follicular Helper T Cells in Human Blood and Tonsils Using High-Dimensional Mass Cytometry Analysis. Cell Rep. 2015;11(11):1822-33.
147. Chen W, Jin W, Hardegen N, Lei KJ, Li L, Marinos N, et al. Conversion of peripheral CD4+CD25- naive T cells to CD4+CD25+ regulatory T cells by TGF-beta induction of transcription factor Foxp3. J Exp Med. 2003;198(12):1875-86.
148. Davidson TS, DiPaolo RJ, Andersson J, Shevach EM. Cutting Edge: IL-2 is essential for TGF-beta-mediated induction of Foxp3+ T regulatory cells. J Immunol. 2007;178(7):4022-6.
149. Burchill MA, Yang J, Vogtenhuber C, Blazar BR, Farrar MA. IL-2 receptor beta-dependent STAT5 activation is required for the development of Foxp3+ regulatory T cells. J Immunol. 2007;178(1):280-90.
150. Takimoto T, Wakabayashi Y, Sekiya T, Inoue N, Morita R, Ichiyama K, et al. Smad2 and Smad3 are redundantly essential for the TGF-beta-mediated regulation of regulatory T plasticity and Th1 development. J Immunol. 2010;185(2):842-55.
151. Tone Y, Furuuchi K, Kojima Y, Tykocinski ML, Greene MI, Tone M. Smad3 and NFAT cooperate to induce Foxp3 expression through its enhancer. Nat Immunol. 2008;9(2):194-202.
152. Martinez GJ, Zhang Z, Chung Y, Reynolds JM, Lin X, Jetten AM, et al. Smad3 differentially regulates the induction of regulatory and inflammatory T cell differentiation. J Biol Chem. 2009;284(51):35283-6.
153. Pandiyan P, Zheng L, Ishihara S, Reed J, Lenardo MJ. CD4+CD25+Foxp3+ regulatory T cells induce cytokine deprivation-mediated apoptosis of effector CD4+ T cells. Nat Immunol. 2007;8(12):1353-62.
154. Qureshi OS, Zheng Y, Nakamura K, Attridge K, Manzotti C, Schmidt EM, et al. Trans-endocytosis of CD80 and CD86: a molecular basis for the cell-extrinsic function of CTLA-4. Science. 2011;332(6029):600-3.
155. Wing K, Onishi Y, Prieto-Martin P, Yamaguchi T, Miyara M, Fehervari Z, et al. CTLA-4 control over Foxp3+ regulatory T cell function. Science. 2008;322(5899):271-5.
156. Jonuleit H, Schmitt E, Kakirman H, Stassen M, Knop J, Enk AH. Infectious tolerance: human CD25(+) regulatory T cells convey suppressor activity to conventional CD4(+) T helper cells. J Exp Med. 2002;196(2):255-60.
157. Sundstedt A, O'Neill EJ, Nicolson KS, Wraith DC. Role for IL-10 in suppression mediated by peptide-induced regulatory T cells in vivo. J Immunol. 2003;170(3):1240-8.
158. Annacker O, Pimenta-Araujo R, Burlen-Defranoux O, Barbosa TC, Cumano A, Bandeira A. CD25+ CD4+ T cells regulate the expansion of peripheral CD4 T cells through the production of IL-10. J Immunol. 2001;166(5):3008-18.
159. Umetsu DT, Jabara HH, DeKruyff RH, Abbas AK, Abrams JS, Geha RS. Functional heterogeneity among human inducer T cell clones. J Immunol. 1988;140(12):4211-6.
160. Panzer M, Sitte S, Wirth S, Drexler I, Sparwasser T, Voehringer D. Rapid in vivo conversion of effector T cells into Th2 cells during helminth infection. J Immunol. 2012;188(2):615-23.
161. Murphy KM, Stockinger B. Effector T cell plasticity: flexibility in the face of changing circumstances. Nat Immunol. 2010;11(8):674-80.

162. Lu KT, Kanno Y, Cannons JL, Handon R, Bible P, Elkahloun AG, et al. Functional and epigenetic studies reveal multistep differentiation and plasticity of in vitro-generated and in vivo-derived follicular T helper cells. Immunity. 2011;35(4):622-32.
163. Becattini S, Latorre D, Mele F, Foglierini M, De Gregorio C, Cassotta A, et al. T cell immunity. Functional heterogeneity of human memory CD4(+) T cell clones primed by pathogens or vaccines. Science. 2015;347(6220):400-6.
164. Han A, Glanville J, Hansmann L, Davis MM. Linking T-cell receptor sequence to functional phenotype at the single-cell level. Nat Biotechnol. 2014;32(7):684-92.
165. Koch MA, Tucker-Heard G, Perdue NR, Killebrew JR, Urdahl KB, Campbell DJ. The transcription factor T-bet controls regulatory T cell homeostasis and function during type 1 inflammation. Nat Immunol. 2009;10(6):595-602.
166. Zheng Y, Chaudhry A, Kas A, deRoos P, Kim JM, Chu TT, et al. Regulatory T-cell suppressor program co-opts transcription factor IRF4 to control T(H)2 responses. Nature. 2009;458(7236):351-6.
167. Cossarizza A, Ortolani C, Paganelli R, Barbieri D, Monti D, Sansoni P, et al. CD45 isoforms expression on CD4+ and CD8+ T cells throughout life, from newborns to centenarians: implications for T cell memory. Mech Ageing Dev. 1996;86(3):173-95.
168. Saule P, Trauet J, Dutriez V, Lekeux V, Dessaint JP, Labalette M. Accumulation of memory T cells from childhood to old age: central and effector memory cells in CD4(+) versus effector memory and terminally differentiated memory cells in CD8(+) compartment. Mech Ageing Dev. 2006;127(3):274-81.
169. Sanders ME, Makgoba MW, Sharrow SO, Stephany D, Springer TA, Young HA, et al. Human memory T lymphocytes express increased levels of three cell adhesion molecules (LFA-3, CD2, and LFA-1) and three other molecules (UCHL1, CDw29, and Pgp-1) and have enhanced IFN-gamma production. J Immunol. 1988;140(5):1401-7.
170. Smith SH, Brown MH, Rowe D, Callard RE, Beverley PC. Functional subsets of human helper-inducer cells defined by a new monoclonal antibody, UCHL1. Immunology. 1986;58(1):63-70.
171. Sallusto F, Lenig D, Forster R, Lipp M, Lanzavecchia A. Two subsets of memory T lymphocytes with distinct homing potentials and effector functions. Nature. 1999;401(6754):708-12.
172. Pedron B, Guerin V, Cordeiro DJ, Masmoudi S, Dalle JH, Sterkers G. Development of cytomegalovirus and adenovirus-specific memory CD4 T-cell functions from birth to adulthood. Pediatr Res. 2011;69(2):106-11.
173. Ellefsen K, Harari A, Champagne P, Bart PA, Sekaly RP, Pantaleo G. Distribution and functional analysis of memory antiviral CD8 T cell responses in HIV-1 and cytomegalovirus infections. Eur J Immunol. 2002;32(12):3756-64.
174. Fearon DT, Carr JM, Telaranta A, Carrasco MJ, Thaventhiran JE. The rationale for the IL-2-independent generation of the self-renewing central memory CD8+ T cells. Immunol Rev. 2006;211:104-18.
175. Libri V, Azevedo RI, Jackson SE, Di Mitri D, Lachmann R, Fuhrmann S, et al. Cytomegalovirus infection induces the accumulation of short-lived, multifunctional CD4+CD45RA+CD27+ T cells: the potential involvement of interleukin-7 in this process. Immunology. 2011;132(3):326-39.
176. Gordon CL, Miron M, Thome JJ, Matsuoka N, Weiner J, Rak MA, et al. Tissue reservoirs of antiviral T cell immunity in persistent human CMV infection. J Exp Med. 2017;214(3):651-67.
177. Weiskopf D, Bangs DJ, Sidney J, Kolla RV, De Silva AD, de Silva AM, et al. Dengue virus infection elicits highly polarized CX3CR1+ cytotoxic CD4+ T cells associated with protective immunity. Proc Natl Acad Sci U S A. 2015;112(31):E4256-63.

178. Song K, Rabin RL, Hill BJ, De Rosa SC, Perfetto SP, Zhang HH, et al. Characterization of subsets of CD4+ memory T cells reveals early branched pathways of T cell differentiation in humans. Proc Natl Acad Sci U S A. 2005;102(22):7916-21.
179. Gattinoni L, Lugli E, Ji Y, Pos Z, Paulos CM, Quigley MF, et al. A human memory T cell subset with stem cell-like properties. Nat Med. 2011;17(10):1290-7.
180. Ahmed R, Roger L, Costa Del Amo P, Miners KL, Jones RE, Boelen L, et al. Human Stem Cell-like Memory T Cells Are Maintained in a State of Dynamic Flux. Cell Rep. 2016;17(11):2811-8.
181. Miyama T, Kawase T, Kitaura K, Chishaki R, Shibata M, Oshima K, et al. Highly functional T-cell receptor repertoires are abundant in stem memory T cells and highly shared among individuals. Sci Rep. 2017;7(1):3663.
182. Mpande CAM, Dintwe OB, Musvosvi M, Mabwe S, Bilek N, Hatherill M, et al. Functional, Antigen-Specific Stem Cell Memory (TSCM) CD4(+) T Cells Are Induced by Human Mycobacterium tuberculosis Infection. Front Immunol. 2018;9:324.
183. Orlando V, La Manna MP, Goletti D, Palmieri F, Lo Presti E, Joosten SA, et al. Human CD4 T-Cells With a Naive Phenotype Produce Multiple Cytokines During Mycobacterium Tuberculosis Infection and Correlate With Active Disease. Front Immunol. 2018;9:1119.
184. Fuertes Marraco SA, Soneson C, Cagnon L, Gannon PO, Allard M, Abed Maillard S, et al. Long-lasting stem cell-like memory CD8+ T cells with a naive-like profile upon yellow fever vaccination. Sci Transl Med. 2015;7(282):282ra48.
185. Pulko V, Davies JS, Martinez C, Lanteri MC, Busch MP, Diamond MS, et al. Human memory T cells with a naive phenotype accumulate with aging and respond to persistent viruses. Nat Immunol. 2016;17(8):966-75.
186. Epstein MA, Achong BG, Barr YM. Virus Particles in Cultured Lymphoblasts from Burkitt's Lymphoma. Lancet. 1964;1(7335):702-3.
187. Borza CM, Hutt-Fletcher LM. Alternate replication in B cells and epithelial cells switches tropism of Epstein-Barr virus. Nat Med. 2002;8(6):594-9.
188. Nemerow GR, Mold C, Schwend VK, Tollefson V, Cooper NR. Identification of gp350 as the viral glycoprotein mediating attachment of Epstein-Barr virus (EBV) to the EBV/C3d receptor of B cells: sequence homology of gp350 and C3 complement fragment C3d. J Virol. 1987;61(5):1416-20.
189. Chesnokova LS, Nishimura SL, Hutt-Fletcher LM. Fusion of epithelial cells by Epstein-Barr virus proteins is triggered by binding of viral glycoproteins gHgL to integrins alphavbeta6 or alphavbeta8. Proc Natl Acad Sci U S A. 2009;106(48):20464-9.
190. Taylor GS, Long HM, Brooks JM, Rickinson AB, Hislop AD. The immunology of Epstein-Barr virus-induced disease. Annu Rev Immunol. 2015;33:787-821.
191. Young LS, Arrand JR, Murray PG. EBV gene expression and regulation. In: Arvin A, Campadelli-Fiume G, Mocarski E, Moore PS, Roizman B, Whitley R, et al., editors. Human Herpesviruses: Biology, Therapy, and Immunoprophylaxis. Cambridge2007.
192. Sinclair AJ, Brimmell M, Shanahan F, Farrell PJ. Pathways of activation of the Epstein-Barr virus productive cycle. J Virol. 1991;65(5):2237-44.
193. Fixman ED, Hayward GS, Hayward SD. trans-acting requirements for replication of Epstein-Barr virus ori-Lyt. J Virol. 1992;66(8):5030-9.
194. Henderson S, Huen D, Rowe M, Dawson C, Johnson G, Rickinson A. Epstein-Barr virus-coded BHRF1 protein, a viral homologue of Bcl-2, protects human B cells from programmed cell death. Proc Natl Acad Sci U S A. 1993;90(18):8479-83.
195. Bellows DS, Howell M, Pearson C, Hazlewood SA, Hardwick JM. Epstein-Barr virus BALF1 is a BCL-2-like antagonist of the herpesvirus antiapoptotic BCL-2 proteins. J Virol. 2002;76(5):2469-79.

196. Quinn LL, Williams LR, White C, Forrest C, Zuo J, Rowe M. The Missing Link in Epstein-Barr Virus Immune Evasion: the BDLF3 Gene Induces Ubiquitination and Downregulation of Major Histocompatibility Complex Class I (MHC-I) and MHC-II. J Virol. 2016;90(1):356-67.
197. Zuo J, Currin A, Griffin BD, Shannon-Lowe C, Thomas WA, Ressing ME, et al. The Epstein-Barr virus G-protein-coupled receptor contributes to immune evasion by targeting MHC class I molecules for degradation. PLoS Pathog. 2009;5(1):e1000255.
198. Hislop AD, Ressing ME, van Leeuwen D, Pudney VA, Horst D, Koppers-Lalic D, et al. A CD8+ T cell immune evasion protein specific to Epstein-Barr virus and its close relatives in Old World primates. J Exp Med. 2007;204(8):1863-73.
199. Rowe M, Glaunsinger B, van Leeuwen D, Zuo J, Sweetman D, Ganem D, et al. Host shutoff during productive Epstein-Barr virus infection is mediated by BGLF5 and may contribute to immune evasion. Proc Natl Acad Sci U S A. 2007;104(9):3366-71.
200. Zeidler R, Eissner G, Meissner P, Uebel S, Tampe R, Lazis S, et al. Downregulation of TAP1 in B lymphocytes by cellular and Epstein-Barr virus-encoded interleukin-10. Blood. 1997;90(6):2390-7.
201. Quinn LL, Zuo J, Abbott RJ, Shannon-Lowe C, Tierney RJ, Hislop AD, et al. Cooperation between Epstein-Barr virus immune evasion proteins spreads protection from CD8+ T cell recognition across all three phases of the lytic cycle. PLoS Pathog. 2014;10(8):e1004322.
202. Zuo J, Thomas WA, Haigh TA, Fitzsimmons L, Long HM, Hislop AD, et al. Epstein-Barr virus evades CD4+ T cell responses in lytic cycle through BZLF1-mediated downregulation of CD74 and the cooperation of vBcl-2. PLoS Pathog. 2011;7(12):e1002455.
203. Ressing ME, van Leeuwen D, Verreck FA, Keating S, Gomez R, Franken KL, et al. Epstein-Barr virus gp42 is posttranslationally modified to produce soluble gp42 that mediates HLA class II immune evasion. J Virol. 2005;79(2):841-52.
204. Ressing ME, van Leeuwen D, Verreck FA, Gomez R, Heemskerk B, Toebes M, et al. Interference with T cell receptor-HLA-DR interactions by Epstein-Barr virus gp42 results in reduced T helper cell recognition. Proc Natl Acad Sci U S A. 2003;100(20):11583-8.
205. Cohen JI, Lekstrom K. Epstein-Barr virus BARF1 protein is dispensable for B-cell transformation and inhibits alpha interferon secretion from mononuclear cells. J Virol. 1999;73(9):7627-32.
206. Strockbine LD, Cohen JI, Farrah T, Lyman SD, Wagener F, DuBose RF, et al. The Epstein-Barr virus BARF1 gene encodes a novel, soluble colony-stimulating factor-1 receptor. J Virol. 1998;72(5):4015-21.
207. Young LS, Rickinson AB. Epstein-Barr virus: 40 years on. Nat Rev Cancer. 2004;4(10):757-68.
208. Hsieh JJ, Hayward SD. Masking of the CBF1/RBPJ kappa transcriptional repression domain by Epstein-Barr virus EBNA2. Science. 1995;268(5210):560-3.
209. Grossman SR, Johannsen E, Tong X, Yalamanchili R, Kieff E. The Epstein-Barr virus nuclear antigen 2 transactivator is directed to response elements by the J kappa recombination signal binding protein. Proc Natl Acad Sci U S A. 1994;91(16):7568-72.
210. Sinclair AJ, Palmero I, Peters G, Farrell PJ. EBNA-2 and EBNA-LP cooperate to cause G0 to G1 transition during immortalization of resting human B lymphocytes by Epstein-Barr virus. EMBO J. 1994;13(14):3321-8.
211. Mannick JB, Cohen JI, Birkenbach M, Marchini A, Kieff E. The Epstein-Barr virus nuclear protein encoded by the leader of the EBNA RNAs is important in B-lymphocyte transformation. J Virol. 1991;65(12):6826-37.
212. Zhao B, Marshall DR, Sample CE. A conserved domain of the Epstein-Barr virus nuclear antigens 3A and 3C binds to a discrete domain of Jkappa. J Virol. 1996;70(7):4228-36.
213. Robertson ES, Lin J, Kieff E. The amino-terminal domains of Epstein-Barr virus nuclear proteins 3A, 3B, and 3C interact with RBPJ(kappa). J Virol. 1996;70(5):3068-74.

214. Tomkinson B, Robertson E, Kieff E. Epstein-Barr virus nuclear proteins EBNA-3A and EBNA-3C are essential for B-lymphocyte growth transformation. J Virol. 1993;67(4):2014-25.
215. Wang D, Liebowitz D, Kieff E. An EBV membrane protein expressed in immortalized lymphocytes transforms established rodent cells. Cell. 1985;43(3 Pt 2):831-40.
216. Kaye KM, Izumi KM, Kieff E. Epstein-Barr virus latent membrane protein 1 is essential for B-lymphocyte growth transformation. Proc Natl Acad Sci U S A. 1993;90(19):9150-4.
217. Uchida J, Yasui T, Takaoka-Shichijo Y, Muraoka M, Kulwichit W, Raab-Traub N, et al. Mimicry of CD40 signals by Epstein-Barr virus LMP1 in B lymphocyte responses. Science. 1999;286(5438):300-3.
218. Eliopoulos AG, Gallagher NJ, Blake SM, Dawson CW, Young LS. Activation of the p38 mitogen-activated protein kinase pathway by Epstein-Barr virus-encoded latent membrane protein 1 coregulates interleukin-6 and interleukin-8 production. J Biol Chem. 1999;274(23):16085-96.
219. Eliopoulos AG, Stack M, Dawson CW, Kaye KM, Hodgkin L, Sihota S, et al. Epstein-Barr virus-encoded LMP1 and CD40 mediate IL-6 production in epithelial cells via an NF-kappaB pathway involving TNF receptor-associated factors. Oncogene. 1997;14(24):2899-916.
220. Horie K, Ohashi M, Satoh Y, Sairenji T. The role of p38 mitogen-activated protein kinase in regulating interleukin-10 gene expression in Burkitt's lymphoma cell lines. Microbiol Immunol. 2007;51(1):149-61.
221. Longnecker R. Epstein-Barr virus latency: LMP2, a regulator or means for Epstein-Barr virus persistence? Adv Cancer Res. 2000;79:175-200.
222. Portis T, Dyck P, Longnecker R. Epstein-Barr Virus (EBV) LMP2A induces alterations in gene transcription similar to those observed in Reed-Sternberg cells of Hodgkin lymphoma. Blood. 2003;102(12):4166-78.
223. Barth S, Pfuhl T, Mamiani A, Ehses C, Roemer K, Kremmer E, et al. Epstein-Barr virus-encoded microRNA miR-BART2 down-regulates the viral DNA polymerase BALF5. Nucleic Acids Res. 2008;36(2):666-75.
224. Jung YJ, Choi H, Kim H, Lee SK. MicroRNA miR-BART20-5p stabilizes Epstein-Barr virus latency by directly targeting BZLF1 and BRLF1. J Virol. 2014;88(16):9027-37.
225. Fields BN, Knipe DM, Howley PM, Griffin DE. Fields virology. 4th ed. Philadelphia: Lippincott Williams & Wilkins; 2001. xix, 3087 p. p.
226. Shinozaki-Ushiku A, Kunita A, Isogai M, Hibiya T, Ushiku T, Takada K, et al. Profiling of Virus-Encoded MicroRNAs in Epstein-Barr Virus-Associated Gastric Carcinoma and Their Roles in Gastric Carcinogenesis. J Virol. 2015;89(10):5581-91.
227. Nachmani D, Stern-Ginossar N, Sarid R, Mandelboim O. Diverse herpesvirus microRNAs target the stress-induced immune ligand MICB to escape recognition by natural killer cells. Cell Host Microbe. 2009;5(4):376-85.
228. Xia T, O'Hara A, Araujo I, Barreto J, Carvalho E, Sapucaia JB, et al. EBV microRNAs in primary lymphomas and targeting of CXCL-11 by ebv-mir-BHRF1-3. Cancer Res. 2008;68(5):1436-42.
229. Albanese M, Tagawa T, Bouvet M, Maliqi L, Lutter D, Hoser J, et al. Epstein-Barr virus microRNAs reduce immune surveillance by virus-specific CD8+ T cells. Proc Natl Acad Sci U S A. 2016;113(42):E6467-E75.
230. Tagawa T, Albanese M, Bouvet M, Moosmann A, Mautner J, Heissmeyer V, et al. Epstein-Barr viral miRNAs inhibit antiviral CD4+ T cell responses targeting IL-12 and peptide processing. J Exp Med. 2016;213(10):2065-80.
231. Murer A, Ruhl J, Zbinden A, Capaul R, Hammerschmidt W, Chijioke O, et al. MicroRNAs of Epstein-Barr Virus Attenuate T-Cell-Mediated Immune Control In Vivo. MBio. 2019;10(1).
232. Draborg AH, Duus K, Houen G. Epstein-Barr virus in systemic autoimmune diseases. Clin Dev Immunol. 2013;2013:535738.

233. Levin LI, Munger KL, O'Reilly EJ, Falk KI, Ascherio A. Primary infection with the Epstein-Barr virus and risk of multiple sclerosis. Ann Neurol. 2010;67(6):824-30.
234. Handel AE, Williamson AJ, Disanto G, Handunnetthi L, Giovannoni G, Ramagopalan SV. An updated meta-analysis of risk of multiple sclerosis following infectious mononucleosis. PLoS One. 2010;5(9).
235. Khan G, Hashim MJ. Global burden of deaths from Epstein-Barr virus attributable malignancies 1990-2010. Infect Agent Cancer. 2014;9(1):38.
236. Paya CV, Fung JJ, Nalesnik MA, Kieff E, Green M, Gores G, et al. Epstein-Barr virus-induced posttransplant lymphoproliferative disorders. ASTS/ASTP EBV-PTLD Task Force and The Mayo Clinic Organized International Consensus Development Meeting. Transplantation. 1999;68(10):1517-25.
237. Cohen JI. Epstein-Barr virus lymphoproliferative disease associated with acquired immunodeficiency. Medicine (Baltimore). 1991;70(2):137-60.
238. Erikson J, ar-Rushdi A, Drwinga HL, Nowell PC, Croce CM. Transcriptional activation of the translocated c-myc oncogene in burkitt lymphoma. Proc Natl Acad Sci U S A. 1983;80(3):820-4.
239. Gregory CD, Rowe M, Rickinson AB. Different Epstein-Barr virus-B cell interactions in phenotypically distinct clones of a Burkitt's lymphoma cell line. J Gen Virol. 1990;71 (Pt 7):1481-95.
240. Mesri EA, Feitelson MA, Munger K. Human viral oncogenesis: a cancer hallmarks analysis. Cell Host Microbe. 2014;15(3):266-82.
241. Kutok JL, Wang F. Spectrum of Epstein-Barr virus-associated diseases. Annu Rev Pathol. 2006;1:375-404.
242. Middeldorp JM, Brink AA, van den Brule AJ, Meijer CJ. Pathogenic roles for Epstein-Barr virus (EBV) gene products in EBV-associated proliferative disorders. Crit Rev Oncol Hematol. 2003;45(1):1-36.
243. Fiola S, Gosselin D, Takada K, Gosselin J. TLR9 contributes to the recognition of EBV by primary monocytes and plasmacytoid dendritic cells. J Immunol. 2010;185(6):3620-31.
244. Zauner L, Nadal D. Understanding TLR9 action in Epstein-Barr virus infection. Front Biosci (Landmark Ed). 2012;17:1219-31.
245. Severa M, Giacomini E, Gafa V, Anastasiadou E, Rizzo F, Corazzari M, et al. EBV stimulates TLR- and autophagy-dependent pathways and impairs maturation in plasmacytoid dendritic cells: implications for viral immune escape. Eur J Immunol. 2013;43(1):147-58.
246. Quan TE, Roman RM, Rudenga BJ, Holers VM, Craft JE. Epstein-Barr virus promotes interferon-alpha production by plasmacytoid dendritic cells. Arthritis Rheum. 2010;62(6):1693-701.
247. Iwakiri D, Zhou L, Samanta M, Matsumoto M, Ebihara T, Seya T, et al. Epstein-Barr virus (EBV)-encoded small RNA is released from EBV-infected cells and activates signaling from Toll-like receptor 3. J Exp Med. 2009;206(10):2091-9.
248. Gaudreault E, Fiola S, Olivier M, Gosselin J. Epstein-Barr virus induces MCP-1 secretion by human monocytes via TLR2. J Virol. 2007;81(15):8016-24.
249. Biron CA. Activation and function of natural killer cell responses during viral infections. Curr Opin Immunol. 1997;9(1):24-34.
250. Tomkinson BE, Wagner DK, Nelson DL, Sullivan JL. Activated lymphocytes during acute Epstein-Barr virus infection. J Immunol. 1987;139(11):3802-7.
251. Williams H, McAulay K, Macsween KF, Gallacher NJ, Higgins CD, Harrison N, et al. The immune response to primary EBV infection: a role for natural killer cells. Br J Haematol. 2005;129(2):266-74.

252. Zhang Y, Wallace DL, de Lara CM, Ghattas H, Asquith B, Worth A, et al. In vivo kinetics of human natural killer cells: the effects of ageing and acute and chronic viral infection. Immunology. 2007;121(2):258-65.
253. Balfour HH, Jr., Odumade OA, Schmeling DO, Mullan BD, Ed JA, Knight JA, et al. Behavioral, virologic, and immunologic factors associated with acquisition and severity of primary Epstein-Barr virus infection in university students. J Infect Dis. 2013;207(1):80-8.
254. Azzi T, Lunemann A, Murer A, Ueda S, Beziat V, Malmberg KJ, et al. Role for early-differentiated natural killer cells in infectious mononucleosis. Blood. 2014;124(16):2533-43.
255. Chijioke O, Muller A, Feederle R, Barros MH, Krieg C, Emmel V, et al. Human natural killer cells prevent infectious mononucleosis features by targeting lytic Epstein-Barr virus infection. Cell Rep. 2013;5(6):1489-98.
256. Palendira U, Rickinson AB. Primary immunodeficiencies and the control of Epstein-Barr virus infection. Ann N Y Acad Sci. 2015;1356:22-44.
257. Parvaneh N, Filipovich AH, Borkhardt A. Primary immunodeficiencies predisposed to Epstein-Barr virus-driven haematological diseases. Br J Haematol. 2013;162(5):573-86.
258. Hislop AD, Annels NE, Gudgeon NH, Leese AM, Rickinson AB. Epitope-specific evolution of human CD8(+) T cell responses from primary to persistent phases of Epstein-Barr virus infection. J Exp Med. 2002;195(7):893-905.
259. Long HM, Chagoury OL, Leese AM, Ryan GB, James E, Morton LT, et al. MHC II tetramers visualize human CD4+ T cell responses to Epstein-Barr virus infection and demonstrate atypical kinetics of the nuclear antigen EBNA1 response. J Exp Med. 2013;210(5):933-49.
260. Annels NE, Callan MF, Tan L, Rickinson AB. Changing patterns of dominant TCR usage with maturation of an EBV-specific cytotoxic T cell response. J Immunol. 2000;165(9):4831-41.
261. Pudney VA, Leese AM, Rickinson AB, Hislop AD. CD8+ immunodominance among Epstein-Barr virus lytic cycle antigens directly reflects the efficiency of antigen presentation in lytically infected cells. J Exp Med. 2005;201(3):349-60.
262. Woodberry T, Suscovich TJ, Henry LM, Davis JK, Frahm N, Walker BD, et al. Differential targeting and shifts in the immunodominance of Epstein-Barr virus--specific CD8 and CD4 T cell responses during acute and persistent infection. J Infect Dis. 2005;192(9):1513-24.
263. Abbott RJ, Quinn LL, Leese AM, Scholes HM, Pachnio A, Rickinson AB. CD8+ T cell responses to lytic EBV infection: late antigen specificities as subdominant components of the total response. J Immunol. 2013;191(11):5398-409.
264. Catalina MD, Sullivan JL, Bak KR, Luzuriaga K. Differential evolution and stability of epitope-specific CD8(+) T cell responses in EBV infection. J Immunol. 2001;167(8):4450-7.
265. Callan MF, Tan L, Annels N, Ogg GS, Wilson JD, O'Callaghan CA, et al. Direct visualization of antigen-specific CD8+ T cells during the primary immune response to Epstein-Barr virus In vivo. J Exp Med. 1998;187(9):1395-402.
266. Silins SL, Sherritt MA, Silleri JM, Cross SM, Elliott SL, Bharadwaj M, et al. Asymptomatic primary Epstein-Barr virus infection occurs in the absence of blood T-cell repertoire perturbations despite high levels of systemic viral load. Blood. 2001;98(13):3739-44.
267. Jayasooriya S, de Silva TI, Njie-jobe J, Sanyang C, Leese AM, Bell AI, et al. Early virological and immunological events in asymptomatic Epstein-Barr virus infection in African children. PLoS Pathog. 2015;11(3):e1004746.
268. Abbott RJ, Pachnio A, Pedroza-Pacheco I, Leese AM, Begum J, Long HM, et al. Asymptomatic Primary Infection with Epstein-Barr Virus: Observations on Young Adult Cases. J Virol. 2017;91(21).
269. Amyes E, Hatton C, Montamat-Sicotte D, Gudgeon N, Rickinson AB, McMichael AJ, et al. Characterization of the CD4+ T cell response to Epstein-Barr virus during primary and persistent infection. J Exp Med. 2003;198(6):903-11.

270. Precopio ML, Sullivan JL, Willard C, Somasundaran M, Luzuriaga K. Differential kinetics and specificity of EBV-specific CD4+ and CD8+ T cells during primary infection. J Immunol. 2003;170(5):2590-8.
271. Appay V, Zaunders JJ, Papagno L, Sutton J, Jaramillo A, Waters A, et al. Characterization of CD4(+) CTLs ex vivo. J Immunol. 2002;168(11):5954-8.
272. Brooks JM, Long HM, Tierney RJ, Shannon-Lowe C, Leese AM, Fitzpatrick M, et al. Early T Cell Recognition of B Cells following Epstein-Barr Virus Infection: Identifying Potential Targets for Prophylactic Vaccination. PLoS Pathog. 2016;12(4):e1005549.
273. Lelic A, Verschoor CP, Ventresca M, Parsons R, Evelegh C, Bowdish D, et al. The polyfunctionality of human memory CD8+ T cells elicited by acute and chronic virus infections is not influenced by age. PLoS Pathog. 2012;8(12):e1003076.
274. Klarenbeek PL, Remmerswaal EB, ten Berge IJ, Doorenspleet ME, van Schaik BD, Esveldt RE, et al. Deep sequencing of antiviral T-cell responses to HCMV and EBV in humans reveals a stable repertoire that is maintained for many years. PLoS Pathog. 2012;8(9):e1002889.
275. Leen A, Meij P, Redchenko I, Middeldorp J, Bloemena E, Rickinson A, et al. Differential immunogenicity of Epstein-Barr virus latent-cycle proteins for human CD4(+) T-helper 1 responses. J Virol. 2001;75(18):8649-59.
276. Long HM, Haigh TA, Gudgeon NH, Leen AM, Tsang CW, Brooks J, et al. CD4+ T-cell responses to Epstein-Barr virus (EBV) latent-cycle antigens and the recognition of EBV-transformed lymphoblastoid cell lines. J Virol. 2005;79(8):4896-907.
277. Long HM, Leese AM, Chagoury OL, Connerty SR, Quarcoopome J, Quinn LL, et al. Cytotoxic CD4+ T cell responses to EBV contrast with CD8 responses in breadth of lytic cycle antigen choice and in lytic cycle recognition. J Immunol. 2011;187(1):92-101.
278. Haigh TA, Lin X, Jia H, Hui EP, Chan AT, Rickinson AB, et al. EBV latent membrane proteins (LMPs) 1 and 2 as immunotherapeutic targets: LMP-specific CD4+ cytotoxic T cell recognition of EBV-transformed B cell lines. J Immunol. 2008;180(3):1643-54.
279. Adhikary D, Behrends U, Moosmann A, Witter K, Bornkamm GW, Mautner J. Control of Epstein-Barr virus infection in vitro by T helper cells specific for virion glycoproteins. J Exp Med. 2006;203(4):995-1006.
280. Lam JKP, Hui KF, Ning RJ, Xu XQ, Chan KH, Chiang AKS. Emergence of CD4+ and CD8+ Polyfunctional T Cell Responses Against Immunodominant Lytic and Latent EBV Antigens in Children With Primary EBV Infection. Front Microbiol. 2018;9:416.
281. Paludan C, Bickham K, Nikiforow S, Tsang ML, Goodman K, Hanekom WA, et al. Epstein-Barr nuclear antigen 1-specific CD4(+) Th1 cells kill Burkitt's lymphoma cells. J Immunol. 2002;169(3):1593-603.
282. Bickham K, Munz C, Tsang ML, Larsson M, Fonteneau JF, Bhardwaj N, et al. EBNA1-specific CD4+ T cells in healthy carriers of Epstein-Barr virus are primarily Th1 in function. J Clin Invest. 2001;107(1):121-30.
283. Munz C, Bickham KL, Subklewe M, Tsang ML, Chahroudi A, Kurilla MG, et al. Human CD4(+) T lymphocytes consistently respond to the latent Epstein-Barr virus nuclear antigen EBNA1. J Exp Med. 2000;191(10):1649-60.
284. Marshall NA, Vickers MA, Barker RN. Regulatory T cells secreting IL-10 dominate the immune response to EBV latent membrane protein 1. J Immunol. 2003;170(12):6183-9.
285. Cardenas Sierra D, Velez Colmenares G, Orfao de Matos A, Fiorentino Gomez S, Quijano Gomez SM. Age-associated Epstein-Barr virus-specific T cell responses in seropositive healthy adults. Clin Exp Immunol. 2014;177(1):320-32.
286. Ning RJ, Xu XQ, Chan KH, Chiang AK. Long-term carriers generate Epstein-Barr virus (EBV)-specific CD4(+) and CD8(+) polyfunctional T-cell responses which show immunodominance hierarchies of EBV proteins. Immunology. 2011;134(2):161-71.

287. Khanna R, Burrows SR, Thomson SA, Moss DJ, Cresswell P, Poulsen LM, et al. Class I processing-defective Burkitt's lymphoma cells are recognized efficiently by CD4+ EBV-specific CTLs. J Immunol. 1997;158(8):3619-25.
288. Landais E, Saulquin X, Scotet E, Trautmann L, Peyrat MA, Yates JL, et al. Direct killing of Epstein-Barr virus (EBV)-infected B cells by CD4 T cells directed against the EBV lytic protein BHRF1. Blood. 2004;103(4):1408-16.
289. Nikiforow S, Bottomly K, Miller G, Munz C. Cytolytic CD4(+)-T-cell clones reactive to EBNA1 inhibit Epstein-Barr virus-induced B-cell proliferation. J Virol. 2003;77(22):12088-104.
290. Bibas M, Antinori A. EBV and HIV-Related Lymphoma. Mediterr J Hematol Infect Dis. 2009;1(2):e2009032.
291. Leruez-Ville M, Seng R, Morand P, Boufassa F, Boue F, Deveau C, et al. Blood Epstein-Barr virus DNA load and risk of progression to AIDS-related systemic B lymphoma. HIV Med. 2012;13(8):479-87.
292. Carbone A. AIDS-related non-Hodgkin's lymphomas: from pathology and molecular pathogenesis to treatment. Hum Pathol. 2002;33(4):392-404.
293. Rezk SA, Weiss LM. Epstein-Barr virus-associated lymphoproliferative disorders. Hum Pathol. 2007;38(9):1293-304.
294. Said JW. Immunodeficiency-related Hodgkin lymphoma and its mimics. Adv Anat Pathol. 2007;14(3):189-94.
295. Flinn IW, Ambinder RF. AIDS primary central nervous system lymphoma. Curr Opin Oncol. 1996;8(5):373-6.
296. Fafi-Kremer S, Morand P, Brion JP, Pavese P, Baccard M, Germi R, et al. Long-term shedding of infectious epstein-barr virus after infectious mononucleosis. J Infect Dis. 2005;191(6):985-9.
297. Hislop AD, Kuo M, Drake-Lee AB, Akbar AN, Bergler W, Hammerschmitt N, et al. Tonsillar homing of Epstein-Barr virus-specific CD8+ T cells and the virus-host balance. J Clin Invest. 2005;115(9):2546-55.
298. Woon HG, Braun A, Li J, Smith C, Edwards J, Sierro F, et al. Compartmentalization of Total and Virus-Specific Tissue-Resident Memory CD8+ T Cells in Human Lymphoid Organs. PLoS Pathog. 2016;12(8):e1005799.
299. Janz A, Oezel M, Kurzeder C, Mautner J, Pich D, Kost M, et al. Infectious Epstein-Barr virus lacking major glycoprotein BLLF1 (gp350/220) demonstrates the existence of additional viral ligands. J Virol. 2000;74(21):10142-52.
300. Cohen JI. Vaccine Development for Epstein-Barr Virus. Adv Exp Med Biol. 2018;1045:477-93.
301. Gu SY, Huang TM, Ruan L, Miao YH, Lu H, Chu CM, et al. First EBV vaccine trial in humans using recombinant vaccinia virus expressing the major membrane antigen. Dev Biol Stand. 1995;84:171-7.
302. Sokal EM, Hoppenbrouwers K, Vandermeulen C, Moutschen M, Leonard P, Moreels A, et al. Recombinant gp350 vaccine for infectious mononucleosis: a phase 2, randomized, double-blind, placebo-controlled trial to evaluate the safety, immunogenicity, and efficacy of an Epstein-Barr virus vaccine in healthy young adults. J Infect Dis. 2007;196(12):1749-53.
303. Goldacre MJ, Wotton CJ, Yeates DG. Associations between infectious mononucleosis and cancer: record-linkage studies. Epidemiol Infect. 2009;137(5):672-80.
304. Hjalgrim H, Askling J, Rostgaard K, Hamilton-Dutoit S, Frisch M, Zhang JS, et al. Characteristics of Hodgkin's lymphoma after infectious mononucleosis. N Engl J Med. 2003;349(14):1324-32.
305. Rees L, Tizard EJ, Morgan AJ, Cubitt WD, Finerty S, Oyewole-Eletu TA, et al. A phase I trial of epstein-barr virus gp350 vaccine for children with chronic kidney disease awaiting transplantation. Transplantation. 2009;88(8):1025-9.

306. Perez EM, Foley J, Tison T, Silva R, Ogembo JG. Novel Epstein-Barr virus-like particles incorporating gH/gL-EBNA1 or gB-LMP2 induce high neutralizing antibody titers and EBV-specific T-cell responses in immunized mice. Oncotarget. 2017;8(12):19255-73.
307. Ruiss R, Jochum S, Wanner G, Reisbach G, Hammerschmidt W, Zeidler R. A virus-like particle-based Epstein-Barr virus vaccine. J Virol. 2011;85(24):13105-13.
308. van Zyl DG, Tsai MH, Shumilov A, Schneidt V, Poirey R, Schlehe B, et al. Immunogenic particles with a broad antigenic spectrum stimulate cytolytic T cells and offer increased protection against EBV infection ex vivo and in mice. PLoS Pathog. 2018;14(12):e1007464.
309. Lin CL, Lo WF, Lee TH, Ren Y, Hwang SL, Cheng YF, et al. Immunization with Epstein-Barr Virus (EBV) peptide-pulsed dendritic cells induces functional CD8+ T-cell immunity and may lead to tumor regression in patients with EBV-positive nasopharyngeal carcinoma. Cancer Res. 2002;62(23):6952-8.
310. Chia WK, Wang WW, Teo M, Tai WM, Lim WT, Tan EH, et al. A phase II study evaluating the safety and efficacy of an adenovirus-DeltaLMP1-LMP2 transduced dendritic cell vaccine in patients with advanced metastatic nasopharyngeal carcinoma. Ann Oncol. 2012;23(4):997-1005.
311. Taylor GS, Jia H, Harrington K, Lee LW, Turner J, Ladell K, et al. A recombinant modified vaccinia ankara vaccine encoding Epstein-Barr Virus (EBV) target antigens: a phase I trial in UK patients with EBV-positive cancer. Clin Cancer Res. 2014;20(19):5009-22.
312. Hui EP, Taylor GS, Jia H, Ma BB, Chan SL, Ho R, et al. Phase I trial of recombinant modified vaccinia ankara encoding Epstein-Barr viral tumor antigens in nasopharyngeal carcinoma patients. Cancer Res. 2013;73(6):1676-88.
313. Roskrow MA, Suzuki N, Gan Y, Sixbey JW, Ng CY, Kimbrough S, et al. Epstein-Barr virus (EBV)-specific cytotoxic T lymphocytes for the treatment of patients with EBV-positive relapsed Hodgkin's disease. Blood. 1998;91(8):2925-34.
314. Bollard CM, Gottschalk S, Torrano V, Diouf O, Ku S, Hazrat Y, et al. Sustained complete responses in patients with lymphoma receiving autologous cytotoxic T lymphocytes targeting Epstein-Barr virus latent membrane proteins. J Clin Oncol. 2014;32(8):798-808.
315. Chia WK, Teo M, Wang WW, Lee B, Ang SF, Tai WM, et al. Adoptive T-cell transfer and chemotherapy in the first-line treatment of metastatic and/or locally recurrent nasopharyngeal carcinoma. Mol Ther. 2014;22(1):132-9.
316. Smith C, Tsang J, Beagley L, Chua D, Lee V, Li V, et al. Effective treatment of metastatic forms of Epstein-Barr virus-associated nasopharyngeal carcinoma with a novel adenovirus-based adoptive immunotherapy. Cancer Res. 2012;72(5):1116-25.
317. Straathof KC, Bollard CM, Popat U, Huls MH, Lopez T, Morriss MC, et al. Treatment of nasopharyngeal carcinoma with Epstein-Barr virus--specific T lymphocytes. Blood. 2005;105(5):1898-904.
318. Icheva V, Kayser S, Wolff D, Tuve S, Kyzirakos C, Bethge W, et al. Adoptive transfer of epstein-barr virus (EBV) nuclear antigen 1-specific t cells as treatment for EBV reactivation and lymphoproliferative disorders after allogeneic stem-cell transplantation. J Clin Oncol. 2013;31(1):39-48.
319. Haque T, Wilkie GM, Jones MM, Higgins CD, Urquhart G, Wingate P, et al. Allogeneic cytotoxic T-cell therapy for EBV-positive posttransplantation lymphoproliferative disease: results of a phase 2 multicenter clinical trial. Blood. 2007;110(4):1123-31.
320. Krensky AM, Reiss CS, Mier JW, Strominger JL, Burakoff SJ. Long-term human cytolytic T-cell lines allospecific for HLA-DR6 antigen are OKT4+. Proc Natl Acad Sci U S A. 1982;79(7):2365-9.
321. Maimone MM, Morrison LA, Braciale VL, Braciale TJ. Features of target cell lysis by class I and class II MHC-restricted cytolytic T lymphocytes. J Immunol. 1986;137(11):3639-43.

322. Fleischer B. Acquisition of specific cytotoxic activity by human T4+ T lymphocytes in culture. Nature. 1984;308(5957):365-7.
323. Juno JA, van Bockel D, Kent SJ, Kelleher AD, Zaunders JJ, Munier CM. Cytotoxic CD4 T Cells-Friend or Foe during Viral Infection? Front Immunol. 2017;8:19.
324. Watson AM, Lam LK, Klimstra WB, Ryman KD. The 17D-204 Vaccine Strain-Induced Protection against Virulent Yellow Fever Virus Is Mediated by Humoral Immunity and CD4+ but not CD8+ T Cells. PLoS Pathog. 2016;12(7):e1005786.
325. Terahara K, Ishii H, Nomura T, Takahashi N, Takeda A, Shiino T, et al. Vaccine-induced CD107a+ CD4+ T cells are resistant to depletion following AIDS virus infection. J Virol. 2014;88(24):14232-40.
326. Quezada SA, Simpson TR, Peggs KS, Merghoub T, Vider J, Fan X, et al. Tumor-reactive CD4(+) T cells develop cytotoxic activity and eradicate large established melanoma after transfer into lymphopenic hosts. J Exp Med. 2010;207(3):637-50.
327. Petersen JL, Morris CR, Solheim JC. Virus evasion of MHC class I molecule presentation. J Immunol. 2003;171(9):4473-8.
328. Schwartz O, Marechal V, Le Gall S, Lemonnier F, Heard JM. Endocytosis of major histocompatibility complex class I molecules is induced by the HIV-1 Nef protein. Nat Med. 1996;2(3):338-42.
329. Wiertz EJ, Jones TR, Sun L, Bogyo M, Geuze HJ, Ploegh HL. The human cytomegalovirus US11 gene product dislocates MHC class I heavy chains from the endoplasmic reticulum to the cytosol. Cell. 1996;84(5):769-79.
330. Soghoian DZ, Jessen H, Flanders M, Sierra-Davidson K, Cutler S, Pertel T, et al. HIV-specific cytolytic CD4 T cell responses during acute HIV infection predict disease outcome. Sci Transl Med. 2012;4(123):123ra25.
331. Raeiszadeh M, Pachnio A, Begum J, Craddock C, Moss P, Chen FE. Characterization of CMV-specific CD4+ T-cell reconstitution following stem cell transplantation through the use of HLA Class II-peptide tetramers identifies patients at high risk of recurrent CMV reactivation. Haematologica. 2015;100(8):e318-22.
332. Zhou X, McElhaney JE. Age-related changes in memory and effector T cells responding to influenza A/H3N2 and pandemic A/H1N1 strains in humans. Vaccine. 2011;29(11):2169-77.
333. Vogel AJ, Brown DM. Single-Dose CpG Immunization Protects Against a Heterosubtypic Challenge and Generates Antigen-Specific Memory T Cells. Front Immunol. 2015;6:327.
334. Aslan N, Yurdaydin C, Wiegand J, Greten T, Ciner A, Meyer MF, et al. Cytotoxic CD4 T cells in viral hepatitis. J Viral Hepat. 2006;13(8):505-14.
335. Casazza JP, Betts MR, Price DA, Precopio ML, Ruff LE, Brenchley JM, et al. Acquisition of direct antiviral effector functions by CMV-specific CD4+ T lymphocytes with cellular maturation. J Exp Med. 2006;203(13):2865-77.
336. Pachnio A, Ciaurriz M, Begum J, Lal N, Zuo J, Beggs A, et al. Cytomegalovirus Infection Leads to Development of High Frequencies of Cytotoxic Virus-Specific CD4+ T Cells Targeted to Vascular Endothelium. PLoS Pathog. 2016;12(9):e1005832.
337. Shabir S, Smith H, Kaul B, Pachnio A, Jham S, Kuravi S, et al. Cytomegalovirus-Associated CD4(+) CD28(null) Cells in NKG2D-Dependent Glomerular Endothelial Injury and Kidney Allograft Dysfunction. Am J Transplant. 2016;16(4):1113-28.
338. Gamadia LE, Rentenaar RJ, van Lier RA, ten Berge IJ. Properties of CD4(+) T cells in human cytomegalovirus infection. Hum Immunol. 2004;65(5):486-92.
339. Patil VS, Madrigal A, Schmiedel BJ, Clarke J, O'Rourke P, de Silva AD, et al. Precursors of human CD4(+) cytotoxic T lymphocytes identified by single-cell transcriptome analysis. Sci Immunol. 2018;3(19).

340. Wilkinson TM, Li CK, Chui CS, Huang AK, Perkins M, Liebner JC, et al. Preexisting influenza-specific CD4+ T cells correlate with disease protection against influenza challenge in humans. Nat Med. 2012;18(2):274-80.
341. Xie Y, Akpinarli A, Maris C, Hipkiss EL, Lane M, Kwon EK, et al. Naive tumor-specific CD4(+) T cells differentiated in vivo eradicate established melanoma. J Exp Med. 2010;207(3):651-67.
342. Zhang X, Gao L, Meng K, Han C, Li Q, Feng Z, et al. Characterization of CD4(+) T cell-mediated cytotoxicity in patients with multiple myeloma. Cell Immunol. 2018;327:62-7.
343. Zaunders JJ, Munier ML, Kaufmann DE, Ip S, Grey P, Smith D, et al. Early proliferation of CCR5(+) CD38(+++) antigen-specific CD4(+) Th1 effector cells during primary HIV-1 infection. Blood. 2005;106(5):1660-7.
344. Johnson S, Eller M, Teigler JE, Maloveste SM, Schultz BT, Soghoian DZ, et al. Cooperativity of HIV-Specific Cytolytic CD4 T Cells and CD8 T Cells in Control of HIV Viremia. J Virol. 2015;89(15):7494-505.
345. Brown DM, Lee S, Garcia-Hernandez Mde L, Swain SL. Multifunctional CD4 cells expressing gamma interferon and perforin mediate protection against lethal influenza virus infection. J Virol. 2012;86(12):6792-803.
346. Hua L, Yao S, Pham D, Jiang L, Wright J, Sawant D, et al. Cytokine-dependent induction of CD4+ T cells with cytotoxic potential during influenza virus infection. J Virol. 2013;87(21):11884-93.
347. Brown DM, Kamperschroer C, Dilzer AM, Roberts DM, Swain SL. IL-2 and antigen dose differentially regulate perforin- and FasL-mediated cytolytic activity in antigen specific CD4+ T cells. Cell Immunol. 2009;257(1-2):69-79.
348. Qui HZ, Hagymasi AT, Bandyopadhyay S, St Rose MC, Ramanarasimhaiah R, Menoret A, et al. CD134 plus CD137 dual costimulation induces Eomesodermin in CD4 T cells to program cytotoxic Th1 differentiation. J Immunol. 2011;187(7):3555-64.
349. Workman AM, Jacobs AK, Vogel AJ, Condon S, Brown DM. Inflammation enhances IL-2 driven differentiation of cytolytic CD4 T cells. PLoS One. 2014;9(2):e89010.
350. Moore TC, Vogel AJ, Petro TM, Brown DM. IRF3 deficiency impacts granzyme B expression and maintenance of memory T cell function in response to viral infection. Microbes Infect. 2015;17(6):426-39.
351. Zhang J, Scordi I, Smyth MJ, Lichtenheld MG. Interleukin 2 receptor signaling regulates the perforin gene through signal transducer and activator of transcription (Stat)5 activation of two enhancers. J Exp Med. 1999;190(9):1297-308.
352. Pipkin ME, Sacks JA, Cruz-Guilloty F, Lichtenheld MG, Bevan MJ, Rao A. Interleukin-2 and inflammation induce distinct transcriptional programs that promote the differentiation of effector cytolytic T cells. Immunity. 2010;32(1):79-90.
353. Cruz-Guilloty F, Pipkin ME, Djuretic IM, Levanon D, Lotem J, Lichtenheld MG, et al. Runx3 and T-box proteins cooperate to establish the transcriptional program of effector CTLs. J Exp Med. 2009;206(1):51-9.
354. Alonso-Arias R, Moro-Garcia MA, Vidal-Castineira JR, Solano-Jaurrieta JJ, Suarez-Garcia FM, Coto E, et al. IL-15 preferentially enhances functional properties and antigen-specific responses of CD4+CD28(null) compared to CD4+CD28+ T cells. Aging Cell. 2011;10(5):844-52.
355. Mucida D, Husain MM, Muroi S, van Wijk F, Shinnakasu R, Naoe Y, et al. Transcriptional reprogramming of mature CD4(+) helper T cells generates distinct MHC class II-restricted cytotoxic T lymphocytes. Nat Immunol. 2013;14(3):281-9.
356. Carlier VA, VanderElst L, Janssens W, Jacquemin MG, Saint-Remy JM. Increased synapse formation obtained by T cell epitopes containing a CxxC motif in flanking residues convert CD4+ T cells into cytolytic effectors. PLoS One. 2012;7(10):e45366.

357. Malek Abrahimians E, Carlier VA, Vander Elst L, Saint-Remy JM. MHC Class II-Restricted Epitopes Containing an Oxidoreductase Activity Prompt CD4(+) T Cells with Apoptosis-Inducing Properties. Front Immunol. 2015;6:449.
358. Betts MR, Brenchley JM, Price DA, De Rosa SC, Douek DC, Roederer M, et al. Sensitive and viable identification of antigen-specific CD8+ T cells by a flow cytometric assay for degranulation. J Immunol Methods. 2003;281(1-2):65-78.
359. Peters PJ, Borst J, Oorschot V, Fukuda M, Krahenbuhl O, Tschopp J, et al. Cytotoxic T lymphocyte granules are secretory lysosomes, containing both perforin and granzymes. J Exp Med. 1991;173(5):1099-109.
360. Imai T, Hieshima K, Haskell C, Baba M, Nagira M, Nishimura M, et al. Identification and molecular characterization of fractalkine receptor CX3CR1, which mediates both leukocyte migration and adhesion. Cell. 1997;91(4):521-30.
361. Kaech SM, Cui W. Transcriptional control of effector and memory CD8+ T cell differentiation. Nat Rev Immunol. 2012;12(11):749-61.
362. Takeuchi A, Badr Mel S, Miyauchi K, Ishihara C, Onishi R, Guo Z, et al. CRTAM determines the CD4+ cytotoxic T lymphocyte lineage. J Exp Med. 2016;213(1):123-38.
363. van Leeuwen EM, Remmerswaal EB, Vossen MT, Rowshani AT, Wertheim-van Dillen PM, van Lier RA, et al. Emergence of a CD4+CD28- granzyme B+, cytomegalovirus-specific T cell subset after recovery of primary cytomegalovirus infection. J Immunol. 2004;173(3):1834-41.
364. Brien JD, Uhrlaub JL, Nikolich-Zugich J. West Nile virus-specific CD4 T cells exhibit direct antiviral cytokine secretion and cytotoxicity and are sufficient for antiviral protection. J Immunol. 2008;181(12):8568-75.
365. Mahon BP, Katrak K, Nomoto A, Macadam AJ, Minor PD, Mills KH. Poliovirus-specific CD4+ Th1 clones with both cytotoxic and helper activity mediate protective humoral immunity against a lethal poliovirus infection in transgenic mice expressing the human poliovirus receptor. J Exp Med. 1995;181(4):1285-92.
366. Grossman WJ, Verbsky JW, Tollefsen BL, Kemper C, Atkinson JP, Ley TJ. Differential expression of granzymes A and B in human cytotoxic lymphocyte subsets and T regulatory cells. Blood. 2004;104(9):2840-8.
367. Pearce EL, Mullen AC, Martins GA, Krawczyk CM, Hutchins AS, Zediak VP, et al. Control of effector CD8+ T cell function by the transcription factor Eomesodermin. Science. 2003;302(5647):1041-3.
368. Intlekofer AM, Banerjee A, Takemoto N, Gordon SM, Dejong CS, Shin H, et al. Anomalous type 17 response to viral infection by CD8+ T cells lacking T-bet and eomesodermin. Science. 2008;321(5887):408-11.
369. Raveney BJ, Oki S, Hohjoh H, Nakamura M, Sato W, Murata M, et al. Eomesodermin-expressing T-helper cells are essential for chronic neuroinflammation. Nat Commun. 2015;6:8437.
370. Buggert M, Nguyen S, McLane LM, Steblyanko M, Anikeeva N, Paquin-Proulx D, et al. Limited immune surveillance in lymphoid tissue by cytolytic CD4+ T cells during health and HIV disease. PLoS Pathog. 2018;14(4):e1006973.
371. Donnarumma T, Young GR, Merkenschlager J, Eksmond U, Bongard N, Nutt SL, et al. Opposing Development of Cytotoxic and Follicular Helper CD4 T Cells Controlled by the TCF-1-Bcl6 Nexus. Cell Rep. 2016;17(6):1571-83.
372. Oja AE, Vieira Braga FA, Remmerswaal EB, Kragten NA, Hertoghs KM, Zuo J, et al. The Transcription Factor Hobit Identifies Human Cytotoxic CD4(+) T Cells. Front Immunol. 2017;8:325.
373. Masopust D, Choo D, Vezys V, Wherry EJ, Duraiswamy J, Akondy R, et al. Dynamic T cell migration program provides resident memory within intestinal epithelium. J Exp Med. 2010;207(3):553-64.

374. Park CO, Kupper TS. The emerging role of resident memory T cells in protective immunity and inflammatory disease. Nat Med. 2015;21(7):688-97.
375. Schenkel JM, Masopust D. Tissue-resident memory T cells. Immunity. 2014;41(6):886-97.
376. Mackay LK, Wynne-Jones E, Freestone D, Pellicci DG, Mielke LA, Newman DM, et al. T-box Transcription Factors Combine with the Cytokines TGF-beta and IL-15 to Control Tissue-Resident Memory T Cell Fate. Immunity. 2015;43(6):1101-11.
377. Ganusov VV, De Boer RJ. Do most lymphocytes in humans really reside in the gut? Trends Immunol. 2007;28(12):514-8.
378. Hondowicz BD, An D, Schenkel JM, Kim KS, Steach HR, Krishnamurty AT, et al. Interleukin-2-Dependent Allergen-Specific Tissue-Resident Memory Cells Drive Asthma. Immunity. 2016;44(1):155-66.
379. Hondowicz BD, Kim KS, Ruterbusch MJ, Keitany GJ, Pepper M. IL-2 is required for the generation of viral-specific CD4(+) Th1 tissue-resident memory cells and B cells are essential for maintenance in the lung. Eur J Immunol. 2018;48(1):80-6.
380. Kang MC, Choi DH, Choi YW, Park SJ, Namkoong H, Park KS, et al. Intranasal Introduction of Fc-Fused Interleukin-7 Provides Long-Lasting Prophylaxis against Lethal Influenza Virus Infection. J Virol. 2015;90(5):2273-84.
381. Yeon SM, Halim L, Chandele A, Perry CJ, Kim SH, Kim SU, et al. IL-7 plays a critical role for the homeostasis of allergen-specific memory CD4 T cells in the lung and airways. Sci Rep. 2017;7(1):11155.
382. Adachi T, Kobayashi T, Sugihara E, Yamada T, Ikuta K, Pittaluga S, et al. Hair follicle-derived IL-7 and IL-15 mediate skin-resident memory T cell homeostasis and lymphoma. Nat Med. 2015;21(11):1272-9.
383. Strutt TM, Dhume K, Finn CM, Hwang JH, Castonguay C, Swain SL, et al. IL-15 supports the generation of protective lung-resident memory CD4 T cells. Mucosal Immunol. 2018;11(3):668-80.
384. Wang D, Diao H, Getzler AJ, Rogal W, Frederick MA, Milner J, et al. The Transcription Factor Runx3 Establishes Chromatin Accessibility of cis-Regulatory Landscapes that Drive Memory Cytotoxic T Lymphocyte Formation. Immunity. 2018;48(4):659-74 e6.
385. Moguche AO, Shafiani S, Clemons C, Larson RP, Dinh C, Higdon LE, et al. ICOS and Bcl6-dependent pathways maintain a CD4 T cell population with memory-like properties during tuberculosis. J Exp Med. 2015;212(5):715-28.
386. Shiow LR, Rosen DB, Brdickova N, Xu Y, An J, Lanier LL, et al. CD69 acts downstream of interferon-alpha/beta to inhibit S1P1 and lymphocyte egress from lymphoid organs. Nature. 2006;440(7083):540-4.
387. Labiano S, Melendez-Rodriguez F, Palazon A, Teijeira A, Garasa S, Etxeberria I, et al. CD69 is a direct HIF-1alpha target gene in hypoxia as a mechanism enhancing expression on tumor-infiltrating T lymphocytes. Oncoimmunology. 2017;6(4):e1283468.
388. Testi R, Phillips JH, Lanier LL. Leu 23 induction as an early marker of functional CD3/T cell antigen receptor triggering. Requirement for receptor cross-linking, prolonged elevation of intracellular [Ca++] and stimulation of protein kinase C. J Immunol. 1989;142(6):1854-60.
389. Rosato PC, Beura LK, Masopust D. Tissue resident memory T cells and viral immunity. Curr Opin Virol. 2017;22:44-50.
390. Bankovich AJ, Shiow LR, Cyster JG. CD69 suppresses sphingosine 1-phosophate receptor-1 (S1P1) function through interaction with membrane helix 4. J Biol Chem. 2010;285(29):22328-37.
391. Skon CN, Lee JY, Anderson KG, Masopust D, Hogquist KA, Jameson SC. Transcriptional downregulation of S1pr1 is required for the establishment of resident memory CD8+ T cells. Nat Immunol. 2013;14(12):1285-93.

392. Mackay LK, Braun A, Macleod BL, Collins N, Tebartz C, Bedoui S, et al. Cutting edge: CD69 interference with sphingosine-1-phosphate receptor function regulates peripheral T cell retention. J Immunol. 2015;194(5):2059-63.
393. Kumar BV, Ma W, Miron M, Granot T, Guyer RS, Carpenter DJ, et al. Human Tissue-Resident Memory T Cells Are Defined by Core Transcriptional and Functional Signatures in Lymphoid and Mucosal Sites. Cell Rep. 2017;20(12):2921-34.
394. Oja AE, Piet B, Helbig C, Stark R, van der Zwan D, Blaauwgeers H, et al. Trigger-happy resident memory CD4(+) T cells inhabit the human lungs. Mucosal Immunol. 2018;11(3):654-67.
395. El-Asady R, Yuan R, Liu K, Wang D, Gress RE, Lucas PJ, et al. TGF-{beta}-dependent CD103 expression by CD8(+) T cells promotes selective destruction of the host intestinal epithelium during graft-versus-host disease. J Exp Med. 2005;201(10):1647-57.
396. Wong MT, Ong DE, Lim FS, Teng KW, McGovern N, Narayanan S, et al. A High-Dimensional Atlas of Human T Cell Diversity Reveals Tissue-Specific Trafficking and Cytokine Signatures. Immunity. 2016;45(2):442-56.
397. Mackay LK, Minnich M, Kragten NA, Liao Y, Nota B, Seillet C, et al. Hobit and Blimp1 instruct a universal transcriptional program of tissue residency in lymphocytes. Science. 2016;352(6284):459-63.
398. Buggert M, Nguyen S, Salgado-Montes de Oca G, Bengsch B, Darko S, Ransier A, et al. Identification and characterization of HIV-specific resident memory CD8(+) T cells in human lymphoid tissue. Sci Immunol. 2018;3(24).
399. Gebhardt T, Wakim LM, Eidsmo L, Reading PC, Heath WR, Carbone FR. Memory T cells in nonlymphoid tissue that provide enhanced local immunity during infection with herpes simplex virus. Nat Immunol. 2009;10(5):524-30.
400. Mueller SN, Mackay LK. Tissue-resident memory T cells: local specialists in immune defence. Nat Rev Immunol. 2016;16(2):79-89.
401. Dumauthioz N, Labiano S, Romero P. Tumor Resident Memory T Cells: New Players in Immune Surveillance and Therapy. Front Immunol. 2018;9:2076.
402. Amsen D, van Gisbergen K, Hombrink P, van Lier RAW. Tissue-resident memory T cells at the center of immunity to solid tumors. Nat Immunol. 2018;19(6):538-46.
403. Yang L, Yu Y, Kalwani M, Tseng TW, Baltimore D. Homeostatic cytokines orchestrate the segregation of CD4 and CD8 memory T-cell reservoirs in mice. Blood. 2011;118(11):3039-50.
404. Sathaliyawala T, Kubota M, Yudanin N, Turner D, Camp P, Thome JJ, et al. Distribution and compartmentalization of human circulating and tissue-resident memory T cell subsets. Immunity. 2013;38(1):187-97.
405. Teijaro JR, Turner D, Pham Q, Wherry EJ, Lefrancois L, Farber DL. Cutting edge: Tissue-retentive lung memory CD4 T cells mediate optimal protection to respiratory virus infection. J Immunol. 2011;187(11):5510-4.
406. Gebhardt T, Whitney PG, Zaid A, Mackay LK, Brooks AG, Heath WR, et al. Different patterns of peripheral migration by memory CD4+ and CD8+ T cells. Nature. 2011;477(7363):216-9.
407. Iijima N, Iwasaki A. T cell memory. A local macrophage chemokine network sustains protective tissue-resident memory CD4 T cells. Science. 2014;346(6205):93-8.
408. Purwar R, Campbell J, Murphy G, Richards WG, Clark RA, Kupper TS. Resident memory T cells (T(RM)) are abundant in human lung: diversity, function, and antigen specificity. PLoS One. 2011;6(1):e16245.
409. Chapman TJ, Lambert K, Topham DJ. Rapid reactivation of extralymphoid CD4 T cells during secondary infection. PLoS One. 2011;6(5):e20493.

410. Vukmanovic-Stejic M, Sandhu D, Seidel JA, Patel N, Sobande TO, Agius E, et al. The Characterization of Varicella Zoster Virus-Specific T Cells in Skin and Blood during Aging. J Invest Dermatol. 2015;135(7):1752-62.
411. Ganesan AP, Clarke J, Wood O, Garrido-Martin EM, Chee SJ, Mellows T, et al. Tissue-resident memory features are linked to the magnitude of cytotoxic T cell responses in human lung cancer. Nat Immunol. 2017;18(8):940-50.
412. Park SL, Buzzai A, Rautela J, Hor JL, Hochheiser K, Effern M, et al. Tissue-resident memory CD8(+) T cells promote melanoma-immune equilibrium in skin. Nature. 2019;565(7739):366-71.
413. Bunce M. PCR-sequence-specific primer typing of HLA class I and class II alleles. Methods Mol Biol. 2003;210:143-71.
414. Quigley MF, Almeida JR, Price DA, Douek DC. Unbiased molecular analysis of T cell receptor expression using template-switch anchored RT-PCR. Curr Protoc Immunol. 2011;Chapter 10:Unit10 33.
415. Lefranc MP, Pommie C, Ruiz M, Giudicelli V, Foulquier E, Truong L, et al. IMGT unique numbering for immunoglobulin and T cell receptor variable domains and Ig superfamily V-like domains. Dev Comp Immunol. 2003;27(1):55-77.
416. Shugay M, Bagaev DV, Zvyagin IV, Vroomans RM, Crawford JC, Dolton G, et al. VDJdb: a curated database of T-cell receptor sequences with known antigen specificity. Nucleic Acids Res. 2018;46(D1):D419-D27.
417. Roederer M, Nozzi JL, Nason MC. SPICE: exploration and analysis of post-cytometric complex multivariate datasets. Cytometry A. 2011;79(2):167-74.
418. Rajnavolgyi E, Nagy N, Thuresson B, Dosztanyi Z, Simon A, Simon I, et al. A repetitive sequence of Epstein-Barr virus nuclear antigen 6 comprises overlapping T cell epitopes which induce HLA-DR-restricted CD4(+) T lymphocytes. Int Immunol. 2000;12(3):281-93.
419. Mautner J, Bornkamm GW. The role of virus-specific CD4+ T cells in the control of Epstein-Barr virus infection. Eur J Cell Biol. 2012;91(1):31-5.
420. Amyes E, McMichael AJ, Callan MF. Human CD4+ T cells are predominantly distributed among six phenotypically and functionally distinct subsets. J Immunol. 2005;175(9):5765-73.
421. Petrara MR, Freguja R, Gianesin K, Zanchetta M, De Rossi A. Epstein-Barr virus-driven lymphomagenesis in the context of human immunodeficiency virus type 1 infection. Front Microbiol. 2013;4:311.
422. Mautner J, Pich D, Nimmerjahn F, Milosevic S, Adhikary D, Christoph H, et al. Epstein-Barr virus nuclear antigen 1 evades direct immune recognition by CD4+ T helper cells. Eur J Immunol. 2004;34(9):2500-9.
423. Adhikary D, Behrends U, Feederle R, Delecluse HJ, Mautner J. Standardized and highly efficient expansion of Epstein-Barr virus-specific CD4+ T cells by using virus-like particles. J Virol. 2008;82(8):3903-11.
424. Tamaru Y, Miyawaki T, Iwai K, Tsuji T, Nibu R, Yachie A, et al. Absence of bcl-2 expression by activated CD45RO+ T lymphocytes in acute infectious mononucleosis supporting their susceptibility to programmed cell death. Blood. 1993;82(2):521-7.
425. Akbar AN, Borthwick N, Salmon M, Gombert W, Bofill M, Shamsadeen N, et al. The significance of low bcl-2 expression by CD45RO T cells in normal individuals and patients with acute viral infections. The role of apoptosis in T cell memory. J Exp Med. 1993;178(2):427-38.
426. Curtsinger JM, Agarwal P, Lins DC, Mescher MF. Autocrine IFN-gamma promotes naive CD8 T cell differentiation and synergizes with IFN-alpha to stimulate strong function. J Immunol. 2012;189(2):659-68.
427. Harari A, Vallelian F, Pantaleo G. Phenotypic heterogeneity of antigen-specific CD4 T cells under different conditions of antigen persistence and antigen load. Eur J Immunol. 2004;34(12):3525-33.

428. Makedonas G, Betts MR. Polyfunctional analysis of human t cell responses: importance in vaccine immunogenicity and natural infection. Springer Semin Immunopathol. 2006;28(3):209-19.
429. Gerlach C, Moseman EA, Loughhead SM, Alvarez D, Zwijnenburg AJ, Waanders L, et al. The Chemokine Receptor CX3CR1 Defines Three Antigen-Experienced CD8 T Cell Subsets with Distinct Roles in Immune Surveillance and Homeostasis. Immunity. 2016;45(6):1270-84.
430. Bottcher JP, Beyer M, Meissner F, Abdullah Z, Sander J, Hochst B, et al. Functional classification of memory CD8(+) T cells by CX3CR1 expression. Nat Commun. 2015;6:8306.
431. Saez-Borderias A, Guma M, Angulo A, Bellosillo B, Pende D, Lopez-Botet M. Expression and function of NKG2D in CD4+ T cells specific for human cytomegalovirus. Eur J Immunol. 2006;36(12):3198-206.
432. Munier CML, van Bockel D, Bailey M, Ip S, Xu Y, Alcantara S, et al. The primary immune response to Vaccinia virus vaccination includes cells with a distinct cytotoxic effector CD4 T-cell phenotype. Vaccine. 2016;34(44):5251-61.
433. Hislop AD, Taylor GS, Sauce D, Rickinson AB. Cellular responses to viral infection in humans: lessons from Epstein-Barr virus. Annu Rev Immunol. 2007;25:587-617.
434. Bade B, Boettcher HE, Lohrmann J, Hink-Schauer C, Bratke K, Jenne DE, et al. Differential expression of the granzymes A, K and M and perforin in human peripheral blood lymphocytes. Int Immunol. 2005;17(11):1419-28.
435. Zaunders JJ, Dyer WB, Munier ML, Ip S, Liu J, Amyes E, et al. CD127+CCR5+CD38+++ CD4+ Th1 effector cells are an early component of the primary immune response to vaccinia virus and precede development of interleukin-2+ memory CD4+ T cells. J Virol. 2006;80(20):10151-61.
436. Doisne JM, Urrutia A, Lacabaratz-Porret C, Goujard C, Meyer L, Chaix ML, et al. CD8+ T cells specific for EBV, cytomegalovirus, and influenza virus are activated during primary HIV infection. J Immunol. 2004;173(4):2410-8.
437. Li Causi E, Parikh SC, Chudley L, Layfield DM, Ottensmeier CH, Stevenson FK, et al. Vaccination Expands Antigen-Specific CD4+ Memory T Cells and Mobilizes Bystander Central Memory T Cells. PLoS One. 2015;10(9):e0136717.
438. van Aalst S, Ludwig IS, van der Zee R, van Eden W, Broere F. Bystander activation of irrelevant CD4+ T cells following antigen-specific vaccination occurs in the presence and absence of adjuvant. PLoS One. 2017;12(5):e0177365.
439. Balfour HH, Jr., Holman CJ, Hokanson KM, Lelonek MM, Giesbrecht JE, White DR, et al. A prospective clinical study of Epstein-Barr virus and host interactions during acute infectious mononucleosis. J Infect Dis. 2005;192(9):1505-12.
440. Callan MF. The immune response to Epstein-Barr virus. Microbes Infect. 2004;6(10):937-45.
441. Mattoo H, Mahajan VS, Maehara T, Deshpande V, Della-Torre E, Wallace ZS, et al. Clonal expansion of CD4(+) cytotoxic T lymphocytes in patients with IgG4-related disease. J Allergy Clin Immunol. 2016;138(3):825-38.
442. Schreeder DM, Pan J, Li FJ, Vivier E, Davis RS. FCRL6 distinguishes mature cytotoxic lymphocytes and is upregulated in patients with B-cell chronic lymphocytic leukemia. Eur J Immunol. 2008;38(11):3159-66.
443. Maini MK, Gudgeon N, Wedderburn LR, Rickinson AB, Beverley PC. Clonal expansions in acute EBV infection are detectable in the CD8 and not the CD4 subset and persist with a variable CD45 phenotype. J Immunol. 2000;165(10):5729-37.
444. Lima M, Teixeira Mdos A, Queiros ML, Santos AH, Goncalves C, Correia J, et al. Immunophenotype and TCR-Vbeta repertoire of peripheral blood T-cells in acute infectious mononucleosis. Blood Cells Mol Dis. 2003;30(1):1-12.

445. Bitmansour AD, Waldrop SL, Pitcher CJ, Khatamzas E, Kern F, Maino VC, et al. Clonotypic structure of the human CD4+ memory T cell response to cytomegalovirus. J Immunol. 2001;167(3):1151-63.
446. Crompton L, Khan N, Khanna R, Nayak L, Moss PA. CD4+ T cells specific for glycoprotein B from cytomegalovirus exhibit extreme conservation of T-cell receptor usage between different individuals. Blood. 2008;111(4):2053-61.
447. Dietrich PY, Walker PR, Schnuriger V, Saas P, Perrin G, Guillard M, et al. TCR analysis reveals significant repertoire selection during in vitro lymphocyte culture. Int Immunol. 1997;9(8):1073-83.
448. Pu Z, Carrero JA, Unanue ER. Distinct recognition by two subsets of T cells of an MHC class II-peptide complex. Proc Natl Acad Sci U S A. 2002;99(13):8844-9.
449. Song I, Gil A, Mishra R, Ghersi D, Selin LK, Stern LJ. Broad TCR repertoire and diverse structural solutions for recognition of an immunodominant CD8(+) T cell epitope. Nat Struct Mol Biol. 2017;24(4):395-406.
450. Alfieri C, Birkenbach M, Kieff E. Early events in Epstein-Barr virus infection of human B lymphocytes. Virology. 1991;181(2):595-608.
451. Venturi V, Price DA, Douek DC, Davenport MP. The molecular basis for public T-cell responses? Nat Rev Immunol. 2008;8(3):231-8.
452. Stubbington MJT, Lonnberg T, Proserpio V, Clare S, Speak AO, Dougan G, et al. T cell fate and clonality inference from single-cell transcriptomes. Nat Methods. 2016;13(4):329-32.
453. Kjer-Nielsen L, Clements CS, Purcell AW, Brooks AG, Whisstock JC, Burrows SR, et al. A structural basis for the selection of dominant alphabeta T cell receptors in antiviral immunity. Immunity. 2003;18(1):53-64.
454. Miles JJ, Bulek AM, Cole DK, Gostick E, Schauenburg AJ, Dolton G, et al. Genetic and structural basis for selection of a ubiquitous T cell receptor deployed in Epstein-Barr virus infection. PLoS Pathog. 2010;6(11):e1001198.
455. Nguyen TH, Bird NL, Grant EJ, Miles JJ, Thomas PG, Kotsimbos TC, et al. Maintenance of the EBV-specific CD8(+) TCRalphabeta repertoire in immunosuppressed lung transplant recipients. Immunol Cell Biol. 2017;95(1):77-86.
456. Lim A, Trautmann L, Peyrat MA, Couedel C, Davodeau F, Romagne F, et al. Frequent contribution of T cell clonotypes with public TCR features to the chronic response against a dominant EBV-derived epitope: application to direct detection of their molecular imprint on the human peripheral T cell repertoire. J Immunol. 2000;165(4):2001-11.
457. Venturi V, Chin HY, Asher TE, Ladell K, Scheinberg P, Bornstein E, et al. TCR beta-chain sharing in human CD8+ T cell responses to cytomegalovirus and EBV. J Immunol. 2008;181(11):7853-62.
458. Fazilleau N, Cabaniols JP, Lemaitre F, Motta I, Kourilsky P, Kanellopoulos JM. Valpha and Vbeta public repertoires are highly conserved in terminal deoxynucleotidyl transferase-deficient mice. J Immunol. 2005;174(1):345-55.
459. Galperin M, Farenc C, Mukhopadhyay M, Jayasinghe D, Decroos A, Benati D, et al. CD4(+) T cell-mediated HLA class II cross-restriction in HIV controllers. Sci Immunol. 2018;3(24).
460. Tian Y, Babor M, Lane J, Schulten V, Patil VS, Seumois G, et al. Unique phenotypes and clonal expansions of human CD4 effector memory T cells re-expressing CD45RA. Nat Commun. 2017;8(1):1473.
461. Gallimore A, Glithero A, Godkin A, Tissot AC, Pluckthun A, Elliott T, et al. Induction and exhaustion of lymphocytic choriomeningitis virus-specific cytotoxic T lymphocytes visualized using soluble tetrameric major histocompatibility complex class I-peptide complexes. J Exp Med. 1998;187(9):1383-93.

462. Remmerswaal EB, Klarenbeek PL, Alves NL, Doorenspleet ME, van Schaik BD, Esveldt RE, et al. Clonal evolution of CD8+ T cell responses against latent viruses: relationship among phenotype, localization, and function. J Virol. 2015;89(1):568-80.
463. Trautmann L, Rimbert M, Echasserieau K, Saulquin X, Neveu B, Dechanet J, et al. Selection of T cell clones expressing high-affinity public TCRs within Human cytomegalovirus-specific CD8 T cell responses. J Immunol. 2005;175(9):6123-32.
464. Davenport MP, Price DA, McMichael AJ. The T cell repertoire in infection and vaccination: implications for control of persistent viruses. Curr Opin Immunol. 2007;19(3):294-300.
465. Venturi V, Kedzierska K, Price DA, Doherty PC, Douek DC, Turner SJ, et al. Sharing of T cell receptors in antigen-specific responses is driven by convergent recombination. Proc Natl Acad Sci U S A. 2006;103(49):18691-6.
466. Thorley-Lawson DA, Gross A. Persistence of the Epstein-Barr virus and the origins of associated lymphomas. N Engl J Med. 2004;350(13):1328-37.
467. Anagnostopoulos I, Hummel M, Kreschel C, Stein H. Morphology, immunophenotype, and distribution of latently and/or productively Epstein-Barr virus-infected cells in acute infectious mononucleosis: implications for the interindividual infection route of Epstein-Barr virus. Blood. 1995;85(3):744-50.
468. Pallett LJ, Davies J, Colbeck EJ, Robertson F, Hansi N, Easom NJW, et al. IL-2(high) tissue-resident T cells in the human liver: Sentinels for hepatotropic infection. J Exp Med. 2017;214(6):1567-80.
469. Hara T, Jung LK, Bjorndahl JM, Fu SM. Human T cell activation. III. Rapid induction of a phosphorylated 28 kD/32 kD disulfide-linked early activation antigen (EA 1) by 12-o-tetradecanoyl phorbol-13-acetate, mitogens, and antigens. J Exp Med. 1986;164(6):1988-2005.
470. Zundler S, Becker E, Spocinska M, Slawik M, Parga-Vidal L, Stark R, et al. Hobit- and Blimp-1-driven CD4(+) tissue-resident memory T cells control chronic intestinal inflammation. Nat Immunol. 2019;20(3):288-300.
471. Oja AE, Piet B, van der Zwan D, Blaauwgeers H, Mensink M, de Kivit S, et al. Functional Heterogeneity of CD4(+) Tumor-Infiltrating Lymphocytes With a Resident Memory Phenotype in NSCLC. Front Immunol. 2018;9:2654.
472. Beura LK, Wijeyesinghe S, Thompson EA, Macchietto MG, Rosato PC, Pierson MJ, et al. T Cells in Nonlymphoid Tissues Give Rise to Lymph-Node-Resident Memory T Cells. Immunity. 2018;48(2):327-38 e5.
473. Thome JJ, Yudanin N, Ohmura Y, Kubota M, Grinshpun B, Sathaliyawala T, et al. Spatial map of human T cell compartmentalization and maintenance over decades of life. Cell. 2014;159(4):814-28.
474. Freeman BE, Hammarlund E, Raue HP, Slifka MK. Regulation of innate CD8+ T-cell activation mediated by cytokines. Proc Natl Acad Sci U S A. 2012;109(25):9971-6.
475. Wherry EJ, Ha SJ, Kaech SM, Haining WN, Sarkar S, Kalia V, et al. Molecular signature of CD8+ T cell exhaustion during chronic viral infection. Immunity. 2007;27(4):670-84.
476. Schenkel JM, Fraser KA, Masopust D. Cutting edge: resident memory CD8 T cells occupy frontline niches in secondary lymphoid organs. J Immunol. 2014;192(7):2961-4.
477. Ugur M, Schulz O, Menon MB, Krueger A, Pabst O. Resident CD4+ T cells accumulate in lymphoid organs after prolonged antigen exposure. Nat Commun. 2014;5:4821.
478. Marriott CL, Dutton EE, Tomura M, Withers DR. Retention of Ag-specific memory CD4(+) T cells in the draining lymph node indicates lymphoid tissue resident memory populations. Eur J Immunol. 2017;47(5):860-71.
479. Glennie ND, Volk SW, Scott P. Skin-resident CD4+ T cells protect against Leishmania major by recruiting and activating inflammatory monocytes. PLoS Pathog. 2017;13(4):e1006349.

480. Bergsbaken T, Bevan MJ. Proinflammatory microenvironments within the intestine regulate the differentiation of tissue-resident CD8(+) T cells responding to infection. Nature Immunology. 2015;16(4):406-14.
481. Mackay LK, Rahimpour A, Ma JZ, Collins N, Stock AT, Hafon ML, et al. The developmental pathway for CD103(+)CD8(+) tissue-resident memory T cells of skin. Nature Immunology. 2013;14(12):1294-+.
482. Carlson CM, Endrizzi BT, Wu J, Ding X, Weinreich MA, Walsh ER, et al. Kruppel-like factor 2 regulates thymocyte and T-cell migration. Nature. 2006;442(7100):299-302.
483. Cannons JL, Lu KT, Schwartzberg PL. T follicular helper cell diversity and plasticity. Trends Immunol. 2013;34(5):200-7.
484. Haynes NM, Allen CD, Lesley R, Ansel KM, Killeen N, Cyster JG. Role of CXCR5 and CCR7 in follicular Th cell positioning and appearance of a programmed cell death gene-1high germinal center-associated subpopulation. J Immunol. 2007;179(8):5099-108.
485. Hardtke S, Ohl L, Forster R. Balanced expression of CXCR5 and CCR7 on follicular T helper cells determines their transient positioning to lymph node follicles and is essential for efficient B-cell help. Blood. 2005;106(6):1924-31.
486. Kim CH, Rott LS, Clark-Lewis I, Campbell DJ, Wu L, Butcher EC. Subspecialization of CXCR5+ T cells: B helper activity is focused in a germinal center-localized subset of CXCR5+ T cells. J Exp Med. 2001;193(12):1373-81.
487. Lee JY, Skon CN, Lee YJ, Oh S, Taylor JJ, Malhotra D, et al. The transcription factor KLF2 restrains CD4(+) T follicular helper cell differentiation. Immunity. 2015;42(2):252-64.
488. Zotos D, Coquet JM, Zhang Y, Light A, D'Costa K, Kallies A, et al. IL-21 regulates germinal center B cell differentiation and proliferation through a B cell-intrinsic mechanism. J Exp Med. 2010;207(2):365-78.
489. Linterman MA, Beaton L, Yu D, Ramiscal RR, Srivastava M, Hogan JJ, et al. IL-21 acts directly on B cells to regulate Bcl-6 expression and germinal center responses. J Exp Med. 2010;207(2):353-63.
490. Bryant VL, Ma CS, Avery DT, Li Y, Good KL, Corcoran LM, et al. Cytokine-mediated regulation of human B cell differentiation into Ig-secreting cells: predominant role of IL-21 produced by CXCR5+ T follicular helper cells. J Immunol. 2007;179(12):8180-90.
491. Spolski R, Kim HP, Zhu W, Levy DE, Leonard WJ. IL-21 mediates suppressive effects via its induction of IL-10. J Immunol. 2009;182(5):2859-67.
492. Yusuf I, Kageyama R, Monticelli L, Johnston RJ, Ditoro D, Hansen K, et al. Germinal center T follicular helper cell IL-4 production is dependent on signaling lymphocytic activation molecule receptor (CD150). J Immunol. 2010;185(1):190-202.
493. Kragten NAM, Behr FM, Vieira Braga FA, Remmerswaal EBM, Wesselink TH, Oja AE, et al. Blimp-1 induces and Hobit maintains the cytotoxic mediator granzyme B in CD8 T cells. Eur J Immunol. 2018;48(10):1644-62.
494. Kaech SM, Wherry EJ. Heterogeneity and cell-fate decisions in effector and memory CD8+ T cell differentiation during viral infection. Immunity. 2007;27(3):393-405.
495. Ranasinghe S, Flanders M, Cutler S, Soghoian DZ, Ghebremichael M, Davis I, et al. HIV-specific CD4 T cell responses to different viral proteins have discordant associations with viral load and clinical outcome. J Virol. 2012;86(1):277-83.
496. Kurth J, Hansmann ML, Rajewsky K, Kuppers R. Epstein-Barr virus-infected B cells expanding in germinal centers of infectious mononucleosis patients do not participate in the germinal center reaction. Proc Natl Acad Sci U S A. 2003;100(8):4730-5.